Stabilisation of Low Temperature Biocatalysts

Ekta Yogesh Rayani

A thesis submitted for the degree of Doctor of Philosophy to
University College London

Department of Biochemical Engineering
University College London
Torrington Place
London
WC1E 7JE

January 2022

Declaration

I, Ekta Yogesh Rayani, confirm that this thesis is my own. Additional information sourced from other sources has been identified in this thesis.

Abstract

Cold marine environments represent a rich resource for bioprospecting of low temperature enzymes from the polar waters surrounding the Antarctic.

Psychrophilic lipase candidates were identified using *in silico* bioprospecting methods from two different genomic resources. The *Tara* Ocean database for bacterial candidates using motif searches identified a 921bp lipase gene (PL001). The exploration of eukaryotic lipases from assembled genomes of the *Salpa thompsoni*, a marine tunicate, discovered a 1761bp pancreatic like lipase sequence (PL002). Recombinant bacterial expression produced only PL002 at 10°C followed by affinity purification. Hydrolysis of the synthetic substrate ρ-nitrophenyl butyrate (PNPB) revealed that PL002 is a cold active lipase with an optimal activity temperature and pH profile of 20°C and pH 7 and a specific activity of 3.16U/mg that was maintained at over 60% in temperatures from 15 to 25°C. A meta-analysis of lipase activities towards PNPB showed that PL002 displays a higher activity at lower temperatures relative to reported lipases. Site directed covalent immobilisation, using chemically activated cellulose nanofiber membranes (CNF), was trialled to improve lipase stability and activity. Using the Lilly-Hornby equation to determine the Michaelis-Menten constant, K_M, it was established that the K_M in the free and immobilised systems were comparable and therefore the mass transfer properties exhibited in CNF are favourable with immobilised lipases. Lipase mediated decomposition of polyurethane-polyesters (PUs) has potential to reduce waste accumulation. The greater ester cleaving potential demonstrated by positive control, *Candida antarctica* lipase B, presented further analysis to characterise the degradation capabilities by assessing enzyme loading on CNF. Over a 12-hour period the lower loaded membranes degraded more of the 0.01 mg/ml PU substrate (56%), and at higher rate of 3.78 $x10^{-03}$mg/ml/hr than the free enzyme in solution (33% and 3.53 $x10^{-03}$mg/ml/hr). The findings underline the potential of a CNF immobilisation system for process intensification, and monomer recycling from PU degradation.

Impact Statement

Despite the broad geographic coverage of low temperature marine environments, they remain underexplored from a bioprospecting perspective due to their remote locations and challenges with accessibility. Yet there is an untapped resource for psychrophilic enzymes for biocatalysis and bioconversion. There is a need to create a pipeline for enzyme discovery from eukaryotic organisms that are cold active.

This thesis demonstrates a pipeline for enzyme discovery from this unique set of organisms by linking *in silico* bioprospecting with the *in vitro* expression of a lipase gene of interest. It is the first time a cold-adapted lipase from a marine tunicate, *Salpa thompsoni* (Salps), has been characterised. Salps are an ecologically important set of organisms in the marine carbon cycle, through their rapid and explosive growth and contribution to deposition of material as marine snow. Using a case study of *Salpa thompsoni,* we created a publicly available digestive tract RNA dataset, (accession numbers SRX13276964 and SRX13276963) to identify lipase candidates. Cold active lipases have been reported to reduce the temperature at which regular enzymatic reactions can take place leading to a reduction in energy usage. Lipases can catalyse a multitude of different reactions therefore the ideal enzymatic candidate for future use in the biotechnology industry. The enzyme characterised in this study has been shown to have cold activity preference, exhibiting over 60% activity at temperatures below 25 °C. The short chain substrate specificity of this candidate also provides insight to the hydrolysis ability suitable for future applications.

Polyurethane polyesters are a plastic material traditionally used as coating or adhesive in everyday items. It is estimated that total annual production is 8 million tonnes and grows by up to 5% every year (Matsumura, Soeda and Toshima, 2006). Therefore, there is a need to consider end of life management that is both cost effective and sustainable. Significant strides in the biodegradation of this material have been made in the recent years, with novel enzymes being discovered to degrade a variety of different plastics. However, there is a lack of understanding in establishing a method to produce an immobilised enzyme scale up system to biodegrade liquid polyesters. In this thesis lipases immobilised onto chemically functionalised cellulose nanofiber, are optimised for use in a recirculating batch flow of liquid polyester polyurethanes. This demonstrates the potential for both the salp lipase, and commercial

candidate, *Candida antarctica* lipase B (Cal B) as a biocatalyst in the biodegradation of thermolabile pseudoplastic, Dispercoll® U 2682. The cold activity demonstrated by Cal B encouraged the development of a system was optimised for use at 20°C, this is the first time that low temperatures have been utilised in a biodegradation application and represents an important first step in the recovery and recycling of polyester monomers. Alternative detection methods based on prior work conducted by Biffinger *et al.*, (2015) using Impranil® DLN, were optimised to identify the hydrolysis of ester bonds within the plastic. This will facilitate future efforts to identify a multienzyme flow based degradation system. As the first study to investigate the biodegradability of Dispercoll using Cal B, the data will serve as an important benchmark for future scale up studies and technoeconomic evaluations of application of immobilised lipases in biotechnology industries.

Acknowledgements

Firstly, I am grateful to my supervisors, Dr Brenda Parker (UCL) and Dr William Goodall-Copestake (SAMS) for all their words of encouragement and support throughout the project. Brenda, there's been many a time where things were going wrong and I was unsure what to do, your invaluable support has really helped me to see the bigger picture. Will, thank you for helping me with understanding the importance of *in silico* bioinformatics and priceless advice and feedback on my thesis.

I would also like to thank Professor John Ward (UCL) and Dr Maria Bawn (UCL), for all their guidance and support when applying new concepts of plastic degradation by cold enzymes.

This work could not have taken place without collaboration with Cytiva Ltd. Thank you, Dr Iwan Roberts, and the team, for all their technical support.

There are many individuals that have given up their time as well as their invaluable advice. Thank you to Alexander Cotton for all things salp at UCL. A special mention to my friends in the department, you guys have kept me sane when assays and fermentations were getting away from me!

This research was conducted in the Department of Biochemical Engineering at University College London (UCL) with funding provided from the Engineering Physical Science Research Council has also been vital in supporting my work.

Thanks to my AG friends for always being around and supporting me (even though you don't know what I have been doing for the past few years!)

Finally, I am thankful to all my parents, Yogesh and Jayshri and my sister, Neha. I couldn't have gotten this far without your care and support throughout all my studies.

I would like to dedicate this thesis to you.

Table of Contents

Index of Figures

Index of Tables

Index of Abbreviations

4-NP	4-Nitrophenol, ρ-nitrophenolate ion
BP	Base pairs
Cal B	*Candida antarctica* lipase B
CDS	Coding sequence
CFPS	Cell Free Protein Synthesis
Cys	Cysteine
DNA	Deoxyribonucleic acid
E. coli	*Escherichia coli*
FTIR	*Fourier-transform infrared spectroscopy*
His Tag	6x Histidine tag
IPTG	Isopropyl β-D-1-thiogalactopyranoside
kDa	Kilodalton
LB	Lysogeny Broth
MM	Magic Media
MW	Molecular Weight
NCBI	National Centre for Biotechnology Information
NMR	Nuclear magnetic resonance
OD	Optical Density
ORF	Open Reading Frame
PDB	Protein Data Bank
PI	Isoelectric Point
PL001	Psychrophilic Lipase 1, Tara Oceans bacterial lipase
PL002	Psychrophilic Lipase 2, Salp pancreatic like lipase
PNPB	ρ-nitrophenyl butyrate
PNPP	ρ-nitrophenyl palmitate
PU	Polyester polyurethane
RNA	Ribonucleic acid
RPM	Revolutions Per Minute
RT PCR	Reverse Transcription Polymerase Chain Reaction
Salp	*Salpa thompsoni, S. thompsoni*
SDS PAGE	Sodium dodecyl-sulfate polyacrylamide gel electrophoresis

SEC HPLC	Size Exclusion High Pressure Liquid Chromatography
SEM	Scanning Electron Microscope
TB	Terrific Broth
tBLASTN	Basic local alignment search tool for nucleotides
tBLASTP	Basic local alignment search tool for proteins
TBS	Tris-buffered saline
TBST	Tris-buffered saline (TBS) and Polysorbate 20 (Tween)
TBSTM	tris-buffered saline (TBS), Polysorbate 20 (Tween), Milk
UCL	University College London (UK)

Nomenclature

ΔG	Gibbs free energy ($kJmol^{-1}$)
°C	Degrees centigrade
C	Reaction capacity (mol.h-1)
kcat	Enzyme turnover rate (s-1)
Km	Michaelis Menten constant (mM)
Km (app)	Apparent Michaelis Menten constant (mM)
P	The fraction of substrate reacted in the column
Q	Volumetric flow rate (mL.h-1)
So	Substrate concentrations (mM)
T	Temperature (°C)
Vmax	Maximum velocity at saturating substrate concentration (mM.s-1)

List of Publications

Original Research Papers:

Rayani, E, Cotton, A, Roberts, I, Ward, J, Goodall-Copestake, W, Parker, B.
2022. Recombinant expression and characterisation of a lipase from the Antarctic zooplankton. *Salpa thompsoni* BioRxiv https://doi.org/10.1101/2022.11.18.517127 (Chapters 2 to 4)

Rayani, E, Bawn, M, Ward, J, Hailes, H, Roberts, I, Parker, B. 2022.
Immobilisation of Cal B lipase on cellulose nanofiber as an effective method to degrade polyesters. (Chapters 5 and 6) – manuscript in preparation

Conference Posters:

Rayani, E, Cotton, A, Roberts, I, Ward, J, Goodall-Copestake, W, Parker, B.
November 2018. Identification of novel lipase candidates. British Antarctic Survey Annual Conference. Cambridge, UK. (Chapter 2)

Rayani, E, Cotton, A, Roberts, I, Ward, J, Goodall-Copestake, W, Parker, B.
April 2022. Novel cold-adapted lipase from marine tunicate, *Salpa thompsoni* and applications. Microbial Engineering II. Albufeira, Portugal. (Chapters 2 to 6)

Chapter 1: Introduction

1.1 From Bioprospecting to Biocatalysis

Biocatalysis, or the use of biologically derived systems to catalyse reactions, has been employed in the biotechnology field for many years. Since the 1990s the use of "Green Chemistry", when using enzymes, or whole cells, in a commercial setting, has reduced the requirement for harsh conditions that were previously exhausted when these sustainable alternatives were unavailable (Mhetras, Mapare and Gokhale, 2021).

Enzyme discovery is defined as the characterisation of new enzymes using reference based enzyme discovery. This is through the known structural functions found in previously characterised families obtained from enzyme expansion studies, specifically geographical regions of known interest based upon operating parameters (Robinson, Piel and Sunagawa, 2021). Bioprospecting has been defined as the search of new molecular material from nature (Oyemitan, 2017). The most logical source for bioprospecting of novel enzymes is from organisms inhabiting low temperature environments.

The marine environment covers over 70 % of the Earth's surface with temperatures close below 5 °C (Pesant *et al.*, 2015). Psychrotroph organisms are cold adapted or tolerant organisms which have an optimal activity between 0 °C to 30 °C (Lee, Jang and Chung, 2017). Often cold active enzymes are not only adapted to low temperatures but are usually adapted to various other environmental factors that can also be beneficial to the bioprocessing industry. These include resistance to extreme saline conditions and even survival in conditions which are low in nutrients (Feller and Gerday, 2003). Thus, the exploration into the Antarctic polar regions represent a rich treasure trove of cold active biocatalysts adapted to function under extreme environmental conditions.

Genomic DNA can be obtained from multiple microscopic communities that are gathered from environmental samples; from which bioinformatic techniques are used to discover genes of interest. This is defined as metagenomic analysis and can be utilised for the identification of novel enzymes for any evolutionary profiles that may exist (Thomas, Gilbert and Meyer, 2012).

An example of this is the *Tara* Oceans project (2009 – 2013) and the metagenomic sequences that were identified during this marine expedition.

Whole genomes of hundreds of species have been annotated and are publicly available for mining of enzyme candidates from the collective archive known as the International Nucleotide Sequence Database (INSDC). By 2021, there were over 800 eukaryotic genomes available on INSDC for enzyme mining endeavours (available: www.ncbi.nlm.nih.gov/genome/annotation_euk/) (Sayers *et al.*, 2022). The annotated genomes of species provide opportunities for directly obtaining candidate enzymes of interest and a useful reference to obtain such enzymes from related species for which only unannotated genomic data is currently available. For example, the model organism and tunicate *Ciona intestinalis* has an annotated genome which can be used to guide the screening of other unannotated tunicate genomes for the purposes of enzyme mining. In this thesis, the annotated *C. intestinalis* genome was used to guide bioprospecting of an unannotated genome of the tunicate S*alpa thompsoni* gene sequence data.

Extraction of novel enzymes can also be conducted by harvesting the proteins from its original source. This is vital when understanding the performance of the protein in systems that are yet to be characterised; especially for proteomic and metabolomic studies. The extraction process provides a useful understanding to the digestive enzymes and thus the ecological impact on the food web (Martínez-Pérez *et al.*, 2020; Xin *et al.*, 2020). However, this requires further studies into optimising purification for large scale manufacturing (Franca-Oliveira, Fornari and Hernández-Ledesma, 2021).

The industrial application of enzyme discovery from unusual or unculturable organisms requires the protein to be made in bulk through recombinant expression in microorganisms such as bacteria (Rosano and Ceccarelli, 2014). *Escherichia coli* cells for protein production have been studied for numerous years with great advancement in the field of genome engineering; whereby issues associated with *E. coli* hosts can be avoided. For example, rare codon expression. Codon usage of the recombinant genes may include specific codons, which do not occur naturally in the host system (Agashe *et al.*, 2013). *Escherichia coli* tRNA are then exhausted, resulting in truncation of proteins (Gustafsson, Govindarajan and Minshull, 2004). Therefore, to circumvent this issue, the use of codon optimisation takes place whereby the genes are optimised for successful expression (Welch *et al.*, 2009). However, there are also

key disadvantages to *E. coli* cell lines. Depending on the expression of the protein, the cell will require lysis mechanisms, which can cause protein disruptions; these include mechanical, chemical or physical mechanisms (Walker, 2009). Over-expression of recombinant proteins in this host can cause protein aggregation and the formation of inclusion bodies (Peternel and Komel, 2011). Inclusion bodies can be refolded (Akbari *et al.*, 2010), however, this may cause negative effects on activity and can be laborious for bulk manufacturing (Soto, 2001). Bacterial lipases are generally favoured towards bacterial hosts as their post translational folding patterns and codon usage system are similar. Complex post translational folding mechanisms exhibited by eukaryotic lipases, such as glycosylation cannot take place in bacterial hosts (Almeida *et al.*, 2020). In such cases, a yeast based eukaryotic protein production host can be employed.

Yeast based systems are an alternative platform that have also been optimised for recombinant protein production. *Pichia pastoris* is a known methyl inducing cell line and has the ability to secrete proteins, which evades the need for cell lysis processes that are used with *E.coli* systems (Kurtzman, 2009; Park *et al.*, 2019) Yeast cell lines have been utilised to produce high concentration of protein biologics such as eukaryotic based recombinant insulin (Gomes *et al.*, 2018). However, the secretary nature of this host system may reach its capacity, resulting in the amassing of unfolded proteins in the endoplasmic reticulum which activates unfolded protein response factors. These factors increase the production of molecular chaperones and reduce or inhibit target protein formation (Contesini *et al.*, 2020). Yeast based glycosylation patterns have the potential to produce immunogenic sugars whilst producing some eukaryotic proteins (Burnett and Burnett, 2020). Suggestions for employing mammalian host cell sources for proteins that require such modifications for expression purposes can be attempted.

Mammalian cell lines can be used to produce proteins that require specific glycosylation folding patterns. This includes N-glycosylation, which mimics human protein translation, however, further modifications and optimisations are required (Demain and Vaishnav, 2009). Chinese hamster ovary cells are traditionally utilised for therapeutic protein production following this approach. This is a highly expensive resource especially for scale-up purposes. Nonetheless, if successful, in the cases of antibody manufacturing, the reward is lucrative (Griffin *et al.*, 2007).

A novel expression system, Cell Free Protein Synthesis (CFPS) can also be attempted for expression of recombinant proteins. CFPS employs the mechanistic ability of protein

production without the cumbersome metabolic pathways of the host cell line. This reduces the ability of any host cell reactions that interfere with protein production (Colant *et al.*, 2021). A caveat here is that this process requires sufficient production of cell free extracts that can be expensive and laborious (Park *et al.*, 2011).

As with all protein expression methods, optimisation is required to generate maximal yield. Downstream protein processing factors will then need to be utilised to ensure that high purity is determined. Therefore, the trade-off between yield and purity will come into effect (Doran, 2013). It is vital to determine a protein's structure to deduce its applied nature in biotechnology.

Finally, in terms of implementation, the cost and lack of recovery of free enzyme can be a significant barrier to implementation. Immobilised enzymes are also more convenient to handle in a solid format. The key advantage to immobilised enzymes is the easy separation of product from the enzyme: substrate complex, reducing the risk of contamination. This also facilitates better separation between the enzyme and the product if enzymatic inhibition occurs. A method of continuous product generation and also potential reduction in the risk of contamination encourages the use of immobilised enzymes in the bioprocessing industry (Sheldon and van Pelt, 2013). However, the chemical processes that are used to attach the enzymes to the surface of interest can cause inactivation or denaturing if processed incorrectly. This is due to the potentially toxic or active site denaturing substances used in the process, such as EDTA (Mateo, Grazu, *et al.*, 2007). Continuous processing using immobilised enzyme has been beneficial in the food industry. A continuous process to produce vitamin C (L-Ascorbic) a water-soluble natural antioxidant was developed. Cal B was used as a biocatalyst in transesterification reactions to produce a fatty acid ester of adapted vitamin C. This process has the ability for bioconversion at 95% (Burham *et al.*, 2009; Basso and Serban, 2019) The caveat of processes such as this is the cost of the immobilisation system and the reaction time. Therefore, if these two factors were minimised, immobilisation provides an attractive solution for the bioprocessing industry.

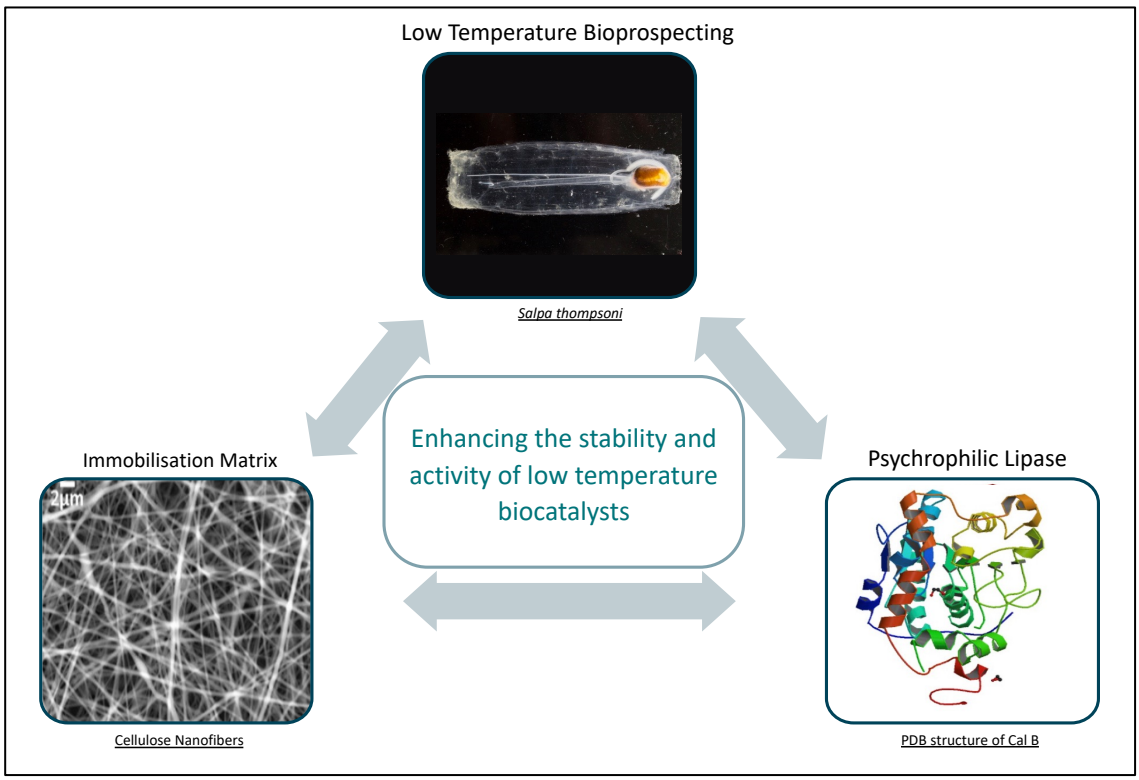

Figure 1.1 Stabilisation of Low temperature Biocatalysts

Depicted to improve current bioprocessing methods in industry

1.2 A Significant Biocatalyst: The Lipase

Lipases (EC: 3.1.1.3) are a form of triglyceraldehyde hydrolases and part of the structural superfamily of alpha/beta-hydrolases. Their primary function, in natural conditions, is to hydrolyse carboxylic ester bonds in hydrophobic compounds. Pharmaceutical industries have also made use of these enzymes in the production of specific drug compounds; specifically as digestive aids to reduce cholesterol levels (Tanokura *et al.*, 2015; Chandra *et al.*, 2020).

Lipases possess the ability to catalyse a wide variety of molecular reactions, making them valuable for several biocatalytic applications. These have been optimised for use in the biotechnology industry and therefore lipase candidates are a sought after biocatalyst, and the model enzyme for this work. Reactions implemented at scale include hydrolysis, esterification, and transesterification reactions. Hydrolysis reactions have been conducted using immobilised lipase from *Rhodothermus marinus* for the production of ibuprofen esters (Memarpoor-Yazdi, Karbalaei-Heidari and Doroodmand, 2018). Flavour esters have been synthesised by esterification reactions using *Candida antarctica* Lipase B (De Souza *et al.*, 2017). Transesterification reactions have been used in the production of biodiesels by lipases of *Streptomyces* origin (Cho *et al.*, 2012). Infrequent reactions conducted by lipases are acidolysis, alcoholysis and aminolysis reactions, (Figure 1.2.1).

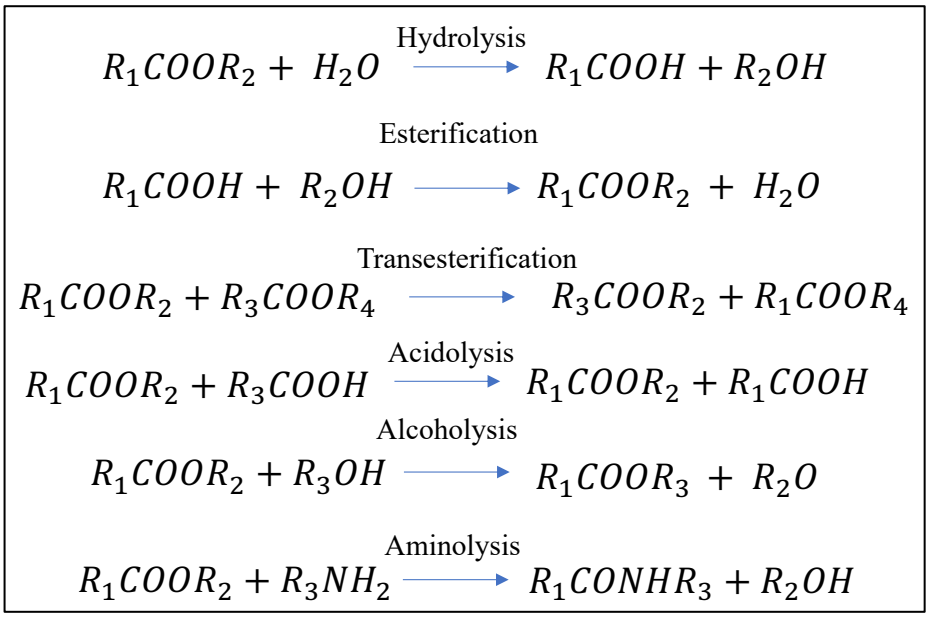

Figure 1.2.1 Common lipase catalysed reactions

Hydrolysis, esterification, and transesterification reactions are commonly utilised in industrial applications. Adapted from (Chandra *et al.*, 2020).

Lipase Structure, Classification and Function

Lipase structures can be used to determine the expression and activity profile of the catalyst. Here, a brief search into bacterial and eukaryotic lipase classification, Table 1.2.2, and Table 1.2.3, was conducted to determine the types of lipases that can be harnessed for industrial applications.

Lipases have a general structure of a catalytic triad and nucleophilic elbow. This catalytic triad is a highly conserved structural feature of the enzyme (Ollis *et al.*, 1992). The active site of a general lipase consists of serine, histidine, and an interchangeable glutamic acid or aspartic acid which is common to all serine hydrolases of the structural superfamily of alpha/beta-hydrolases. The serine acts as a nucleophile, histidine as the basic residue and the aspartic acid or glutamic acid as the acid residue (Joseph, Ramteke and Thomas, 2008). The active site in lipases has been found to be shielded by a mobile lid; also referred to as a nucleophilic elbow whereby the catalytic serine residue resides (Brocca *et al.*, 2003).

Lipases from the fungus *Candida rugosa* were used to identify the role of the lid domain in lipase activity. It was found that by exchanging the lids of the enzymes, there was no significant decrease in enzyme activity. However, this is the most variable region within the lipase structure that, if altered drastically, can have detrimental repercussions on enzyme activity (Brocca *et al.*, 2003). When open, the substrate can easily access the active site, whilst, when closed, the enzyme remains inactive. A substrate binding site is located inside the pocket on top of the central beta sheet. The binding site is dependent on the size and geometry of the substrate specificity (Joseph, Ramteke and Thomas, 2008).

The mode of action of lipases involves interfacial activity. This is usually conducted when a substrate with limited water solubility is used for activity. The lipase follows standard steady state kinetics until reaching the substrate molecules. Free lipase then can become adsorbed onto the substrate molecule using the nucleophilic lid as a means of attachment. This increases the activity of the lipase as the lid is no longer hindering the active site from substrate and is known as interfacial activation (Rodrigues *et al.*, 2019). The flexibility of the lid encourages greater

protection of the vulnerable active site to be shielded against unwanted reactions (Khan *et al.*, 2017).

The bacterial lipase superfamily consists of 8 families and all members have a catalytic triad of Ser-Asp-His unless otherwise specified (Table 1.2.2). Since then, alternative representation and classification of lipases have occurred which include recent work identified by Hitch and Clavel, (2019). However, the most popular and cited form of lipase classification has been utilised here (Arpigny and Jaeger, 1999). Family I, also known as the true lipases, mainly consists of lipases from *Pseudomonas* species (Yabuuchi *et al.*, 1992). These lipases were the first to be identified and generally synthesise longer chained substrates (Messaoudi *et al.*, 2010). Family II, the GDSL family, does not contain nucleophilic elbow, Gly-X-Ser-X-Gly, instead they contain a Gly- Asp-Ser-(Leu) domain with active sites at the serine residue (Akoh *et al.*, 2004). Family III contains traditional protein folding equivalent to other lipases within the alpha/beta-hydrolase family. There is also 20% amino acid sequence identity with human plasma platelet activating factor-acetylhydrolase (Angkawidjaja and Kanaya, 2006). The hormone-sensitive lipase, Family IV, has similar structural and functional characteristics as the human lipase (ØSterlund *et al.*, 1999). Family V has lipases that originate from a mesophilic nature, this is common with Family IV as well. Family VI and VII have similarities to eukaryotic lipases (Arpigny and Jaeger, 1999). Family IIX has a conserved sequence of Ser-X-X-Lys (Nishizawa *et al.*, 1995). These bacterial lipase superfamilies and example applications of these biocatalysts in industry have been summarised (Table 1.2.2).

Eukaryotic lipases can be classified into 5 subfamilies: gastric, pancreatic, hormone-sensitive hepatic and monoacylglycerol. Gly-X-Ser-X-Gly has been identified as the conserved sequence for all the members of the eukaryotic lipase family. In addition, there is a catalytic triad, Ser-Asp-His whereby the serine has been determined as the catalytic source (Winkler, D'Arcy and Hunziker, 1990; Roussel *et al.*, 1999). These properties are useful in identifying novel lipase candidates from eukaryotic sources (Table 1.2.3).

Table 1.2.2: Bacterial lipases characteristics and industrial applications

Bacterial lipases have been categorised using classifications derived from (Arpigny and Jaeger, 1999). Industrial applications of these candidates have also been outlined. Unless specified all examples operate at standard operating parameters.

Lipase Family	**Example**	**Characteristics**	**Industry application**
I – True Lipases	Subfamily 1: *Pseudomonas* Species	First to be studied (Arpigny and Jaeger, 1999) (Messaoudi *et al.*, 2010).	Isoamyl ester production using *Pseudomonas* species (Dhake, Thakare and Bhanage, 2013)
	Subfamily 2: *Burkholder* Species	First crystallised structure and generally larger in size (33 kDa). Amino acid sequence forms anti-parallel double β-strand at the surface of the molecule (Arpigny and Jaeger, 1999).	*Burkholde*r species used for biocatalytic transesterification of allylic alcohol (Brenna *et al.*, 2011)
	Subfamily 3: - *Pseudomonas fluorescens* - *Serratia marcescens*	A higher molecular mass is found in these lipases and there is an absence of an N-terminal signal peptide and of Cys residues (Arpigny and Jaeger, 1999).	*Serratia marscens* used for detergent formulation and biodiesel production (García-Silvera *et al.*, 2018)
	Subfamily 4: *Bacillus*	Conserved pentapeptide referring to nucleophilic elbow, Ala-X-Ser-X-Gly. Optimal parameters include a high pH and thermophilic tendencies (Arpigny and Jaeger, 1999).	*Bacillus thuringiensis* variety was used as a waste water treatment (Montiel, Tyagi and Valero, 2001).

	Subfamily 5: *Staphylococcal*	Structure and function similar to phospholipases (Arpigny and Jaeger, 1999).	Production of flavour esters using *Staphylococcal* derived lipases (Karra-Châabouni *et al.*, 2006)
	Subfamily 6: - *Propionibacterium acnes* - *Streptomyces cinnamoneus*	High similarities (>50%) to *Burkholder* Species. (Arpigny and Jaeger, 1999).	*Propionibacterium acnes* investigated for proinflammatory activities (McLaughlin *et al.*, 2019)
II – GDSL Family	Examples: - *Aeromonas hydrophila* - *Pseudomonas aeruginosa* - *Salmonella typhimurium* - *Photorhabdus luminescens*	Conserved motif, Gly-Asp-Ser-(Leu) with catalytic serine residue. Similar structure to the α1 subunit of the platelet-activating-factor acetylhydrolase (α1PAF-AH) from bovine brain (Arpigny and Jaeger, 1999).	Biodiesel production from *Streptomyces sp* (Cho *et al.*, 2012)
III	Examples: - *Streptomyces exfoliates* - *Streptomyces albus* - *Moraxella species*	An extracellular lipases with standard folding characteristic of other of alpha/beta-hydrolases and conserved Ser-Asp-His catalytic triad (Arpigny and Jaeger, 1999).	Antimicrobial implications of *Streptomyces albus* (Deepa *et al.*, 2012)
IV- Hormone sensitive lipases	Examples: - *Alicyclobacillus acidocaldarius* - *Pseudomona*s sp. B11-1	Similar in structure to the mammalian Hormone Sensitive lipase, and research suggest that this could have been evolved through a common ancestor. Potentially cold adapted as high activity is present at lower temperatures	*Alicyclobacillus acidocaldarius* as Biosensor for the Detection of Organophosphate Pesticide (Febbraio *et al.*, 2011).

	- *Archaeoglobus fulgidus* - *Alcaligenes eutrophus* - *Escherichia coli* - *Moraxella species* - *Psychrobacter immobilis*	(species *Moraxella species and Psychrobacter immobilis)*. Conserved sequences are HGGGF and GDSAGGXLA. (Arpigny and Jaeger, 1999).	
V	Examples - *Pseudomonas oleovorans* - *Haemophilus influenzae* - *Psychrobacter immobilis* (Cold Tolerant) - *Moraxella sp. (Cold Tolerant)* - *Acetobacter pasteurianus*	Similarity (20–25%) to bacterial non-lipolytic enzymes, epoxide hydrolases, dehalogenases and haloperoxidases. Contains structural folding in line with alpha/beta-hydrolases. Catalytic triad Ser-Asp- His exists (Arpigny and Jaeger, 1999).	Multiple applications of *Pseudomonas oleovorans* including aromatic compounds derived from lignin (Weimer *et al.*, 2020)
VI	Examples - *Synechocystis sp.* - *Spirulina platensis* - *Pseudomonas fluorescens* - *Rickettsia prowazekii* - *Chlamydia trachomatis*	Small lipase, between 23–26 kDa. Alpha/beta-hydrolase fold and Ser-Asp-His catalytic triad exists. Prefers activity towards shorter chained substrates. Human lysophospholipase shares 40% sequence similarity (Arpigny and Jaeger, 1999).	Triacylglycerol and phytyl ester synthesis in *Synechocystis* (Aizouq *et al.*, 2020)

VII	Examples - *Arthrobacter oxydans Bacillus subtilis* - *Streptomyces coelicolor*	Large lipase, (55 kDa) however efficiently hydrolyses ρ-nitrophenyl compounds (Arpigny and Jaeger, 1999).	Herbicide degradation using *Arthrobacter oxydans.* (Pohlenz *et al.*, 1992)
VIII	Examples - *Arthrobacter globiformis* - *Streptomyces chrysomallus* - *Pseudomonas fluorescens SIK W1*	Ser-X-X-Lys motif identified in the N-terminus. Conserved catalytic triad does not exist within all species of this family (Arpigny and Jaeger, 1999).	Isoamyl ester production using *Pseudomonas* species (Dhake, Thakare and Bhanage, 2013)

Table 1.2.3: Eukaryotic lipase characteristics and industrial applications

Common eukaryotic lipases have been classified alongside industrial applications (Winkler, D'Arcy and Hunziker, 1990; Roussel *et al.*, 1999).

Family	Sub-family	Characteristics	Industrial application
Lipase	Gastric	Classical catalytic triad (Ser-153, His-353, Asp-324) contains oxyanion hole (NH groups of Gln-154 and Leu-67) (Roussel *et al.*, 1999)	Lamb gastric lipase for dairy manufacturing (rennet production) (Richardson, Nelson and Farnham, 1971)
	Pancreatic	Triglyceride lipases with ser-asp-his residues for catalysis. N-terminal domain at the C-terminal edge of a doubly wound parallel β-sheet. (Winkler, D'Arcy and Hunziker, 1990).	Pancreatic enzyme replacement therapy for malabsorption in advanced pancreatic cancer (Landers, Brown and Strother, 2019)
	Hormone Sensitive	Nucleophilic elbow, G-X-S-X-G with Ser-Asp-His residues for catalysis. Examples of cold adapted lipases are found in the family, which include similarities to similar to bacterial *Moraxella* (Langin *et al.*, 1993).	Dairy, oil and fat industries (Sánchez-Carbente *et al.*, 2017)
	Hepatic	Ser-Asp-His residues for catalysis whereby serine resides in the Gly-X-Ser-X-Gly, nucleophilic elbow. Centre of the protein contains cysteine clusters. (Perret *et al.*, 2002)	Use of Hepatic lipases in lipoprotein metabolism (Connelly, 1999)

	Monoacylglycerol	Small protein, 33-kDa, with GXSXG consensus whereby Ser-asp-his residues for catalysis. (Karlsson *et al.*, 1997)	Applications of monoacyl lipases in food industry (cake manufacture) (Guy and Sahi, 2006)
Phospholipase	A1	Ser-asp-his residues for catalysis whereby serine resides in the Gly-X-Ser-X-Gly, nucleophilic elbow. Difficult to express this lipase using heterologous expression patterns (Aoki *et al.*, 2002).	Applications of porcine derived phospholipase in food manufacturing (egg development) (Guerrand, 2016)

Lipases are commonly compatible with a range of different sized and types of substrates. These include synthetic substrates such as ρ-nitrophenyl derivatives in addition to commercially available polyesters. There is a high chemo and steroselectivity with the use of lipases. This means that the secondary alcohols within the reaction orient towards the active site. For example, Cal B, a cold adapted lipase, has a high enantioselectivity towards chiral secondary alcohols (Joseph, Ramteke and Thomas, 2008). A high process stability enables the production of these lipases to be cheap and affordable (Ansorge-Schumacher and Thum, 2013).

1.3 Cold Active Enzymes

Psychrophilic biocatalysts are cold active enzymes that enable organisms to flourish in seemingly inhospitable climates. A benefit of using psychrophilic biocatalysts for the bioprocess industry is that their lower temperature requirements translate into increased economic viability and can also minimise any undesirable chemical reactions that usually occur at higher temperatures, which may include active site denaturing (Cavicchioli *et al.*, 2011). This encourages the use of cold adapted immobilised enzymes in improving green chemistry of the bioprocessing industry.

Flexible structure of cold enzymes

Cold active lipases have been found to have a more flexible structure. This is due to the polypeptide chain allowing for easier accessibility of substrates at lower temperatures. They have a very flexible structure that compensates for the low kinetic energy found in low temperature environments. A common feature of many psychrophilic biocatalysts is that there is a flexible active site which occurs through the reduced number of noncovalent interactions (Feller, 2013). An example would be the psychrophilic carbonic anhydrase (Chiuri *et al.*, 2009).

It has been determined that some psychrophilic microorganisms have over expressed RNA helicases. This enables them to unwind RNA secondary structures for translation purposes (Cartier *et al.*, 2010). Increased RNA helicase levels are thought to represent an evolved adaptive mechanism that enables protein synthesis to occur efficiently in colder temperatures (Feller, 2013).

Stability of low temperature enzymes

The stability of an enzyme can be measured by the change Gibbs free energy, ΔG, to measure the thermodynamic stability of a protein. This can be calculated using the equation, $\Delta G = -RT \ln K$; where K, a constant, can be determined at varying temperature (T) at the constant gas constant 8.31 $J.K^{-1}.mol^{-1}$ (-R) (Siddiqui and Cavicchioli, 2006). The ΔG of psychrophilic, mesophilic, and thermophilic enzymes occur at successively higher temperatures. DNA Ligase

of *Thermus scotod*uctus, a thermophile, has a ΔG of 60.4 kJmol^{-1}, whereas a cold adapted DNA ligase, of *Pseudoalteromoas haloplanktis*, has a ΔG of 27 kJmol^{-1} which determines its weak stability (Georlette *et al.*, 2003).

The hypothetical psychrophilic lipase reaction profile and a mesophilic lipase reaction profile can graphically determine Gibbs free energy change, (Figure 1.3.1). This shows that the energy required to create the same product with a psychrophilic catalyst is less than that of a mesophilic catalyst. Therefore, when optimised to work within industrial applications, the assumptions that can be made is that the amount of energy saved with a cold active enzyme would be much greater than that of a thermophilic or mesophilic biocatalyst (Feller, 2013)

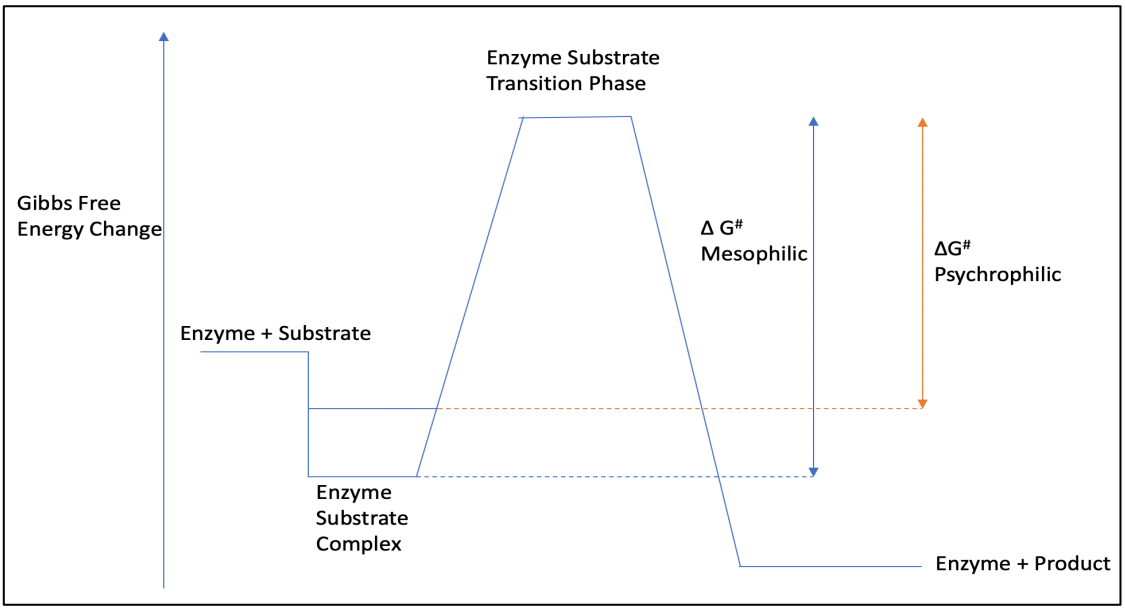

Figure 1.3.1: Energy reaction profiles of mesophilic and psychrophilic enzymes

It has been established here that psychrophilic candidates require less energy to reach the same enzyme substrate phase in comparison to mesophilic candidates. Adapted from (Feller, 2013).

Model Lipase Biocatalyst*: Candida antarctica* Lipase B

Psychrophilic biocatalysts are cold active enzymes that are frequently identified in organisms inhabiting low temperature environments, highly active below 30 °C (D'Amico *et al.*, 2003; Feller and Gerday, 2003) and are defined as having optimal temperature for growth at about 15 °C or lower (Lee, Jang and Chung, 2017).

Candida antarctica Lipase B (Cal B) is a highly optimised lipase used extensively throughout the biotechnology industry. Cal B, originally found from an Antarctic based yeast, is one of the few psychrophilic lipase candidates used for commercial synthesis in processes ranging from the synthesis of scented compounds, (Kundys *et al.*, 2018), to immobilised Cal B used for the synthesis of medicinal intermediates (Truppo and Hughes, 2011).

Cal B is a 33 kDa lipase consisting of the conserved catalytic triad, Ser-105, His-224 and Asp-187. Interestingly, the lipase does not contain the conserved nucleophilic elbow pentapeptide, GXSXG, however, it contains a TWSQG sequence. Initial crystallography analysis suggests that the protein remains in an open state with the lipase remaining closed or open, which could be due to a very small, if present, lid domain (Uppenberg *et al.*, 1995) (Figure 1.3.2). This lipase cannot be able to undertake the standard interfacial activation phenomena. The lack of nucleophilic lid present within the lipase suggests that there is no hinderance towards activating with substrate molecules found within the reaction mix as is the case with traditional lid bearing lipases (Stauch, Fisher and Cianci, 2015). Cal B has also shown to have a wide span of activity throughout different temperature conditions, from 20 °C to 50 °C (Ganjalikhany *et al.*, 2012; Siódmiak *et al.*, 2020). Thus, providing an efficient biocatalyst for industrial applications.

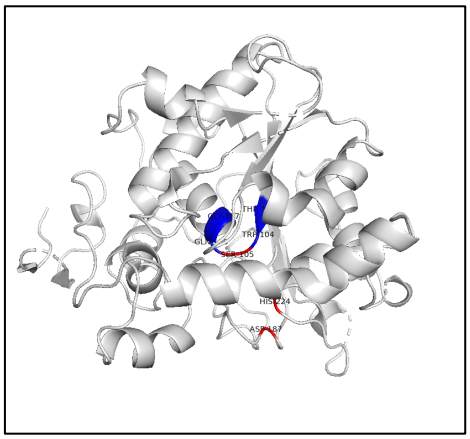

Figure 1.3.2: Three dimensional model of *Candida antarctica* Lipase B

Red regions indicate the catalytic triad, and blue indicate the hypothesised pentapeptide.

Image generated on PyMOL using PDB reference: 1TCA.

Cal B has high thermostability, remaining active up to 60 °C (Lee, Jang and Chung, 2017). Using directed evolution, it was found to have improved resistance towards thermal inactivation. For example, a mutant Cal B displayed an increase in K_{cat}, the number of substrate molecule each enzyme site converts to product per unit time, from 84 min^{-1} to 1900 min^{-1} (Zhang *et al.*, 2003).

1.4 Sourcing Cold Active Enzymes

Marine environments present temperatures between 2°C to 4°C below 1000 meters sea level (Pesant *et al.*, 2015). These regions host a vast cornucopia of unresearched organisms for the mining of low temperature biocatalysts. In this work, two sources of cold-active enzymes were explored: The metagenomic data gathered from the *Tara* Oceans expeditions, and the genomic information from an Antarctic eukaryote, *Salpa thompsoni.*

Extreme Microbiome Project – *Tara* Ocean Metagenome

The *Tara* Ocean expedition was set out with similar concepts as the H.M.S Beagle and its voyage with the great Charles Darwin, in mind. The expedition began in 2009 and ended in 2013 and sampled 210 ecosystems in 20 geographic locations from which 35,000 samples were collected. The samples were of both seawater and plankton (Pesant *et al.*, 2015). The *Tara* Ocean expedition aimed to enable a greater access to validated data sets. Access is available to all the data collections whether in nucleotides or environmental data. This is available from the European Nucleotide Archive or the PANGAEA open access library (Gimmler *et al.*, 2016). Processed genomic data can be found through the online database of samples collected through this project (Pesant *et al.*, 2015) which enables the identification of novel cold adapted lipases.

The area of interest for this work was identified as, the Southern Ocean due to its proximity to the Antarctic as well as its similarity to the locations where the salp environmental samples were taken. Sampling site 085 occurs off the remote Antarctic Coastline, (coordinates: -62.2231N, -49.2139E) and was sampled on the 6th of January 2011 during the *Tara* Ocean expedition. Each sample site has three readings, corresponding to three different ocean levels, the deep chlorophyll layer, the surface and the mesopelagic zones (Pesant *et al.*, 2015). The deep chlorophyll maxima layer was investigated due to the presence of algal blooms in this region, and therefore, potentially also the presence of digestive enzymes. Associated identifiers for the material are saline water (ENVO:00002010) and marine biome (ENVO:00000447). This material was size-fractionated (0.22-3 micrometres), preserved on board with RNA-Later, and stored in liquid nitrogen for later detection of prokaryote nucleic acid sequences by pyrosequencing methods, and for later metagenomics/transcriptomics analysis (Gimmler *et al.*, 2016).

The metagenomic sequence data for *Tara* Ocean sample 085 was unannotated. Therefore, to mine these unannotated sequences for genes of interest a conserved protein motif was used as a reference point for enzyme discovery. This motif was identified through the background literature research on lipases, for which the conserved motifs are listed (Tables 1.1.1 and 1.1.2). Once a conserved lipase motif was identified in the 085 sequence data, the DNA surrounding this was further characterised using bioinformatic software to identify the full gene sequence.

Figure 1.4.1: Map of the Southern Ocean

Sampling sites from the *Tara* Ocean project and salp events are highlighted in red.

Tara Ocean sample site 085 is located at -49.3, -62.14 coordinates, the two salp events are at E20 coordinates -55.5, -53.3 and E242 coordinates -60.5, -61.3

Whole organisms – the *Salpa thompsoni*

Salpa thompsoni, is a species of salp commonly found in the Southern Ocean surrounding Antarctica. *S. thompsoni* adults are barrel shaped, up to 10 centimetres long, and feed by a tangential flow filtration mechanism, capturing algal cells and other food particles on a fine mucous mesh at a low velocity. Thus, being regarded with one the most efficient filter feeders in the ocean (Sutherland, Madin and Stocker, 2010). It is a tunicate which is a sister lineage of vertebrates (Bourlat *et al.*, 2006), and as such, is an important resource for studying the evolution of developmental mechanisms (Racioppi *et al.*, 2017).

Current research includes the important role of salps in the carbon cycle, and this gives rise to its importance to environmental scientists. The difficult-to-process algae that salps consume is repackaged in their faecal matter as carbon which then sinks to the bottom of the ocean and that has been estimated to contribute highly to the removal of carbon from the surface (Stone and Steinberg, 2016). The contribution of salps to this 'biological carbon pump' makes them very interesting to both the ecologists and biochemical engineers. Due to the broad range of food particles salps filter out of the ocean, it seems reasonable to assume that they might express a range of digestive enzymes within the gut, with the key enzyme of interest to this study being the fatty acid digesting lipase (Zeldis and Décima, 2020). The pancreatic lipases are one of the main digestive enzymes used to break down dietary fats molecules in animals (Zhu *et al.*, 2021).

Salps have a unique reproduction mechanism as they can sexually and asexually reproduce. Fertilized eggs produce oozoid. (Figure 1.4.2) and are generally found as a solitary variety and produce clones, known as asexually reproduced blastozooids, through budding (Goodall-Copestake, 2014). These chained salps grow into long strings that live in social harmony communicating via electrical signals. Salps can use this to synchronise their swimming and move swiftly through sea currents (Käse and Geuer, 2018) to reproduce forming further oozoid (Goodall-Copestake, 2014).

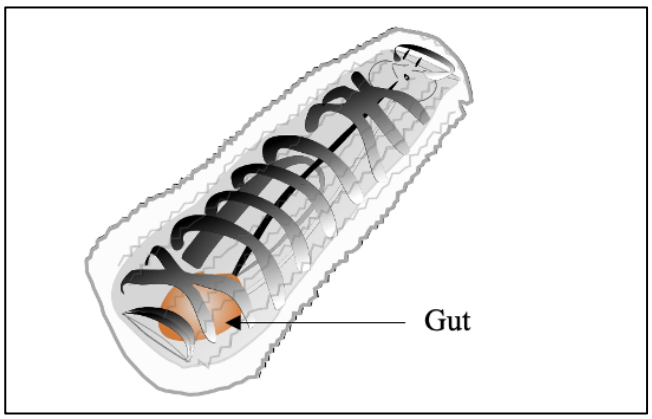

Figure 1.4.2: Diagramatic representation of *Salpa thompsoni*

Single salp, an oozoid, with highlighted digestive gut (orange)

The *Salpa thompsoni* mapped genome was used to identify novel cold temperate lipases. Currently two versions of the genome are available, a unannotated draft assembly (Jue *et al.*, 2016) and unannotated assembly of expressed gene sequence data from 48 separate salp sequence datasets (Batta-Lona *et al.*, 2017). The expressed gene sequence data provides the most appropriate resource for identifying lipase candidates. However, the unannotated nature of these sequences required the annotated *C. intestinalis* genome to guide bioprospecting attempts at identifying enzyme candidates.

Further salp gene sequence data was obtained from sequence read archive; AC_e20 and AC_e242, accession numbers SRX13276964 and SRX13276963, respectively. This data corresponds to cDNA sample of the salp gut generated for PhD thesis (Cotton, 2021). The dataset was generated from salp samples from the event 20 and 242 during the British Antarctic Survey (BAS) cruise JR26. The event took place in the South Atlantic Ocean and Drakes Passage respectively (coordinates -55.5, -53.3 and -60.5, -61.3) in December 1997, (Figure 1.4.1). These samples were preserved at -80°C. Further analysis took place for RNA extraction from the salp gut; where it is believed that many digestive enzymes occur (Bone, Carre and Ryan, 2000) (Figure 1.3.2). The purified gut mRNA was sequenced using Illumina Truseq Stranded Total RNA Kit at the University of Bristol. Quality analysis took place using GeneiousPrime version 2021.1 (https://www.geneious.com) (Kearse et al., 2012) These databases containing sequenced *S. thompsoni* mRNA were used to corroborate identified genes of interest.

1.5 Stability and Activity of Immobilised Lipases

Enzyme immobilisation is a strategy to increase reusability of biocatalysts (Zhang, Yuwen and Peng, 2013), as well as means of overcoming substrate or product inhibition and offers a mechanism for continuous production (Basso and Serban, 2019). The activity of an enzyme usually declines due to inhibition either by medium or products; this effect is reduced by immobilisation (Almeida *et al.*, 2021).

Immobilised enzymatic structures have two distinct roles, which are comprised of their catalytic activity and their non-catalytic functions (Liu and Dong, 2020). Catalytic activity, which are integral in the function of the biocatalyst by decreasing the activation energy usually present in free enzyme reactions. This in turn can save the amount of time and energy required to generate a product (Boudrant, Woodley and Fernandez-Lafuente, 2020). Whereas the non-catalytic functions can include the physical and chemical structure of the surface where the enzyme will be immobilised. This includes the shape, size, spacer arms and other chemical modifications which are required to enable adherence to the immobilisation surface (Liu and Dong, 2020).

Immobilisation strategies

There are a wide range of techniques employed that enable different types of immobilisations to take place. This includes covalent, affinity and ionic immobilisation. The different types of immobilisations each have their advantages and disadvantages that have been summarised in Table 1.5.1.

Table 1.5.1: Advantages and disadvantages of common immobilisation techniques

Affinity, Covalent and Ionic methods have been evaluated from (Ansorge-Schumacher and Thum, 2013; Franssen *et al.*, 2013; Redeker *et al.*, 2013)

Immobilisation Techniques	Advantages	Disadvantages
Affinity	Reversible	Stability is unreliable
		Storage
Covalent	Minimize steric hindrance	Protein denaturation during coupling reactions
	Improve binding efficiency	Irreversible
	Greater mobility	
	Controlled protein orientation	
Ionic	Commercialised immobilised lipase (Novozyme 435)	Weak unstable bonds
		Leaching

There are many factors that influence the performance of immobilised enzymes. The effect on enzyme activity post immobilisation should be taken into consideration. Different immobilisation matrixes play a part in the role of enzyme recovery and the biocompatibility of enzyme candidates. Here some commonly utilised immobilisation matrixes have been summarised and the role they play in the domain of immobilised enzymes.

Table 1.5.2: Example immobilisation matrices and their properties

Popular immobilisation matrixes and example applications have been discussed.

Immobilisation Matrix	Properties	Application
Electrospun nanofiber	Chemically functionalised cellulose nanofiber membranes (CNF) provide a covalent based technique for immobilisation. The biocompatibility of this material ensures sufficient lifecycle assessment. The addition of the enzyme onto the surface, requires the need of a chemical coupling agent. These enable a greater improvement in the binding efficiency, provide a greater mobility and minimize steric hindrance (Park *et al.*, 2012).	Chemically generated linkers have been optimised for *Candida rugosa* immobilisation studies, Huang et al., has used $NaIO_4$ to generate aldehyde chemical linkers. Average diameter 200nm (Huang *et al.*, 2011).
Foams	Polyurethane based foams provide a covalent form of immobilisation. External mass transfer and substrate diffusion limitations (Kamble, Shinde and Yadav, 2016)	Kinetic resolution of (R, S)-α-tetralol catalysed by crosslinked Cal B enzyme supported on mesocellular foam. Average size spherical 40 nm sized mesocellular pores connected by 5–20 nm sized mesoporous windows (Kamble, Shinde and Yadav, 2016)
Gels	Generally used for entrapment style immobilisation. Flexibility of the matrix is limited and has produced fewer active biocatalysts as with other method. Generally used as a whole cell system than	Lipases from *Burkholderia cepacia* and *Candida antarctica* were entrapped in silica aerogels. Average pore size of 10 nm (Sheldon and van Pelt, 2013)

	free enzyme (Ansorge-Schumacher and Thum, 2013).	
Monoliths	Monolith structures usually have porous channels increasing convective mass transfer for operations at high flowrates (Hardick *et al.*, 2013). High storage and thermal properties were also obtained using this system (Cheng *et al.*, 2019).	*Candida antarctica* lipase was trapped in the pores of silica monoliths to hydrolyse synthetic substrate ρ-nitrophenyl butyrate. Average pore size of 9 to 16 nm (Alotaibi *et al.*, 2018)
Nanoparticles	Nanoparticles provide a high surface to volume ratio with increased binding capacity. Covalent structures provide highly specific binding patterns and prevent enzyme contaminations (Ansari and Husain, 2012).	Silicone and iron based materials are more common (Zdarta *et al.*, 2018). Fe3O4 magnetic nanoparticles, covalent immobilisation with carbodiimide interactions using *Candida rugosa* for the hydrolysation of p nitrophneyl compounds. Mean diameter was 12.8 nm (Huang, Liao and Chen, 2003).
Porous Beads	Ion exchange based resin is a commercial favourite and used for the immobilisation of multiple candidates. Weaker interaction which may cause enzyme leakage. Mass transfer limitation and protein loading capacities are also affected (Dods *et al.*, 2015).	*Candida antarctica* lipase B, immobilised in Lewatit VP OC 1600, a macro-porous resin with a hydrophobic surface. The average particle size of 315–1000 μm (SÁ *et al.*, 2017).

Immobilisation strategy

Chemically functionalised electrospun cellulose nanofiber membranes (CNF) are a novel porous membrane adsorbent that is an alternative to current chromatography media, such as monoliths (Hardick *et al.*, 2015). These membranes are produced by electrospinning regenerated cellulose to generate fibres material with very small porous diameters; between 10 to 100s of nanometres (Feng *et al.*, 2014). The biocompatibility and biodegradability of cellulose fibres provides an alternative to current industry applications for immobilisation (Menkhaus *et al.*, 2010) The enzyme immobilisation field has had a multitude of new developments that encourage the concept of the use of CNF as a suitable support for enzyme immobilisation. The Cellulose nanofiber (CNF) used in this project were supplied by Cytiva Ltd.

The cellulose structure of these membranes provides the material to be generated for all types of immobilisations methods (Rather *et al.*, 2022). The ability for these membranes to be chemically functionalised provide a covalent based technique for immobilisation. The sturdy nature of covalent bonds minimises enzyme leakage from the support into the medium. This attributes to the stability of the biocatalyst system as there is no barrier between the localisation of the enzyme onto the support (Park *et al.*, 2012). Reactive groups between the membrane and the enzyme are summarised, (Table 1.5.3).

Table 1.5.3: Reactive groups between the membrane and the enzyme

Sites of reaction on the solid support, the chemical coupling mechanism, followed by the interaction with the reactive group on the enzyme. Adapted from (Sulaiman *et al.*, 2014)

Reactive group on the Solid Support	Chemical Coupling mechanism	Reactive group on the Enzyme
-NH2	Carbodiimide	-COOH
-SH	Cysteine	-SH
-OH	Cyanogen Bromide	-NH2

Factors influencing immobilisation

Site Specific Covalent Immobilisation

Site specific immobilisation requires a known chemical group or sequence introduced in the protein at the site-specific location, (Figure 1.5.4). This leads to chemical coupling mechanisms; also known as a spacer arm or a ligand. Spacer arm or a ligand is a known method of tethering an enzyme to immobilise it onto a surface, (Table 1.5.3). This known chemical group must be biorthogonal whereby the chemical group does not appear or react with any of the known amino acid residues within the active site, (Figure 1.5.4B). Site directed immobilisation techniques enable a more controllable and homogeneous protein orientation which can be highly advantageous for sensitivity and reproducibility of assays (Redeker *et al.*, 2013).

Amino acids found on the outside of the enzyme are used as the key interaction point for immobilising the enzyme. These functional groups are usually found to be amine, in lysine residues, or carboxyl, in aspartic acid or glutamic acid amino acids, (Figure 1.5.4A). Thiol groups, found in cysteine, are also frequently used as an immobilisation functional group (Foley *et al.*, 2007).

Non-Specific Covalent Immobilisation

Non-specific covalent immobilisation involves covalent bonding of two mutually reactive chemical groups on the protein and the substrate surface, (Table 1.5.3). The reaction must be able to be performed under physiological conditions, such as a neutral pH and aqueous buffers, to avoid protein denaturation during coupling reactions. There are a few naturally occurring functional groups found in amino acids that are used for covalent immobilisation. These include amines and thiols, which are good nucleophiles, and carboxylic acid groups which are reactive towards these nucleophiles, (Figure 1.5.4A and Figure 1.5.4B). As the covalent coupling reactions are not unique to the protein, multiple protein orientations can occur at the substrate surface which can cause hard to predict protein orientations that can reduce enzyme activity (Redeker *et al.*, 2013).

Porous support materials are a favourable approach to covalent immobilisation. The open structure provides a larger surface area making it beneficial for bioprocessing production. One promising application of covalent porous structures in the biorenewables field. For example, carbon molecules were modified with ethylene diamine which the lipase of *Pseudomonas gessardi* was immobilised. This was used for the hydrolysis of olive oil. Sixty-five percent of its original activity after 50 cycles was publicised to demonstrate the stability of the immobilised lipase (Franssen *et al.*, 2013).

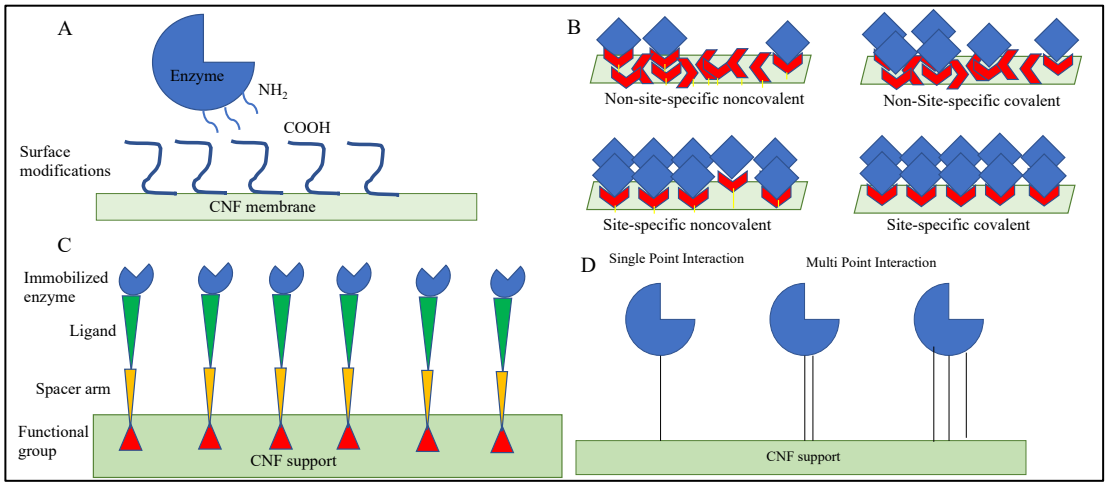

Figure 1.5.4: Immobilisation mechanisms

Covalent enzyme immobilisation between the amide bond formed by carboxyl and amine groups (A), Non-site and site-specific enzyme bonding (B) immobilised enzyme on a CNF support using a chemical coupling mechanism (C), Comparison of single point or multipoint interaction mechanism on a CNF membrane (D)

Adapted from (Redeker *et al.*, 2013; Jia, Narasimhan and Mallapragada, 2014; Sulaiman *et al.*, 2014)

Immobilised enzymes can form single or multipoint interactions dependent on the functional groups surrounding them, (Figure 1.5.4D). Single point enables flexibility and easy access to the functional group. However, they are not as strong when comparing to multipoint interactions. Multipoint interactions enable rigidity; however, they can prevent interactions such as protein extraction. Generally, multipoint interactions include the use of a spacer arm and a ligand (Sulaiman *et al.*, 2014). Multipoint immobilisation should have a large internal surface area to support the strength of the interaction. The reactive groups involved in the immobilisation should be stable to ensure a long-term immobilisation (Mateo, Palomo, *et al.*, 2007).

The use of epoxy groups as an example of multipoint covalent attachment has been deemed successful. Epoxy groups have also been found to increase the stability of the proteins when combined with multipoint attachment (Ismail and Baek, 2020). They have short spacer arms that enable reactions with nucleophilic groups found on the protein surface, such as lysine (Foley *et al.*, 2007).

Advantages of CNF

Cellulose nanofiber can easily be manipulated through the incorporation of functional groups to tailor them for different applications. Using a high surface area of nano sized support provides a high number of immobilised enzymes producing efficient processes (Ismail and Baek, 2020). The even flow distribution and fouling resistance properties of CNF make it an ideal support to maximise the potential of immobilised enzymes (Jia, Narasimhan and Mallapragada, 2014). Nanofiber adsorbents have shown an increase in purification productivity due to their larger surface areas due to their electrospun nature (Hardick et al., 2013). In addition, they offer the ability to be customised by shapes (to scale up in volume) as well as reduce as mass transfer and pressure drop limitations that may occur with beaded alternatives, such as Immobead (Dods *et al.*, 2015).

Table 1.5.5: Advantages of CNF when used for enzyme immobilisation

Factors that encourage advantageous enzyme immobilisation on CNF have been outlined. Adapted from (Sulaiman *et al.*, 2014)

Factors	Advantages
Surface area to volume ratio	It provides a high surface area to volume ratio for enzyme interaction.
Functional groups	CNF can possess a range of surface functional groups; therefore, increasing the types of enzyme interactions
Flow rate	It behaves stably when monodispersed in aqueous suspension
Mass transfer effects	High surface area of CNF support provides increased enzymatic activity and stability
Easily recovery	The enzyme is easily recovered from reaction media in comparison to freely suspended enzymes
Design of enzymatic bioreactor	CNF have high flexibility; they can be easily prepared as membrane

Disadvantages of CNF

Disadvantages of CNF include a chance of crosslinking unless the site specific modulations of the immobilised enzymes are known (Jonkheijm *et al.*, 2008). In addition, unless amino acid residues that will be adhering to the chemically treated nanofiber is located at a distance from the active site, there is a chance that the enzyme will bind to the membrane causing a decrease in activity and stability (Sulaiman *et al.*, 2014). This form of immobilisation may require the use of toxic chemicals as an immobilisation blocking step or at membrane generation stages, which may lead to enzyme inactivation (Cao, 2006; Mateo, Grazu, *et al.*, 2007).

The trade-off between the cost of immobilisation and single use of biocatalyst must be ascertained to determine the stability and activity of biocatalysts. Physical attempts to optimise the membrane can be made by comparing enzyme density and assessing the use of multipoint enzymatic interactions. Biological modifications can also include modulating enzymes to contain more chemical coupling mechanisms, such as cysteine residues for thiol bonds, to compare attachment to the membranes. These modifications can determine the assessment of the rate of enzyme recovery and the lifetime recycle rate (Nair *et al.*, 2007).

1.6 Applications of Immobilised Lipase Biocatalysts

The highly applicable nature of lipases provides it to be a model biocatalyst for the synthesises of multitude different reactions. These biological catalysts have a wide range of substrate specificity enabling them to be a high value enzyme in the field of biochemical engineering.

The low temperature optimal activity of cold active lipases provides a low energy alternative in industrial applications. Lipases have been commercially optimised for laundry detergents for many years as their ability to withstand detergents and their thermostable nature encourage its use in a nontoxic system (Cherif *et al.*, 2011). One of the first lipases optimised for commercial use are two bacterial candidates called, 'Lumafast' from *Pseudomonas mendocina* and 'Lipomax' from *P. alcaligenes by* Genencor Limited. These lipases were recombinantly produced to mass scale due to their ability to operate at cooler temperatures and stability in harsher chemical environments (Kavitha, 2016; Sahay and Chouhan, 2018). High value compounds have been produced using lipase biocatalysts. *Geotricum candidum* lipase is used in the presence of toluene to produce key phosphonic acid intermediate and diethyl ester in the synthesis pathway of squalene synthase inhibitor, an anti-cholesterol drug at lower temperatures of 27°C (Patel, Banerjee and Szarka, 1997; Jiang *et al.*, 2014; Mhetras, Mapare and Gokhale, 2021). This provides a method to decrease operating costs and provide a useful alternative to current bioprocessing standards.

Immobilised enzymes have been using cellulose based matrixes for innovative applications. Commercially available cellulose membrane marketed as the Sartobind Cellulose Membrane has been utilised for immobilised lipases; for example, *Candida rugero*so lipase has been successfully immobilised using aldehyde groups as the coupling mechanism. The immobilised system was successfully reused 8 times before the activity declined to 30% of its original value (Huang *et al.*, 2011). The activity and stability of the enzyme was significantly higher than that of its free source. Thus, making it a suitable method of immobilisation.

Lipases have been used in the fat and oils industry in hydrolysis, esterification and interesterification reactions. These include the modification of inexpensive lipids, such as olive oil, into higher value compounds such as biodiesel. (Sharma, Chisti and Banerjee, 2001).

Immobilised lipases have also been used in transesterification reactions within the same industry. Immobilised *Rhizomucor miehei* lipases have been used to replace the palmitic acid in palm oil with stearic acid (Sharma, Chisti and Banerjee, 2001). Steric acid is known as a 'healthy acid' as it reduces the bad cholesterol in the body (Grande, Anderson and Keys, 1970).

Novozyme 435 was one of the first commercially available lipases. *Candida antarctica* lipase B has been immobilised using ionic interactions. This immobilised system has been used in a range of different applications which include the production of high value compounds, such a esters (Ortiz *et al.*, 2019). However, due to the method of immobilisation there is a high risk in enzyme leaching. At higher temperatures it has been reported that the enzyme detaches from the immobilisation surface (De Souza *et al.*, 2017). Therefore, covalent immobilisation of lipases, including the use of spacer arms, are a more suitable method for the stabilisation of these cold tolerant lipases. The rate of enzyme recovery and the lifetime recycle rate must be high for immobilised enzymes to be cost beneficial (Nair *et al.*, 2007). The use of immobilised lipases may provide an alternative method to current methods of polyurethane degradation.

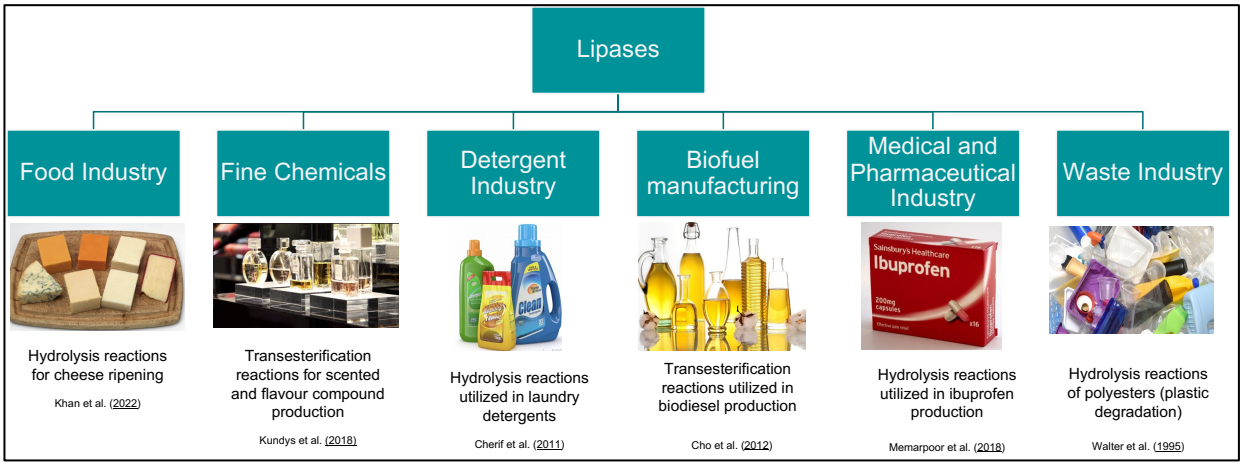

Figure 1.6: Broad range of lipase derived applications

1.7 Aims and Objectives

The overall aim for this project is to identify novel cold active enzyme candidates to investigate improved stability and activity whilst immobilised as an application for the biotechnology industry. Immobilisation of low temperature lipases can be highly beneficial for flow based production systems with reduced energy costs. Here five objectives were identified to accomplish this goal. These objectives and the experimental plan conducted are summarised in Figure 1.7.

Objectives

1. Identification of novel psychrophilic lipase candidates

The discovery of these cold active lipase candidates will be conducted using mining techniques from two datasets, the metagenomic resource *Tara* Oceans project, and the whole organism genome from *Salpa thompsoni*. The selected lipase candidates will then be characterised for cold properties using *in silico* bioinformatics techniques to identify cold activity.

2. Recombinant expression and purification

The production of these candidates for further applications requires a robust and optimised expression system therefore *E. coli* based fermentation is preferred. Successful expression parameters will be optimised for scale up techniques followed by affinity based nickel purification methods.

3. Characterising lipase activity

The cold activity of the lipase candidates will be established using a plate based assay in an *in vitro* form. This will be used to determine protein characteristics such as substrate affinity and pH determinations and thus its kinetic potentials for subsequent applications.

4. Investigating stability and activity of the lipases using immobilisation techniques

Lipase immobilisation will take place using chemically activated cellulose nanofiber membranes, provided by Cytiva Ltd. Here physical and biological modifications will be considered for the improvement of stability and activity of the biocatalyst. Physical modifications will be determined by modifications of lipase density and effects on the stability and activity of the enzyme. Biological modifications to the lipase will also be trialled, this includes the use of cysteine tags adhered to the protein to lipase stability and activity

5. Examine a model system for the application of these immobilised lipases

Applying the cold active lipases candidates to a model application will be trialled by assessing the plastic degradation capabilities of these enzymes. A flow based immobilised system will be issued to optimise plastic degradation.

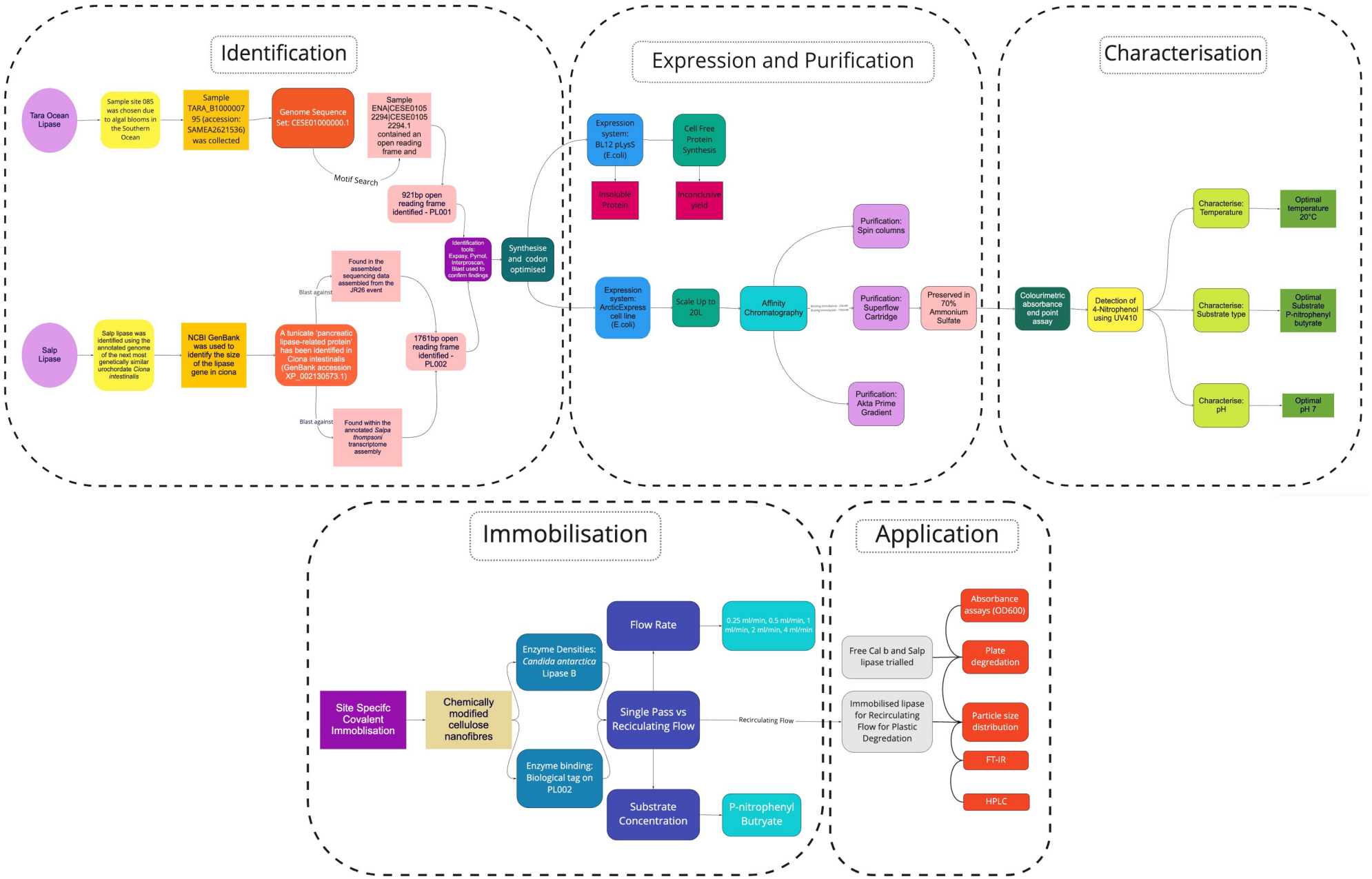

Figure 1.7: Flow chart of experimental stages in relation to key objectives

Chapter 2: Identifying Novel Lipase Candidates for Recombinant Expression

2.1 Introduction

Low temperature enzymes can be mined from, by volume, the most abundantly cold marine environments. For this study, organisms from the polar waters surrounding the Antarctic were targeted as a potential source for psychrophilic lipases. The temperatures in these waters remain below 5°C all year around (Feller, 2013), thus well below the 30°C optimum activity range of what are considered as psychrophilic enzymes (D'Amico *et al.*, 2002).

Genomic DNA or expressed gene (RNA) sequences isolated from candidate organisms of interest represent valuable resources from which to develop novel enzyme products. These sequences can be derived in-house using purification techniques followed by gene sequencing as described for the *Salpa thompsoni* (salp) gut RNA in the introduction (Jue *et al.*, 2016; Batta-Lona *et al.*, 2017). However, such de novo generation of data may not always be necessary as there is an ever-increasing archive of publicly available genomic sequences that can be mined for enzyme candidates, collectively known as the International Nucleotide Sequence Database (INSDC). INSDC houses nucleotide sequence data from collaborations with the European Nucleotide Archive (ENA) at the European Molecular Biology Laboratory's European Bioinformatics Institute (EMBL-EBI) in Hinxton, UK; and GenBank at National Centre for Biotechnology Information (NCBI) for over 30 years (Arita *et al.*, 2021). Lipases have previously been mined from these resources. These include the cold-active Lip1 lipase from the Antarctic bacterium *Pseudoalteromonas haloplanktis* (de Pascale *et al.*, 2008) that was isolated from genomic DNA sequence data, and a lipase candidate from *Rhizopus microsporus* that was identified from expressed gene 'transcriptomic' data (Xiang *et al.*, 2021). The mining of existing genomic resources, such as alignments can be used to propose a new family of bacterial lipase (Kim *et al.*, 2009), suggest the scope for undiscovered enzymes from expensive samples ready for metagenomic mining.

In silico enzyme discovery lies in favour of obtaining lipase catalysts due to their ability to catalyse multiple reactions. It was identified that over 84% of enzymes discovered between

January 2014 and March 2017 belong to either the lipase/esterase or cellulase/hemicellulose classes. A further 82% were discovered by activity-based screening. This provides a thorough understanding of obtaining enzymatic candidates from this class as multiple templates of prior discovery are available (Berini *et al.*, 2017; Robinson, Piel and Sunagawa, 2021).

Publicly available genomic resources were mined for identifying lipase candidates, more specifically those located in the polar regions surrounding the Antarctic. A microbial genomic resource was targeted to identify bacterial candidates, this is the *Tara* Ocean Database. And another from a zooplankton that feeds on this microbial lipase, the *Salpa thompsoni* genome. The *Tara* Ocean expedition identified, samples site 085 due to proximity to the Antarctic. This was of interest due to the potential of algal grazers and therefore the existence of digestive enzymes. Protist grazers within subsurface chlorophyll maxima and deep chlorophyll maxima regions of the Ocean and mesozooplankton predators have been identified to migrate here (Moeller *et al.*, 2019). *Salpa thompsoni* are interesting marine invertebrates and their ability to perform metabolic digestive activity at cold temperatures makes them a valuable organism for the harvesting of cold active lipases. The ability to digest nonselective long chain fatty acid diatoms presents evidence that lipase genes are expressed (von Harbou *et al.*, 2011). Location of the sampling sites are presented in Figure 1.4.1, Chapter 1.

The search for these cold active lipases was carried out with two different strategies. The *Tara* Ocean lipase and the salp lipase are subsequently referred to as PL001 and PL002 respectively. PL001 was identified using the bioinformatic technique of motif searching. This involves identifying amino acid sequence motifs for the gene of interest and using this to screen *Tara* Ocean sequence data from target genomes for matches. Lipases possess the highly conserved, GXSXG and SDH feature of the alpha/beta hydrolases family which encourages the mining for putative lipase candidates in genomic datasets (Ollis *et al.*, 1992). It can be deduced that these residues would be identifiers in psychrophilic candidates. The serine residue, bound within the glycopeptide, is a conserved amino acid that is required for catalytic activity, as demonstrated in *Candida antarctica* lipase B (Pleiss, Fischer and Schmid, 1998). Further characteristic sequence motifs have been used to identify enzymes (Table 1.2.2 and 1.2.3 from Chapter 1). The sequences generated from the water samples of the *Tara* Ocean voyage were assembled DNA shotgun sequencing reads used to reconstruct microbial community genomes. Genes were predicted on these "contigs" (Sunagawa *et al.*, 2015). Therefore, to fully identify these genes further investigation using NCBI's conserved domain database to detect the

presence of protein domains is required. This method has been utilised to identify other enzyme candidates in scientific literature, (Zarafeta *et al.*, 2016). The salp lipase, PL002, was identified using annotated transcriptomic *Salpa thompsoni* resources available on GenBank. Searching annotated DNA sequence archive meta-data for names of candidate enzymes provide a direct method for identifying genes of interest. However, in the instance that this is not available, target gene sequences can be obtained from annotated genomes of related species. These can be used as a template to screen the assembled genome to identify genes of interest.

Sequence level verification is required to confirm the presence of lipase candidates. Computational approaches to define cold activity can reveal structural adaptations of proteins for their function (Åqvist, Isaksen and Brandsdal, 2017). Conserved amino acids can be used to determine the cold activeness of the genes. Glycine residue analysis has been conducted as small side chains of this amino acid residue encourage greater local mobility. This has been verified in multiple enzymatic sequences (Mavromatis *et al.*, 2002; Siddiqui and Cavicchioli, 2006; Veno *et al.*, 2019). There are numerous features that separate psychrophilic lipases from mesophilic and thermophilic adapted candidates. Firstly, there is an increased quantity of hydrophobic groups on the protein surface and an increased sum of hydrophilic groups within protein cavities that contributes towards confirmational stability and ionic reactions (Metpally and Reddy, 2009). Lysine residues for cold adaptations has been demonstrated by the increase in lysine to arginine amino acid residues (Siddiqui *et al.*, 2006). Lysine distribution on the protein surface increase hydrophilicity and provides mesophilic tendencies of modified proteins (Ahmad *et al.*, 2020).

Amino acid content can also be an indicator for identifying cold protein stability. A lower content of proline residues, of up to 40%, are found in the loops of the structure than in the alpha helices (Kulakova *et al.*, 2004). It was also found that there was a reduced number of salt bridges, aromatic/aromatic interactions and disulphide bridges (Cavicchioli *et al.*, 2011) which are the key molecular structures found within psychrophilic biocatalysts. In cold adapted enzymes, the catalytic amino acids are further buried within the structure. The Van der Waals forces are distance related and are weaker and shorter in range. The enzyme could be destabilised due to the increased movement between the internal molecular groups (Saunders *et al.*, 2003). Therefore, amino acids with an ability to pack closer are key to increased activity and stability of cold proteins.

Recombinant expression is a suitable method for the bulk production of cold active lipase candidates for the use in biotechnology. Methods to optimise the production of these biocatalysts include *in vitro* gene production either through cloning procedures or direct synthesis into expression vectors. Gene sequences can also be modified in this appraoch to include biological tags, such as 6xHis tag, for useful downstream processing including purification by affinity chromatography. It is more advantageous than the extraction of the whole organism whereby bulk expression is limited. Cloning lipases requires a template RNA of the lipase source and primer design of the gene sequence. This is then followed by RT-PCR and molecular transformation to expression into host cells (Robinson, Piel and Sunagawa, 2021). However, synthesis of novel genes is an alternative. Here, genes of interest are synthesised in expression vectors of interest by an external provider, and this provides some flexibility towards modifications such as codon optimisation to encourage protein expression. This occurs by reducing codon usage limitations that can occur to increase successful bacterial expression. This was important as the origins of the *Tara Oceans* lipase is unknown, and the eukaryotic nature of the salp may cause tRNA abundance differences between the lipase origin and the host cell interactions (Welch *et al.*, 2009). Example lipases have been sourced using a similar approach, (Tian *et al.*, 2015; Sander *et al.*, 2021).

In this chapter, two identification processes to obtain putative cold temperature lipase gene candidates from a *Tara Ocean*, a bacterial source, PL001, and the *Salpa thompsoni* genome, a eukaryotic source, PL002, are contrasted. Modifications made to the sequences, including codon optimisation and addition of histidine tags, prior to commercial synthesis, have been described. Here *in silico* attempts are made to characterise the cold temperature nature of the lipase candidates and derive full length lipase genes for expression and purification purposes.

2.2 Methods and Materials

Identification of PL001, *Tara Ocean* lipase

The Tara Oceans sample site was selected as 085. The sample TARA_B100000795 (accession:SAMEA2621536)(https://www.ebi.ac.uk/ena/browser/view/SAMEA2621536). These reads, when sequenced, provided a collection of short reads that were used to determine the marine metagenome genome assembly, Whole Genome Shotgun sequence set, (accession: CESE01000000) containing assembly contigs from CESE01000001-CESE01277195. This assembly was downloaded as a FASTA file onto in the software package GeneiousPrime version 2021.1 (https://www.geneious.com) (Kearse et al., 2012). The tBLASTP algorithm was used to search the bacterial assembly contig dataset, WGS Sequence Set: CESE01000000.1, with GXSXG as a query to identify sequences that contain this motif (Altschul, 1997; Agarwala *et al.*, 2018). Multiple entries that contained the conserved pentapeptide sequences were found. Sample ENA|CESE01052294|CESE01052294.1 was selected as it was the first match to contain a full open reading frame and conserved motif. This was identified as putative lipase candidate, PL001. Annotation tools were used to further bioinformatically characterise the sequence to reveal a hypothetical protein coding region (CDS) based on patterns established from NCBI and other public databases, from which the final sequence of PL001 was derived.

Identification of PL002, *Salpa thompsoni* lipase

Salp lipase was identified using the annotated genome of the next most genetically similar urochordate *Ciona intestinalis.* The *Ciona intestinalis* genome has been successfully annotated and assembled and with neighbouring ancestry, it would be expected that their digestive enzymes would be homologous (Godeaux, 1981). NCBI GenBank was used to identify the lipase gene in *Ciona intestinalis.* This was conducted using "Ciona intestinalis"[Organism] AND lipase [All Fields] in the search function (Altschul, 1997; Agarwala *et al.*, 2018). A match was identified as a tunicate 'pancreatic lipase-related protein' in the model species *Ciona intestinalis*, (accession: XP_002130573.1). One of the homologous gene sequences, an orthologue, was identified within the unannotated *Salpa thompsoni* transcriptome assembly (GenBank accession: GFCC00000000.1) by using the tBLASTN function with the *Ciona*

intestinalis lipase accession XP_002130573.1 using GeneiousPrime (Kearse *et al.*, 2012; Batta-Lona *et al.*, 2017). A full length pancreatic-like lipase gene open reading frame was identified in the *S. thompsoni* assembly sequence, (accession: GFCC01067991). To further verify this putative salp lipase candidate, short read archive data generated from *S. thompsoni* digestive tract RNA (samples AC_e20 and AC_e242, accession numbers SRX13276964 and SRX13276963, respectively) was screened for matching sequences using the Map to Reference method in Geneious under the LSF setting (word length 24, index word length 14, maximum mismatches per read 10). This tool is used for assembly of sequences to a reference, in this case the salp lipase GenBank accession: GFCC00000000.1 to the S. *thompsoni* digestive tract RNA.

Protein Identification Tools

A range of different protein identification tools were used to characterise *in silico* cold activity. The Expasy Protein Parameter tool was used to identify various physical and chemical parameters for the lipase candidates. The computed parameters include the molecular weight and amino acid composition which was used to identify conserved residues (Gasteiger *et al.*, 2005; Artimo P, 2020). InterProScan analysis was used to identify predictive domains within the lipases using genome-scale protein function classification (Jones *et al.*, 2014). NCBI tBLASTP encourages further structural confirmations and annotated protein alignments to the hypothesised lipases (Altschul, 1997). SWISS-MODEL Repository was used to identify near crystal structures providing further indications into the sequence origins (Bienert *et al.*, 2017; Waterhouse *et al.*, 2018).

2.3 Results

Two putative cold active lipase candidates were identified from open resource databases; PL001 and PL002. These lipases included conserved sequences corresponding to nucleophilic elbow required for catalysis, the motifs are G-X-S-X-G (Mala and Takeuchi, 2008), and an open reading frame spanning the length of the lipase gene.

Identification of lipase PL001 from The *Tara* Ocean Database

The conserved motif, GXSXG revealed a hit in the Tara Ocean metagenome sample ENA|CESE01052294|CESE01052294.1, (Figure 2.1). A 920bp protein was identified as putative lipase candidate, PL001. Sequence characterisation methods, such as homology modelling, employed by SWISS-MODEL, identified two crystal structures with sequence identity, 22% sequence coverage, *Rhizomucor miehei* lipase (PDB: 6QPP) and 19% sequence coverage, phospholipase A1 (PDB: 2YIJ).

Figure 2.1: Open Reading Frame and tBLASTN hit PL001

The NCBI tBLASTN hit (orange) with the inferred lipase conserved domain sequence (yellow) within the sample ENA|CESE01052294|CESE01052294.1. The yellow annotation indicates a hypothetical protein coding region (CDS) as a lipase. The full open reading frame translation of PL001 can be found in appendix A.

InterProScan tool was used to identify functional analysis of the lipase by predicting domains from Pfam and SUPERFAMILY databases. Here, Pfam identifies the putative lipase candidate as a bacterial lipase of family 1.3 (Mistry *et al.*, 2021). The SUPRFAMILY database identifies this as a member of the alpha/beta hydrolases (Wilson *et al.*, 2009) which corroborates the conserved motif search conducted. The nucleophilic elbow, GXSXG, is annotated in red (position 177 to 181). Expasy ProtPram identified 7% of all amino acids as glycine, distribution is visualised in pink, (Figure 2.2). In addition to this, the cysteine content was identified as 0.7% and molecular characteristics, theoretical pI: 5.39 and molecular weight of 34.79 kDa determined.

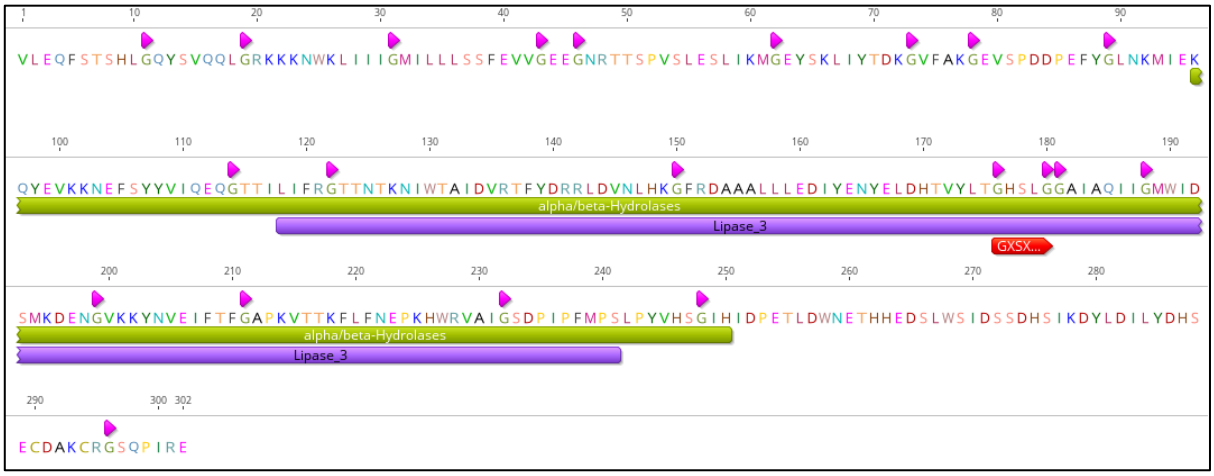

Figure 2.2: InterProScan analysis identifying predicative domains in PL001

Lipase domains identified through Pfam databases (Mistry *et al.*, 2021). Alpha/beta hydrolase family identified through SUPERFAMILY databases (Gough *et al.*, 2001; Wilson *et al.*, 2009).

NCBI BLASTP results from a search conducted with the lipase open reading frame translation identified that 87% of the first 100 hits (with e value lower than 2e-10) were lipase candidates. The full list of hits obtained can be found in appendix A. The first annotated hit was a 40% identity match to bacterium *Oleispira antarctica* (Yakimov *et al.*, 2003). The molecular chaperonins underlying protein folding in this bacterium confer cold active adaptations. These chaperonins have been characterised and inserted into *E.coli* for expression purposes as a commercially available cell line for expression, ArcticExpress (DE3) (Hartinger *et al.*, 2010).

While the top, unannotated tBLASTP hit was to a sequence of phage origin, (accession: KT997808.1), all remaining hits from the first 100 were to sequences of bacterial or single celled archaeal origin. The fact that the remaining hits were to non-eukaryotes, suggests that PL001 is of bacterial or archaeon origin.

Identification of lipase PL002 from *Salpa thompsoni*

A putative 1761bp salp lipase, subsequently referred to as PL002., was identified within the salp transcriptome assembly sequence GFCC01067991 using bioinformatic methods. This had a 46% amino acid identity to the pancreatic lipase accession XP_002130573.1. Additionally the SWISS MODEL homology tool provided a 41% structural similarity to pancreatic lipase related protein 2 from horse (PDB:1w52) and 40% similarity to that of the Human Pancreatic Lipase (PDB: 2ppl) (Waterhouse *et al.*, 2018). Thus, suggesting that PL002 is a pancreatic like lipase Identical DNA sequence transcripts were found within cDNA reads isolated from the *S. thompsoni* digestive tract sample AC-E20 and 99.7% identical transcript sequences were recovered from sample AC-E242, (Figure 2.3). This corroborated the identification of this lipase as of salp origin and demonstrated that it is expressed in the digestive tract consistent with a digestive function.

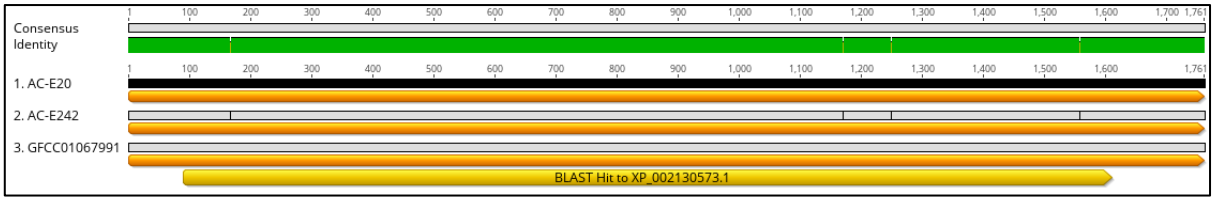

Figure 2.3: PL002 identified in three different digestive tract sources

A consensus was generated using the samples from E20 and E242 and the GFCC01067991 sequencing data from (Batta-Lona *et al.*, 2017).

InterProScan analysis predicted domains within the salp lipase were inferred from multiple databases and classified using conserved sites and molecular functions from the NCBI's directory (Lu *et al.*, 2020) (Figure 2.4). They included the PLAT (Polycystin-1, Lipoxygenase, Alpha-Toxin) and LH2 (Lipoxygenase homology) domains that are found within membrane or lipid associated proteins (Bateman and Sandford, 1999) and conserved motifs characteristic of lipases (Attwood *et al.*, 2003; Mistry *et al.*, 2021). Lipases have derived from common ancestry

of the alpha/beta fold hydrolases superfamily containing conserved histidine residues for catalytic function (Gough *et al.*, 2001; Wilson *et al.*, 2009).

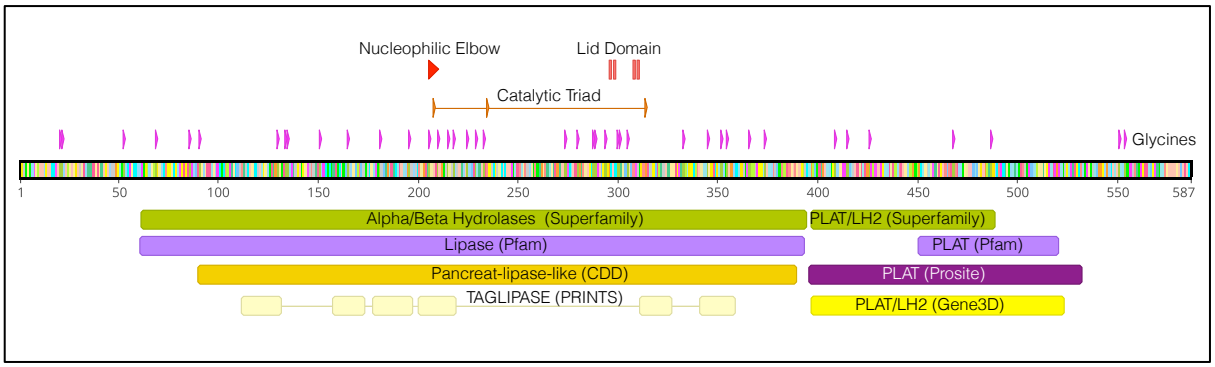

Figure 2.4: InterProScan analysis putative pancreatic salp lipase, PL002

Annotated structural features are displayed. InterProScan results identified multiple domains. PLAT (Polycystin-1, Lipoxygenase, Alpha-Toxin) domains were identified from Superfamily (Gough *et al.*, 2001; Wilson *et al.*, 2009), and Pfam (Mistry *et al.*, 2021) databases. Lipase domains identified through PRINTS(Attwood *et al.*, 2003), Pfam (Mistry *et al.*, 2021), CDD (Lu *et al.*, 2020). LH2 (Lipoxygenase homology) identified through Superfamily (Gough *et al.*, 2001; Wilson *et al.*, 2009)

Expasy protein parameter identifies 7% of amino acids at glycine with 50% clustered around the active site, (Figure 2.4). In addition to this, a 2% cysteine content was identified. Molecular weight of 66 kDa and a theoretical pI: 9.62 was also established. NCBI tBLASTP identified multiple predictive domains; these include a predictive active site/lid, catalytic triad including a serine nucleotide. Protein similarities included *Ciona intestinalis* (accession: XP_002130573.1) however newer assemblies have been submitted for organism *Phallusia mammillata* (accession: CAB3264979.1). In addition to this, 94% of BLAST alignments identified as lipase, particularly pancreatic like with e value lower than 3e-76.

Codon optimisation

Codon optimisation increased the GC content of PL001 by 51% and PL002 to 55%. The genes for PL001 and PL002 were synthesised by Genscript, USA. These, with the addition of a His-tag and codon optimisation, were inserted into pET-28a (+) expression vectors and were delivered in freeze-dried format.

2.4 Discussion

Two putative lipase candidates were identified and synthesised for *in vitro* expression. A bacterial lipase from family 1.3, PL001, identified from the *Tara* Ocean project open genomic resources, and a eukaryotic pancreatic like lipase, PL002, identified from the *Salpa thompsoni* genome archived on GenBank.

The *Tara* Ocean Lipase, PL001, was synthesised with the assumption for this lipase to have a bacterial nature. This lipase was identified using one conserved motif, GXSXG. Therefore hits identified from the genome could produce other enzymatic candidates from the alpha/beta hydrolase family whereby this sequence is also conserved, such as GDSL family of esterases (Akoh *et al.*, 2004) or acyltransferases (Poust *et al.*, 2014). This method is useful to determine lipase candidates using available motif searching functions, however further verification, including functional analysis and *in vitro* characterisation, is required to confirm the cold activity. In contrast, PL002 identification required the next most genetically similar organism to contain an annotated and fully assembled genome, in this case the *Ciona intestinalis* genome. A lipase identified here was used to construct a salp lipase from the Batta-Lona assembled genome (Batta-Lona *et al.*, 2017). The use of the whole gene from *Ciona intestinalis* provided verification that the sequence of interest was a lipase. NCBI tBLASTP results further confirmed this and substantiated the lipase classification, as a pancreatic-like lipase. The method used here included confirmation of relevant lipase motifs in addition to template genes for identification purposes. Therefore, the method of identifying lipases from annotated genomes provide an effective and robust confirmation of enzyme discovery.

PL001 was identified using saline water samples collected from the *Tara* Ocean expedition. This is an assortment of bacterial candidates that were spliced and sorted as a metagenome for identification purposes. Therefore, there is some uncertainty in the origins of the lipase. Origins of the lipase can aid the determinisation of other enzymes within the species to have been cold adapted and exhibit cold characteristics that can be used to identify similar features in PL001. It has been suggested that there are three-dimensional folding and active site structures that lead towards cold adaptiveness from an evolution perspective (Papaleo *et al.*, 2011). In contrast, PL002 was identified from a single organism with verifications of origins from salp gut cDNA. The use of two different genomic datasets, both encoding identical lipase sequences as well as the fully annotated nature of the genomic data set from Batta-Lona et al, produces a

pipeline to detect further putative biocatalysts within the salp gut. Therefore, the identification of genes from known genomes provides future endeavours to identify enzymatic candidates from interesting organisms, such as the marine tunicate, the salp.

NCBI tBLASTP function facilitates further structural confirmations to be annotated on the hypothesised lipases. Aside from the conserved glycopeptide sequence in PL001, Gly-176, His-177, Ser-178, Lys-179 and Gly-180 there are no other structural identification factors identified here, (Figure 2.4). Lipase classification suggests that this protein may belong to the Family VIII bacterial lipolytic enzymes as there is no presence of a catalytic triad. The conserved serine and InterProScan results present evidence that the protein is with the alpha/beta hydrolase family, following the classification outlined by (Arpigny and Jaeger, 1999). Functional biochemistry is required to confirm this. Methods to classify lipases by structure and function have had many attempts. Each method to classify lipases does so differently based upon structure, function, sequence homology or conserved motifs. Therefore as there are multiple different analysis parameters, the one chosen to classify PL001 was through (Arpigny and Jaeger, 1999) has done so by for other cold active lipase classification; for example (Zhang and Zeng, 2008; Wang *et al.*, 2013).

The annotated sequences on the salp lipase revealed further structural features to confirm the presence of a lipase. The salp lipase contains a predicted lid domain, a catalytic triad, and a nucleophilic elbow, (Figure 2.5). The nucleophilic elbow has been identified as Gly-206, Phe-207, Ser-208, Leu-209 and Gly-210. The predictive lid domain is a highly conserved feature of lipases and found within the catalytic domain. The PL002 sequence that occurs within the catalytic domain was Cys-295, His-296, Val-311 and Cys-312. Fluctuations in the lid domain can be used to determine substrate affinity of the lipase (Ollis *et al.*, 1992; Saavedra *et al.*, 2018). Temperature dependent studies identify that the lid structure in cold active lipases is far smaller than at higher temperatures (Khan *et al.*, 2017). As identified with other marine invertebrate neutral lipases of microcrustacean (*Daphnia pulux*) (Colbourne *et al.*, 2011). It has been suggested that the cysteine residues contribute towards a disulfide bridge, this has been observed in mammalian pancreatic lipases, particularly that of the secondary fold, the β9 loop (Lowe, 2002). The catalytic triad consists of Ser-208, from the conserved pentapeptide, Asp-235 and His-314 , which is critical for lipase activity (Winkler, D'Arcy and Hunziker, 1990; Brumlik and Buckley, 1996) and common to all enzymes from the serine hydrolases family. Alpha-beta hydrolases structurally locate the nucleophilic serine across the two other residues

of the catalytic triad (Denesyuk *et al.*, 2020). These residues acts as charged molecules (Uppenberg, Oehrner, *et al.*, 1994; Uppenberg, Patkar, *et al.*, 1994; Uppenberg *et al.*, 1995) and convergent evolution has established this triad to exist in two other digestive enzymes, trypsin and subtillisin (Joseph, Ramteke and Thomas, 2008).

Glycine residues are highly valued in cold active enzymes. Due to the small side chain, a single hydrogen, the enzymes are provided further flexibility and stability (Yan and Sun Qing, 1997). PL001 has an even placement of glycine molecules dispersed through the gene sequence. This can provide structural flexibility throughout the molecule. Protein folding studies are required to determine the role of glycine and enzymatic activity. PL002 has the same glycine content as PL001, however, the clustered nature around the active site encourages greater flexibility of the active site, consistent with the synthesis of large substrates (von Harbou *et al.*, 2011). This characteristic is homologous with the other psychrophilic enzymes, the alkaline phosphatase from the Antarctic strain TAB5, which has a great distribution of glycine residues close to the active site (Mavromatis *et al.*, 2002; Siddiqui *et al.*, 2006). It has also been demonstrated that rationally engineered glycines modulated in the active site of the thermoalkalophilic *Geobacillus thermocatenulatus* active site for enhanced flexibility and improved thermostability (Wang *et al.*, 2021).

PL001 has a larger ratio of lysine to arginine, 7% to 3%, whereas PL002 has an equal amount of both residues. These positively charges amino acids are able to determine protein solubility, where increased lysine content provides conformational stability (Ahmad *et al.*, 2020). This suggests that it may be hypothesised that PL001 is able to be more expressed in soluble format recombinantly than the salp lipase.

NCBI tBLASTP results indicate that PL001 identifies all known sequences as origins of a marine bacterial species. However, as 13% of hits are of hypothetical or unknown in nature, there is difficulty in characterising the cold nature of the protein using *in silico* methods. PL001 alignments share 35% identity with a lipase gene from *Oleispira antarctica* an oil degrading species, identified as a psychrophilic gram-negative, aerobic, spiral-shaped bacterium that belongs to the family *Oceanospirillaceae.* It has been previously been isolated from seawater samples from Antarctic coastal marine environments (Rod Bay, Ross Sea) (Yakimov *et al.*, 2003). Biological chaperonins required to assist with protein folding of cold enzymes have been isolated and optimised for grow of a transgenic *E.coli* strain (Strocchi *et al.*, 2006). It can

be inferred that due to the genetic ancestry between these two organisms being so close, there may be similar protein folding mechanism embedded in PL001, suggesting soluble recombinant protein formation.

In silico analysis has determined PL002 has cold active tendencies. The prominent identity towards cold water originated vase tunicate, *Ciona intestinalis*, at 46% (Dybern, 1967) suggests the cold nature of the salp lipase. Further structural patterns can be used to characterise the cold nature, including identifying surface residues and those surrounding the active site. PDB structures can be used to build hypothetical models however X-ray crystallography of structures genetically like the target lipases are required to provide further confidence in the results. PDB and SWISS-MODEL are useful homology tools to provide information on protein families. they are unable to identify novel structural patterns that may belong to protein candidates of an unannotated source and thus, as of yet, very few structures are fully identified using these structural predicting software (Robinson, Piel and Sunagawa, 2021).

Residues or structural functions of cold proteins have been identified using molecular biology methods to confirm the psychrophilic tendencies of these enzymes. Known residues that determine cold activity of proteins have been altered to determine protein functional changes. A metanalysis compared different *Pseudomonas* lipases to determine a significant difference in the amino acid content; especially glycine, arginine and cysteine residues of cold proteins (Ganasen *et al.*, 2016). Similar mutagenic studies can be conducted with PL001 and PL002. It has been postulated that the serine residue within the nucleophilic elbow of PL001 is of a catalytic nature.

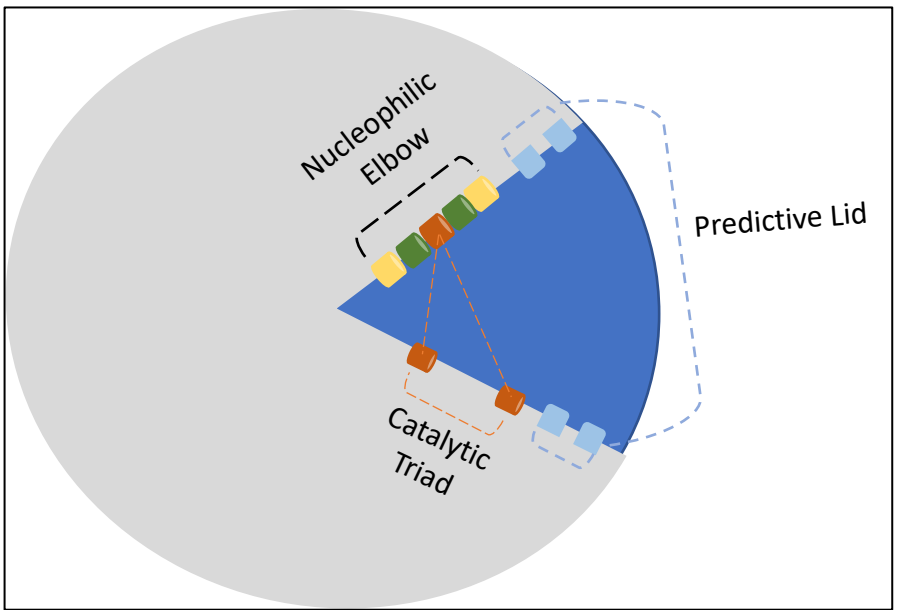

Figure 2.5: Key features pictorially depicted on a representative lipase

Blue region resembles the active site region. Predictive lid domain (light blue), catalytic triad (orange) and nucleophilic elbow (yellow, green, and orange) have been annotated. The nucleophilic elbow has two green regions which are variable amino acids whereby the yellow are conserved glycines. The middle amino acid is a highly conserved serine molecule which is present in the catalytic triad too.

As other structural features are unknown, this residue can be modulated to determine if the activity differs. Additionally, glycine residues can be exchanged for proline residues to determine if the cold nature of the lipase changes (Kulakova *et al.*, 2004). Site directed mutagenesis can be used to compare the cold activity of these proteins *in vitro* using with a temperature based enzymatic assay. It was established that by altering amino acid residues, substrate specificity towards different chain lengths altered greatly. As amino acid residues were modulated on the surface and near the active site, the longer chain specificity was acquired for proteins that operated at higher temperatures (Gatti-Lafranconi *et al.*, 2010). This suggests that shorter or tightly packed amino acids are in the active site of the enzyme to increase substrate specificity longer chained substrates. Therefore, functional analysis, such as plate assays, can be used to determine cold adaptations of enzymes.

Codon optimisation was utilised to increase the expression of recombinant proteins by reducing limitations relating to codon usage (Gustafsson *et al.*, 2012; Brown and James, 2016). As the expression system utilised requires the need of a bacterial host system, the protein

synthesis may be restricted by rare codons (Angov *et al.*, 2008). Codon usage of the gene can occur as 20 amino acids are encoded by 61 codons (Mauro, 2018). Apart from methionine and tryptophan, other amino acids are specified by up to six codons. This variability increases the chances sequences with different codon usage can encode the same polypeptide (Welch *et al.*, 2009; Supek, 2016). Therefore, synthesis of genes including codon optimisation reduced the risk of codon biases when the proteins undergo heterologous expression. This will be determined experimentally to investigate the soluble nature of the expression systems. Codon optimisations produce an increase in the GC content of the lipase genes leading to increased overexpression in the next stages of the enzyme production pipeline. By including this in the synthesis of the protein, there is a greater chance of producing stable and soluble recombinant protein.

Table 2.5: Summary of identified lipases and their features

Enzyme nomenclatures	**Lipase features**	**Structural features of cold proteins**
PL001 – *Tara* Oceans lipase	Molecular size: 920 bp (35kDa)	35% homology identity with a cold tolerant lipase from *Oleispira antarctica*
	Nucleophilic elbow Gly-176, His-177, Ser-178, Lys-179 and Gly-180	larger ratio of lysine to arginine, 7% to 3%,
		Even placement of glycine residues (7%)
		0.7% of amino acid content are cysteine
PL002 – *Salpa thompsoni* lipase	Molecular size: 1761 bp (66kDa)	7% of amino acids at glycine with 50% clustered around the active site
	Nucleophilic elbow- Gly-206, Phe-207, Ser-208, Leu-209 and Gly-210	2% cysteine content was identified
	Predictive lid - Cys-295, His-296, Val-311 and Cys-312.	
	Catalytic lid - Ser-208, Asp-235 and His-314	

2.5 Conclusion

This study combined *in silico* bioprospecting to identify two lipase genes from genomic data sources. PL001 was identified in the metagenomic data procured through the *Tara* Oceans expedition. This provided a 921bp novel lipase candidate mined using conserved sequences from WGS Sequence Set: CESE01000000.1 of the sampling point of 085, in the Southern Ocean. Here reliance on bioinformatic software, such as motif hunting and BLAST alignments, was required to confirm the presence of a lipase. The irregularities from the BLAST alignments, such as low identity matches to known genomes, provided unreliability in the gene identified. However, if the datasets presented BLAST hits to be closer in identity to other bacterial lipase genes, this method would be a robust system to identify other lipase candidates. At present, there has not been any other enzymes identified using this WGS sequencing data. Therefore, the origins of the lipase gene are unknown which reduced the amount of *in silico* determination of cold activeness that could be provided without attempting *in vitro* studies to determine function.

PL002, a putative 1761bp pancreatic like lipase was identified in the salp transcriptome assembly sequence GFCC01067991 using bioinformatic methods. Initial identification of PL002 included determining an annotated lipase gene in the closest familial match, *Ciona intestinalis*, as a template to identify a salp lipase. In addition, the in house cDNA of salp species was also used to corroborate lipase presence. The *in silico* approach applied here has greater degrees of certainty as multiple genome sources are available to confirm the presence of the lipase. Additionally, cold adaptations and lipase structures were identified using the amino acid sequence generated. Conserved lipase structures were identified here, the nucleophilic elbow, the active site, and the catalytic triad. Therefore, this methodology opens the doors towards the identification of other digestive enzymes.

Codon optimisation was required for both lipase candidates. PL001, the origins of the lipase were unknown, so synthesis and codon optimisation were required to increase successful expression in an *E. coli* host system. It deemed time appropriate to also have PL002 synthesised whereby codon optimisation would have occurred to increase solubility whilst attempting to produce a eukaryotic lipase in a bacterial expression system.

Chapter 3: Expression and Purification of Cold Active Lipases

3.1 Introduction

An *in silico* approach has great value to aid the identification and initial characterisation of putative lipase candidates, however, *in vivo*, or *in vitro* assessments are required to test the cold nature of these candidates. Through these assessments the expression conditions of the recombinant lipases can be identified, and their psychrophilic nature ascertained. Cold adapted enzymes, or psychrophilic biocatalysts, are highly prevalent in organisms inhabiting low temperature environments with optimal activity below 30 °C (D'Amico *et al.*, 2003; Feller and Gerday, 2003) and are defined as having optimal gene expression temperatures at about 15°C or lower (Lee, Jang and Chung, 2017).

Approaches to assess the expression of lipase candidates include extracting enzymes directly from host sources, recombinant expression using yeast or bacteria based host cells and novel Cell Free Protein Synthesis (CFPS). Each system would need to be optimised to produce lipase candidates.

Direct extraction of enzymatic candidates from multicellular organisms is traditionally optimised to include methods of homogenisation for crude extraction followed by multiple purification steps. For example, specimens of cannonball jellyfish *Stomolophus sp. 2* were homogenised and gastric pouches extracted for analysis of phospholipase activity (Martínez-Pérez *et al.*, 2020). This method provides significant insight into activities of the lipase in its native biological format. However, it does not provide a pure candidate without difficulty, which was a necessary requirement for the work of this project. Lipases have been extracted from Antarctica krill using a similar process and was optimised to include a series of purification steps, precipitation of ammonium sulfate, ion exchange and gel filtration methods (Xin *et al.*, 2020). This work benefitted from prior studies on the production of krill lipases and hence known parameters could be used to identify the molecular size of the protein of interest.

Recombinant protein production includes the use of yeast-based host systems for expression. These have the potential to improve protein recovery and optimise yield from eukaryote recombinant genes. Yeast based platforms require successful optimisation to generate highly

active recombinant lipases in bulk (Wang *et al.*, 2018). However, multiple recombinant fungal lipases have been recombinantly expressed using yeast candidate, *Pichia pastoris.* Cold active lipase candidate from *Rhizopus microsporus* was recombinantly expressed and purified using ion exchange principles (Xiang *et al.*, 2021). This suggests an alternative method for expression of lipases.

An alternative for recombinant protein production involves the use of *E. coli* host systems. The fast growth kinetics of the bacterial host system and its relatively robust laboratory set up make it a suitable method of heterologous expression of enzymatic candidates and mass production by known methodologies for upstream large scale fermentation are relatively uncomplicated (Rosano and Ceccarelli, 2014). The high expression rate produced by the pET-28a (+) expression vector makes it a suitable backbone for the expression of recombinant proteins (Shilling *et al.*, 2020). For the optimisation of expression, a range of different cell lines, media, pH, and temperature conditions were utilised to determine successful parameters for protein expression. Biological chaperones, such as the Takara Plasmid set, can be trialled alongside chemical based chaperones, such as the addition of sorbitol, to encourage successful protein folding. Low temperature *E. coli* based expression systems optimised for the bulk production of recombinant proteins can also be exploited. Hydrophobic or insoluble proteins are generally formed through increased temperature conditions (Sahdev, Khattar and Saini, 2008). Therefore, optimising parameters to include colder temperatures suggest successful expression. Modified system, ArcticExpress (DE3) *E. coli* cells has been co-transformed with chaperonins from the Antarctic bacteria, *Oleispira* sp (Ferrer *et al.*, 2003) to operate at 10°C. Difficult to solubilise proteins, especially those from a cold climate, employ the use of this cell line to provide a psychrophilic expression system. The genetically modified cell line encodes has two chaperones, Cpn 10 (10 kDa) and Cpn 60 (57 kDa) which enhance the protein folding and promote solubility (Strocchi *et al.*, 2006). The chaperones have a 70% and 50% functional similarity to the *E.coli* chaperones GroEL and GroES (Ferrer *et al.*, 2003). The *in vivo* properties of GroEL and GroES were compared with Cpn 10 and Cpn 60 to demonstrate that these chaperones promote the folding for proteins and are able to be utilised under low temperature conditions (Ferrer *et al.*, 2003). The modified ArcticExpress bacterial host system, as employed in this study, ensures a clearer route for the production of cold active enzymes (Hartinger *et al.*, 2010) as there is yet to be a comparable yeast based cell line available as an alternative for cold expression.

A further alternative expression using bacterial systems is using a Cell Free Protein Synthesis (CFPS). Difficult to express proteins have been synthesised using CFPS (Schumann and Ferreira, 2004). It has been determined that proteins expressed in this way have better activity and thermal stability (Park *et al.*, 2011). Successful expression of proteins using CFPS is to ensure that target enzymes should not interfere with another host cellular pathways, including regular cell metabolism. This has been demonstrated by successful expression and screening of Cal B (Park *et al.*, 2011).

Purification systems can include all forms of chromatography as methods to sperate the protein of interest. The most common methods include size exclusion, ion exchange and affinity purification. Ion exchange and size exclusion principles require optimisation of multiple steps before yielding protein (Sharma, Chisti and Banerjee, 2001). Affinity chromatography provides an alternative single step approach to purification. Histidine tagged proteins (6xHis) allow for successfully purifying proteins. Hexahistadine residues have a relatively uncharged nature, small molecular size (<0.84 kDa) and are suitable candidates for purification by affinity chromatography (Spriestersbach *et al.*, 2015). Immobilised metal affinity chromatography is employed due to the affinity of the histidine reduced for the immobilised metal ions, usually nickel or copper. These ions are immobilised on various chromatography matrixes and are available packed into columns and can be regenerated for further use. Therefore, this bind and elute system can be optimised to perform with multiple different column sizes and buffering systems (Spriestersbach *et al.*, 2015).

Expression and purification factors have been explored in several studies reported to contain an *E. coli* based expression system followed by affinity chromatography for purification purposes (Table 3.1). These suggest that the single step his-tag purification system is a preferred method due to ease of protein recovery and high yield. This system will be explored in the expression of cold lipase candidates, PL001 and PL002.

Table 3.1: Expression and purification conditions of recombinant proteins

Recombinant enzyme production systems and downstream purification pathways have been summarised. The brief literature research encouraged subsequent methods.

Enzyme Classification	Species	Expression		Purification	Reference
		Vector	System		
Esterase	*Lactobacillus fermentum LF-12*	pCzn1	*E. coli* ArcticExpress™ (DE3)	Affinity Chromatography	(Liu *et al.*, 2020)
Esterase	*Thermogutta terrifontis*	pLATE31	*E. coli* ArcticExpress™ (DE3) 48 hours at 12 °C	Affinity Chromatography	(Sayer *et al.*, 2015)
Lipase	*Sulfolobus acidocaldarius lipase*	pET-28a (+)	*E. coli* BL21(DE3) 16 hours at 20°C	Affinity Chromatography	(Glogauer *et al.*, 2011)
Lipase	*Indian hot spring*	pET-28a (+)	*E. coli* BL21(DE3) 16 to 18 hours at 37 °C	Affinity Chromatography	(Sander *et al.*, 2021)
Lipase	*Pseudomonas sp. LSK25*	pET-32b (+)	*E. coli* BL21(DE3) for 16 hours at 25 °C	Affinity Chromatography	(Salwoom *et al.*, 2019)
Cytochrom p450	*Sulfolobus acidocaldarius*	pET-20b	*E. coli* BL21(DE3) overnight at 37°C	Affinity Chromatography	(Aslantas and Surmeli, 2019)
Lipase	*Candida antarctica* (B)	pPICZaA	*E. coli* BL21-StarTM (DE3) Plasmids for Cell Free Protein Synthesis		(Park *et al.*, 2011)

A need for a cell culture media that would increase the cell density without compromising the expression pathway was required as the low temperatures of expression resulted in low yields of protein. Commonly, Lysogeny Broth (LB) media is the medium of choice for culturing *E. coli*. It's simple preparation and high nutrient content ensures optimal growth for cells. However, a major caveat is that the cell densities are unable to deliver high yields (Sezonov, Joseleau-Petit and D'Ari, 2007). In the expression system of choice and for the bacterial lipase PL001 this media might not cause a concern. In the recombinant expression of PL002, a eukaryotic protein in a bacterial host, the yield obtained using this media may not be optimal. Terrific Broth (TB) is an alternative media which has been optimised to contain additional glucose to increase yield (Madurawe *et al.*, 2000). Other options include the use of autoinductive media instead of inductive media. Autoinductive media reduce the need to change expression parameters once induced. Glucose, the main component of this media, is used for metabolism of the cells, lactose uptake is prevented and therefore there is no need for cell induction, as with TB and LB (Studier, 2014). Traditional IPTG induced cell cultures use the induction sugar that is usually lactose. In autoinduction media lactose is added directly to the media prior to inoculation (Fox and Blommel, 2009). The use of autoinductive media and increasing the optical density of the cell culture enables a greater yield of protein. MagicMedia™ *E. coli* expression medium can increase the yield of the protein. This media encourages a greater cell biomass however it is a costlier media. Modified TB enriched with glycerol is ~£9.47 per litre whereas MagicMedia™ is £40.66 per litre (Sigma, UK). It has been observed that an auto inductive media can produce a higher cell density, this will be trialled to assess protein production (Krause, Neubauer and Neubauer, 2016). Therefore, considerations for scale up processes would be much costlier if this media was employed.

PL001 and PL002 lipases (EC:3.1.1.3) have been successfully identified as a bacterial lipase candidate and eukaryotic lipase, respectively. These lipases were sourced from marine genomic data; the *Tara* Ocean metagenome database and an assembled Batta-Lona salp transcriptome. The 33 kDa *Tara Ocean* and 66 kDa *S. thompsoni* lipase sequences were synthesised and codon optimised by GenScript (Leiden, Netherlands). Codon optimisation increased the GC content by 51% and 55%, as established in Chapter 2. This encourages protein expression by reducing limitations that may occur due to codon usage and tRNA abundance differences between the organism encoding the gene of interest and the host system chosen, *E. coli*. Furthermore, three methods of purification were trialled to identify the most suitable purification system.

3.2 Methods and Materials

Molecular biology methods have been used in the expression and purification stages of novel cold active lipases PL001 and PL002. PL001 was synthesised prior to expression stages. Direct cDNA amplicon cloning attempts were initiated for the salp lipase PL002, however, due to time constraints this gene was also codon optimised and synthesised. These attempts can be found in appendix B.

4 µg of lyophilised plasmid DNA of both lipases was synthesised by Genscript (Leiden, Netherlands). This was resolubilised with the addition of 20 µl of sterilised water and gently vortexed for 1 minute prior to storage at -20 °C. Transformation stages occurred immediately after solubilisation.

Expression

PL001 and PL002 transformation was carried out using NEB® 5-alpha competent *E. coli* (High Efficiency) to produce clones for storage.

The Genscript lipase constructs were transformed into *E. coli* BL21 pLysS (DE3) and *E. coli* ArcticExpress (DE3) cell lines using a heat shock methodology for protein overexpression following the manufacturers protocols. The recombinant clones obtained were plated on agar containing the appropriate selective antibiotics (Sambrook, 1983; Strocchi *et al.*, 2006). Overnight incubation at 37 °C 250 rpm, resulted in clear plaque growths indicative of a successful transformation process. Positive colonies were selected for 10ml starter cultures containing TB media and relevant antibiotics. Overnight growth of these starter cultures was used to prepare glycerol stocks, containing 50% glycerol and 50% starter culture, that were subsequently stored at -80°C.

The *E. Coli* BL21 (DE3) pLysS PL001 overnight cultures were scaled up to a 1 in 50 ratio. This was then grown at 37°C to an optical density of 0.8. IPTG was then added to the cultures at a final concentration of 1mM. Successful protein expression was achieved by including a post expression temperature decrease to 10 °C in a shaking incubator set at 120 rpm for 24 and 72 hours. Cells were then harvested by centrifugation (10,000g, 10 min, 4 °C). And these pellets were stored in -20°C freezer for SDS-PAGE Analysis (Akbari *et al.*, 2010).

PL002 was successfully expressed using ArcticExpress (DE3) Cell Line with TB media in soluble form. The overnight cultures were scaled up (1:50) at 30°C until the optimal optical density of 4 was obtained. The cultures were cooled to 10 °C and induced using IPTG to a final concentration of 1mM. The cultures were then left to incubate for a further 24 hours at 10 °C, 180rpm. Cells were then harvested using the methods described above.

Trials to optimise protein expression by altering media and cell density conditions were conducted. Autoinductive media, MagicMedia™ at optical densities of 0.8 and 2 were compared to TB media conditions in the expression of PL002. Overnight cultures were scaled up to 1:50 and incubated in their respective media conditions at 30°C until the required optical density was obtained. Samples were then treated with IPTG, if required, and incubated at 10°C for a further 24 hours; followed by cell harvest, as above.

A large scale up expression of PL002 was also carried out using a Biostat® Cplus (Sartorius) stainless steel bioreactor. 20 litres of TB containing relevant antibiotics and was inoculated with 400 ml of seed culture, previously grown overnight as described. Once the OD 600 reached 4, PL002 expression was induced with 1mM IPTG. The 20L culture was then incubated at 11 °C for 24 hours, harvested, and stored at -20 °C

Cell Free Protein Synthesis

Cell free protein synthesis (CFPS) was used to attempt expression of PL001. The protocol for CFPS reaction was performed as described in (Colant *et al.*, 2021) with the following modifications: Two BL21-Star (DE3) based extracts were used, one that had been induced with IPTG during extract preparation and one that had not. These samples were not subjected to sonication but were immediately sampled for SDS-PAGE analysis. Parameters investigated included two different temperature conditions (10 °C and 15 °C), cell extracts that were treated with and without IPTG. The negative control used was the empty plasmid vector, pET-28a (+).

Analysis

SDS page analysis was used to confirm if protein expression was successful. The inclusion of 6xHis protein tag encourages the use of Western Blot analysis as an alternative means of proving protein expression.

SDS-PAGE Analysis

The cell pellets from harvested cultures (<1 g wet weight cells) were suspended in 50mM phosphate buffer followed by 10 cycles of 10 s sonication. Further centrifugation was carried out at 5,000g, 30 minutes, 4 °C to pellet the soluble fraction. The supernatant, also referred to as the lysate or soluble fraction, was removed and kept on ice for SDS-PAGE analysis and purification. The pellet was resuspended with 8M urea. After ten cycles of 10 s sonication the insoluble fraction was able to be used for SDS-PAGE analysis. The samples were then prepared using Bolt™ Sample buffers and Reducing Agents as per the manufacture's guidelines. To detect the recombinant protein, between 5 – 10 µl of the samples, were loaded onto 12% Bolt™ Minigels for gel electrophoresis. The 12% gels were then stained with Coomassie brilliant blue for SDS analysis. Gels were visualised using Amersham™ Imager 600 (GE healthcare, USA).

Western Blot Analysis

Western blotting (Burnette, 1981) was carried out using the Bio-Rad Trans-Blot® TurboTM Transfer System (Bio-Rad, Thermo Scientific, United States). SDS-PAGE was performed as stated previously. The gels were transferred to an 8 mm by 8 mm nitrocellulose membrane using the Bio-Rad Trans-Blot® TurboTM Transfer System. Subsequent methodologies were adapted from (Colant, 2020). The membrane was incubated with the primary antibody: Anti-His mouse monoclonal antibody (ab18184, Abcam, Cambridge, MA, USA) diluted 1:1000 in TBST-M for two hours. The membrane was washed with TBST before being incubated with the secondary antibody: Goat anti-mouse HRP conjugated antibody (HAF007, Biotechne, USA), diluted 1:1000 in TBST-M. Imaging took place using The Pierce ECL Western Blotting Substrate (Thermo Fisher Scientific, USA) for 1-2 minutes in darkness then exposed and imaged using Amersham™ Imager 600 (GE healthcare, USA).

Purification

His-tagged recombinant proteins can be easily purified using nickel-based affinity chromatography. The successful expression of PL002 allows for the use of protein purification. Cell pellets were resuspended in lysis buffer on ice, 50mM sodium phosphate pH 8.0, 300 mM NaCl, 10 mM imidazole (Spriestersbach *et al.*, 2015) followed by 10 cycles of 10 s sonication

(Soniprep 150, MSE Centrifuges). Samples were then centrifuged at 5,000 g for 30 minutes at 4 °C to pellet the insoluble fraction. The soluble supernatant was clarified using a 0.22µM PES syringe filter and analysed using the three methods for purification outlined below.

Step Imidazole Elution using Spin Columns

HisPur™ Cobalt Spin Columns (Thermo Scientific, USA), 0.2 mL, were initially used for His-tag Purification of PL002. These columns were used using the manufactures guidelines, at 4°C. Five wash stages took place using the following imidazole concentrations, 10 mM, 25 mM, and 50 mM. This was prepared in 50 mM sodium phosphate, 300 mM NaCl buffer at pH 8.0, supplemented with the various imidazole concentrations. Four elution stages took place (150 mM, 50 mM sodium phosphate, 300 mM NaCl buffer at pH 8.0). All wash and elution flowthroughs were stored at 4°C for SDS-PAGE analysis, or the protein precipitated at 70% ammonium sulfate for further analysis.

Step Imidazole Elution using Gravity

Ni-NTA Superflow Cartridges (QIAGEN, Germany), 1ml, were used for affinity chromatography purification of the lysate. This was loaded onto the pre-equilibrated column at a rate of 1ml/min using an infusion pump. After washing the column and matrix with ten column volumes of wash buffer (50 mM sodium phosphate pH 8.0, 300 mM NaCl, 25 mM imidazole). The salp lipase was eluted using the equilibration solution consisting of 50 mM sodium phosphate pH 8.0, 300 mM NaCl, 150 mM imidazole (Spriestersbach *et al.*, 2015). Ammonium sulfate, at 70%, was used to precipitate and store the protein at 4 °C.

Gradient Elution using AKTA Prime Chromatography

A HisTrap™ High Performance (Cytiva, United States) 1ml column was used in the AKTA Prime chromatography unit (Cytiva, United States) in a gradient elution form. This system was used following the manufactures guidelines at 4°C. In brief, a standard HiTrap Desalting programme was employed in which 2 buffers were mixed at different concentrations to perform increasing wash and elution stages: lysis buffer and elution buffer (500mM imidazole 20mM Sodium Phosphate, 500mM NaCl, pH 7.6). All wash and elution flowthroughs were stored at 4°C for SDS-PAGE analysis.

Protein quantification

Protein quantification occurred using Bradford reagent. Known concentrations of Bovine Serum Albumin (BSA) (25 µg/ml, 0.50 mg/ml, 0.75 mg/ml, 1 mg/ml, 1.25 mg/ml, 1.5 mg/ml, and 2mg/ml) were used to identify protein yield. 5 µl of standard concentration was incubated with 150 µl of Bradford reagent and absorbance values at 595nm were obtained. These were used to produce a standard calibration curve, from which sample protein concentration can be calculated. A 5ul of sample, for example clarified lysate or elution fractions was used in the same style to obtain the protein concentration.

Protein Precipitation

Ammonium sulfate crystals were added to the protein elution to 70% working concentration. This was rotated at 4 °C to dissolve. Centrifuge for 10 minutes at 6000 rpm, 10°C to remove the buffer for characterisation studies. 70% saturated ammonium sulfate was used to reconstitute the protein pellet for storage at 4 °C.

3.3 Results

Heterologous *E. coli* expression methods were trialled to recombinantly express PL001 and PL002. PL001 was expressed in truncated and insoluble form thus CFPS systems were attempted. This too produced insufficient protein to confirm expression. Therefore, this candidate would not be pursued further. PL002 was successfully expressed using psychrophilic expression strain and then purified using affinity chromatography.

Bacterial sourced lipase from the *Tara* Ocean Database, PL001

The synthetic PL001 gene was inserted into the expression vector, pET-28a (+), within the molecular cloning sites, NcoI and XhoI. A 6xHis affinity tag can be found at the N terminus and a kanamycin resistance gene is also present. The full plasmid backbone can be found in appendix B.

Expression of lipase PL001 from The Tara Ocean Database

Initial expression of PL001 (34.79 kDa) was conducted using *E. coli* BL21 PlysS and ArcticExpress (DE3) cell lines for expression trials. SDS-PAGE highlights inferred soluble truncated PL001 (25 kDa) using BL21 PlysS, after 24 hour incubation, (Figure 3.2 lane 2). Interestingly there was not clear PL001 production in the ArcticExpress (DE3) cell line, Figure 3.2 lanes 5 to 8. Insoluble expression of PL001 could also be seen clearly using BL21 pLysS after 72 hour incubation, (Figure 3.3 lane 2). The bands of expression were not found in the control samples, empty pET-28a (+) vector, (Figure 3.2 lane 4 and Figure 3.3 lane 4).

Additional expression platforms and processes were also trialled; these are summarised in appendix B.

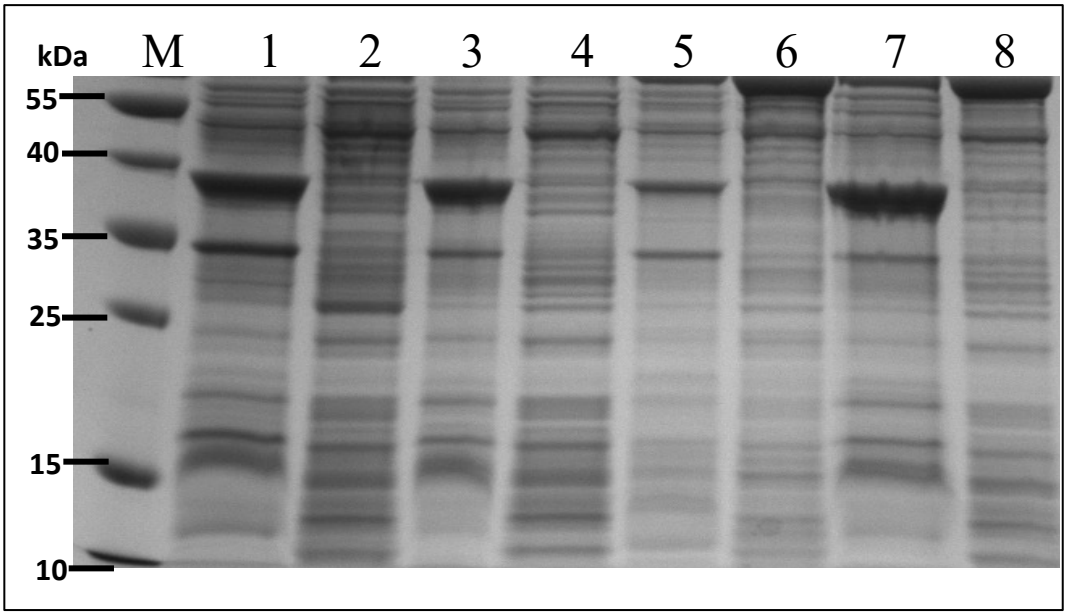

Figure 3.2: Recombinant expression of PL001 10 °C for 24 hours

BL21 pLysS (lane 1-4) and ArcticExpress (DE3) (lane 5-8) *E. coli* cells harvested after 24 hours

Lane 1, 2, 5,6: PL001 clarified lysate and insoluble fraction. Lane 3,4,7,8: Control pET-28a (+) empty vector clarified lysate and insoluble fraction

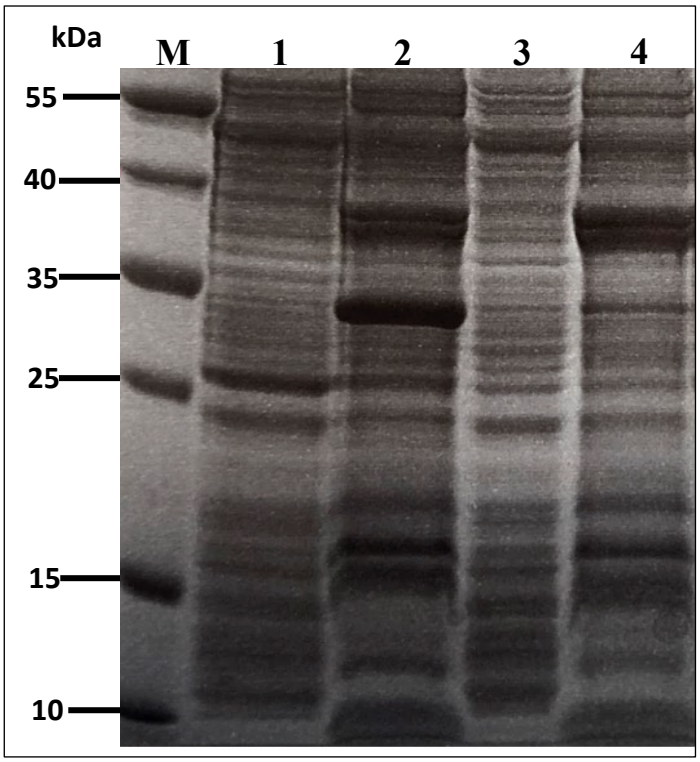

Figure 3.3: Recombinant expression of PL001 10 °C for 72 hours

BL21 pLysS *(E. coli)* cells were harvested after 72 hours

Lanes 1 and 3 contain clarified lysate, soluble fractions, of PL001 and empty vector control, pET-28a (+). Lanes 2 and 4 contain insoluble fraction of PL001 and empty vector control, pET-28a (+)

Cell Free Protein Synthesis

CFPS samples, treated with and without IPTG, display protein production at 35 kDa mark, (Figure 3.4 B). However, sufficient target protein expression was not observed.

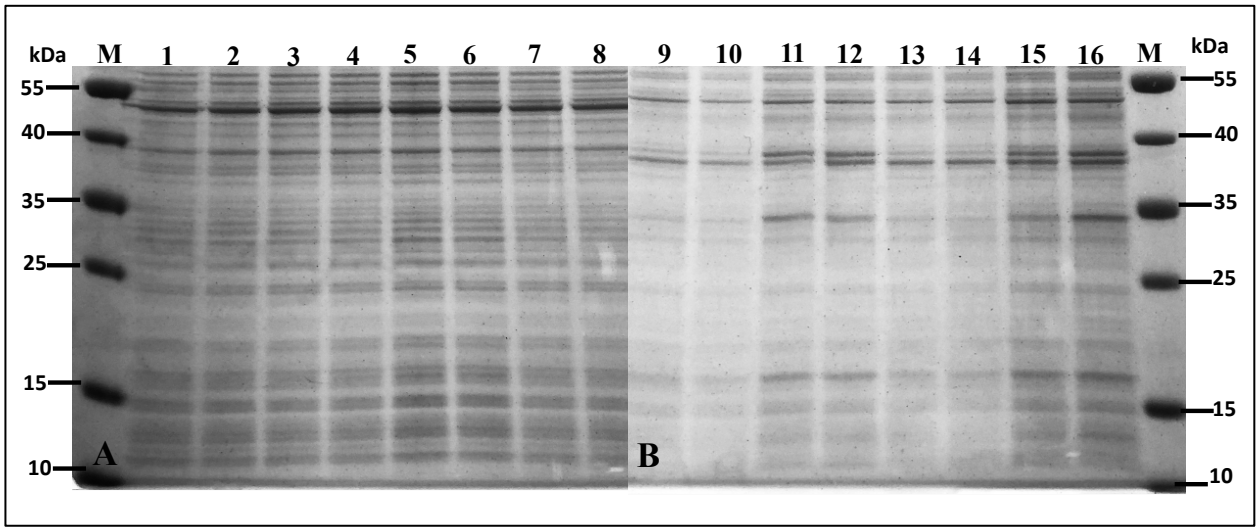

Figure 3.4: Cell Free Protein Synthesis of PL001

Lanes 1-8 are the insoluble fractions (A). Lanes 9-16 are the soluble fractions (B)
PL001 samples: lanes 1 and 9 at 10 °C with IPTG, lanes 3 and 11 at 10 °C without IPTG, lanes 5 and 13 at 15 °C with IPTG, lanes 7 and 15 at 15 °C without IPTG
PET-28a (+) samples (control): lanes 2 and 10 at 10°C with IPTG, lanes 4 and 12 at 10°C without IPTG, lanes 5 and 14 at 15°C with IPTG, lanes 8 and 16 at 15°C without IPTG

Pancreatic-like lipase from *Salpa thompsoni*, PL002

The salp lipase gene, PL002, was inserted into the pET-28a (+) expression vector with molecular cloning sites, BamHI and HindIII. A 6xHis affinity tag can be found at the N terminus and the kanamycin resistance gene was also present. Full plasmid backbone can be found in appendix B.

Expression

The gene encoding PL002, the salp lipase, was successfully expressed using ArcticExpress DE3 *(E. coli)* after a 24 hour incubation period at 10 °C. Due to the similarity in size between Cpn 2 (60 kDa) and PL002 (66 kDa), a His-tag Western Blot analysis was employed to visualize PL002 more clearly to verify successful expression. The SDS-PAGE and Western Blot analysis carried out after harvesting sample PL002, negative controls, pET-28a (+) and

just the ArcticExpress cells, respectively, (Figure 3.5). There was unclear separation between PL002 and the chaperones throughout the SDS Page gel. By contrast, the Western Blot showed clear, definitive expression of the salp lipase.

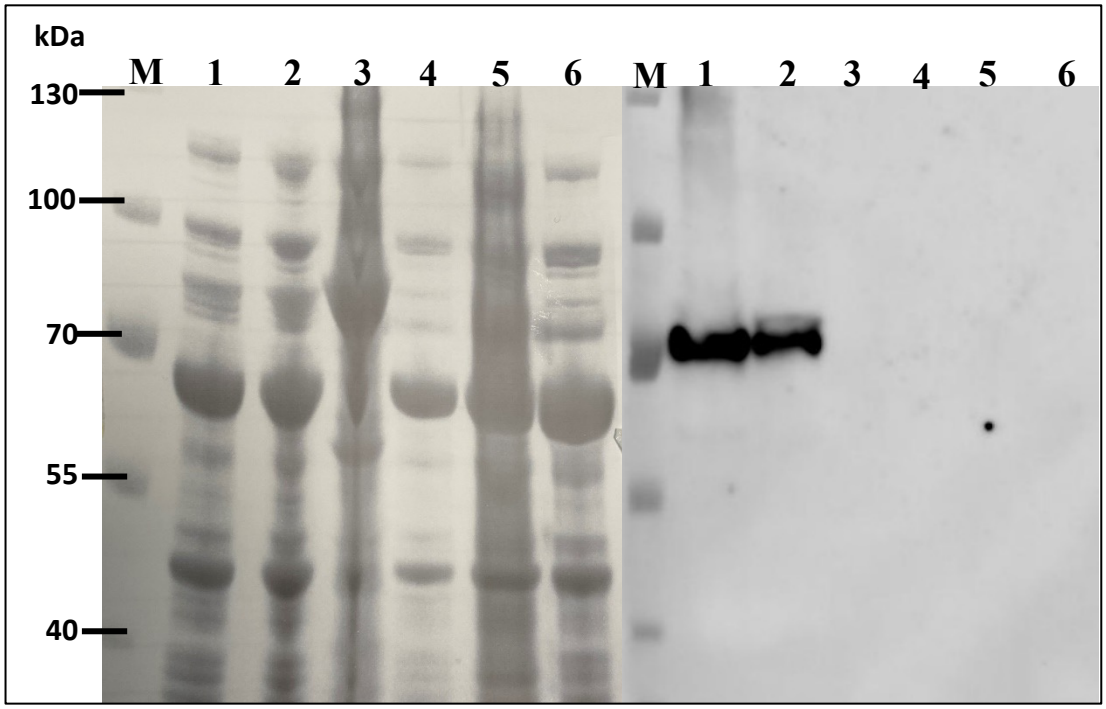

Figure 3.5: Recombinant expression of PL002

Analysis conducted using SDS-PAGE (A) and Western Blot (B)

ArcticExpress DE3 *(E. coli)* after a 24 hour incubation period at 10 °C

Lanes 1 and 2: PL002 clarified lysate and insoluble fraction. Lanes 3 and 4: control pET-28a (+) empty vector clarified lysate and insoluble fraction. Lanes 5 and 6: control untransformed arctic express cells clarified lysate and insoluble fraction

Media Comparison

Optimising the growth conditions of PL002 revealed that the highest protein expression was obtained when the inducible media had an optical density reading of 2 in TB, (Figure 3.6). Optimising the growth conditions was vital as there was a low yield of protein generated under the low temperature conditions. The SDS-PAGE compares the clarified lysates harvested from samples with OD readings of 0.8 and 2, and media conditions, IPTG induced TB media and autoinductive MagicMedia™ (MM). MM expressed PL002 had the highest protein

concentration at the indicative 70 kDa marker, (Figure 3.6). However, for scale up fermentations, TB would be a more cost effective system than MM.

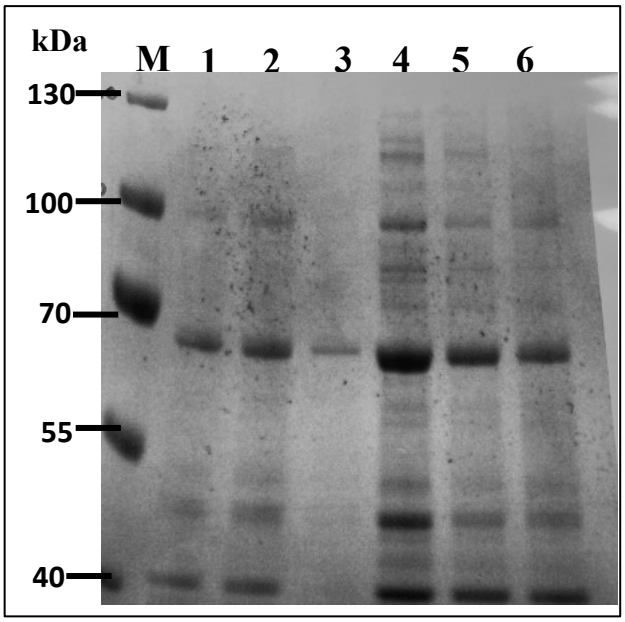

Figure 3.6: Recombinant expression of PL002 with various media and cell density

ArcticExpress DE3 *(E. coli)* after a 24 hour incubation period at 10 °C

Lane 1-4 Magic Media expression: PL002 (OD 0.8), pET-28a (+) (OD 0.8), Just AE cells (OD 0.8), PL002 (OD 2). Lane 5 and 6 Terrific Broth expression: PL002 (OD 2), pET-28a (+) (OD 2)

Purification

Successful expression of soluble PL002 determined affinity-based nickel-purification was the next stage for soluble protein collection. Initial purification was conducted using gravity assisted, Ni-NTA Superflow Cartridges, for affinity chromatography and a 50 ml frozen pellet from small scale harvest. SDS PAGE analysis of purification strategy using imidazole concentrations, 10 mM, 25 mM, and 50 mM for the wash steps and three 150 mM elution steps. Elution fractions, lane 6 and. 7, were pooled for ammonium sulfate precipitation, (Figure 3.7).

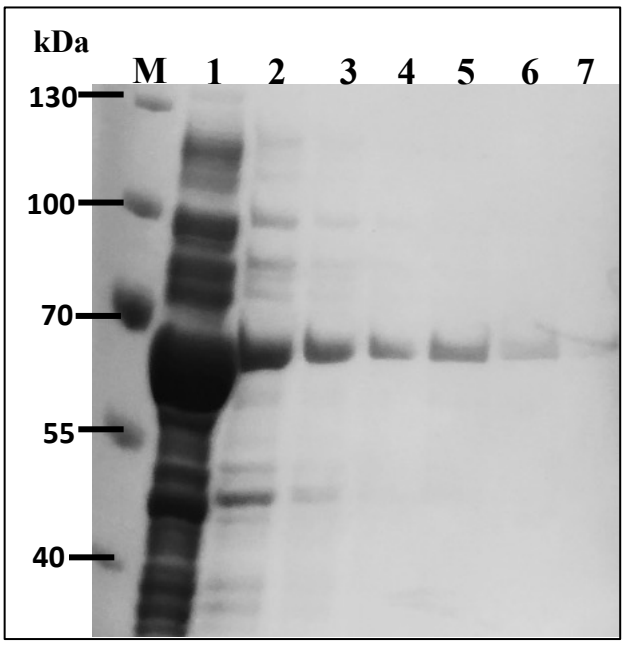

Figure 3.7: Small scale expression and purification of PL002

ArcticExpress DE3 *(E. coli)* after a 24 hour incubation period at 10 °C

Lane 1: PL002 clarified lysate. Lane 2-4: imidazole wash stages (10mM, 25mM and 50mM). Lane 5-7: imidazole elution stages (150mM)

Large Scale Expression

A 500ml, total volume, cell culture pellet was defrosted from the large scale batch fermentation. This was clarified and lysate extracted for purification using Ni-NTA Superflow Cartridge chromatography gravity assisted, (Figure 3.8). Purification steps were optimised to include a further imidazole wash and elution steps: 2x 10 mM, 2x 25 mM and 1x 50 mM for the wash steps followed by 4x 150 mM elution steps. Elution fractions, lane 10 and 11, were pooled for ammonium sulfate precipitation to preserve the protein.

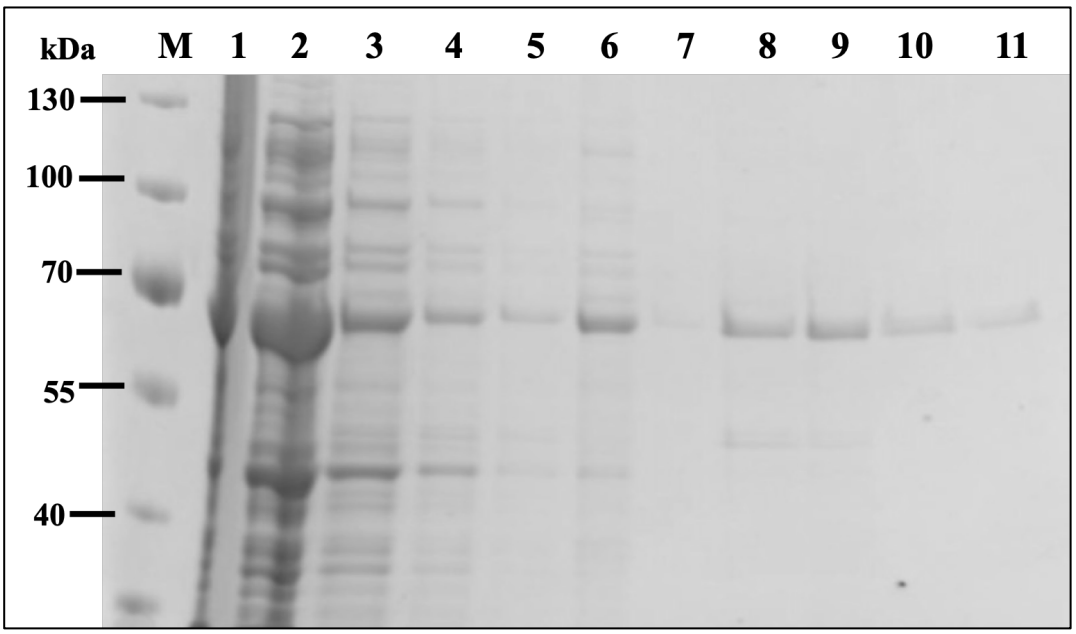

Figure 3.8: Large-scale expression and purification of PL002

ArcticExpress DE3 *(E. coli)* after a 24 hour incubation period at 10 °C conducted using Biostat® Cplus (Sartorius) stainless steel bioreactor

Lane 1 and 2: insoluble and soluble fractions of PL002. Lanes 3 and 4: imidazole wash steps (10 mM). Lanes 5 and 6: imidazole wash steps (25 mM). Lane 7: imidazole wash step (50 mM). Lane 8-11; imidazole elusion steps (150 mM).

The three systems provided affinity tag purification systems however the binding of the proteins was far greater in the gravity assisted, Superflow cartridge method. Figure 3.9 shows an improved protein purification pathway with fewer steps. Gradient elution, (Figure 3.10), depicts residue host proteins, perhaps eluting from the column or host cell proteins that bind to the column. Therefore, Superflow cartridges have been used henceforth.

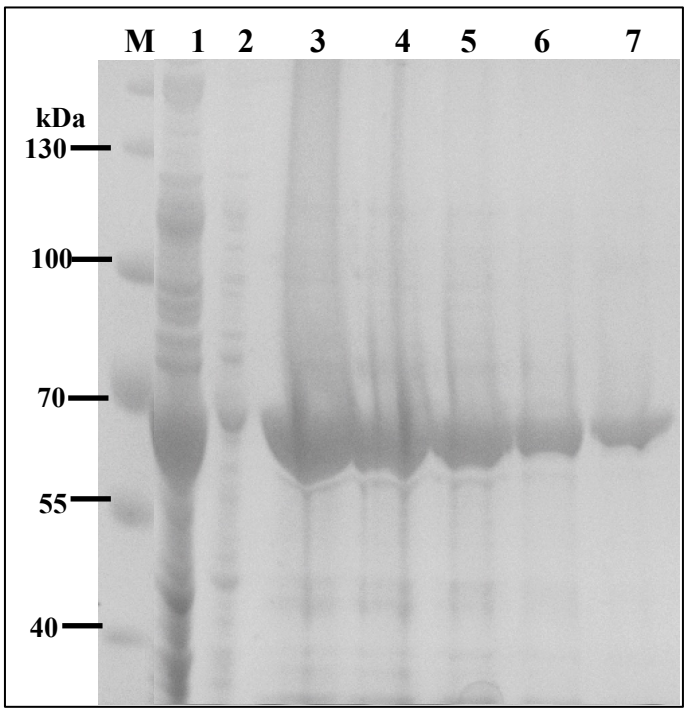

Figure 3.9: PL002 purification using gravity flow

Ni-NTA Superflow cartridge was used in in step imidazole elution.

Lane 1 and 2: Flowthrough and wash fraction (50 mM) of PL002. Lane 3-7: imidazole elusion steps (150 mM)

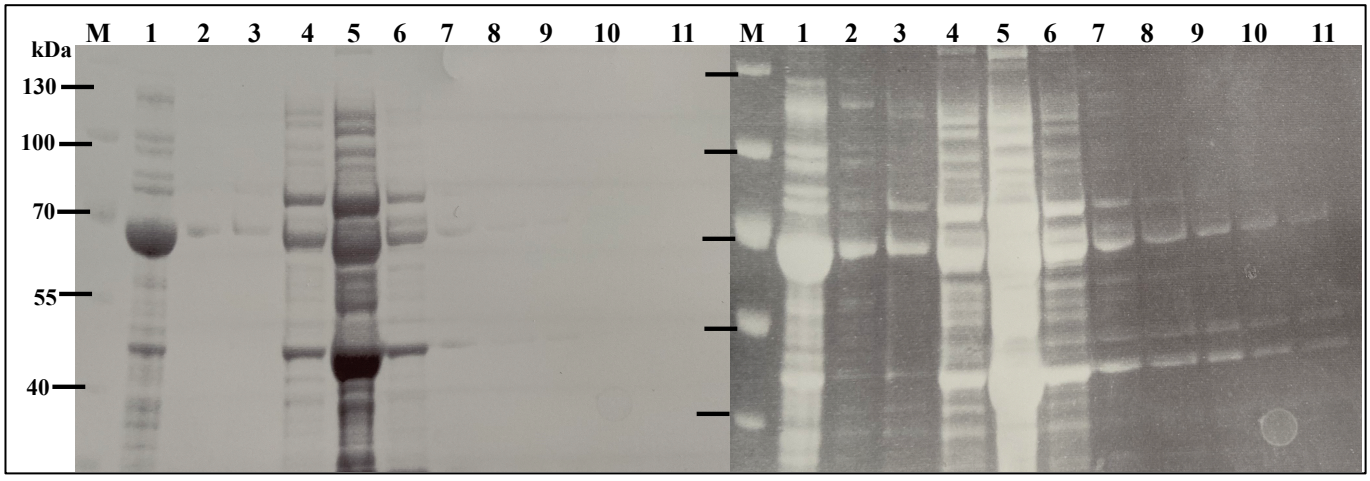

Figure 3.10: PL002 purification using automated systems

HiTrap™ High Performance column used in AKTA Prime Chromatography in gradient elution.

Lane 1 and 2: Flowthrough and wash fractions of PL002. Lane 3-7; imidazole elusion steps (150 mM).

3.4 Discussion

PL001, the *Tara* Ocean lipase, was expressed insolubly using BL21 pLysS (DE3) after post induction conditions of 72-hour growth period at 10 °C using TB media. Cell free synthesis was trialled to increase protein solubility, however to no avail. PL002, the salp lipase, was successfully expressed and purified using the ArcticExpress (DE3) competent cells at post induction conditions of 10 °C for 24 hours. Optimised expression conditions included increasing cell density prior to induction using TB media. Purification was optimised at bench top scale using Ni-NTA Superflow cartridge. Therefore, the salp lipase candidate, PL002, was taken forward for characterisation and application purposes. PL001 was set aside for consideration for future work.

Bacterial sourced lipase from the *Tara Ocean* Database, PL001

The recombinant expression attempts of PL001 resulted in an insoluble protein at
(35 kDa) and a truncated protein (25 kDa). An increased incubation time, at 72 and 96 Hours with the temperature at 10°C, exhibited a 35 kDa protein in the insoluble range, which is likely to be PL001 (Figure 3.3). Insoluble protein production took place at 72 hours post induction which could have transpired due to over expression (Terpe, 2006). Therefore, there is probability of soluble protein production to occur at a shorter duration. Subsequent analysis could include Western Blot and activity assays to confirm the PL001 protein presence. Methods to convert the insoluble protein to a refolded active state can take place, proposals may formulate a less active and lower yields of the target candidates (Sahdev, Khattar and Saini, 2008). PL001 expression was also trialled with ArcticExpress (DE3) at post-induction incubation temperatures of 15 °C, 10 °C, and at 5 °C to increase solubility, however, this was unsuccessful.

Due to the slow growth at these lower temperatures, suggestion for an increase in the post induction incubation times could be trialled to reduce the truncation issues. It can also be postulated that due to errors in the ORF prediction truncation of proteins transpired (Saunders *et al.*, 2003). A highly likely situation as bioinformatic prediction methods to identify the protein, (Chapter 2), relied upon annotation tools and BLASTP results. The outcomes of which were unannotated BLASTP hits. Therefore, there may have been differences in codon usage

that resulted in truncation leading to proteolysis or premature termination of protein translation (Angov *et al.*, 2008).

Alternative expression systems can provide a robust expression system. For example, selecting a closest taxonomic relative can provide a greater yield of protein expression. For example, Fe-S flavoenzymes from *Clostridium scidens* were discovered by expression in a *Clostridium* expression strain (Funabashi *et al.*, 2020; Robinson, Piel and Sunagawa, 2021). This may be a suitable method of expression for PL001 as alternative strains like *Candidatus sp.* identified in the BLASTP results can be used for successful recombinant protein production Chapter 2.

CFPS demonstrated unclear expression levels of PL001, (Figure 3.4). BL21 *E. coli* cells have a range of host proteins which discourage the certainty of identifying/visualising successful PL001 expression when using CFPS (Swartz, 2001). A host cell protein, Glyceraldehyde-3-phosphate dehydrogenase, is of a similar molecular size to PL001, between 34 to 38 kDa (accession: A0A140N783) and expression of this protein may be occurring (Bateman *et al.*, 2021). Therefore, it is inconclusive if CFPS is a viable alternative to cell-based systems and Western Blot analysis should be used to confirm PL001 expression.

Pancreatic-like lipase from *Salpa thompsoni*, PL002

Cloning attempts of PL002 were plagued by plasmid self-ligation; and as such, alternative synthesis methods were employed. The process of cloning is rather lengthy and expensive, the molecular biology kit for PCR retails at £232.00 for 25 reactions (in 2018). Thus, it was decided that gene synthesis would be a more cost effective and time saving solution. Further details are provided in appendix B.

PL002 was successfully expressed using ArcticExpress (DE3) in TB media following post induction conductions of 24 hours at 10 °C, (Figure 3.5). Scale up was successful in production of 20 L of protein in a 30 L bioreactor using the same operating conditions which enables mass protein production to be frozen for future analysis. The traditional temperature for *E.coli* host systems is between the range of 23 to 40 °C (Kumar and Libchaber, 2013) and has been employed in the scale-up of lipases for commercial purposes. However, to produce PL002 using this psychrophilic cell line requires a greater energy consumption. The energy required

to heat and cool the bioreactors at a stable 10 °C temperature for over 24 hours can incur expenses that would not occur for expression systems that require more moderate temperatures for shorter durations (Xia *et al.*, 2015).

Recombinant expression of PL002 yielded very little protein. Alternative protein expression systems, such as the use of secretory yeast cells may provide an increased yield. For example, lipase gene from *Y. lipolytica* was expressed in secretory yeast strain *S. cerevisiae* with high yields (Darvishi, 2012). The high expression levels of this eukaryotic protein in a eukaryotic expression strain may suggest an alternative for route for expression. In addition, the ability for yeast systems to secrete recombinant proteins may reduce any loses that occur due to cell disruption techniques as commonly employed by bacterial systems.

Purification

The soluble salp lipase, PL002, was purified using three different forms of affinity chromatography: Spin Columns, Superflow Cartridges and AKTA Prime chromatography.

Initial purification of His-tagged proteins was conducted using spin columns. The method is optimised for use at 4 °C in a microcentrifuge which reduces the risk of protein degradation (Lee *et al.*, 2010). There is a requirement to optimise the imidazole concentration through multiple wash and elution stages before obtaining pure protein. Therefore, the Superflow cartridges were employed using the optimised conditions as determined from the spin columns. The use of an injection pump here creates a semi-automatic system operated at room temperature which, in this method, was optimal for low nonspecific binding. It has been reported that nickel based affinity purification has a higher binding affinity than cobalt systems (such as the spin columns) (Bornhorst and Falke, 2000). Thus, suggesting a greater yield using the gravity assisted methods.

Ideally, the gradient elution chromatography method produces a less labour-intensive method than that of the two step systems employed. However, the gradient elution analysis depicted multiple host cell proteins bound to the column and eluted into the fractions, (Figure 3.10). There is a high risk of contamination in this cold operated system, and use of psychrophilic proteins, may encourage a higher binding of nonspecific proteins, such as Cpn 60, that mask the presence of PL002. Step elution protocols for purifications have been utilised to remove this chaperonin (Hartinger *et al.*, 2010). A higher imidazole concentration of binding buffer

demonstrated little to no protein of interest binding to the column. Alternative methods to remove the 60 kDa chaperonin include an additional wash stage of 1 M urea after the wash stages (Belval *et al.*, 2015). Due to the need to further optimise the gradient elution method, it was established that the Ni-NTA Superflow cartridges were preferable.

3.5 Conclusion

PL001 was recombinantly expressed in an insoluble form (33 kDa) and another in a truncated form (25 kDa) using heterogenous bacterial expression. This lipase was then trialled in a cell free protein system to improve production and solubility but to no avail. The insoluble proteins could have expressed due to the long expression stages (72 hours). Assessing that the correct proteins have expressed can be evaluated using Western Blot analysis; following this affinity purification and then activity assessments should be made. If this protein is then inactive, refolding stages could occur to solubilise the protein. It has been proposed that errors in the ORF prediction may have caused the proteins to form truncations. Successive analysis of Western Blots should be conducted to confirm the presence of the protein.

The salp lipase, PL002, was successfully expressed and purified. Expression conditions included the cold adapted *E. coli* cell line, ArcticExpress (DE3), operated at post induction conditions of 10 °C for 24 hours which followed a bind and elute Ni-NTA affinity chromatography purification. ArcticExpress (DE3) has biological chaperonins that aid the protein folding and stability of recombinant proteins such as PL002. Affinity purification was also an ideal method as it is a single step nickel based system that was optimised for use using a Superflow cartridge. The method to express and purify cold active lipases were easily optimised for large scale bulk manufacture and therefore can be applied to produce future low temperature enzymes. The successful expression and purification of the salp lipase ensures that cold active characterisation using functional assays can be performed.

Chapter 4: Characterisation of Cold Active Lipases

4.1 Introduction

Salpa thompsoni is a marine invertebrate found in the Southern Ocean surrounding Antarctica. Commonly referred to as a salp, it is a zooplankton from the tunicate group. *Salpa thompsoni* appears to have evolved as a low temperature adapted species (Goodall-Copestake, 2018) and was selected as a source to mine cold active lipase candidates (Chapter 2 and 3). These candidate enzymes are hypothesised to perform enzymatic reactions at lower temperatures. After successful expression and purification of soluble pancreatic-like lipase, PL002, (Chapter 3), it was deemed that the lipase is of psychrophilic nature (growth below 15°C) (Lee, Jang and Chung, 2017). Functional characterisation, using *in vitro* methods, can provide further insight into cold activity of protein candidates.

In addition to biochemical characterisation, homology modelling provides key insight into folding patterns of novel protein structures. Through sequence alignment and mapping onto crystal structures published in the protein data bank, three dimensional (3D) structures of unknown proteins which can be used to establish an understanding of protein folding (Wen, Scoles and Facelli, 2014). Structural features of cold proteins are used to determine cold activity, in particular cysteine residues. It has been identified that these residues unique capabilities of disulfide bridge formations add greater stability to the proteins. In the case of cold active alpha-amylase, the protein activity was significantly improved (Siddiqui *et al.*, 2005). Additionally, cysteines located around the lid domain provide increased thermostability (Veno *et al.*, 2019). Therefore, to determine cold activity, and subsequent investigations on immobilisation of cold active lipases, it would be vital to determine the positioning of these residues. A 3D graphical representation of proteins is also required to identify the positioning of critical catalytic residues which can be useful in determining substrate and protein interactions in addition to subsequent analysis on protein stability using immobilisation methods, (Chapter 5).

Characterisation of functional properties of lipases generally occurs using the ester cleaving potential present with lipases, through hydrolysis or esterification reactions (Lopes *et al.*,

2011). These reactions are traditionally optimised for assessing activity parameters. Frequently used functional assays for determining lipase activity include titrimetric or spectrophotometric assays. Titrimetric assays, using the hydrolysis of substrates such as tributyrin, are generally time consuming and unsuitable for large scale characterisation of lipases. However they have the capacity to be water soluble which can be beneficial for characterising flow based biocatalysis (Wrolstad *et al.*, 2004). Spectrophotometric assays include the use of ρ-nitrophenyl ester compounds. These systems are highly sensitive; however, the longer chain compounds have low solubility in water. In addition to this, the substrate has a risk of naturally decomposing with temperature changes or prolonged exposure to light (Sigma SDS: N9876). Following successful characterisation of lipases in their soluble homogeneous free form, immobilisation of the lipase on to a flow based catalyst is required so consideration must be taken to include substrates that are generally water-soluble and that do not tend to precipitate and cause disruptions in the flow systems. Longer chained ρ-nitrophenyl substrates require solubilisation in solvents, such as ρ-nitrophenyl palmitate. To avoid these shortcomings of longer chained compounds, the shorter carbon chain ρ-nitrophenyl butyrate (C4) (PNPB) can be used for initial characterisations of lipases (Quinn *et al.*, 1982).

The hydrolysis of this compound is demonstrated, (Figure 4.1). Here a yellow ρ- nitrophenolate (4-NP or 4 Nitrophenol) ion is formed following successful hydrolytic cleavage of the PNPB substrate. The yellow colour can be easily scanned using a UV based plate assay.

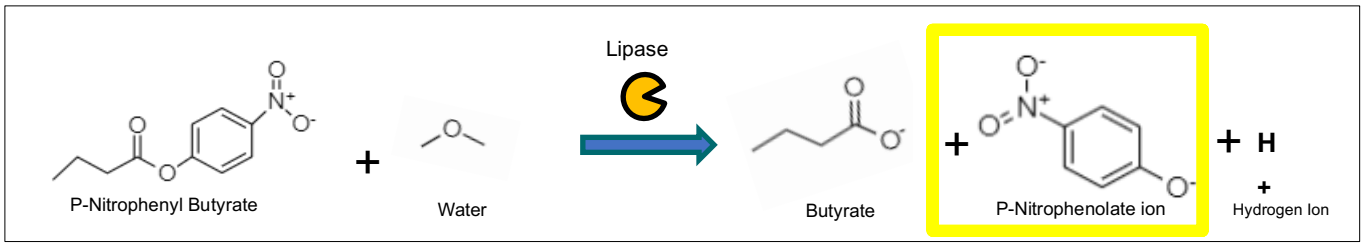

Figure 4.1: The hydrolysis of ρ-nitrophenyl butyrate to ρ-nitrophenolate ion

A lipase catalysed hydrolysis reaction to produce 4-NP. The reaction is adapted from (Pliego *et al.*, 2015)

PNPB substrate can be used in both end point and continuous assays. These assays can be used to determine optimum temperature, pH, and kinetic parameters of the lipases. End point assays are commonly used to rapidly determine a proteins optimum characteristics, as done so by (Tišma *et al.*, 2019; Kumar *et al.*, 2020) The reaction mix is stopped at a specified time point with a pH altering solution. This ensures that the enzyme is inactivated and therefore the reaction is quenched. The blocking of residual activity of the enzyme is required to ensure that there is no change in the colour intensity (Kanwar *et al.*, 2005). The Beer-Lambert law was used to predict the product formation based upon the molar absorption coefficients has been frequently used for determining cold protein parameters (Bender and Turnquest, 1957; Gupta *et al.*, 2003; Sander *et al.*, 2021) These reactions are very useful in determining the activity of proteins whereby extreme environmental conditions need to be monitored.

Continuous assays can be used to determine the rate at which a lipase hydrolyses substrates. The analysis of the kinetic parameters takes place by calculating the product formation from the absorbance readings at specified time points. The major practical caveat here is that depending on the initial findings of optimum temperature for maximal activity, plate readers are unable to reach sufficiently low temperature operating systems. Therefore, end point assays are generally explored to determine characteristics of psychrophilic enzyme candidates. Kinetic parameters are important as they will be used to compare the free system to the immobilised biocatalyst (Ozcan *et al.*, 2009). Kinetic parameters will be explored using Michaelis-Menten kinetics to determine the K_M and V_{max}. It is assumed that steady state parameters occur with the lipase and that there will not be a propensity to form dimerization.

In this chapter, the short carbon chain substrate PNPB was used for end point and continuous assays to characterise a candidate cold active lipase PL002 derived from *S. thompsoni* in comparison to a commercially available lipase *Candida antarctica* lipase B (Cal B).

4.2 Methods and Materials

Homology Model

Homology model of the hypothetical structures of the lipases was drawn on PyMOL **(**http://pymol.sourceforge.net/**)** using I-TASSER (A Roy, A Kucukural, 2010). Known x-ray crystal structures available on the Protein Data Bank are used as templates for this process. Template structures for PL002 was generated using a PDB entry of a crystal structure of a proteolyzed form of pancreatic lipase related protein (PDB entry:1W52), rat pancreatic lipase (PDB: 1BU8), human pancreatic lipase (PDB: 2PPL), porcine triacylglycerol lipase (PDB 1ETH), and dog pancreatic lipase (1RP1). Previous tBLASTp alignments provided PL002 with a 41% sequence identity to the horse pancreatic like lipase. Cal B homology modelling using PyMOL was conducted with the PDB entry: 1TCA. C-score and TM-value outputs from this modelling system were used to determine confidence in the structures.

End Point Assay

Cal B (Sigma Aldrich 62288) was used at concentrations of 0.5mg/ml. PL002 was used at a working concentration of 0.5mg/ml from the precipitated material generated in Chapter 3. A lipase activity assay was performed using ρ-nitrophenyl substrates with modifications (Winkler and Stuckmann, 1979). Substrate affinity was explored with the comparison of short chain ρ-nitrophenyl butyrate (C4) and longer chain ρ-nitrophenyl palmitate (C22). However, for subsequent reaction, shorter chain ρ-nitrophenyl butyrate was used. The reaction mixture consisted of 125 µl of 55 mM phosphate buffer adjusted to pH 7 (components from Sigma Aldrich) and 10 µl of the substrate 1 mM ρ-nitrophenyl butyrate (PNPB) (Sigma) homogenised in 2-propanol. The mixture was pre-reacted at 20°C for 10 minutes and then 15 µl of the 0.5mg/ml enzyme solution was subsequently added. After 15 minutes of incubation at 20°C, the reaction was terminated using an equal volume of 0.25M sodium carbonate pH 10.5 (Ozcan *et al.*, 2009) and ethanol. The absorbance of the liberated 4-Nitrophenol was measured at 410 nm using multi-well plate reader (Clariostar, BMG Labtech, UK). One unit (U) of lipase activity was defined as the amount of enzyme that released 1 µmol of 4-Nitrophenol per minute. Lipase concentration was measured by the method of Bradford with bovine serum albumin as a standard (Bradford, 1976).The temperature profile of the salp lipase was measured at 5 to 60

°C for 15 minutes. A pH stability test was performed by pre-incubating the lipase for 10 minutes at 4 °C in the buffers and assessing activity at the optimum temperature. The effect of pH on lipase activity was assayed at pH 6–9 by measuring the amount of 4-Nitrophenol liberated using PNPB (C4) as a substrate. The buffer systems used to assess pH effects were: 55mM sodium phosphate buffer (pH 6–8), 55mM Tris–HCl buffer (pH 9). Substrate affinity was determined by comparing ρ-nitrophenyl butyrate (C4) and ρ-nitrophenyl palmitate (C22) at 1 mM concentration. Maximum substrate concentration was also calculated by increasing PNPB concentration to 40mM.

Unless stated otherwise, activity profiles were expressed in relation to the maximum value (=100%). Each value represents the mean ± standard deviation (SD) of five replicate assays.

Continuous Assay

A continuous lipase assay to determine kinetic parameters was adapted from (Ruiz *et al.*, 2004). Substrate concentrations were made from a 2 ml substrate stock of 10 mM of PNPB. This was prepared in 2ml of isopropanol and adjusted to working concentrations of 5mM, 2.5mM, 1.25mM, 0.6mM and 0.3mM 0.15mM, 0.06mM, 0.03mM by serial dilution. The reaction mixture consisted of 125 µl of 55 mM phosphate buffer adjusted to pH 7 (components from Sigma Aldrich) and 10 µl of substrate. Samples were dispensed in triplicates. The detection limit of this lipase assay was characterized by a dilution series of 4-Nitrophenol. The plates were preincubated for 15 minutes at 23 °C. 15 µl of Cal B and PL002 was added in 5 reactions each at a concentration of 0.5mg/ml. The multi-well plate reader (Clariostar, BMG Labtech, UK) measured the absorbance at 410nm from the top of the plate. The plate was read at 10 reads per well for 37 minutes of reaction time. Michaelis-Menten kinetics were used to determine enzyme activity for this assay by calculating the reaction rate or velocity against various substrate concentrations. These curves were then fitted to the Michaelis-Menten equation $v0 = V_{max}[S]/ ([S] + K_M)$, using OriginPro 2017 (Academic) software, allowing determination of the maximum reaction rate of the enzyme (V_{max}) and Michaelis-Menten constant (K_M) which is the substrate concentration when the reaction rate is half of V_{max}. Turnover (K_{cat}) could then be obtained using the equation $K_{cat} = V_{max}/ [E]$. K_{cat} is defined as the turnover number which is the number of substrate molecules converted to the product per unit of time (Cornish-Bowden, 1979).

For these homogenous assays, it has been assumed that the activity parameters of the salp lipase with and without the cysteine modification is the same. This was a pragmatic assumption based upon time limitations.

Statistics

A Student's t-Test was used to determine significance difference between the positive control, the commercially available lipase Cal B, and the salp lipase PL002. A P-value of less than 0.05 was considered to represent a statistically significant difference between the positive control and the examined protein.

4.3 Results

Homology modelling was conducted to visually identify the active site region and cysteine placements of PL002, and positive control Cal B. Biochemical functional based assays can be used to derive the cold activeness of the psychrophilic candidates. This determined that PL002 is a cold active lipase due to optimal activity at temperature conditions of 20°C.

Homology Modelling

Visualisation of PL002, modified salp lipase, PL002/cys and Cal B was used to identify as locations of conserved residues (Chapter 2) that provide catalytic activity. Conserved active site residues, serine-aspartate-histidine, have been identified in models, shown in red (Figure 4.2). These correspond to the catalytic triad as identified in Chapter 2. The putatively catalytic cysteine residues have been highlighted green, (Figure 4.2). It has been suggested that the cysteine residues contribute towards a disulfide bridge, this has been observed in mammalian pancreatic lipases, particularly that of the secondary fold, the β9 loop (Lowe, 2002). The model generated for Cal B was conducted using known crystal structures and catalytic residues previously generated by Uppenberg *et al.*, (2002) and therefore structure predictor I-TASSER was not required.

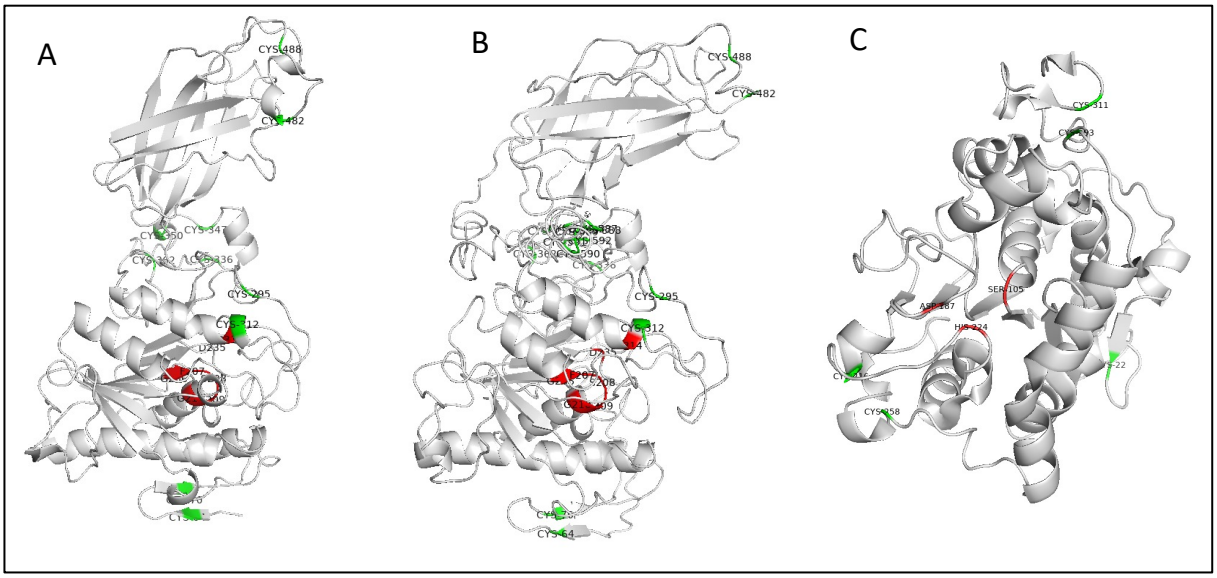

Figure 4.2: 3D Models of PL002 (A), cysteine modified PL002 (B) and Cal B (C)

Cal B model has been adapted from (Uppenberg *et al.*, 1995)

Cysteine residues are highlighted in green and the active site in red. These structures have been annotated using structure visualisation software, PyMOL.

The C-score and TM-score of PL002 and PL002/Cys were -2.46, 0.46 +/- 0.15 and -2.62, 0.45 +/- 0.14, respectively. These scores were calculated as averages across 5 hypothetical model outputs for each protein structure. The limits to this confidence score are -5 to 2 whereby a greater C-score provides better confidence in the model (Yang *et al.*, 2015). TM-scores are used to determine structural similarities and accuracy of the predicted structures. A TM-score >0.5 indicates a model of correct protein folding and a TM-score <0.17 suggests a random similarity (Zhang and Skolnick, 2004). The results obtained here for PL002 suggest a moderate confidence in the model and protein folding.

<u>End Point Assays</u>

It was identified that PL002 has optimum temperature 20°C and at pH 7 using 1mM of PNPB as the substrate, (Figure 4.3 and 4.4). These lipases candidates prefer shorter chained substrate, PNPB, (Figure 4.6). The optimal activity determined for Cal B is 8.57 +/- 0.23 U/mg and PL002 was 3.16 +/- 0.14 U/mg using 1mM of PNPB, at 20 °C with a pH 7. Activity profiles were determined as the mean ± standard deviation (SD) of five replicate assays. Unless stated

otherwise, these are expressed in relation to the maximum value (=100%). P-values < 0.03 were determined.

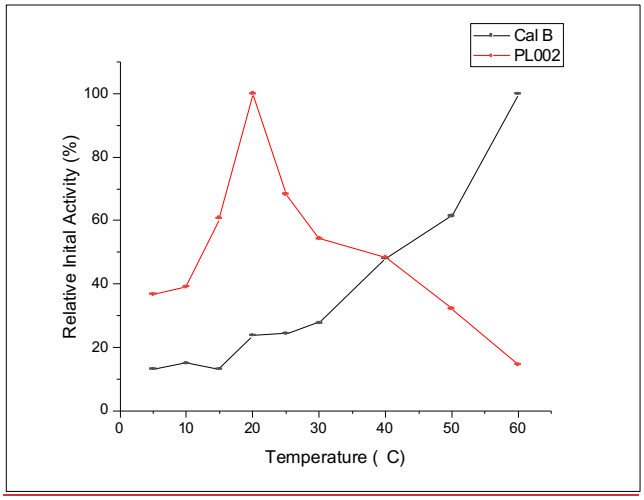

Figure 4.3: Effect of temperatures on lipase activity

Cal B and PL002 activity at pH 7 at increasing temperature increments using 1mM of PNPB. PL002 shows distinct activity at 20°C whereas Cal B prefers warmer temperatures although activity still being present at lower temperatures. Each data point represents the mean ± standard deviation (SD) of five replicate assays. Activity profiles were expressed in relation to the maximum value (=100%).

At 20 °C, the optimum lipolytic activity for PL002 is consistent with unpublished characterisations of other *in vitro* expressed salp digestive enzymes (Cotton, 2021). There was retained activity above 60% between 15 and 25 °C although PL002 loses close to 90% of its activity at temperatures greater than 50 °C.

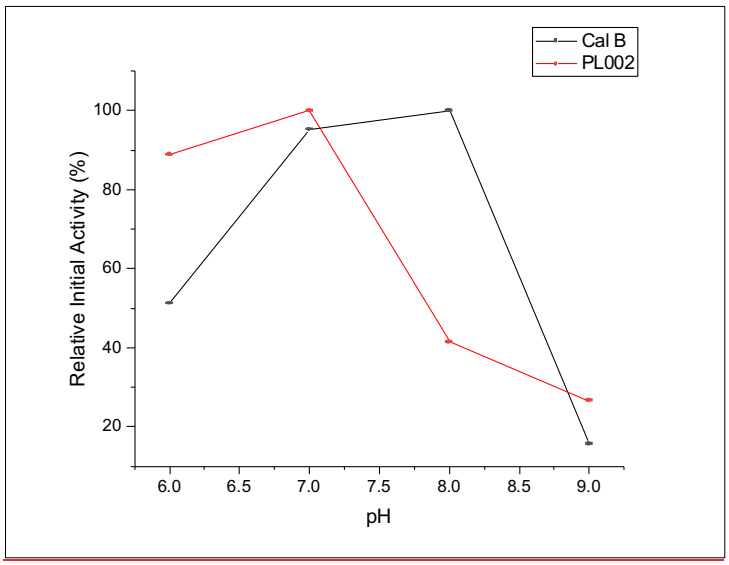

Figure 4.4: Effect of pH on lipase activity

Cal B and PL002 activity with 1mM of PNPB at 20°C. PL002 has pH preference of 7 whereas Cal B prefers pH conditions of 8. Each data point represents the mean ± standard deviation (SD) of five replicate assays. Activity profiles were expressed in relation to the maximum value (=100%).

The pH 7 optima inferred for this enzyme was also similar to other *in vitro* expressed salp digestive enzymes (Cotton, 2021). Alongside activations of other pancreatic lipases from eukaryotic sources this is within the range; 6.2 and 7 (van Kuiken and Behnke, 1994; Xin *et al.*, 2020).

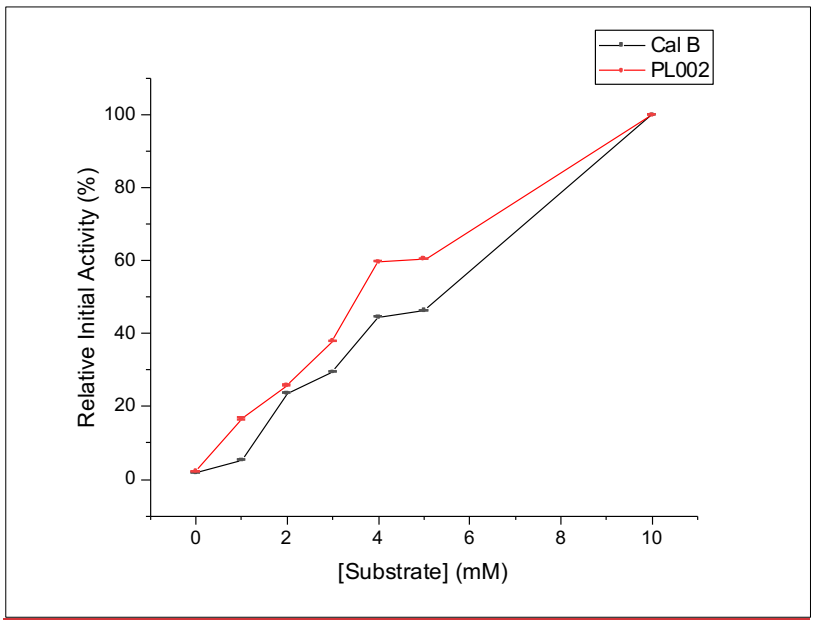

Figure 4.5: Effect of substrate concentration on lipase activity

Cal B and PL002 activity at pH 7 at 20°C with varying concentrations of PNPB. Each data point represents the mean ± standard deviation (SD) of five replicate assays. Activity profiles were expressed in relation to the maximum value (=100%).

Activity assays exploring substrate size revealed that both Cal B and PL002 preferred the shorter chained substrate, PNPB (C4), than a longer chained substrate, PNPP (C22), (Figure 4.6). There was 4 fold greater affinity for the shorter substrate.

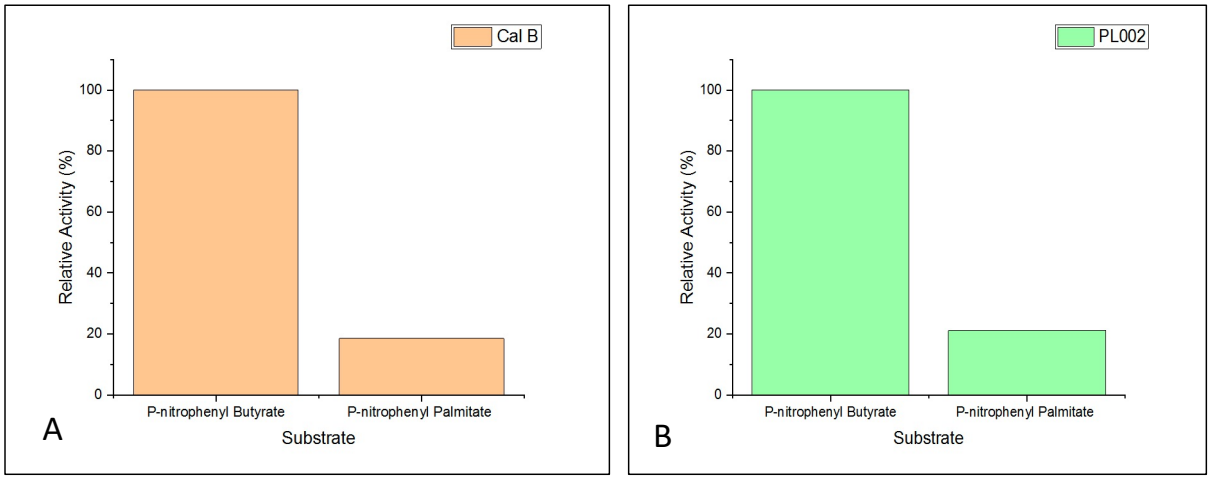

Figure 4.6: Assessing activity of different substrates

Cal B and PL002 activity at pH 7 at using 1mM of PNPB and 1mM of PNPP at 20°C. PNPB has carbon chain length of 4 and PNPP has a longer carbon chain length, 22. There is clear preference for. The shorter chained substrate for both enzymes candidates.

Continuous Assay to determine kinetic parameters

Activity profiles were expressed in relation Michaelis-Menten kinetics. Experiments were conducted at pH 7 at 23°C.

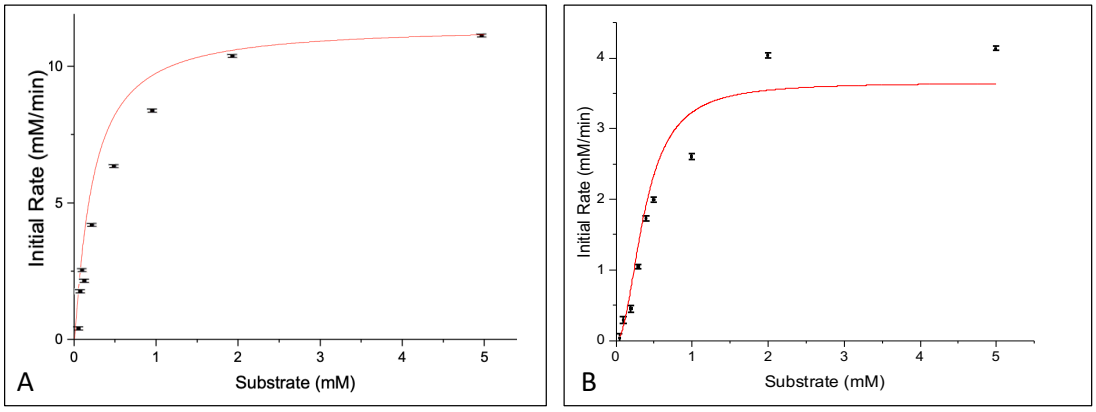

Figure 4.7: Assessing kinetic parameters of Cal B (A) and PL002 (B)

This was conducted in continuous assay using PNPB substrate concentrations 5mM, 2.5mM, 1.25mM, 0.6mM and 0.3mM, 0.15mM, 0.06mM, 0.03mM at 23°C pH 7. Each value represents the mean ± standard deviation (SD) of five replicate assays. Enzyme concentrations were at 0.5 mg/ml.

The highest K_{cat}/K_M was 71.61 mM/s $^{-1}$ with Cal B therefore suggesting a 10 fold greater catalytic efficiency than the salp lipase, 7.13mM/s^{-1}. Additional kinetics parameters were defined, (Table 4.8). It was established that when hydrolysing PNPB, maximal initial reaction velocity is 11.47mM/min and 3.65mM/min for Cal B and PL002.

Table 4.8: Kinetic values of Cal B and PL002

Enzyme	K_M (mM)	V_{max} (mM/min)	K_{cat} (s^{-1})	K_{cat}/K_M (s^{-1}/mM)
Cal B	0.2202 +/- 0.009	11.47 +/- 0.013	15.77	71.61
PL002	0.3761 +/- 0.009	3.65 +/- 0.021	2.68	7.13

As identified, (Figure 5.3), Cal B has a great span of activity across the temperature range. It should be noted that the kinetic parameters presented here for Cal B are only representative of the conditions favourable to PL002, i.e., at pH 7 and temperature of 20°C.

4.4 Discussion

Homology modelling using I-TASSER to determine protein 3D structures provided tentative locations for the catalytic triad and cysteine residues in the lipases PL002, modified PL002 and Cal B, (Figure 4.2). Structural identification of conserved nucleophilic serine residues, residing within the activity site of the lipase, can aid in the understanding of lipase activity (Joseph, Ramteke and Thomas, 2008). In addition, cysteine residues have been found to confer a greater thermostability to cold active proteins (Siddiqui *et al.*, 2005; Veno *et al.*, 2019); assessed further in Chapter 5. The assessment of these models was conducted on PyMOL using PDB structures. Whereby the PDB structure of Cal B was formulated using a previously x-ray crystallised protein, (Uppenberg, Patkar, *et al.*, 1994). However, for the salp lipase, the confidence values for the hypothetical structures generated by I-TASSER are at the lower end of the spectrum. The C-score is negative values of both models in comparison to the optimal value of close to 2 and TM-score is below the values indicating correct protein folding. Zarafeta et al., generated models in a similar method for bacterial esterases to provide prediction scores of C-score 0.61 and TM-score 0.8 ± 0.09 (Zarafeta *et al.*, 2016). This suggests that the template sequence similarities used to generate models for PL002 and PL002/cys has a degree of variation to the actual protein. As this is the first lipase characterised biochemically from the *Salpa thompsoni,* it is expected that the crude 3D structures would require further refinement to fully understand the protein folding.

Biochemical analysis of *in silico* characterised lipases is important in establishing the cold nature of these digestive enzymes. The novel cold active pancreatic-like lipase from *S. thompsoni* characterised here presented activity towards the synthetic substrate ρ-nitrophenyl compounds. This lipase loses close to 90% of its activity at temperatures greater than 50 °C, (Figure 4.3), which implies that the protein is cold active (Gatti-Lafranconi *et al.*, 2010) and a candidate for consideration in the bioprocessing industry. PH is crucial to maintaining the proper form of the lipolytic lid in lipases, which is composed of charged residues required for substrate binding. Changes in pH will disrupt the ionic bonds that form the lipase structure, the impact of which was apparent for PL002 in this assay at only a moderate alkalinity of pH 8, (Figure 4.4). Therefore, to have a comparable positive control, Cal B was operated at conditions favourable to PL002; despite a pH optimum of 8, (Figure 4.4).

Michaelis-Menten kinetics were evaluated to determine steady state parameters. Here the maximum velocity (V_{max}) of Cal B is close to 4 fold greater than that of the salp lipase. Although temperature and substrate conditions differ, this parabolic velocity profile is consistent with other literature examples using Cal B (Gkini *et al.*, 2020). The turnover constant, K_{cat}, was also calculated to be 5 fold greater than that of the salp lipase which demonstrates the heightened catalytic efficiency of Cal B. The K_M constant is a useful indicator for substrate affinity to the lipase. The affinity towards PNPB was greater with Cal B than with the salp lipase, as demonstrated by the K_{cat}/ K_M ratio. Cal B has a modified structure to that of a 'True Lipase', whereby the traditional nucleophilic lid is much smaller, and in some mutations non-existent. The conserved pentapeptide consistent with lipases and corresponding to amino acid sequence, GXSXG, is present in Cal B as TWSQG (Uppenberg, Oehrner, *et al.*, 1994). This suggests that without the lid present the regulation to the active site does not occur as the lipase is always structurally open for substrate presence and therefore does not react as the majority of lipases do with the use of interfacial activation (Stauch, Fisher and Cianci, 2015). Protein engineering and associated activity and structural confirmation studies have been used to optimise Cal B to the extent that it is not surprising that this enzyme outperforms PL002 in *in vitro* characterisation (Palomo *et al.*, 2002; Suen *et al.*, 2004; Xie *et al.*, 2014). As previously noted in the thesis introduction, (Chapter 1), Cal B has been used to catalyse reactions on an industrial scale due to its active state in a wide range of temperatures (Ganjalikhany *et al.*, 2012).

Both lipase candidates, Cal B and PL002, were found to prefer the shorter chained substrates in the activity assays, (Figure 4.6). However, traditionally, true lipases are considered to have a preference for hydrolysing longer chain fatty acid-based substrates while esterases prefer shorter chain substrates, such as PNPB with a carbon chain of 4, (De Santi *et al.*, 2014). To further explore this apparent discrepancy between the lipases Cal B and PL002 and traditional expectations, a literature review was conducted to obtain lipase activity estimates against PNPB. Data from a wide range of bacterial, fungal and plant mesophilic lipases - that have been cultivated in both a recombinant fashion as well as natural expression methods – were obtained, all of which presented considerable activity towards PNPB substrates, (Figure 4.9, appendix Table C). Ali et al, proposes a method of lipase classification dependent on bio-physico-chemical preferences based upon their ability to hydrolyse lipids. This separates non lipolytic esters from lipolytic esters and then further definition to hydrolase and lipase candidates (Ali, Verger and Abousalham, 2012). This suggests that traditional assumptions

regarding classification of alpha/beta hydrolases dependent on substrate preferences need to be reconsidered.

The PNPB lipase activity estimates obtained from the literature review were categorised according their taxonomic origin and also following the psychrophilic, mesophilic or thermophilic classification of (D'Amico *et al.*, 2003). This revealed that the level of activity for PL002 is higher than that for the other animal lipases for which data was extracted from the literature review, (Figure 4.9). Furthermore, PL002 also emerged as the coldest active animal lipase and one of the coldest active lipases overall, as was anticipated given the Antarctic habitat of *S. thompsoni* from which PL002 was isolated. The majority (66%) of reports of lipase activities with the PNPB substrate come from enzymes produced recombinantly in either bacteria or yeast. *Bacillus licheniformis* has great thermophilic activity (Figure 4.9). As with other extremophiles, this candidate has the ability to perform at high pH as well as temperature (Ugras, 2017). Mutations have also been found for this bacterial lipase to be cold tolerant (Zhao *et al.*, 2021). Similar analysis can occur with the salp lipase. Subsequent temperature studies should include a salp lipase from a warmer climate. This will encourage further understanding in characterising eukaryotic cold candidates.

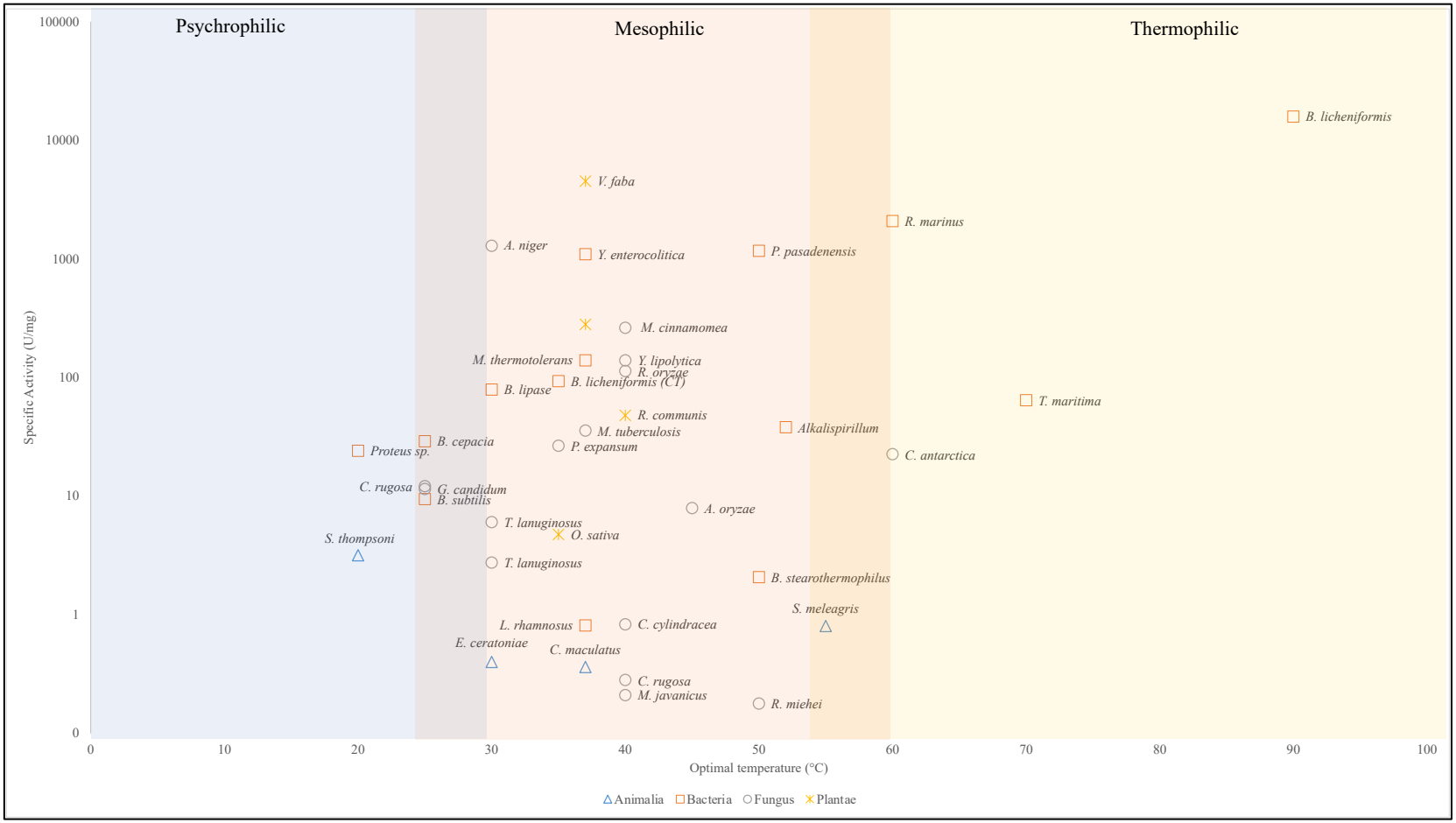

Figure 4.9: Specific activity (U/mg) of PNPB active lipases from Bacteria, Animalia, Fungus and Plantae

A metanalysis on recently classified lipase candidates with activity towards PNPB has been summarised with relation to temperature optima. Temperature domains adapted from (D'Amico *et al.*, 2003). Animalia and plantae lipases have been labelled. The lipases described here do not consider equal purity and reaction conditions do differ. Further information for each lipase and its class can be found in the appendix C.

Beyond the impact of the inherent protein sequence of salp lipase PL002 on its activity, it is also worth considering the impact of the modifications made to this during the expression and purification of this enzyme, for example the addition of a histidine tag to aid affinity purification, (Chapter 3). Specifically, the addition of affinity tags, including hexahistadine tags which have been shown to diminish ρ-nitrophenyl ester hydrolysis activity (de Almeida *et al.*, 2018). It has been demonstrated that an N terminal His tag alters the specific activity, the chain length selectivity and the thermostability of the *Staphylococcus aureus lipase,* (Horchani *et al.*, 2009). In another case, it was reported that there was a 33% increase in specific activity as preference towards medium length chain fatty acid pNP-laurate (C12) of untagged recombinantly produced lipase from *Geobacillus kaustophilus* (Özdemir, Tülek and Erdoğan, 2021). There has also been evidence that indicates that this hexahistadine tag can alter the quaternary structure of proteins (Carson *et al.*, 2007), impacting their specific activities. As such, it is plausible that such a modification may have altered the activity of the recombinantly produced affinity tagged protein PL002. Subsequent analyses could explore this further through a comparison against histidine cleaved proteins generated at both the expression and characterisation stages of *in vitro* enzyme production.

Activity profile and kinetic parameters defined using synthetic substrate, PNPB, suggest that substrates commonly metabolised by *S. thompsoni* may have a difference in activity. It has been identified in other marine invertebrates that optimal activity of lipases was displayed when the substrates of a similar source to their feed source was used as an alternative to the synthetic substrate used here. This was established in white leg shrimp *Penaeus vannamei* (Rivera-Pérez and García-Carreño, 2011). Further biochemical characterisations of marine invertebrate lipases are required to investigate activity profiles of digestive enzymes. Using candidate lipase substrates typically found within *S. thompsoni* and its food items would allow for a more thorough and ecologically revealing characterisation of PL002 activity. Recombinant mammalian pancreatic lipases have been characterised using triacylglycerides (Kawaguchi *et al.*, 2018) such as tributyrin. Catalytic properties of the pancreatic like lipase can be determined using alternative substrates for affinity purposes.

Additional functional assays should be utilised to determine the potential of the salp lipase as an industrial biocatalyst. For example, the supplementation of co-factors, specifically metal calcium ions, has shown to increase activity of eukaryotic pancreatic like lipases (Alvarez and

Stella, 1989). Site directed mutagenesis should be investigated to establish key residues required for cold activity. This approach considers the *in silico* cold protein characterisation, (Chapter 4), and its functional use. The exchange of glycine residues located around the active site to other residues may help to understand the flexible nature of the lipase (Yan and Sun Qing, 1997). Protein thermostability can also be assessed in a similar nature. Seven amino acids were substituted in a mutant variant of psychrophilic protease subtilisin S41 using site directed mutagenesis and evolutionary methods. Here it was identified that the activity, turnover rate (K_{cat}/K_M), and metal ion affinity had increased greatly. This approach could be adapted to subsequent analysis with PL002 to understand. the thermostability capacity of the lipase without effecting the activity (Miyazaki *et al.*, 2000).

Characterisation of other lipases encoded within the genome of *S. thompsoni* would also be revealing, not only to place the activity of PL002 into context but also to assess if this zooplankton species possesses a multi-lipase digestive system consistent with the diversity of food items it obtains through filter feeding. Such a multi-lipase digestive system would not be unexpected given the metanalysis of marine invertebrates conducted by Rivera-Perez, (2015) that identified multiple lipase genes in the eukaryotic digestion system that display different specificities towards different substrate sizes (eukaryotic lipases have been identified in Table 1.2.3 in the introduction). However, it is conceivable that *S. thompsoni* may have a more specialised lipase profile, such that found for the lipolytic enzymes sourced from the gastric pouches of the jellyfish (*Stomolophus sp. 2*), that favoured shorter and medium length triacylglycerides than lipases from other invertebrates (Martínez-Pérez *et al.*, 2020).

4.5 Conclusion

A novel pancreatic-like lipase gene was *in vitro* characterised following heterologous expression and purification using an *E. coli* cell line. This is the first time, to our knowledge, such an approach has been used to characterise a lipase from a marine tunicate. The lipase was identified from *S. thompsoni* and exhibited psychrophilic characteristics in accordance with the cold Antarctic marine habitat of this organism, retaining over 60% activity between 15 to 25 °C and optimal conditions of pH 7. Cold active nature of the salp lipase established in this chapter provides initial empirical data that can be used to understand the metabolic nature of the salp. Accordingly, this study provides initial understanding to unlocking the biochemical potential of lipolytic candidates available to be mined within invertebrates. It was also determined that commercially available lipase, *Candida antarctica* lipase B (Cal B) was also active at this temperature. The positive control, Cal B, was typically 4 folds higher in activity when using ρ-nitrophenyl butyrate, a 4 carbon chain length, synthetic substrate. The structural configurations of commercial Cal B suggest that the lack of lid present encourages a greater substrate affinity than the salp lipase (Uppenberg *et al.*, 1995). Traditionally, shorter substrates affinity indicates the presence of an ester instead of a lipase. However, it has been identified that other marine vertebrates has also shown similar preferences to shorter substrates due to the digestive profiles of the organisms to contain more than one lipase. The recombinant procurement of PL002 suggests that perhaps the folding of the lipase may be different causing activity fluctuations. In addition to this, the 6xhis tag used for purification purposes was not cleaved whilst determining protein characteristics which has been identified to cause difference in activity. *In vitro* characterisation of cold active lipases provides scope to understanding the metabolic profile of a complex collection of digestive enzymes that can provide green alternatives to currently used industrial biocatalysts.

Chapter 5: Stability and Activity of Immobilised Lipases

5.1 Introduction

Immobilisation of lipases, can increase the reusability of biocatalysts (Nair *et al.*, 2007). One emerging technique for enzyme immobilisation is the use of cellulose nanofiber as described in Chapter 1. Chemically functionalised cellulose nanofiber (CNF), provided by Cytiva (UK), are formed an immobilisation matrix which is used in comparison to free lipase. In this chapter, the stability and activity of commercially available lipase *Candida antarctica* lipase B (Cal B) and novel cold active lipase, *Salpa thompsoni* (PL002) will be assessed.

CNF membranes have greater mass transfer properties due to the convective flow of the media across the surface of the membrane. The surface area of the membrane is beneficial for immobilisation matrixes as they are not exhibited within the material as with porous bead alternatives (Hardick, Stevens and Bracewell, 2011) thus providing an alternative to current immobilisation matrixes. Surface modification of CNF can encourage a greater stability of the enzymatic system which has been demonstrated previously where *Candida rugosa* lipase was immobilised onto electrospun CNF. Here the thermostability and activity of the immobilised catalyst were significantly enhanced when using ρ-nitrophenyl palmitate substrate in a hydrolysis system (Huang *et al.*, 2011).

Site directed covalent immobilisation system can take place by binding enzymes to the CNF membrane using known residues which interact with the CNF membrane. The molecular structure of cellulose nanofiber, as discussed in Chapter 1, can facilitate chemical treatment to functionalise the membrane for adhesion purposes. Initial understanding on covalent immobilisation methods using the cysteine amino acid has been conducted with chemical cross linking agent, glutaraldehyde (Habeeb and Hiramoto, 1968). This principle has been modified for the formation of the chemically activated CNF membranes for immobilisation purposes. The chemical modifications on the membrane surface provide controllable and homogeneous protein orientation via the thiol groups, found in cysteine residues (Foley *et al.*, 2007). Therefore, they can perform as strong linkers for site directed covalent immobilisation. This is similar to work conducted by Upadhyay and Verma, (2014), whereby cysteine residues were bound with -NH2 based linkers using glutaraldehyde. To this end, site directed covalent

immobilisation was explored as a means of enhancing the membrane performance in tandem with ligand density.

Physical and biological modification to the flow biocatalyst will be assessed to determine effects on stability and activity. PL002 and *Candida antarctica lipase B* (Cal B) has been characterised to hydrolyse ρ-nitrophenyl esters at 20°C, as demonstrated in Chapter 4. The low temperature activity has the potential to provide a greener alternative to commercially available immobilised biocatalysts performing the same reactions at a higher temperature.

Physical modification to the membrane, by assessing enzyme density on the immobilised matrix, can be used to determine stability and activity of the protein. Cal B loading density was trialled to establish the efficiency of the immobilisation matrix. Cal B is a cold active lipase candidate as demonstrated in Chapter 4. This lipase does not have the propensity to form dimers as there is no lid domain it does not form any open or closed confirmation. And thus would not form dimeric aggregation (Zisis *et al.*, 2015). This is highly advantageous for immobilisation as the open confirmation of the protein is orientated to have maximal substrate conversation (Cao, 2006) . This lipase has shown relative activity at 25°C whilst immobilised onto monolith systems using synthetic substrate ρ-nitrophenyl butyrate (PNPB) (Alotaibi *et al.*, 2018). In addition to density studies, it will operate as a positive control to the salp lipase (PL002), as seen in former chapters. 2% of all Cal B residues are cysteine amino acids. As a result, with more Cal B enzymes, the potential to provide further interactions may increase the rate of reaction. Conversely, this could also have adverse effect as the flexibility of the lipase may be hindered by overcrowding. Mateo *et al.*, (2005), has conducted similar studies with glyoxal groups on protein surfaces. Therefore, to establish the optimal conditions of the immobilisation matrix and if the stability and activity of the lipase changes, enzyme density tests will be trialled. Cal B has cysteine residues located on the surface. Figure 5.1 illustrates potential protein orientations available to bind to the matrix. Cal B has fewer cysteine residues located around the active site which ensures that when covalent bonding occurs, the active site remains unaffected.

Biological modification to the protein is an alternative method to assess protein stability and activity to the immobilised matrix. It was hypothesised, that due to this thiol based covalent bonding mechanisms, an increase in cysteine residues may further improve the stability and activity of the lipase whilst immobilised. Therefore, the salp lipase, PL002, was compared with a modified version, PL002/Cys. PL002 has 2% of cysteine residues and PL002/Cys has 3.3% cysteine. The modified salp lipase was supplemented with an additional 6XCysteine tag at the C terminus to encourage greater binding to immobilisation membranes, (Figure 4.2 in Chapter 4). Hypothesised protein orientations are modelled, Figure 5.1. This gene was synthesised by Genscript (USA) for use.

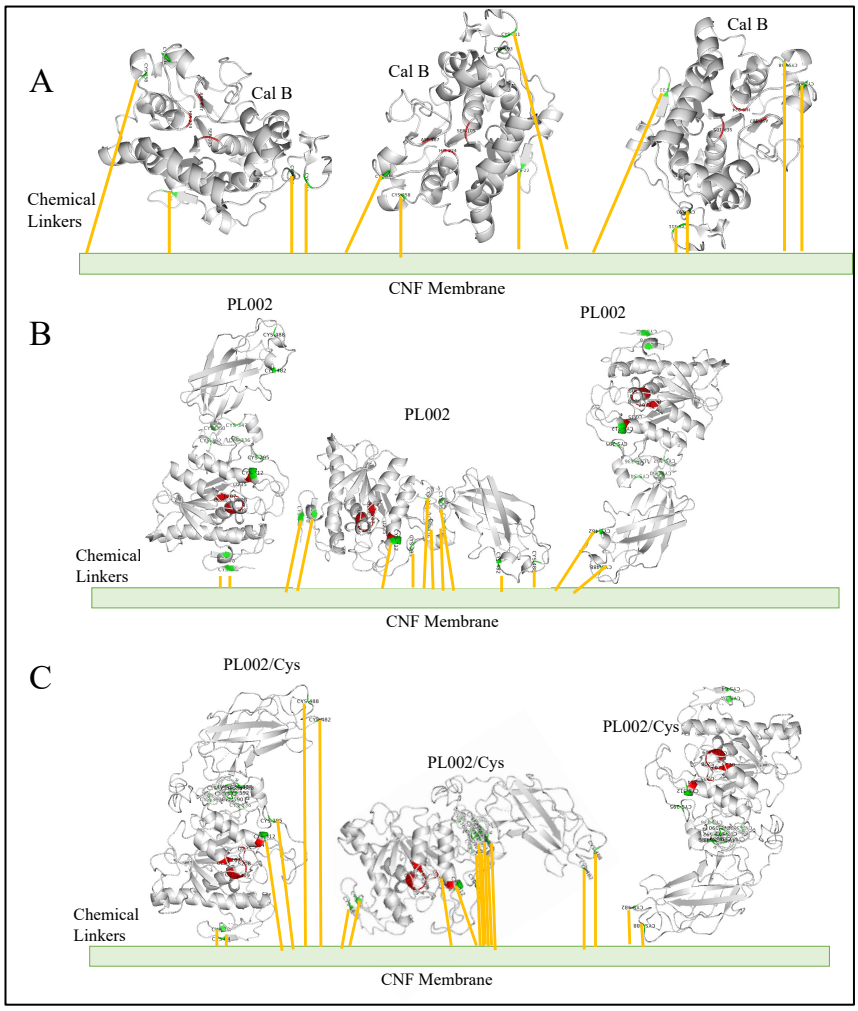

Figure 5.1: Hypothesised binding of lipases to cellulose nanofiber membranes

Orientations of the protein models generated in Chapter 4 are shown to represent the potential binding of cysteine residues to the immobilisation matrix

A) Cal B B) PL002 C) PL002/Cys

Substrate affinity, K_M, will be used to compare the free and immobilised lipase enzyme kinetics. Michaelis-Menten constant, K_M, will be determined using the Lilly-Hornby model. Lilly, Hornby and Crook, (1966), initially developed the method for determining kinetic parameters of an immobilised enzyme, ficin, in a flow system, for the hydrolysis of benzoyl arginine ethyl ester. This was generated by integrating the Michaelis Menten rate equation (Equation 5.2) to derive a method which determines the relationship between flow rate and hydrolysis of the substrate (Equation 5.3).

$$So - St = k3[E]t + K_m ln\left(\frac{St}{So}\right)$$

Equation 5.2: Integrated Michaelis Menten Equation

Adapted from (Lilly, Hornby and Crook, 1966)

Whereby, *so* is the initial concentration of substrate, *St*, is the substrate concentration after time *t*, and K_M, *k3* and *[E]* are the Michaelis constant, the rate constant for the decomposition of the enzyme-substrate complex and the concentration of total enzyme respectively.

The Lilly-Hornby equation is a modified description of the Michaelis Menten equation (Equation 5.2) which can be used to determine kinetic parameters as mass transfer effects are reflected in the calculations and steady state parameters are assumed, (Equation 5.3). The equation is better suited for determining kinetic constraints as flow rate is considered, the system operates in plug flow methods, and the true amount of product generated, substrate consumed, can be calculated.

$$P.\ So = K_{M\ (app)}\ (ln1\text{-}P) + [C/Q]$$

Equation 5.3: The Lilly-Hornby equation to determine enzyme affinity to substrate (K_M)

Adapted from (Lilly, Hornby and Crook, 1966)

Where, *P* is the fraction of substrate reacted in the column, so is the initial substrate concentration, $K_{M\ (app)}$ is the Michaelis-Menten constant relating to enzyme affinity to the substrate, *C* is the reaction capacity of the column and *Q* is the flow rate.

Values of P are measured when, So, substrate concentrations, are passed through the immobilisation matrix at constant flow rates (Q). When $P.\ So$ is plotted against $ln\ (1\text{-}P)$, a straight line with gradient equalling $K_{M\ (app)}$ and y-intercept, C/Q is derived. Reactor capacity, C can be further defined.

$$C=k3E\beta$$

Equation 5.4: Reactor capacity equation

Whereby, $k3$ is an enzymatic constant, E is total amount of enzyme, and β is the column voidage.

This determines a kinetic parameter of apparent K_M at given flow rates. It is important to note that K_M *in* a homogenous system, as seen in Chapter 4, is referred to as apparent K_M ($K_{M\ (app)}$) in a flow based biocatalyst system. This is due to the following assumptions: steady state is assumed in a laminar controlled system and all bound proteins are active and performing at the same rate. Several reports of modified variations of the Lilly-Hornby equation have been employed in assessing immobilised enzyme kinetics in a continuous flow system and therefore this method will be analysed here (Seong, Heo and Crooks, 2003; Abdul, Szita and Baganz, 2013; Carvalho, Marques and Fernandes, 2017; Schmuck, Sandgren and Härd, 2018).

Here single pass systems were compared to the alternative recirculating flow process. Recirculating flow is advantageous due to the potential for full conversion of substrate to product. The hydrolysis of substrate PNPB was used to determine kinetic parameters of immobilised lipases. The reaction profile can be seen in previous kinetic parameter determinations, (Figure 4.7 in Chapter 4), to determine the characteristics of novel cold active lipase, PL002 and positive control, Cal B. However, the substrate is susceptible to light and temperature changes. Therefore, this assay required modifications to the plate-based assay conducted in Chapter 4. The reaction profile of the assay remains the same in an addition to a step of quantifying the product and substrate depletion was introduced using SEC HPLC. In the plate-based assay, a control sample was used to blank the reactions, in this case HPLC ensures that true formation of product was obtained in addition to the rate of degradation which is important to establish kinetic properties using the Lilly-Hornby equation. Heterogeneous catalysis in flow systems have optimised the use of ρ-nitrophenyl based synthetic substrates due to their water soluble nature. This can be used to characterise kinetic studies in flow based systems as previously conducted here (Nair *et al.*, 2007; Souza *et al.*, 2021)

The use of a bespoke rig to enable flow-based measurements to take place facilitates measurement of the biocatalytic performance. The rig system optimised to house immobilised lipases are of similar design used for bioseparation, Figure 5.5 below (Hardick *et al.*, 2013). Using a well-established system of lipase catalysed hydrolysis of PNPB substrates will provide insight into how aspects of biological and physical modification may impact system performance.

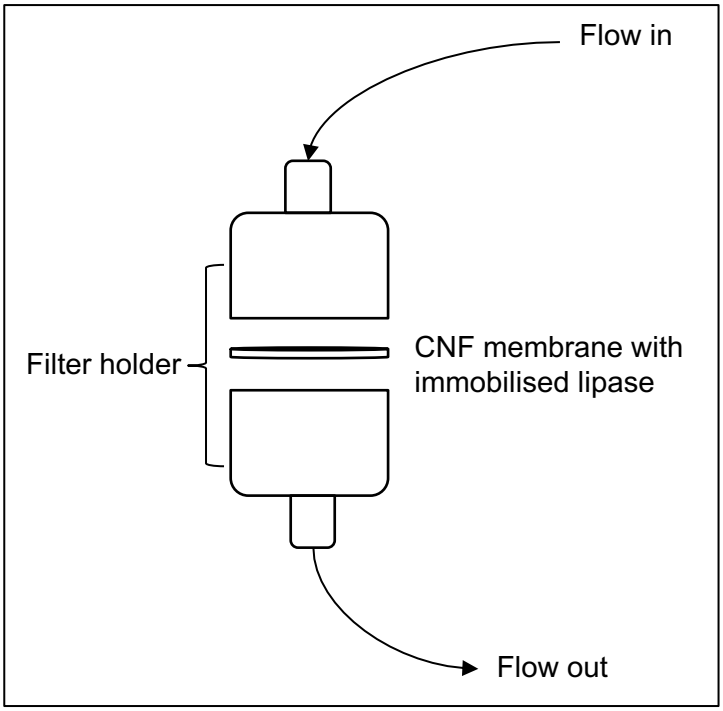

Figure 5.5: Diagram of the CNF membrane in its custom housing.

Adapted from (Hardick *et al.*, 2013).

5.2 Methods and Materials

A commercial lipase, *Candida antarctica* lipase B (Cal B) (Sigma Aldrich 62288) was diluted to working concentrations of 1mg/ml and 5mg/ml. Precipitated recombinant salp lipase was dissolved to a working concentrating of 1.5mg/ml in pH 7 phosphate buffer, as per methods described in Chapter 3. All media salts and additives were purchased from Sigma- Aldrich. The medium for all PNPB assays was 55mM phosphate buffer in RO water adjusted to pH 7. Chemically modified cellulose nanofiber membranes were provided by Cytiva (UK).

CNF membranes immobilised with lipase

All enzymes were prepared to working volume of 2.5 ml by dissolving in 55 mM phosphate buffer at pH 7. This was then added to a 28 mm diameter disc of chemically functionalised CNF material (Cytiva, UK) in a 6-well plate. Immobilisation efficiency was assessed by Bradford assay to determine the mass of enzyme loaded onto the membrane using the following procedure. The plate containing the disc was shaken at 120 rpm for 16 hours. The volume and titre of the remaining liquid (supernatant) was recorded for mass balance calculations. The disc was rinsed with deionised water and shaken on an orbital shaker for 20 minutes. The volume and titre of the washing water was obtained to determine the amount of protein bound and repeated one more time. This method of assessing enzyme bound to an immobilisation matrix is consistent with procedures described for the immobilisation of *Aspergillus niger* lipase on nanoparticles (Osuna *et al.*, 2015). The disk was then blocked for 90 minutes followed by a wash step. Then it was mounted in a custom membrane holder device for flow catalysis studies, as described previously (Hardick *et al.*, 2015). Two Cal B concentrations were trialled, 1 mg/ml and 5 mg/ml which produced enzyme loading values of 15.6 (+/- 0.036) mg/cm^3 and 7.25 (+/- 0.045) mg/cm^3 across three independent repeats. PL002 enzyme loading density was conducted at 4.30 mg/cm^3 and PL002/cys at 4.15 mg/cm^3.

$$Enzyme\ Density = \left(\frac{Cinput\ x\ Vinput - (Csupernatant\ x\ Vsupernatant - Cwash\ 1\ x\ Vwash\ 1)}{Volume\ of\ Disk}\right)$$

Equation 5.6: Mass balance equation used to assess mass of lipase bound to the membrane

This has been adapted from (Osuna *et al.*, 2015) and personal communications from Cytiva (UK).

Ci, Cs, and *Cw* are the initial enzyme, supernatant, and washing solution (deionised water) concentration (mg/ml), whereas *Vi, Vs*, and *Vw* are the volumes of the initial enzyme, supernatant, and washing solution (ml). The volume of the disk is consistent at 0.8cm^3.

To assess the mass of active lipase bound to the membrane, the initial enzyme preparation, supernatant and washing step from the immobilisation processes were used in an end-point assay. There is less than 40% of active protein found in the reservoir liquid after each immobilisation step and suggests protein binding onto the CNF membrane of 59 +/- 2%, (appendix D). A colourimetric characterisation assay, as described in Chapter 4, was used to determine hypothesised active protein bound onto the membrane.

Flow Systems

Experiments were performed on the AKTA Avant (GE healthcare, USA) and the activity of the lipase was monitored by the change in the UV410 detector fitted to the system (Hardick *et al.*, 2013). However, to determine the kinetics of the enzymatic reaction, SEC HPLC was utilised to monitor the degradation of the substrate which was used as input for the Lilly-Hornby equation (Lilly, Hornby and Crook, 1966).

Stability is defined by the immobilised lipase remaining active after 30 different flow tests, the membrane processing volume is 900 ml. Activity is defined by the maximal production of hydrolysed product.

PNPB is a widely used ester for lipase characterisation. Its water-soluble properties were utilised in this reaction, as longer chained esters are unable to dissolve in buffers (Quinn *et al.*, 1982). However, this substrate does have its limitations, it is light and temperature reactive

and thus both were monitored throughout each experiment. A water bath was employed to keep the temperature constant at 20 °C and the feed vessel protected with aluminium foil to reduce light exposure. In addition to this, sample of the substrate was taken before and after each run to optimise the reaction rate and to ensure that exact values of substrate depletion were recorded.

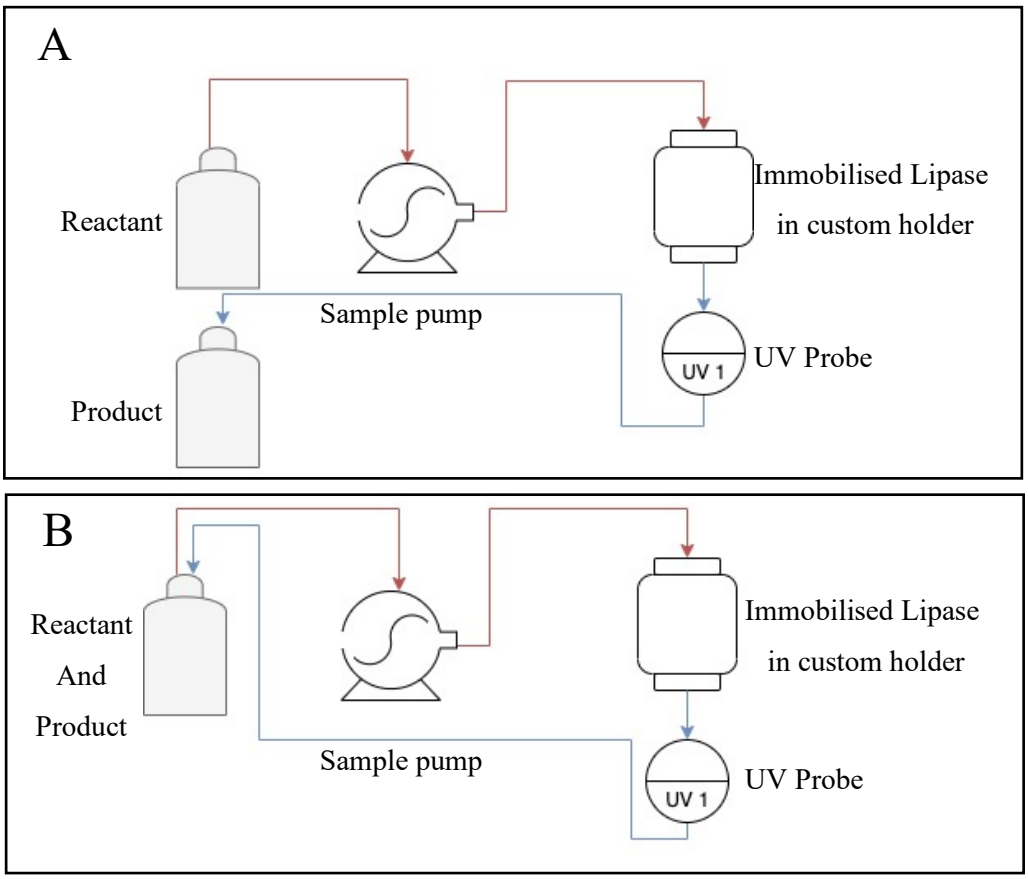

Figure 5.7: Single pass (A) and Recirculating system (B) pathways

The single pass flow system, (Figure 5.7A) collects the flowthrough in a separate vial, whereas in the recirculating flow through it is collected in the same vial, (Figure 5.7B) and recirculated through the flow path. Adapted from initial work connected by (Hardick *et al.*, 2015)

The AKTA Avant system (GE healthcare, USA), software Unicorn 7.4, was used to obtain the initial raw optical density reads which was converted into product formation using standard curves, appendix D. The final flow through was assessed on the HPLC to determine exact product formed and substrate consumed. Here immobilised lipase was trialled with differing flow rates and substrate concentrations to measure the production of product, 4-Nitrophenol

(4-NP). This was carried out in two different flow systems (Figure. 5.7) to assess the apparent effect on product formation as well as the enzyme affinity ($K_{M\ (app)}$). The method has been adapted from a previous study on purifying bovine serum albumin (Hardick *et al.*, 2015). Flow rates tested for each enzyme were 0.25ml/min, 0.5ml/min, 1ml/min, 2ml/min, and 4ml/min. Each flow rate was trialled at three different substrate concentrations: 1mM, 2mM and 4mM. Substrate concentrations were also trialled at 5mM, 2.5mM, 1.25mM, 0.6mM, 0.3mM at 1ml/min flow rate for 30 column volumes for the purpose of determining kinetic parameters and 4-NP production. For all experiments the feed vessel was kept in a 20°C environment using a water bath.

Samples were taken before and after the reaction. 2ml of sample was sterile filtered, with a 0.2um Millipore filter, and analysed by reverse phase HPLC (Agilent 1200) on a C18 column (ACE-121-1546, dimensions are 150 * 4.6mm) using milliQ 0.1% TFA/methanol 0.1% TFA (1:1, vol/vol) as the mobile phase (Mingarro, González-Navarro and Braco, 1995). A 25-minute reaction profile, at 0.5ml/min flowrate, was used whereby step gradient of mobile phase. 0–5-minute 10% mobile phase B, 5-10 minutes 40% B, 10-20 minutes 70% B, 20-25 minutes 100% B. The peak areas of the various reaction products were integrated using the Agilent Chemstation software (Agilent, USA) and compared to respective standards. Compounds and retention times can be found in table 5.8 below.

Table 5.8: The retention times of ρ-nitrophenyl butyrate and 4-Nitrophenol

This was used to analyse samples through SEC HPLC

Compound	**Retention Time**
P-nitrophenyl butyrate	21.5 minutes
4-Nitrophenol	10.9 minutes

Michaelis Menten Kinetics

The Lilly-Hornby equations were employed to determine the *KM* or the $K_{M\ (app)}$ in flow catalysis as shown in Equation 5.3. It has been assumed, (Chapter 5), that the activity parameters of the salp lipase with and without the cysteine modification is the same. This was a pragmatic assumption based upon time limitations.

Productivity of enzyme

Productivity (mg/l/hr) = Amount of product (L) generated per hour (h) per milligram of enzyme (mg)

Equation 5.9: Productivity of the enzyme in a flow system

This was calculated using adapted methods from Abdul, Szita and Baganz, (2013).

5.3 Results

Lipase candidates, *Candida antarctica* lipase B and PL002, the salp lipase were used to assess stability and activity in site directed covalently bound immobilisation systems. Cal B was used to determine if stability and activity is altered by enzyme density; this is equivalent to 7.25 mg/cm^3 and 15.6 mg/cm^3, a twofold difference. PL002 was used in its original form and biologically modified with a cysteine tag to compare enzyme loading. The enzymatic parameter, K_M or enzyme affinity to the substrate was compared with a free form of the lipases.

Flow Systems

Flow catalysis was conducted on the AKTA Avant using single pass and recirculating flow systems. The absorbance of the product, 4-NP was captured thought UV410. A representative example of high-density Cal B hydrolysing differing concentrations of substrate, PNPB, at 2ml/min flowrate, (Figure 5.10). Here it has been established that the higher the substrate concentration, the increased amount of product formation, (Figure 5.10A and 5.10B). In recirculating flow there is a gradual linear increase, whereas in single pass flow the increase of product reaches completion. The recirculating nature of the substrate provides possibilities of full conversion to 4-NP. This can be confirmed if the reaction time was increased as the product formation would plateaux.

The absorbance readings of the product and substrate are the same (410nm), therefore the 4-NP production, (Figure 5.10), does not give true representation of product formation. HPLC analysis is required to determine the exact amount of product formed.

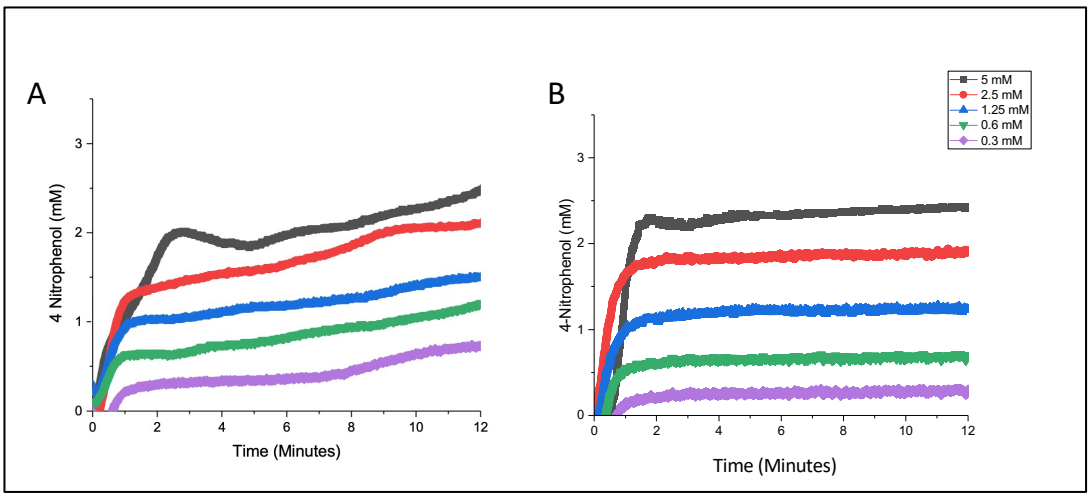

Figure 5.10: AKTA Avant UV readings converted to 4-Nitrophenol production

The flow system here is 15.6 mg/cm^3 (high density immobilised Cal B) in recirculating flow (A) single pass processing (B). PNPB substrate hydrolysis of concentrations: 5 mM, 2 .5mM, 1.25 mM, 0.6 mM, and 0.3 mM. Flow rate was at. 2ml/min (120 ml/hr). 4-NP produced was calculated using standard curves, (appendix D).

HPLC analysis to determine Stability and Activity

The AKTA Avant visualises the absorbance of both product and substrate, however since they are both equally absorbed at 410nm, the SEC HPLC was required to determine the exact change in substrate degradation which is necessary in the Lilly-Hornby equation. Retention times for the product and reactant are different on the HPLC which ensure that the concentration of each sample can be monitored. HPLC analysis was used to compare and quantify the amount of product formed and substrate degraded in the flow system. Example HPLC profile, depicting 0.03mM of PNPB hydrolysation using PL002 to 4-Nitrophenol, (Figure 5.11).

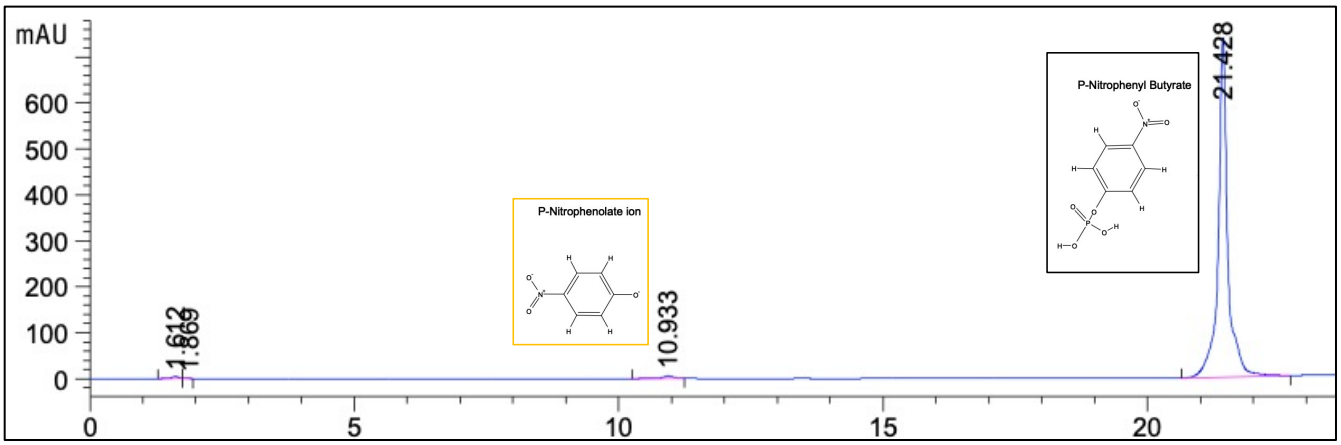

Figure 5.11: HPLC analysis of PNPB hydrolysation

This sample was from immobilised PL002 in single pass processing using 0.3mM of PNPB at flow rate of 60 ml/hr.

It is demonstrating that an increasing flow rate has a great impact on the enzyme ability to hydrolyse the substrate (PNPB) into product. This is experimentally measured using flowrates ranging from high flow rate 240 ml/hr to a lower flow rate 60ml/hr. It was demonstrated that the increased flow rate produced less product, established comparing enzyme densities of commercially available lipase, Cal B. Recircling systems has a greater product formation than a single pass, (Figure 5.11 A and B). The higher enzyme density also provides a twofold greater product formation.

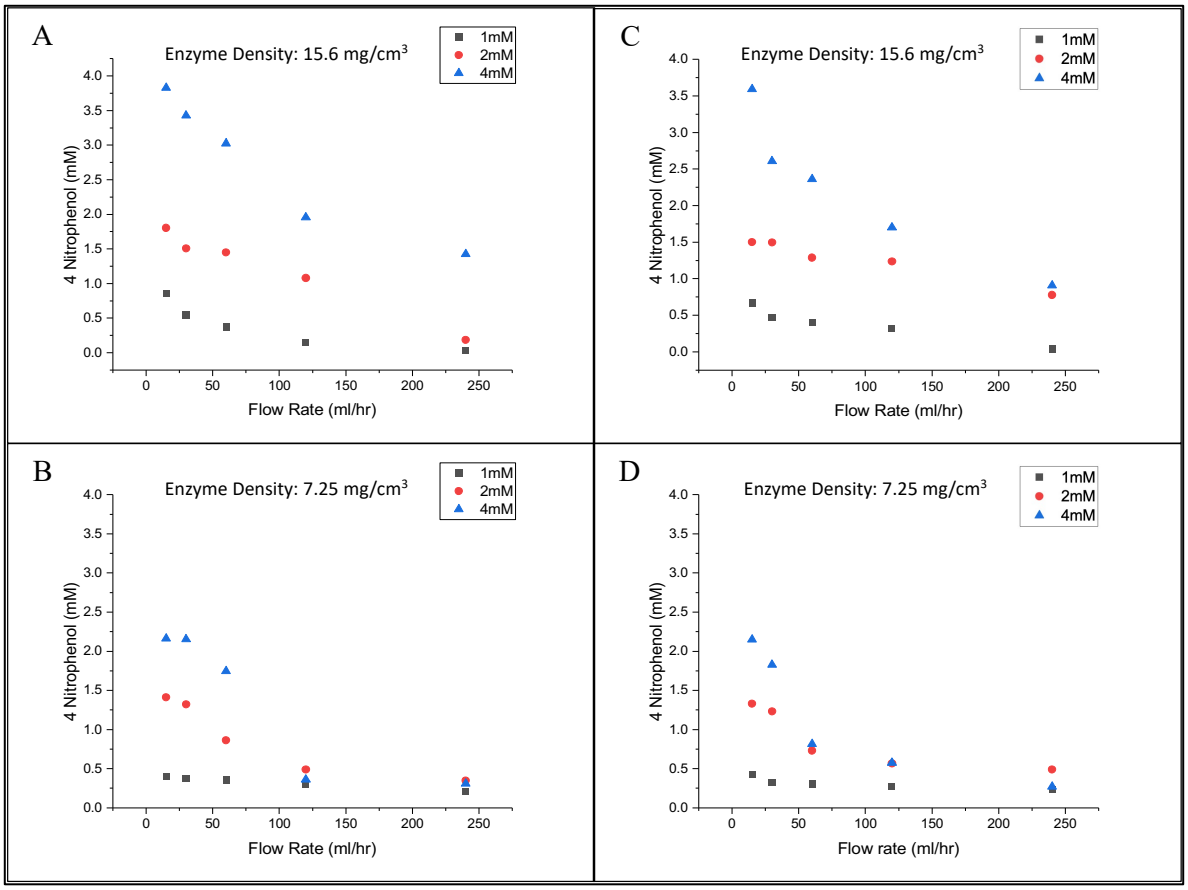

Figure 5.12: HPLC analysis to determine 4-Nitrophenol production using different densities of Cal B

15.6 mg/cm^3 (high density Cal B) in recirculating flow (A) and single pass (C)

7.25 mg/cm^3 (low density Cal B) in recirculating flow (B) and single pass (D)

PL002 without the biological modification of a cysteine tag has a 30% increase in 4-NP formation than with the cysteine tag. This is determined from the comparisons between the two lipases at the slowest flow rate, 15 ml/hr, (Figure 5.11).

A clear difference between the different substrate reactions and flow rate was not observed for PL002, in contrast to Cal B. In addition, there is smaller distinction between the production of 4-NP with relation to the two flow systems (Figure 5.13).

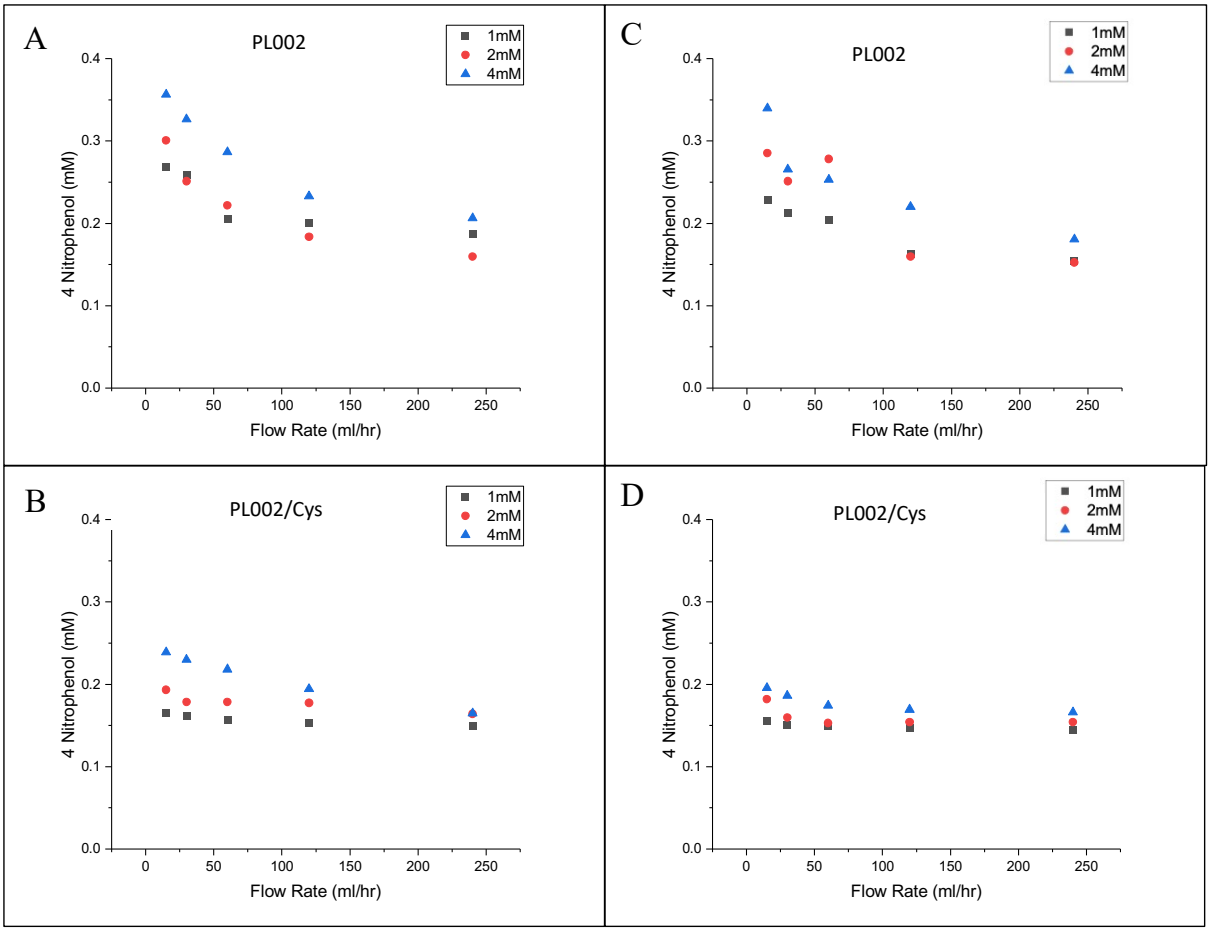

Figure 5.13: HPLC analysis to determine 4-Nitrophenol production using biologically modified salp lipase

PL002 (unmodified) in recirculating flow (A) and single pass (C)

PL002/Cys (modified) in recirculating flow (B) and single pass (D)

Application of Lilly-Hornby Equation

The Lilly-Hornby equation was used to determine an apparent kinetic parameter, the Michaelis Menten constant, K_M, to compare the immobilised system to free lipase. The K_M of the immobilised system was generated using the degree of hydrolysis of the substrate in relation to the flow rate of the system. Here the enzyme density studies were replicated in three technical and experimental repeats.

The degree of hydrolysis (*P. So*) is conducted by the HPLC analysis whereby the *P* is the fraction of the substrate reacted in the system multiplied by the initial substrate concentration (*So*). This can be used to determine the K_M and reactor capacity – *C*.

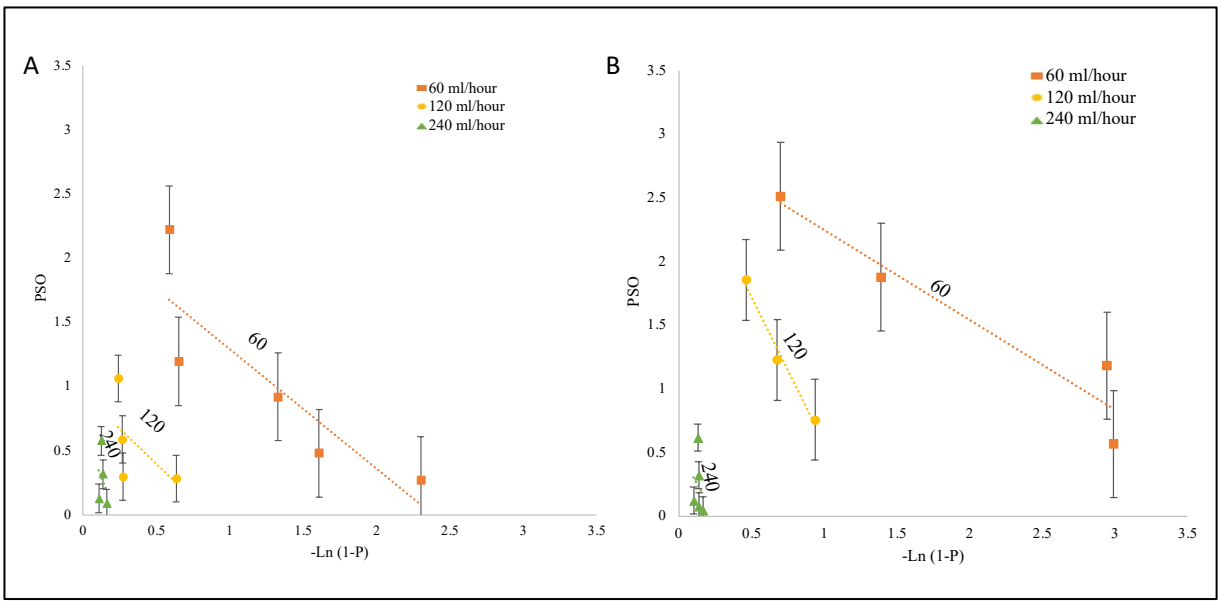

Figure 5.14: Kinetics determination using Lilly-Hornby model for 15.6 mg/cm^3 (high density Cal B) in recirculated flow (A) and single pass flow parameters (B)

Solid lines fitted by linear regression from modified data of Figure 5.12.

Values of $K_{M\,(app)}$ can be obtained from these plots.

A negative linear regression has been established between the degree of hydrolysis of PNPB inverse log functions for high density Cal B in both flow pathways, (Figure 5.14). The gradient corresponds to the Michaelis-Menten constant, $K_{M\,(app)}$, and the y-intercept can be manipulated to derive the reaction capacity, *C*. This profile can be seen throughout all enzymatic reactions, regardless of flow rate. $K_{M\,(app)}$ was determined as a function of flow rate and each flow system. Here the gradient of the Lilly-Hornby equation, equivalent to *KM*, was extrapolated to fit a positive linear regression against flow rate. The value of $K_{M\,(app)}$ was calculated by equating flowrate to be zero. This can be used to compare the K_M of the free lipase system and immobilised. PL002/Cys was not trialled as free lipase, (Figure 5.15 and 5.16).

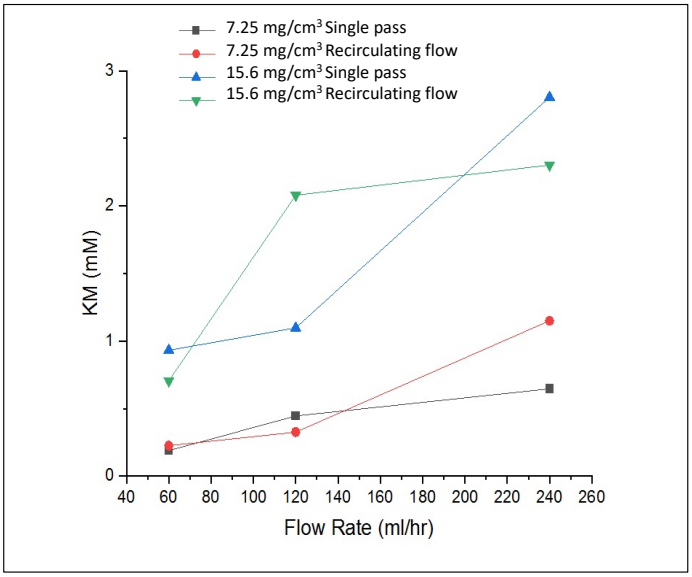

Figure 5.15: Applied Lilly-Hornby Equation to determine K_M in relation to flow rate to *Candida antarctica* Lipase b

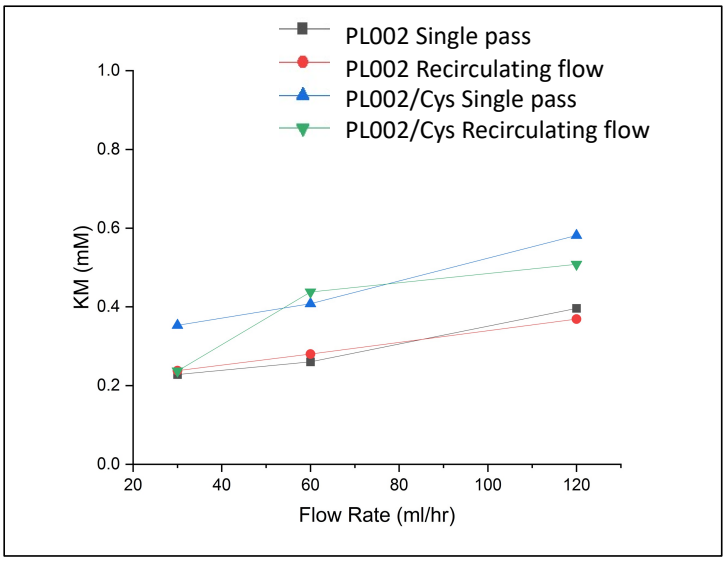

Figure 5.16: Applied Lilly-Hornby Equation to determine K_M in relation to flow rate to the salp lipase

The K_M values determined in the free enzyme system, (Chapter 4), are of comparable level to the observed K_M values in flow biocatalysis, (Table 5.17). There is no significant difference in K_M between the two trialled flow systems however the K_M of the two Cal B densities are 4 fold different.

Table 5.17: Immobilised K_M apparent values

This was calculated when flow rate is zero in comparison to free lipase *KM* values

Enzyme	K_M (mM)		
	Single Pass	**Recirculating Flow**	**Free**
Low (1mg/ml)	0.2708	0.2316	0.2202 +/- 0.009
High (5mg/ml)	0.7248	0.7200	x
PL002	0.3606	0.3868	0.3761 +/- 0.009
PL002/Cys	0.3868	0.3326	x

As the flow rate increases, the reactor capacity (C), decreases. This negative regression linear trend is calculated from y-intercept of the kinetics determination models, (Figure 5.14).

Table 5.18: Enzyme productivity in single pass and recirculating flow reaction

Productivity was calculated for both continuous and batch systems using flowrate conditions to be 15 ml/hr at the highest substrate concentration (4mM of ρ-nitrophenyl butyrate). This was calculated using adapted methods from Abdul, Szita and Baganz, (2013).

Immobilised System	Enzyme Density (mg/cm^3)	Productivity of Single pass system (mg/l/hr)	Productivity of recirculating system (mg/l/hr)
High Cal B Density	15.65	0.360	0.383
Low Cal B density	7.25	1.074	1.082
PL002	4.30	0.113	0.119
PL002/Cys	4.15	0.065	0.080

Cal B has a greater productivity than the salp lipase systems. Further still low density lipase has a threefold greater rate than the higher density system.

5.4 Discussion

The flow based biocatalysis system constructed on initial chromatographic principles here provides a semi-automated flow system. The use of the AKTA Avant to provide the flow pathway and the HPLC optimised for the analysis of the flowthrough, determined a systematic approach to defining kinetic parameters and the rate of product formation.

This immobilised system provides a unique alternative to bead bound immobilised lipases. The CNF membranes in their custom holders provide a plug flow approach towards liquid flow (Menkhaus *et al.*, 2010). Alongside the slow flow rates of the proposed system, this immobilised catalyst can operate in laminar flow fashion (Doran, 2013). The robust structure of CNF membranes encourages substrate enzyme complexes to generate activity at increased flow rates, which has been established in single pass and recirculating flow systems, (Figure 5.12)

Immobilisation Efficiency

Membrane efficiency can be used to determine stability and activity. This has been evaluated by physical and biological modifications to the flow biocatalyst. Physical modifications applied here include changes in enzyme density, or loading, onto the membrane. Biological modifications include using cysteine based modifications to the trialled lipases. These parameters were assessed to determine effects on stability and activity to the lipases.

Stability has been defined as the immobilised lipase membranes remaining active after 30 different flow tests. 30 flow tests were chosen to allow sufficient repeats and testing. Here, stability was measured with relation to the possibility that at later flow trials, the enzyme may begin to denature and render the flow biocatalyst inactive. Both physical and biological modifications to the membrane provided flow based biocatalysts that remained active after the flow tests. However, to further assess stability, studies which include processing a greater volume of reagent in the same flow system, with the same residence time, would be required to determine enzyme leaching and measuring activity of the membranes. This has been conducted in previous studies as reactivation and inactivation studies for characterisation of immobilised lipases (Rodrigues *et al.*, 2019).

Activity has been defined as the immobilised system successfully undergoing the hydrolysis of PNPB. With all such cases, of differing flow rates and substrate concentrations, the flow biocatalyst was active and produced the product, 4-NP, (Figure 5.12 and Figure 5.13).

Application of Lilly-Hornby Kinetics

Here, Lilly-Hornby Kinetics were applied to determine kinetic constant, $K_{M\ (app)}$ and the relationship between the reaction capacity provided by the immobilised system.

$K_{M\ (app)}$ values increase with increasing flow rates across all flow systems. Therefore, as the flow rate reaches 0 ml/hr, the value of K_M should be in line with a free lipase as there is no flow. Higher flowrates should increase the amount of substrate- enzyme interactions, however the residence time for mass transfer therefore decreases which demonstrates that the reduced residence time at higher flow rates limits the substrate in bulk flow to meet the enzymes on the solid surface. This is considered due to the increase in mass transfer ensuring little diffusional limitations as seen with porous bead bound systems which relies on longer residence times (Matte *et al.*, 2017). The mass transfer is sufficient at the lower flow rates to increase efficacy of bound biocatalysts, as observed by the increase in product formation at lower flow rates. This model was demonstrated by (Schmuck, Sandgren and Härd, 2018; Xu *et al.*, 2022).

Reactor capacities (C) of the system is dependent on flow rate, (Equation 5.4). As flow rate increases, the reaction capacity decreases. Therefore, if k3 and β are constant parameters, the E factor would be the result in this difference. It is postulated that the increase in flow reduces the enzyme and substrate contact time. This is reflected in the decrease in product formation, (Figure 5.12 and 5.13). Cal B has been recombinantly produced to provide the highest product yield, it is a well-researched lipase optimised for industrial biocatalysis (Gotor-Fernández, Busto and Gotor, 2006). The activity of this lipase is much greater than the recombinantly produced salp lipase, PL002 and is demonstrated by the product, 4-NP, yield; Cal B enzyme systems produce a 10-fold increase in comparison to the biologically modified salp lipases.

Impact of enzyme density on the stability and activity of immobilised lipases

The initial trials conducted using Cal B, compared two enzyme densities 7.25 mg/cm^3 and 15.6 mg/cm$^{3.}$ The overall, $K_{M\ (app)}$ of the 15.6 mg/cm^3 system has a threefold greater value than that of the lower Cal B density membrane; calculated to be 0.7200mM and 0.2316mM in recirculating flow respectively, (Table 5.16). As the enzymes are the same there should be a similar K_M *observed* across free and immobilised systems. This is true for the low enzyme, 0.2202 +/- 0.009mM which suggests that the affinity to the substrate of the enzyme of both systems is similar and therefore is performing at a comparable rate of reaction (Seong, Heo and Crooks, 2003). However, the higher loading of the lipase may encourage a greater formation of multipoint linkers therefore altering protein orientation and thus reducing the substrate affinity towards the lipases, (Figure 5.19). Multipoint attachment, as discussed in Chapter 1, occurs when multiple membrane reactive sites are found on the lipase. There may have been a conformational difference in the proteins due to overloading, (Figure 5.1).

Cal B has a 2% content of cysteine molecules placed evenly throughout the lipase surface. A higher concentration of lipases may cause enzyme crowding and thus reduce the substrate affinity by impeding accessibility to catalytic residues or perhaps even intermolecular steric hindrances which may lead to limited mass transfer. This is corroborated by (Zhu and Sun, 2012) whereby *Candida rugosa* lipase loading density was trialled on polyvinyl nanofiber activated with glutaraldehyde.

Multipoint attachment can occur by increasing the contact time between the membrane and lipase during immobilisation processes (Mateo, Palomo, *et al.*, 2007). Therefore, Cal B lipase can be trialled for longer incubation times to encourage greater covalent bonds. This is corroborated by Poppe et al., who immobilised Cal B onto Immobead 150 (Poppe *et al.*, 2013) and determined optimal binding to the matrix in similar coupling time based studies. However, there is a risk of reducing flexibility and depending on protein orientation with relation to the active site, there is a risk of decreasing activity (Mateo, Palomo, *et al.*, 2007).

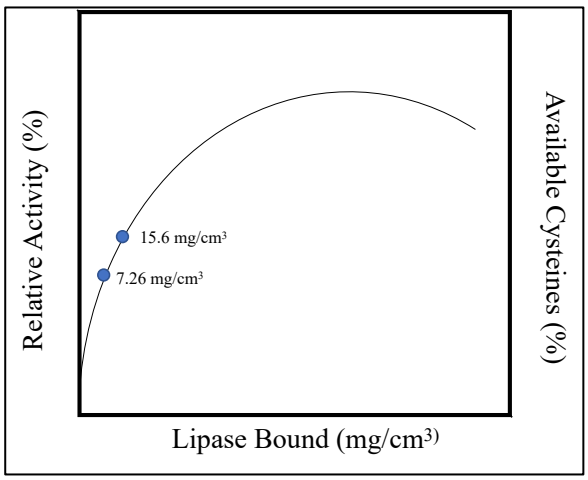

Figure 5.19: Proposed illustration to demonstrate the relationship between activity, enzyme loading and cysteine attachment sites

Loading densities trialled with Cal B is displayed. Adapted from (Pedroche *et al.*, 2007).

Proposed theory to demonstrate the role of enzyme loading in relation to activity and enzyme binding is illustrated, (Figure 5.19). Here, as determined from 4-NP production in Figure 5.12, high loaded Cal B has greater production of product than low loaded membrane. A relationship exists between activity of the lipase, the orientation and how it is bound to matrix for maximal activity, and the maximal enzyme loading on the membrane before instigating a negative effect on the catalyst. This has been hypothesised using the enzyme density studies trialled here, (Figure 5.1). Literature has also cited a similar model referencing lysine based site directed multipoint attachment (Pedroche *et al.*, 2007).

The yield of product formed was used to assess the activity of the immobilised lipase. It was established that when this immobilised system was carried out in a recirculating flow process there was a greater yield of product. The 15.6 mg/cm^3 Cal B has the greatest amount of 4-NP produced. The higher enzyme loaded membrane has a greater enzymatic efficiency at lower flow rates, as previously conducted by (Seong, Heo and Crooks, 2003). Combined with the presence of a small catalytic lid, the active site in Cal B is available for catalytic conversions than in the instance of an enzyme requiring an additional nucleophilic elbow for reaction purposes (Uppenberg, Patkar, *et al.*, 1994), the lipase has the ability to bind efficiently to the membrane as a sufficient alternative to homogenous catalysts.

The productivity was comparable across both the single pass and the recirculating flow systems. There is no significant difference between both operating systems. The comparison of per mass of enzyme bound matrixes identified that the lower enzyme density outperformed the higher density three fold. This suggests that less enzyme is required to carry out a similar rate of reaction. Industrial processes welcome biocatalytic alternatives such as this as a cheaper alternative to free enzymes. The lower reaction temperatures suggest that enzyme stability can increase the product formation by being active for longer durations. Amount of immobilised enzyme used can be optimised to ensure costs are kept at a minimum (Basso and Serban, 2019). Bead based systems require replacement of beads over time which may cause compression of the system (Hardick *et al.*, 2015). This can in turn be detrimental for lipase activity. The CNF membrane reduces this limitation providing a cheaper system in comparison

Impact of biological modification on the stability and activity of immobilised lipases

Biologically modified salp lipase was compared in its cysteine tagged (modified protein) and unmodified (untagged protein) forms. K_M of both proteins was comparable, (Figure 5.17). Therefore, further technical, and analytical repeats must be conducted to confirm this finding. The free enzyme K_M was 0.3761 +/- 0.009 mM which is in a similar range to the K_M calculated using the Lilly-Hornby equation.

Cysteine loading impacts protein orientation, (Figure 5.1). PL002/Cys has a greater number of cysteines, which are located near the active site. This suggests that there is a high chance that the protein orientation on the matrix could inhibit the active site and therefore elucidates the 30% decrease in activity. Suggestions to alter the immobilisation style might be considered here. Adsorption immobilisation offers little to no alternations to the active site, as demonstrated by (Mokhtar *et al.*, 2020).

Biological modifications to the salp gene include a histidine tag at the N terminus in both genes, and an additional cysteine tag for PL002/Cys at the C terminus. Histidine was required for affinity nickel-based purification. However, hydrolytic activity of ρ-nitrophenyl esters has shown to be diminished whilst using proteins with a hexahistadine tag (de Almeida *et al.*, 2018). There has been evidence which indicates that this hexahistadine tag can alter the quaternary structure of the protein (Carson *et al.*, 2007) which contributes to the specific

activity of recombinantly produced affinity tagged proteins; such as the pancreatic like lipase from the *Salpa thompsoni* marine tunicate, PL002. Subsequent reactions to increase activity, and the production of 4-NP, would include the cleavage of the hexahistadine protein, prior to immobilisation, as per Chapter 4, it has been determined that the activity of the protein has the potential to diminish with the addition of a histidine tag. The combined tags on PL002/Cys may contribute towards the reduced activity (as seen in 4-NP graphs). Site directed covalent immobilisation has taken place using cysteines located either naturally, or biologically modified, on Cal B (Blank, Morfill and Gaub, 2006; Zimmermann *et al.*, 2010). It was established here that this cysteine tag had little to no effect on activity or stability. Subsequent analysis should take place whereby a third lipase with neither tag is trialled as a control to confirm this with the salp lipase candidates

PL002 has a 2-fold greater productivity than the modified lipase and a greater 4-NP yield. A possible explanation for this is that there are multiple cysteine residues loaded around the catalytic site of PL002/Cys, (Figure 5.17). With the addition of a higher cysteine count, there is likelihood of protein covalently binding towards the catalytic residues thus reducing the rate of reaction and perhaps even causing protein distortion. This has been observed in covalently immobilised lipase from *Thermomyces lanuginosus* (Rodrigues *et al.*, 2009). To fully confirm this, quantifiable transmission electron microscopy can be used to verify protein orientation, as done so in the characterisation of sol-gel immobilised lipases (Noureddini and Gao, 2007).

5.5 Conclusion

Stability and activity of Cal B and the salp lipase, PL002, was assessed using immobilisation methods. It was identified that the lipase system remains active after processing over 900 ml of substrate. Therefore, stability and activity increase whilst immobilised onto cellulose nanofiber, and can subsequently be used as a flow based application.

The developed biocatalytic platform was operated in single pass and recirculating flow with flow rates and substrate concentrations ranging from 15 ml/hr to 240 ml/hr and 0.3 to 5 mM. The physical modification of the membrane suggested that activity was greater with a higher loading of Cal B (15.6 mg/cm^3). Stability was unable to be confirmed as there was no significant decrease in activity. Productivity, however, was enhanced for the lower loaded lipase, (7.25 mg/cm^3) which suggests a cheaper membrane with less loaded lipase can be utilised. Salp lipase and a cysteine modified salp lipase was used to assess if biological modifications had an improved effect on stability and activity. Here stability of both salp lipase candidates was increased as the lipase remained active. PL002/Cys modified had 30% less activity than unmodified. The site directed covalent binding method of immobilisation suggests that the higher content of cysteine residues surrounding the active site can interfere with the binding; and thus, affecting the activity.

Comparisons between both types of enzymes suggest that there a significant difference between in the productivity, activity, and stability. Subsequent analysis can take place whereby both the systems are modulated with increasing enzyme density. This would clearly determine if the cysteines decreased activity and stability.

The Lilly-Hornby equation was used to assess the kinetics as a comparison between the flow system and the free lipase. The immobilized enzyme presented similar values to determine the affinity towards the substrate *(K_M)*. The calculated $K_{M\,(app)}$ values showed flow rate dependency within the range of conditions used, indicating that the system is likely affected by mass transfer and residence time limitations. This is corroborated with the reactor capacity values. Therefore, it is suggested that the flow rate reduces the enzyme and substrate contact time in turn decreasing product formation.

Chapter 6: Application of Immobilised Lipases

6.1 Introduction

Plastic materials are lightweight and versatile. Their structure can be easily manipulated to be applied to a range of applications from food packaging, to solvents and adhesives (Venkatachalam *et al.*, 2012). The lifespan of plastic objects can be very short, therefore many of these materials are not recycled properly and contribute to the accumulation of more than 5 trillion pieces of plastic waste currently floating in the ocean environment (Eriksen *et al.*, 2014); one of the most common marine plastic pollutants is polyurethanes (Coyle, Hardiman and Driscoll, 2020).

The first urethane was created by Otto Bayer in 1837 as a replacement for rubber (Szycher, 2006), using the then novel method of polyaddition or step polymerisation (Gama, Ferreira and Barros-Timmons, 2018). The synthesis of polyurethanes (PU) includes a reaction between polyester diol and a diisocyanate (Troev *et al.*, 2000). Hydrolysation of this compound occurs by the ester bonds, highlighted in red below, as part of the polyester fraction of the structure, (Figure 6.1A). This forms polyurethane oligomers, glycol, and carboxylic acids (Marjo *et al.*, 2017) for example, adipic acid (Utomo *et al.*, 2020) (Figure 6.1B).

A

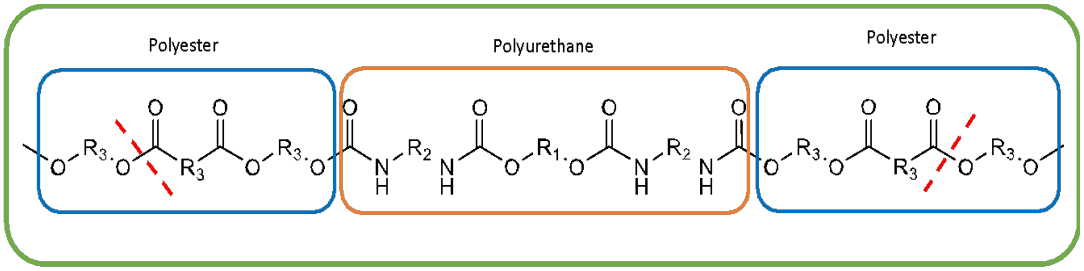

B

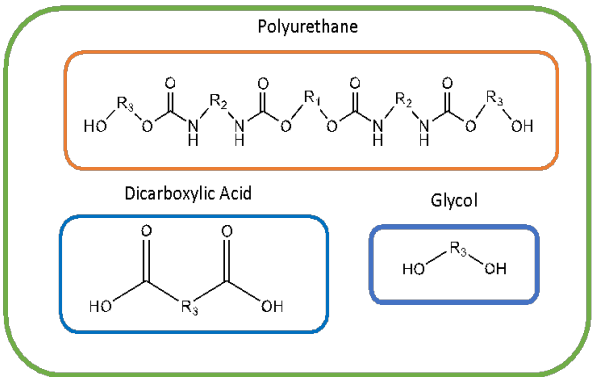

Figure 6.1: Proposed hydrolysis mechanism of polyester polyurethane

A) Structure of a hypothetical polyester polyurethane

B) Hydrolysed PU with glycol and dicarboxylic acid monomers

Adapted from (Marjo *et al.*, 2017)

Previously, biodegradation of commercially available PU , Impranil® DLN, has been conducted using lipases, of the esterase family; this includes the use of highly substrate specified *Pseudomonas* sp (Howard and Blake, 1998; Hung *et al.*, 2016; Utomo *et al.*, 2020). The hydrolysation rate presented by ester cleaving capacities from lipases through partially-clearing, completely clearing, or aggregating Impranil whereby *Pseudomonas* lipase had a 300x greater rate of degradation than the protease (Biffinger *et al.*, 2015). In addition to this, synthetic biologists have discovered ingenious methods of embedding enzymes for the biodegradation of plastics. Proteinase K from *Tritirachium album* was used to biodegrade Poly (L-lactic acid) at temperatures greater than 60 °C over a period of 96 hours (Huang *et al.*, 2020). This provides a wide scope of applied biodegradation of different types of plastics, such as Dispercoll® U 2682, using enzymes optimised for use from the hydrolase superfamily (Ollis *et al.*, 1992; Messaoudi *et al.*, 2010).

PL002 and *Candida antarctica* lipase B (Cal B), has been established to hydrolyse synthetic compounds, ρ-nitrophenyl substrate, (Chapter 4). The initial understanding of the hydrolytic

properties established by the lipases at 20°C suggests the ester cleaving potential of these biocatalysts can be used in the biodegradation of long chain esters. It has been previously demonstrated to degrade an aliphatic polyester-type plastic, such as poly (butylene adipate) copolymers (Okajima *et al.*, 2003). Additionally, arming yeast expressing Cal B on the cell surface has also been analysed for their polymer degradation potential (Shibasaki, 2009); demonstrating novel efforts to combat the plastic problem.

Dispercoll® U 2682, composed of a liquid nature, was chosen to examine the potential for immobilised enzymes in a recirculating batch flow system. It is the model polyester polyurethane (PU), that is water soluble. This property was used to develop a flow based biodegradation model using immobilised lipases, previously demonstrated in Chapter 5. It is a commercially available, proprietary polyester polyurethane, with a polyol backbone; thus, making it a suitable choice to assess its biodegradability using lipases. Dispercoll is a pre-treated material that is an aqueous anionic dispersion, which has compatibility to emulsifiers and thickeners. This PU can be aerobically biodegraded under controlled composting conditions, when incubated at temperatures of ~60°C and requires a total of 100 days to fully compost (Covestro, 2021). However, the flow based catalysis anticipates that a higher degradation rate than that of aerobic biodegradation, could be achieved. Productivity calculations will be used quantify the rate of degradation.

6.2 Methods and Materials

Candida antarctica lipase B (Cal B) (Sigma Aldrich 62288) was used at concentrations of 1 mg/ml and 5 mg/ml. PL002 and PL002/Cys were used at a working concentration of 1.5mg/ml respectively. The medium for all Dispercoll hydrolysis assays was 55mM phosphate buffer per litre RO water (mass in grams): Na2HPO4 (5.8) and NaH2PO4 (3.1) adjusted to pH 7 (components from Sigma Aldrich). Dispercoll® U 2682 (Covestro) was used at 0.01 mg/ml, pH 7 in phosphate buffer. Chemically functionalised cellulose nanofiber membranes prepared for immobilisation were provided by Cytiva Ltd (UK).

Dispercoll 0.01 mg/ml has an OD600 of 3.51 ± 0.07 and allowed for standardisation of the reaction conditions. The process parameters were regulated using the temperature monitor and agitation conditions within the Clariostar® (BMG Labtech, UK)

Free Enzyme Analysis

Plate clearing assay

Initial methods of assessing hydrolysis of Dispercoll were conducted using plate clearing assays, adjusted from previous work (Molitor *et al.*, 2020). Briefly, LB Agar was used as the growth medium supplemented with 0.01 mg/ml of Dispercoll. A 1.5mm biopunch was used to remove agar from the plates for the addition of lipase, followed by incubation at 20°C for 24 hours before inspection.

OD600 Plate assay

Microplate assays using 0.01 mg/ml Dispercoll suspension were conducted with five replicates. Free enzyme solutions were then added. The change in OD600 was monitored over 16 hours in a continuous plate reader (CLARIOSTAR) at a temperature of 20 °C and agitated at 250 rpm before each read.

Batch degradation with free enzyme

Falcon tubes containing 20 ml of Dispercoll 0.01 mg/ml and free lipase were placed in a shaking incubator at a constant temperature of 20 °C and agitated at 250 rpm. Samples of 2ml were taken periodically and degradation measured by the change in OD600 was monitored over 24 hours.

Immobilised Enzymes

CNF Membranes immobilised with Cal B

Lipase dissolved in 55 mM pH 7 phosphate buffer was added to a 28 mm diameter disk of chemically functionalised CNF material (Cytiva, UK) in a 6-well plate. Immobilisation efficiency was assessed by Bradford assay to determine the mass of enzyme loaded onto the membrane. The plate was shaken at 120 rpm for 16 hours. The volume and titre of the supernatant was recorded for mass balance calculations. The disk was rinsed with deionised water and shaken on an orbital shaker for 20 minutes. The volume and titre of the washing water was obtained to determine the amount of protein bound; and repeated. The disk was then blocked for 90 minutes followed by a wash step. Then it was mounted in a custom membrane holder device for PU degradation studies, as shown in (Hardick *et al.*, 2015). Two enzyme concentrations were trialled for commercial lipase, Cal B, 1 mg/ml, and 5 mg/ml which produced enzyme loading values of 15.6 (+/- 0.036) mg/cm^3 and 7.25 (+/- 0.045) mg/cm^3 across three independent repeats. And PL002 enzyme loading density at 4.30 mg/cm^3 and PL002/cys at 4.15 mg/cm^3.

System design of recirculated batch flow of Dispercoll

The method has been adapted from Hardick et al (Hardick *et al.*, 2015), using a peristaltic pump, (Watson and Marlow 500), to continuously circulate 30 ml of 0.01 mg/ml of Dispercoll (Figure 2 below). Samples (n=2) were taken every 24 hours for further analytics. This system was kept in a 20°C environment. To optimise enzyme activity and rate of polyurethane degradation, the system was performed at a constant flow rate of 1 ml/min.

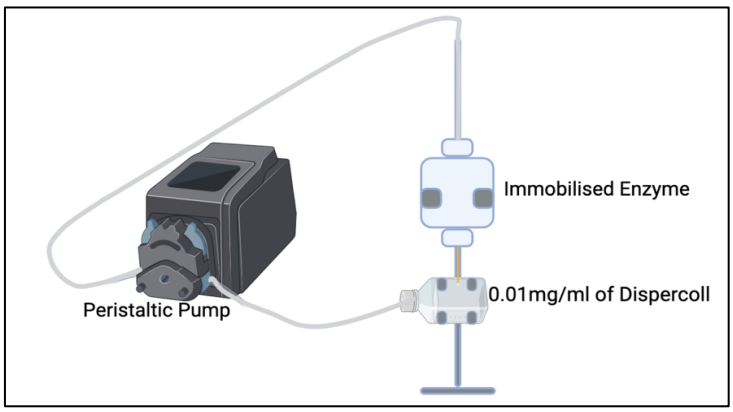

Figure 6.2: System design of a recirculated batch flow of Dispercoll degradation using flow catalysis

This is conducted with immobilised lipase on CNF membranes

After immobilisation of the enzyme, Dispercoll is continuously applied through a system of pumps and peristaltic tubing. This batch system can be manipulated to pump a series of different flow rates to ensure that the immobilised lipase had enough reaction time to carry out the hydrolysis of this polyurethane polyester. The method was adapted from initial work by Hardick et al (Hardick *et al.*, 2015).

Analytical Methods

Fourier-transform infrared spectroscopy (FT-IR)

FT-IR methods were adapted from previous work on the polyurethane Impranil (Partini and Pantani, 2007; Biffinger *et al.*, 2015). Transmission FT-IR spectra were acquired with a PerkinElmer Spectrum Two spectrometer with a universal attenuated total reflectance (UATR) diamond/LiTaO3 accessory arm (PerkinElmer, USA). Spectra were collected at 0.5 cm^{-1} resolution and 32 scans from samples. All spectra were referenced to the soluble material, pH 7 phosphate/Dispercoll stock solution.

Mastersizer

The Hydro MV Mastersizer 3000 was used for the particle size analysis (Malvern Analytical Ltd., UK) and software v.3.71 using standard operating protocols (Pei, Hinchliffe and Minelli, 2021). Two light sources were used in sequence: a helium–neon laser emitting red light (4 mW, wavelength of 632.8 nm) and a blue light-emitting diode (LED) light source (10 mW,

wavelength of 470 nm). The density and refractive index of Dispercoll were set at 1.07 g/cm3 (Covestro, 2021) and 1.49 (Tyagi *et al.*, 2009) respectively. The particle concentrations and stir speed were optimised prior to the measurements.

SEC HPLC

The soluble fraction was collected through centrifugation at 4000rpm at room temperature. The soluble fraction was freeze dried at room temperature for 48 hours. 1mg was then dissolved in 1ml of deionised water; sterile filtered through a 0.22 um filter for SEC HPLC. Adipic acid monomers were detected using ACE5 C18 (150 x 4.6 mm) from Avantor at 30 °C and analysed using Cromeleon 7 software. Acetonitrile and 0.1% phosphoric acid were used as a mobile phase at a flow rate of 0.5 mL/min.

Viscometer

Rotational rheometer measurements were made using a standard loading sequence and protocol on a Kinexus rheometer (Netzch-thermal analysis, UK). All rheology measurements were performed at 25 °C.

Imaging Methods

Scanning electron microscopy images were taken using Phenom Pro Desktop SEM (Phenom-World B.V., The Netherlands). Samples coated with gold using Quorum 150R S and viewed at a 10,000x resolution.

Statistics

Standard deviations were conducted, where possible. To determine significant differences, between mean values, two sample t tests were conducted to determine the p values. The significance threshold was set at 0.05.

6.3 Results

Biodegradation of polyester polyurethane, Dispercoll, has been established by lipase candidate, *Candida antarctica* lipase B. Salp lipase, PL002, was also trialled however the rate of degradation was insufficient to continue analysing degradation. Qualitative and quantitative analytics of the free lipase and immobilised lipase took place to substantiate the hydrolysis of ester bonds.

Qualitative Analysis

The plate clearing assay, shown in Figure 6.3A, demonstrates zones of hydrolysed Dispercoll using Cal B. It should be noted that temperatures higher than 60°C can cause Dispercoll to precipitate, of which some particulates can be seen on the agar (Covestro, 2021).

The higher concentration of Cal B enzyme has a greater degree of hydrolysis; as shown by the larger diameter of clearing zone. Visual degradation is more prevalent in the larger 20 ml samples, (Figure 6.3B). Samples of the larger reaction vessels were taken for the purpose of this image. Degradation is presented by the particle formation after hydrolysation of Dispercoll which has settled to the bottom of the vial. The sample with 1 mg/ml of Cal B is opaquer and has fewer settled particulates. The salp lipases, PL002 and PL002/cys do not indicate much difference in the degree of hydrolysis. The clear solution is the soluble fraction of the hydrolysed Dispercoll and used for further analytical analysis.

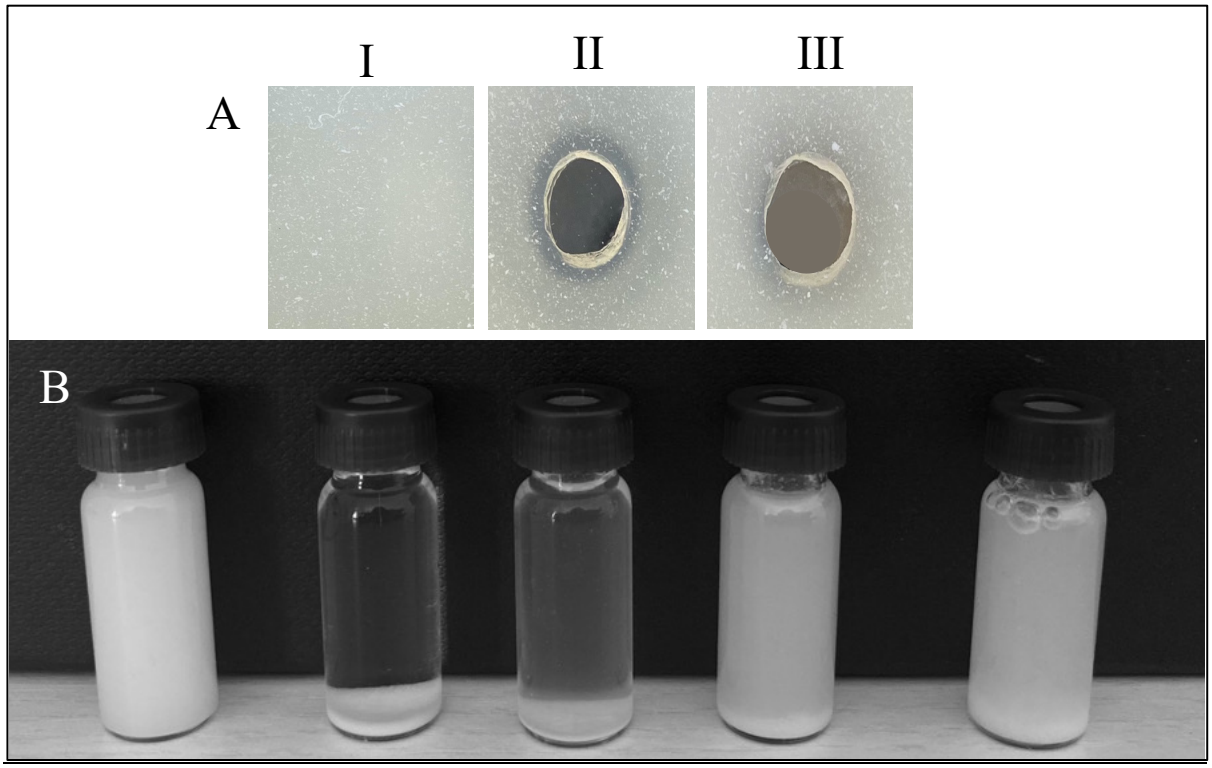

Figure 6.3: Polyesterase activities exhibited by *Candida antarctica* lipase B

A) Agar-based clearing assay I) Control, II) 5 mg/ml of Cal B III) 1 mg/ml of Cal B after 24 hours

B) Photograph of 0.01 mg/ml Dispercoll suspensions before and after exposure to lipases Blank, 5mg/ml of Cal B, 1mg/ml of Cal B, PL002 and PL002/cys (L-R)

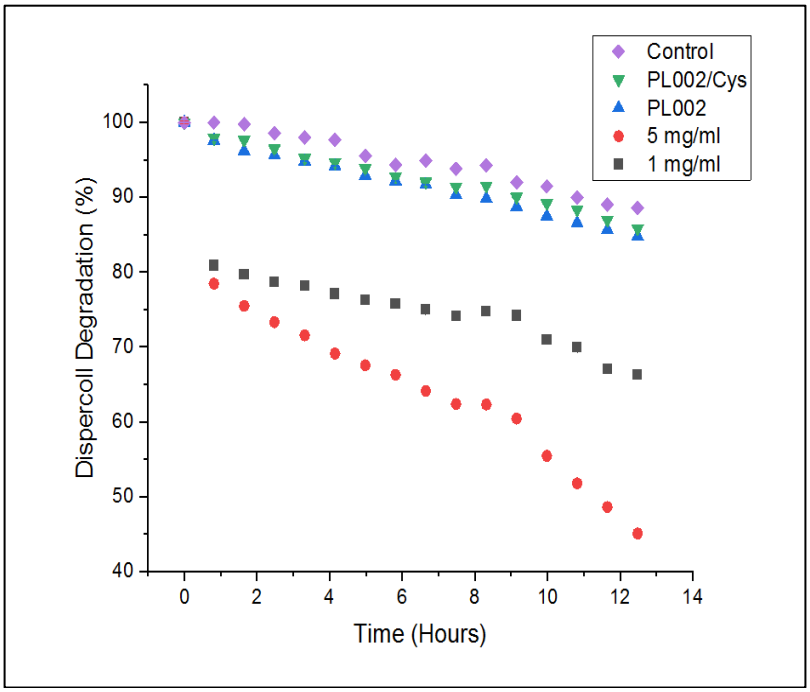

Figure 6.4: Microplate assay of 0.01 mg/ml Dispercoll degradation over 13 hours

The control and the salp lipases show very little difference in degradation (<5%). There is a greater rate of degradation with Cal B and Dispercoll (up to <40%). The values shown are averages of 5 independent experimental repeats with standard deviation bars less than +/- 0.11

To quantify the rate of degradation, free lipase was suspended in 0.01 mg/ml of Dispercoll in a microwell plate assay, (Figure 6.4). Physical agitation increases the rate of reaction and therefore the Dispercoll degradation can be performed more rapidly (Mussatto *et al.*, 2008). Evaporation losses cause a decrease in optical density readings which accounts for the deterioration of the control sample. This deterioration was accounted for in the enzyme treated samples. Degradation of Dispercoll was dependent on enzyme concentration. After 2 hours Dispercoll was degraded by 20%, furthermore after 12 hours more than 50% of Dispercoll had been degraded in the 5 mg/ml system (Figure 6.4). Significant difference was shown between the control and the enzyme induced samples ($p < .0001$). Salp lipases showed very little degradation (less than 5%) therefore further analysis was not conducted.

Two different densities of CNF immobilisation of Cal B were used to compare the rate of hydrolysis in a constant flow system; a lower density (6.25mg/cm^3) and a higher density, two-fold greater (15.6 mg/cm^3). A flow system consistent with Figure 6.2 was established.

Following enzymatic activity, gravity-assisted separation of the insoluble polyurethane oligomers from the soluble material was observed.

SEM images were taken of immobilised membranes to determine fouling of the surface, (Figure 6.5). This was conducted after 72 hours of exposure to Dispercoll in a recirculating flow system. Following enzymatic activity, gravity-assisted separation of the insoluble polyurethane oligomers from the soluble material was observed.

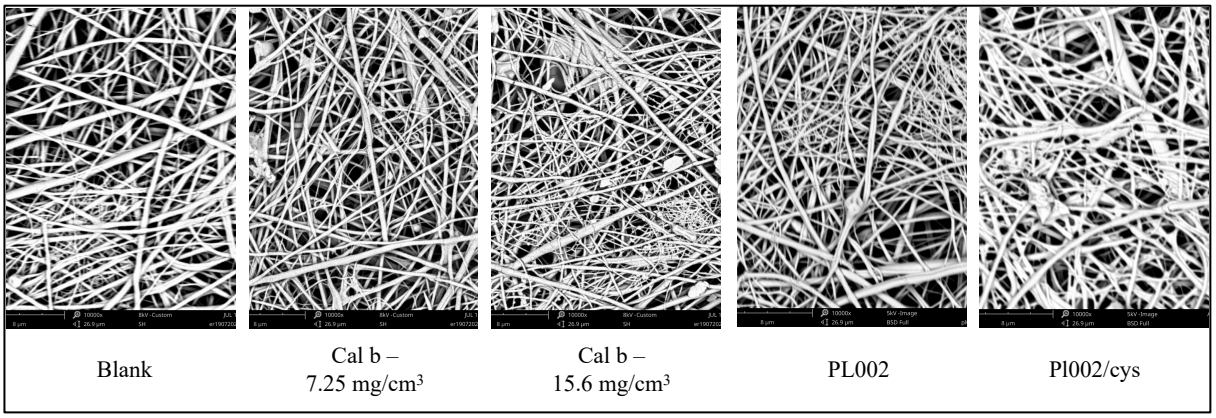

Figure 6.5: SEM images of immobilised lipase membrane after Dispercoll exposure

(L-R) Blank, 7.25 mg/cm^3 of Cal B, 15.6 mg/cm^3 of Cal B, PL002 and PL002/Cys

Images were taken after 0.01mg/ml of Dispercoll exposure in the recirculating flow system of 1ml/min at 20 °C for 72 hours. Cal B 15.6 mg/cm^3 of Cal B has formation of particulates.

FT-IR analysis was performed on the hydrolysed Cal B samples. The soluble fractions of enzymatically treated samples, Figure 6.6 exhibited peaks at 990 and 1080cm^{-1}, which indicate the production of alkene (C=C) and ether (C-O-C) bonds; the 1080cm^{-1} has also been used as a urethane/ester identifier (McCarthy *et al.*, 1997). In contrast, carbonyl stretching (C-O), 1180 cm^{-1} peak, has decreased whilst comparing the control and enzyme treated samples which may suggest a decrease in ester formation.

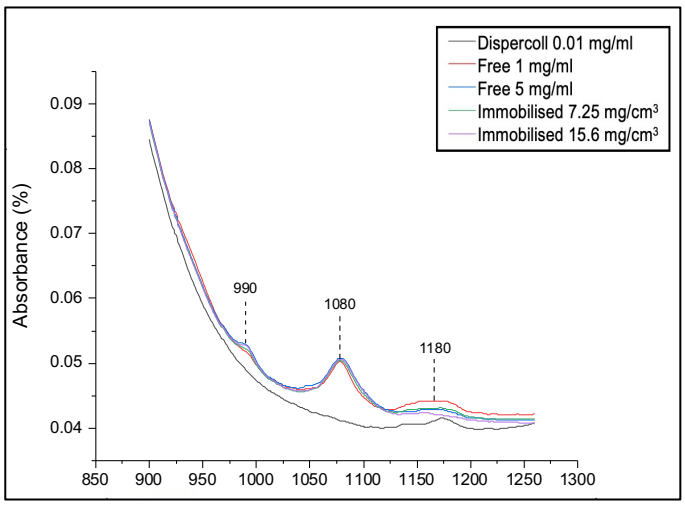

Figure 6.6: FTIR spectroscopy analysis of Dispercoll degradation by Cal B

Immobilised and free sample particle size distribution in relation to untreated 0.01mg/ml Dispercoll control sample after 24 hours of incubations

Overlayed graphs indicating changes reflecting Dispercoll degradation are observed in the signals at 990 cm^{-1} (C=C), 1080 cm^{-1} (C-O-C) and 1180 cm^{-1} (C-O)

The particle size distribution of Dispercoll oligomers was measured for both free enzyme and immobilised enzyme samples. Control, untreated, sample contained a single peak between the 0.1 and 10um size density classification (appendix E). Immobilised Cal B samples generated a lower density of particles in the 0.1 and 10um size density classification (appendix E) than that of the free system. Overall, the 15.6 mg/cm^3 CNF membrane had the lowest volume density of Dispercoll particles compared to other systems suggesting that the rate of degradation was the greatest in a high enzyme density membrane. Peak analysis was considered as degradation of Dispercoll and analysed, (Figure 6.7). Other peaks were disregarded as they could attribute to aggregation of the PU or falling out of solution.

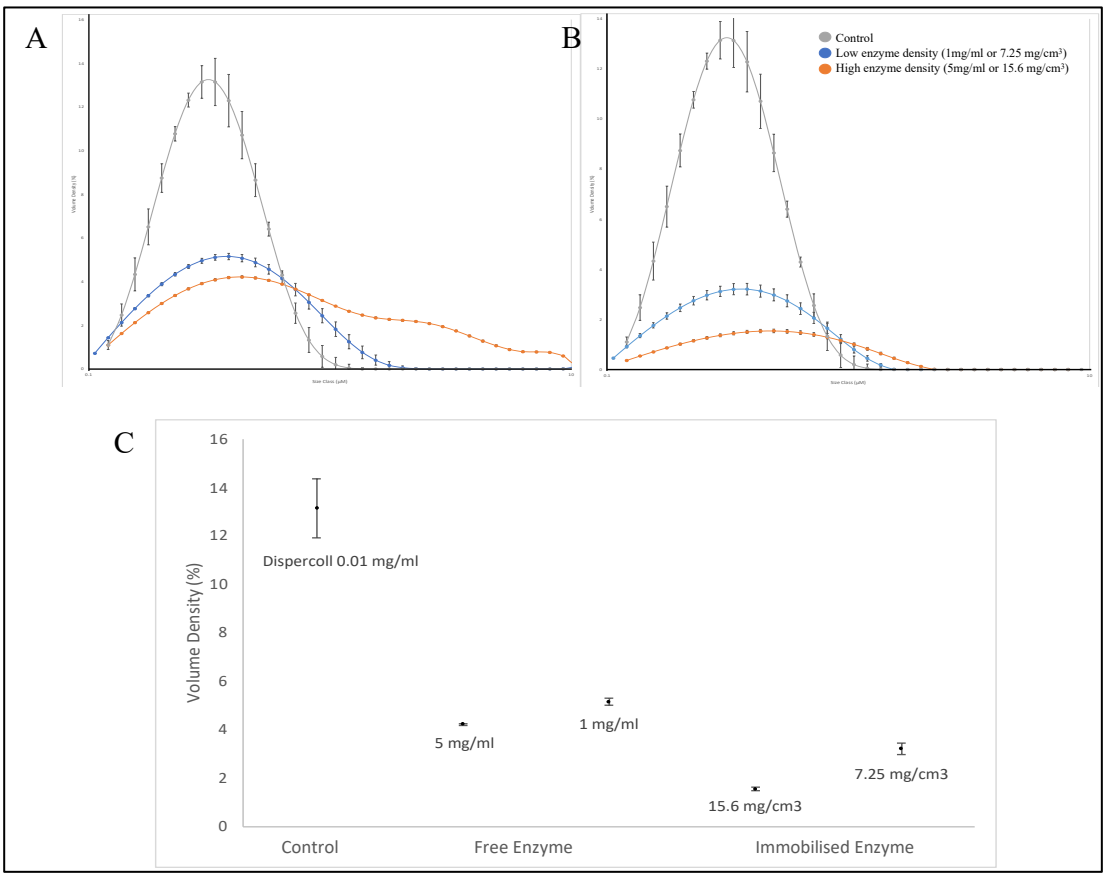

Figure 6.7: Particle size distribution from the hydrolysis of Dispercoll

Immobilised and free sample particle size distribution in relation to untreated 0.01mg/ml Dispercoll control sample.

A) Untreated 0.01 mg/ml Dispercoll (grey) with free Cal B 1 mg/ml (blue), free Cal B 5 mg/ml (orange)

B) Untreated 0.01 mg/ml Dispercoll (grey) with immobilised Cal B 7.25 mg/cm^3 (blue), immobilised Cal B 15.6 mg/cm^3 (orange)

The values shown are averages of 5 independent repeats with standard error bars.

C) Peak analysis comparison of Dispercoll degradation across free and immobilised systems

The values shown are averages of 5 independent repeats with standard error bars

Productivity is defined as the amount of Dispercoll that is hydrolysed in 1 hour per milligram of lipase. This was used to determine the degradability of the PU and the lipase potential. Calculations were adapted from (Abdul, Szita and Baganz, 2013) in (Table 6.8).

Table 6.8: Lipase productivity calculations

Productivity is defined as the millilitres of Dispercoll hydrolysed per hour per milligram of enzyme. Adapted from (Abdul, Szita and Baganz, 2013)

Reaction Conditions	Productivity of the lipase (mg/ml/hr)	Dispercoll Degradation (%)
Immobilised Cal B (15.6mg/ml)	2.33E-03	70
Immobilised Cal B (7.25 mg/ml)	3.78E-03	56
Free Cal B (5 mg/ml)	3.28E-03	55
Free Cal B (1 mg/ml)	3.53E-03	34

It can be inferred that the highest productivity is the immobilised system loaded with 7.25mg/ml. This has a third higher productivity than the higher enzyme loaded membrane. The free lipase systems shows that low enzyme reactions have higher productivity.

To explore the way in which Cal B degrades Dispercoll, assessment of PU hydrolysis was conducted by HPLC analysis of common products of the reaction and material property changes using a Viscometer. Using HPLC, the production of adipic acid, a hypothesised carboxylic acid monomer of PU was used as confirmation of hydrolysis. This has been employed in polyester degradation of other model PUs (Marjo *et al.*, 2017; Utomo *et al.*, 2020). Overall, Cal B produces a greater amount of carboxylic product in a higher enzyme loaded capacity.

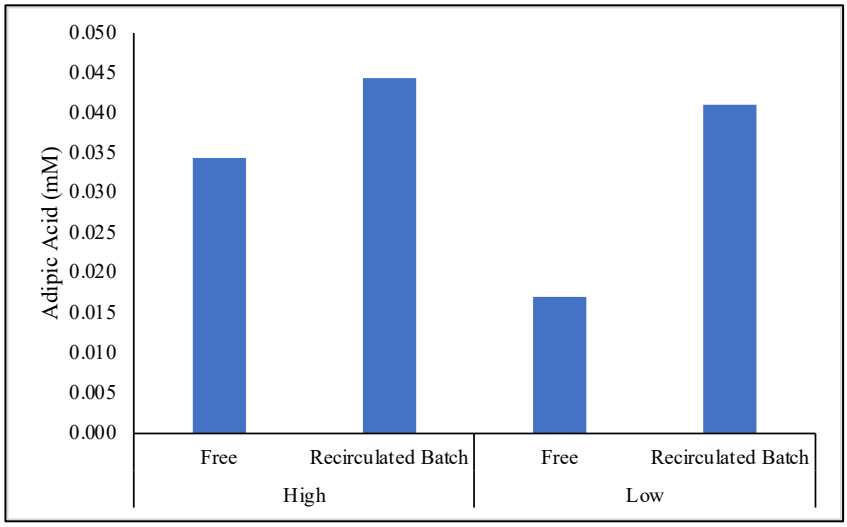

Figure 6.9: Adipic Acid production in hydrolysed samples from Dispercoll Degradation

Hydrolysed material was filtered from immobilised and free enzyme samples compared to a known standard carboxylic acid (Adipic Acid) to determine the amount of carboxylic acid present.

The values represent a single technical repeat.

Adipic acid was used as a reference to determine presence of carboxylic acid production after hydrolysis of polyesters. The high recirculated batch system has the greatest formation of adipic acid like monomers which correlates to the high rate of hydrolysis of this system.

Additionally, changes in the shear rate can also be used to indicate material property, (Figure 6.10). Untreated Dispercoll demonstrates shear rate properties resembling a pseudoplastic (Barnes, 1997).The soluble fraction when applied with the same pressure stress shows a linear trendline corresponding a Newtonian fluid as per Bingham principles (Bingham, 1922), further confirming the hydrolysation of Dispercoll.

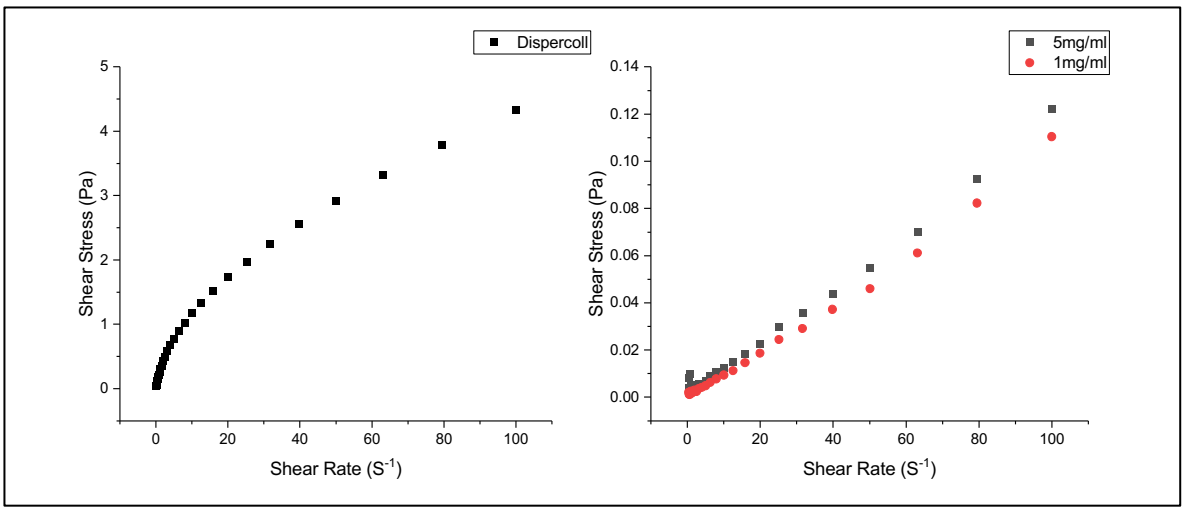

Figure 6.10: Shear rate properties of untreated and enzyme treated Dispercoll

Shear stress as a function of shear rate curve for (A) untreated 0.01 mg/ml of Dispercoll and (B) soluble fraction of Cal B at 1mg/ml and 5 mg/ml treated solution.

6.4 Discussion

Dispercoll is a pre-treated polyurethane polyester which increases its possibilities of hydrolytic cleavage of ester bonds using lipases (Venkatachalam *et al.*, 2012). Cal B possesses highest catalytic activity at optimum temperature ranges between 50 °C and 60 °C, yet activity is detectable at 20 °C. This can be seen in earlier temperature studies with synthetic substrate ρ-nitrophenyl butyrate where a comparable system to the recombinant lipase, PL002 which exhibits maximum activity at 20 °C was determined, Chapter 4. The lower temperature range encourages the use of this lipase without the additional energy costs that are required to increase the temperature for enzyme activation.

Polyester Polyurethane degradation using PL002

It has been identified that there is structural decomposition of urethanes using ammonium sulfate (Montaudo *et al.*, 1984). This can be seen through the work conducted here with the salp lipase and Dispercoll. Ammonium sulfate, in the most part, is removed prior to use. However small increments may remain which can cause Dispercoll to fall out of solution or aggregate, this can be seen in the photograph, (Figure 6.3). Montaudo *et al.*, (1984)., has identified that ammonium particulates encourage hydrolytic cleavage of the polymer chains forming additional tertiary amides. The proprietary structure of Dispercoll suggests that this effect cannot be confirmed. However, subsequent analysis of known tertiary amides can be used to determine if this is present. Analytical methods have been developed for amide separation, (Harada, 2016), this rational can be employed to detect presence of known tertiary amides. Similar approach was conducted in this study with the use of adipic acid to measure the production of carboxylic acid.

The rate of degradation of these long-chained polyester polyurethanes using the salp lipase was insignificant in comparison to the activity profile of Cal B, (Figure 6.4). This is synonymous of substrate comparisons conducted previously in Chapter 4. Here a longer chained synthetic substrate, ρ-nitrophenyl palmitate (C16), had a decreased amount of hydrolysis in comparison to the shorter chain, ρ-nitrophenyl butyrate. Therefore, it can be hypothesised that perhaps a shorter chained PU may be better suited for degradation purposes using PL002.

Polyester Polyurethane degradation using Cal B

Cal B demonstrates 50% of polyester polyurethane degradation after 12 hours, as observed, (Figure 6.4). The initial trials of PU degradation were measured in free lipase, a homogenous catalytic reaction. As mentioned previously, (Chapter 1 and 5), the molecular structure of this lipase is highly beneficial for the degradation of long chained plastic molecules. The lack of a lid domain suggests that the lipase has a highly open conformation which is beneficial for binding onto larger substrates (Ganjalikhany *et al.*, 2012; Zisis *et al.*, 2015) However, a limitation of free enzymatic reactions is that there is a likelihood of substrate inhibition. The high percentage of cysteine residues endorses Cal B as a suitable candidate for cysteine based site directed covalent immobilisation, (Chapter 4). Therefore, an attempt at utilising the CNF systems constant flow capabilities and convective mass transfer principles as a recirculated flow of PU substrate through the hindered enzymes provided a catalytic activity

This immobilised system mimics that of plug flow (no axial diffusion) resulting in a higher efficient biocatalyst (Colli and Bisang, 2011). According to the Stokes-Einstein equation, the mobility difference between the directed flow of polyurethane and the heterogeneous stationary biocatalyst, provides better particle collision than a free enzyme system (Jia *et al.*, 2002; Wang, 2006; Verma and Puri, 2013). Cal B in bead format, Immobead 150, was trialled. However, due to the material composition of the beads, the polyurethane firmly absorbed onto the materials and a flow system was unable to be generated.

Comparative Analysis of Immobilised and Free Systems

FT-IR results do not indicate any difference in the bond stretching between immobilised lipase and free lipase samples, Figure 6.6. Signal assessments have been determined from (Silverstein and Bassler, 1962; McCarthy *et al.*, 1997; Mountaki *et al.*, 2021) using degradation patterns of polyurethane polyester molecules. Due to the large molecular size of polyurethane polyesters, shifts in peaks can occur and identification of molecular changes may become difficult (Szycher, 1991) which must be considered when identifying signal changes in molecules with unknown structures.

Particle size distribution analytics, (Figure 6.7), encouraged a greater understanding of the degradation of Dispercoll. Peak comparison of particulates was conducted to demonstrate that the higher enzyme density membranes and free systems degrades at a greater rate. However, the free system with 5 mg/ml of Cal B has a greater distribution of particles. A suggestion could be that high concentration of free enzyme has degraded or become denatured accounting for the wider spread of particles (Verma *et al.*, 2013). Unreacted Impranil, has shown to have particle size distribution between 0.1 and 0.2 um in size (Biffinger *et al.*, 2015; Magnin *et al.*, 2020) giving further understanding behind the molecular structure of Dispercoll. Subsequent analysis could determine the rate of production of these bonds by analytical analysis of hydrolysed materials at different time points of the reaction.

Technoeconomic evaluations of the process need to be determined which include; overall process economics, associated costs of custom rigs and production of enzymes as well as enzyme discard costs (Rather *et al.*, 2022) to fully determine the true profitability of immobilised enzymes in an biotechnological capacity. Degradation capabilities was compared to analyse the free and immobilised systems. The measure of carboxylic acid production, (Figure 6.9), determined successful degradation of longer chained polyesters with higher loaded system, 15.6mg/ml immobilised lipase to produce the greatest yield of adipic acid. This is synonymous with flow studies determined in Chapter 5. The high lipase loading, in addition to the molecular structure of the lipase, a very small catalytic lid present on Cal B (Uppenberg *et al.*, 1995), determines maximal product conversion. However, there is a third increase in productivity, (Figure 6.8), in the immobilised 7.25 mg/cm^3 loaded membranes, when compared to free systems, which demonstrates that there is less required lipase needed to generate a similar polyurethane degradation system. There is great potential here to generate a polyester degradation by lipolytic systems that can encourage enzyme recovery and safer disposal biologically infused membranes. Industrial applications in flow systems as described here use a maximum cost of 3–10 % w/v of immobilised lipase to moderate operating costs (Basso and Serban, 2019). Therefore, this parameter can be used to determine maximal protein loading that can be used to ensure the system is not cost deficient.

The highly stable method of immobilising enzymes onto CNF membranes ensure that the system can be recycled for membrane reuse multiple times (Lee *et al.*, 2007) to hydrolyse a greater volume of Dispercoll. Previous studies, unpublished, have indicated that the CNF membrane remains active after processing up to 2 litres of solvent across 35 hours. The ability

to recover the lipase-matrix complex from the system further cements the benefits of an immobilised membrane bound catalyst. SEM analysis of immobilised Cal B membrane after Dispercoll exposure at 20 °C for 72 hours detected no visible fouling issues, (Figure 6.5). With little fouling evident the system could be optimised to higher flow rates; however this will decrease the residence time and thus may generate a lower rate of reaction (Nair *et al.*, 2007).

The material property changes identified by the viscometer suggest hydrolysis took place. The change of the material from pseudoplastic nature to Newtonian. This has been corroborated by other thermoplastic PUs (Xian *et al.*, 2018) and vital for its application as a liquid adhesive. To further understand the material property changes, NMR can be used to identify the bond changes, like FT-IR peak comparison experiments. This has been trialled with 13C NMR, (appendix C). However, there are many variables to consider determining a change in treated and untreated PU. Further analysis needs to take place whereby a greater emphasis on controls and internal standards are required to corroborate a shift in peaks to measure the degradation of the polyurethanes polyester.

The use of immobilised lipases in a recirculated flow system provides an alternative method of polyurethane degradation. It has been reported that other pre-treated polyurethanes, such as Impranil DLN, produce a clearing solution comparable to the hydrolysation properties of Cal B and Dispercoll. This suggests that the clearing is attributed to the cleavage of only the ester bonds found within Dispercoll (Biffinger *et al.*, 2015). However, another enzymatic activity is required to hydrolyse the remaining urethane bond of such PUs. Amidases, produced by bacterium, such as *Rhodococcus equi* strain TB-60, has been identified to degrade low molecular weight urethanes by induction of acetanilide (Akutsu-Shigeno *et al.*, 2006). This may be an additional enzyme that can be used in a multienzyme pathway to fully degrade polyester polyurethanes and an alternative to monomer recycling.

Chemically treated CNF membranes have the potential to be scaled up to a variety of different sizes and can be optimised for use in plug flow, batch and continuous reactors to achieve greater productivity (Lee *et al.*, 2007) thus encouraging the scale-up potential of immobilised matrixes. As a proof of concept, this recirculating batch flow demonstrates the potential use of Cal B as a biocatalyst in the biodegradation of liquid polyester polyurethanes. At lower volumes, gravity assisted separation was a useful method to remove the insoluble polyurethane. However, when

considering scale up the addition of a solid's separation method such as filter guards would need to be considered.

The use of immobilised lipases may provide an alternative method to current methods of polyurethane degradation. By successfully demonstrating Cal B activity on the model polyurethane system, and immobilising lipases on cellulose nanofiber, productivity can be compared to provide an alternative solution for the biodegradation of polyester polyurethane-based plastics at ambient temperatures. Therefore, this initial recirculated batch flow of the PU provides a method to biodegrade this material to obtain hydrolysed soluble particulates in a cost effective and suitably rapid system for ease of recyclability.

6.5 Conclusion

This study shows the successful implementation of immobilised Cal B in the degradation of polyester polyurethane, Dispercoll, with specific hydrolytic activity on the ester bond. The adipic acid hydrolysis product was observed by HPLC. Dispercoll biodegradation assays using *Candida antarctica* lipase B in a free and immobilised nature. A recirculating system was engineered to flow Dispercoll at 20 °C for 24 hours. The immobilised system of lower loaded Cal B had a greater rate of degradation. Here 56% was degraded at a rate of 3.78 $x10^{-03}$ mg/ml/hr; a higher degradation system than the free enzyme in solution (33% and 3.53 $x10^{-03}$ respectively). However, the higher loaded system had a greater rate of degradation, 70%. This suggests that there is yet an optimum to be achieved whereby a higher rate of degradation can be productively efficient. The enzyme–nanofiber composites can be used in different types of reactors, of differing sizes, to achieve optimum productivity. These results show that it is necessary to complement clearing studies with quantitative methods to confirm if an organism or enzyme can degrade polymers like Dispercoll. This application has a scope for trials suited with other similar plastics in a multienzyme system.

Chapter 7: Conclusions and Future Directions

7.1 Overall Conclusions

The overarching theme of this research has been to connect the elements of the bioprospecting pipeline to investigate the stabilisation of enzymes for industrial biocatalysis by immobilisation on cellulose nanofiber. This thesis has explored several strategies for the stabilisation of low temperature biocatalysts using a case study of lipases. A bioinformatic approach enabled the discovery of two enzyme candidates followed by heterologous expression and affinity purification and *in vitro* biochemical characterisation. Stability was assessed through immobilisation on cellulose nanofiber to examine the impact on activity of the enzyme candidates. Finally, the flow based system was evaluated for the enzymatic biodegradation of plastic. An overview of the role of each enzyme candidate in the deliverables of the project is shown in Figure 7.1.

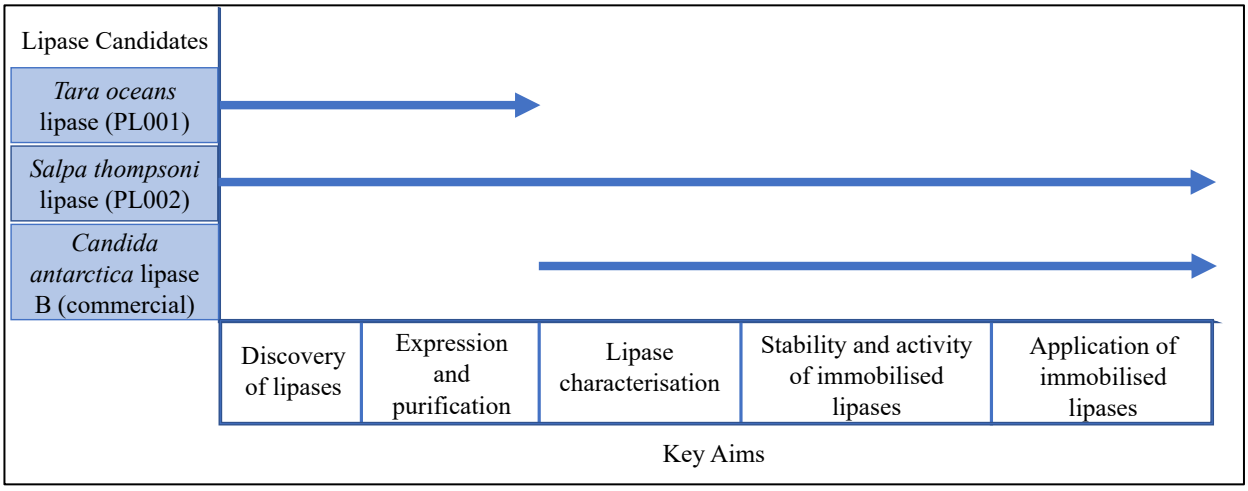

Figure 7.1: Summary of progress in relation to lipase candidates

Metagenomic data from the *Tara* Oceans expedition was mined for putative bacterial lipase candidates in samples collected in the Southern Ocean. In parallel, genomic, and transcriptomic data from a target eukaryotic organism inhabiting polar waters, *Salpa thompsoni,* was mined for sequences containing lipase motifs. This *in silico* approach yielded two lipase candidates, PL001 and PL002 respectively, (Chapter 2). To test the bioinformatic approach for enzyme discovery, recombinant protein production studies were conducted in *E.*

coli. While both enzymes were expressed, only PL002 had sufficient yield to progress to functional characterisation studies, (Chapter 3).

For assay validation and biocatalytic performance, a commercial enzyme *Candida antarctica* lipase B (Cal B) was used as a positive control. Here, synthetic, ρ-nitrophenyl substrate were applied to quantify enzyme activity under a range of conditions. The optimum temperature of PL002 was established to lie in the psychrophilic range, retaining over 60% activity between 15 to 25 °C and optimal conditions of pH 7. However, the overall specific activity is close to 4 folds less when compared to Cal B. The structural configurations of commercial Cal B suggest that the lack of lid present encourages a greater substrate affinity than the salp lipase (Uppenberg *et al.*, 1995). The recombinant procurement of PL002 further contributes to the difference in activity. Catalytic properties of other pancreatic like lipases has been determined using alternative substrates for affinity purposes, such as tributyrin. This may give rise to activity profiles more synonymous to the natural activity of the salp lipase; and thus, a greater activity, (Chapter 4).

The activity profile of these lipase candidates was used as a case study to examine the impact of immobilisation on cellulose nanofiber matrices (CNF) to enhance the stability of the enzyme, (Chapter 5). A flow biocatalysis system was used to assess the performance when immobilised on CNF membrane discs, whereby two factors were examined for their impact on enzyme performance. Firstly, a physical factor was tested which was the CNF enzyme density. Loadings of 7.25 and 15.6 mg/cm^3 were evaluated. While the overall enzyme activity was greater at the higher loading density, the productivity of the low density membrane was higher. The affinity towards the substrate, $K_{M\ (app)}$, of the 15.6 mg/cm^3 system has a threefold greater value than that of the lower Cal B density membrane; calculated to be 0.7200mM and 0.2316mM in recirculating flow respectively. The productivity of the lower enzyme bound system, 7.25 mg/cm^3 has a threefold greater rate of PNPB hydrolysis per hour than the 15.6 mg/cm^3 system suggesting less enzyme is required to function accordingly. Secondly, the impact of a biological modification, the addition of cysteine tag, showed a 30% decrease in activity compared to the unmodified salp lipase. While this did not have a significant impact on the $K_{M\ (app)}$ it was possible to show that it did not have a detrimental effect on stability. PL002 was highly stable whilst immobilised as the flow biocatalyst remained active after multiple flowthroughs, (Chapter 5).

Having established a flow-based system with model substrates, to demonstrate a potential application, the hydrolysis of polyester polyurethanes was tested under conditions of 20°C. Both PL002 and Cal B exhibited activity on Dispercoll, with Cal B exhibiting over 50%

degradation in comparison to 5% by PL002 in free lipase systems. Cal B was then deemed as a more efficient catalyst and thus an immobilised system, in recirculating flow, was derived. The two enzyme densities were evaluated whereby the lower loaded Cal B degraded more of the commercial liquid polyurethane, (56%) and at higher rate of 3.78 $x10^{-03}$ mg/ml/hr. However, the higher loaded system had a greater rate of degradation, 70%. A cost benefit analysis needs to occur to determine the ideal rate of degradation in relation to optimal productivity of the biocatalyst for industrial scale up (Chapter 6).

7.2 Future Directions

Future work on this project could focus on two areas, the identification and expression of candidate enzymes, and the refinement of the immobilisation system. This is summarised in Table 7.2.

7.2.1 Expanding the biocatalytic toolbox of cold active lipases

A pipeline to identify novel cold active lipases has been demonstrated in Chapter 2. Within the scope of this thesis, only one lipase candidate from each source was selected for subsequent characterisation, there is a great deal of potential lipases to be discovered. For instance, searching within the *Ciona intestinalis* genomes, identifies a putative hormone sensitive lipase (accession: XP_002122483.3) and monoacylglycerol lipase (accession: XP_004226795.2). These lipase candidates can be used as template genes for the identification of further lipase in the *Salpa thompsoni* assembled genome (Batta-Lona *et al.*, 2017) . The digestive profiles of this organism can be further defined by corroborating the presence of these putative genes within the short read archive data generated in house from *S. thompsoni* digestive tract RNA (samples AC_e20 and AC_e242, accession numbers SRX13276964 and SRX13276963) that was used to corroborate the presence of PL002.

An alternative approach is to look at transcriptomic genomic data which is a more powerful method to understand which sequences are expressed and have functional roles in a more targeted manner. This has been explored previously as a technique to identify beta-glucosidase enzymes expressed in salps (Cotton, 2021). Cold tolerance could be explored through a comparison of multiple salp species taking into account phylogenetic relationships and adaptation based on habitat (Kocot *et al.*, 2018).

Taking this one step further, proteomic studies could also take place to identify the role of the lipase candidate in relation to the whole organism. Employing a nature-inspired approach, the digestive system of the salp could be further investigated to understand genes implicated in the hydrolysis of algal biomass and hydrolysis of triacyclglycerols. Similar studies on diet have been conducted on *Daphnia pulex.* Multiple lipase genes were identified by conducting feeding

trials that included short and longer chained fatty acids of alga and cyanobacteria (Koussoroplis, Schwarzenberger and Wacker, 2017). It has been elucidated that there is more than one type of lipase gene present in marine invertebrates (Rivera-Perez, 2015). Therefore, to explore this further feeding trials could be a means of ascertaining functional lipases.

Connecting *in silico* enzyme discovery with heterologous expression and characterisation remains a challenge for the full potential of marine bioprospecting to be realised. In terms of expression and characterisation, the *Tara* Oceans lipase, PL001, would merit further investigation. The initial expression studies yielded insoluble protein, which might have been caused by the over expression (Terpe, 2006). Potentially the co-transformation of biological chaperones could be trialled to enhance soluble expression as shown in the recombinant expression *Burkholderia* lipase in *Escherichia coli* using cytoplasmic chaperone GroEL/ES (Narayanan, Khan and Chou, 2011). The addition of fusion tags has also resulted in soluble protein production and could be investigated (Esposito and Chatterjee, 2006).

While the salp lipase was measurable in the ArcticExpress (DE3) *E. coli* cell line, the yield was low. To increase the yield a secretion based expression system, such as the use of yeast cells could be trialled (Gomes *et al.*, 2018). This strategy was shown to be effective for eukaryotic lipase candidates in a yeast based system whereby the secretion system was modulated in yeast *Y. lipolytica* to obtain high yields of Cal B in batch expression systems (Park *et al.*, 2019). The secretory nature circumvents the need for cell disruption which may reduce the yield.

Expanding the range of enzymes that can be produced at scale has several applications. For instance, current medical applications of digestive enzymes, such as the prescription medication Creon ® for the treatment of pancreatic deficiency, uses lipases derived from porcine sources. Therefore it may not be suitable for specific faiths or diets (Kuhn *et al.*, 2010). A recombinant alternative can be a cheaper and more inclusive option.

The use of fluorescent derivatives for the characterisation of enzymes facilitates screening but can be a limitation in terms of characterising novel enzyme activities. A wider range of substrates with differing chain length should also be investigated. Here ρ-nitrophenyl compounds of 4 carbon and 22 carbon were investigated. Mid-sized substrates, such as ρ-nitrophenyl caprate (carbon chain length 10) may help to further determine substrate specificity as conducted with cold active *Pseudomonas fluorescens* lipase whereby substrates

with chain lengths of 2 to 18 were trialled (Elend *et al.*, 2007). This would help to understand the activity profile and substrate specificity. Substrates more consistent with what is consumed by salps may provide higher activity (Rivera-Perez, 2015) and should be investigated. Metal co-factors such as calcium ions have been modulated in similar assays to increase activity. Calcium ions have the propensity to form long chain fatty acids and therefore increase the activity of the lipase as demonstrated on lipase from *Geobacillus stearothermophilus* (Ekinci *et al.*, 2016). Pancreatic lipases from eukaryotic sources have had an increase in activity using calcium ions, (Alvarez and Stella, 1989). As the protein production pipeline has been determined, the assessment of these parameters would be a short term target. Using a diverse range of substrates to assess the temperature and pH stability parameters as described in Chapter 4, which would help to characterise the length of time the lipase remains stable and active in contexts that might be more relevant to biocatalytic reactions. There were also some key limitations to the substrates used in terms of their decomposition.

Modifications to the protein may change the activity and stability relative to the native enzyme. The role of the 6xHis tag has been reported to decreases activity against ρ-nitrophenyl compounds (de Almeida *et al.*, 2018). To more fully understand the salp lipase, comparative assays whereby PL002 containing the His-tag or following cleavage, using TEV protease to remove the histidine tag (Abdullah and Chase, 2005). Might be characterised alongside the native lipase that has been extracted directly from a salp. This would also provide valuable data on the role of the enzyme within the physiological system.

Previous work on the characterisation of key residues for cold adaptation has focussed on site directed mutagenesis (Wang *et al.*, 2021). This could be applied to understand how PL001 and PL002 function in low temperature environments. For example, PL001 was predicted to have a highly active serine residue located within the nucleophilic elbow, Ser-179. This could be modified to alanine, glycine, cysteine or threonine as conducted on hormone sensitive lipase to determine the activity changes (Holm *et al.*, 1994). PL002 has a cluster of glycines around the active site. It has been demonstrated by exchanging these residues to cysteine residues the activity of the lipase changes from cold active to a more mesophilic nature (Veno *et al.*, 2019), this too can also be investigated to determine changes in activity.

However, in the case of both lipases, there is an absence of crystal structure present which suggests that perhaps further validation is required to determine the cold adaptations associated

with protein structures. Homology modelling did provide similar protein structures however the confidence scoring suggests some uncertainty to the protein structures. This makes it difficult to confirm the protein folding patterns of the lipase and any characteristics that may pertain towards cold activeness are uncertain.

7.2.2 Design of systems to enhance performance of immobilised biocatalysts

Immobilisation enables reuse of biocatalysts, reducing cost and offering process flexibility. Electrospun CNF membranes have been demonstrated to be a promising matrix for immobilisation of enzymes due to their increased surface area and mass transfer benefit (Menkhaus *et al.*, 2010). This study explored two possible routes for enhancing CNF immobilisation. Loading, as defined by enzyme density, is an important parameter in this system as it also influences the physical constraints on the enzyme. Recently, loading studies have been conducted on lipase from *Pseudomonas fluorescens* immobilised onto Octyl-Agarose Beads. This has demonstrated that high lipase loading can cause protein-protein interactions effecting the activity of the biocatalyst (Arana-Peña *et al.*, 2020). Therefore, the immobilised system presented, (Chapter 5), can also bare similar implications on stability and activity. A higher loading of Cal B must be trialled to ascertain the full potential of the CNF matrix.

Reuse of the CNF membrane will be a vital determinant in the technoeconomic viability of using this approach. Stability tests to determine membrane lifespan can be assessed through multiple flow throughs at the same flow rate and residence time. Similar studies have been conducted on the production of trans-cinnamic acid (Hong *et al.*, 2021). In addition, to fully determine the rate kinetics, especially the reactor capacity, further flow rates will need to be assessed to determine the effects of mass transfer limitations and impacts on rate constants. Reported flow kinetics derived using Lilly-Hornby kinetics have done so using much lower flow rates (Xiao *et al.*, 2019).

While the experiments conducted in this study were executed in low temperature and aqueous conditions. The ρ-nitrophenyl compounds are universally used to characterise lipase systems, however the scale at which membrane bound lipases have been operated here increases the risk of substrate degradation. Therefore, additional water soluble substrates should be trialled, this

includes the use of tributyrin (Francolini *et al.*, 2020). Substrate degradation suggests subsequent analysis of the immobilised membrane to take place in a similar end-point assay instead of measuring flow catalysis. This may provide a further understanding to the immobilised enzyme kinetics present as done so with enzymes immobilised onto monoliths (Alotaibi *et al.*, 2018). In addition, many lipases reactions take place in solvent systems, such as transesterification reactions for fine chemical production (Tian *et al.*, 2015). Establishing a set of compatible solvents with this biocompatible CNF membrane and constructing a rig design that can keep constant temperature conditions and prohibit solvent evaporation would expand the catalysis remit and purification of products.

In terms of the plastic story application, the degradation of plastic compounds is of timely importance, and enzymes, especially those of the alpha/beta hydrolase family, are being extensively researched for their ability to perform challenging cleavage reactions (Magnin *et al.*, 2020). However, there is still much to do in terms of making this technology cost effective. Lipases have been successfully utilised to hydrolyse polyester molecules, and this was further demonstrated here using Dispercoll. The salp lipase has shown substrate affinity towards shorter chained molecules so PL002 could be trialled with shorter polyesters to determine the hydrolysis activity. Alternative enzyme candidates, such as amidases, have also been identified to degrade polyurethanes (Akutsu-Shigeno *et al.*, 2006). Therefore, a multienzyme pathway to fully degrade the polyester polyurethane can take place. Enzymes may be immobilised on different membranes for sequential reaction, or co-located, potentially even in a multi-enzyme system (Jia, Narasimhan and Mallapragada, 2014). Site specific positional immobilisation can be utilised using biologically tagged enzyme candidates onto known binding sites on the chemically activated cellulose nanofiber for an optimised biodegradation system. This can be orientated to specific positions to optimise the flow catalyst (Schoffelen and van Hest, 2013). To make the system compatible with the large volumes and loadings that might be required in an industrial process there will need to be a redesign of the flow-through system to cope with the pressure and solid loading in a cost suitable system.

Low temperature enzymes in a flow system could have future applications in the synthesis of thermally labile compounds. For example, the production of a rose scented compound, 2-phenylethylacetate, was determined using a lipase catalysed system, (Figure 7.2).

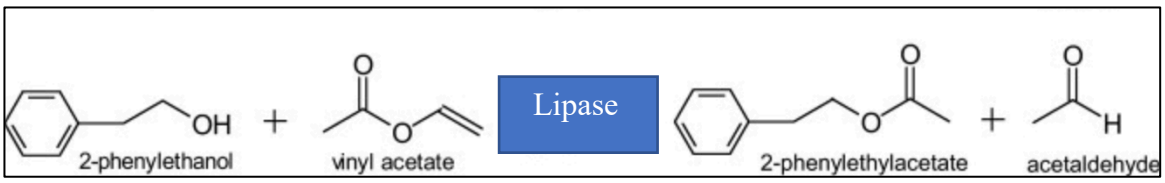

Figure 7.2: Transesterification reaction to produce 2-phenylethylacetate

Adapted from (Białecka-Florjańczyk *et al.*, 2012)

In the CNF system presented here, the immobilised lipase may be tested using a recirculating flow of 2-phenylethanol and vinyl acetate. Intermittent samples would be taken and measured using gas chromatography to determine the presence of 2-phenylethyacetate. Immobilised lipase from *C. rugosa* was utilised in a similar manner however in a closed shaking system instead of flow based catalysis (Kuo *et al.*, 2014).

The versatility of the CNF membrane for flow biocatalysis lends itself to innovative manufacturing applications. As demonstrated in this thesis, this can be fully realised through an understanding of both biological and physical factors on the system.

Table 7.3: Summary of future works

These goals have been categorised based upon colour, green (accomplish in less than 6 months), yellow (accomplish in 6 to 12 months), red (long term goals greater than a year).

<table>
<tr><th colspan="10">Future Direction</th></tr>
<tr><th colspan="2">Lipase Discovery</th><th colspan="2">Lipase Expression and Purification</th><th colspan="2">Lipase Characterisation</th><th colspan="2">Lipase Immobilisation</th><th colspan="2">Lipase based Applications</th></tr>
<tr><th>Aim</th><th>Objectives</th><th>Aim</th><th>Objectives</th><th>Aim</th><th>Objectives</th><th>Aim</th><th>Objectives</th><th>Aim</th><th>Objectives</th></tr>
<tr><td rowspan="3">Identify other candidates</td><td rowspan="2">Other lipases can be identified within the Tara Oceans sample site and salp target genome</td><td rowspan="3">Bacterial based expression systems</td><td rowspan="2">Attempt Western Blot to confirm PL001 production</td><td rowspan="3">Functional assays</td><td rowspan="3">Trial: A full range of ρ-nitrophenyl substrates, Metal co-factors, Temperature, and pH stability tests, nature based substrates</td><td>Activity</td><td>Increase enzyme concentration the membrane to assess if there's detrimental effects on activity</td><td rowspan="3">Hydrolysis reactions: Plastic Degradation</td><td>Multienzyme flow system Trial immobilised membranes of amidases to determine if recirculated flow of polyurethanes can also be degraded</td></tr>
<tr><td>Stability</td><td>Process multiple flow throughs of a single membrane to establish stability</td><td rowspan="2">Optimise the system through scale up methods</td></tr>
<tr><td>Lipases can be identified within</td><td>Purify the truncated PL001 for</td><td>Cal B Parameters</td><td>Trial membrane based upon Cal</td></tr>
</table>

	organisms from warmer regions to compare structural adaptations		characterisation studies. This would be used to assess if the proteins are active.		Compare His tagged recombinant lipase, a His cleaved recombinant lipase and an extracted salp lipase to see activity differences		B optimal conditions		Shorter polyesters to be trialled with the Salp lipase due to preference for smaller substrates
Proteomics and metabolomic studies	Feeding trials to identify digestive enzymes and their pathways.	Yeast based expression systems	Trial this to improve yield and titre of protein due to secretary nature expression system	Site directed mutagenesis	PL001 has a hypothetical nucleophilic serine residue at position 179. This can be modulated to confirm activity.	Substrates	Trial other substrates that are less likely to degrade	Transesterification reactions: Scented Ester Compounds	Determine biocompatibility of cellulose membranes with solvents such as esters
	Lipid analysis can be used to determine the nutritional diet and types of digestive enzymes.	Medical applications	Express and purify lipase candidates for alternative digestive supplements		Cold residues isolated in PL002 can be altered to see activity changes.				Trial flow-based systems to determine a continuous production of high value compounds

Chapter 8: Appendix

Section A: Identification of Lipase Candidates for Recombinant Expression

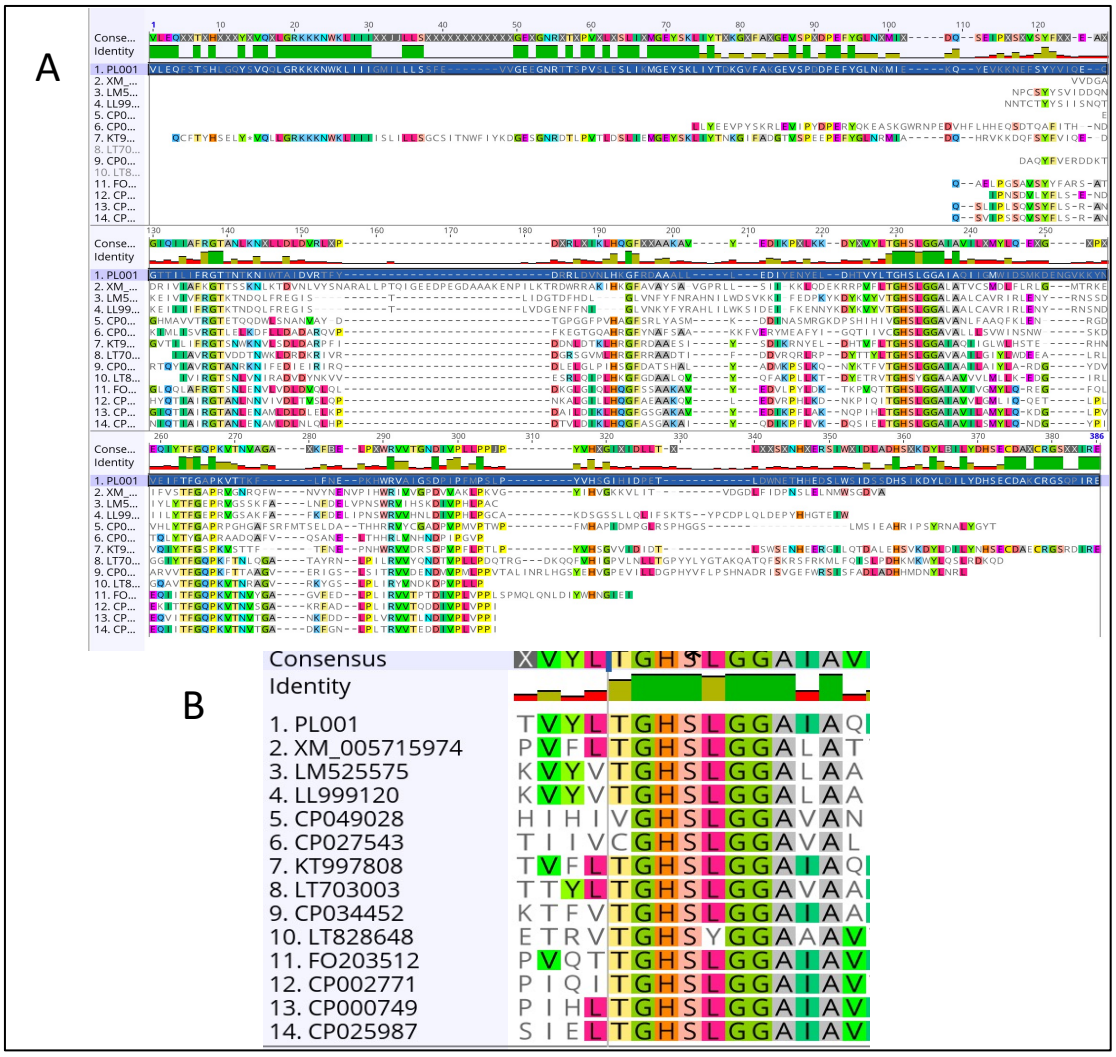

Figure 8.A.1: Sequence alignment of PL001 and other similar organisms

The tBLASTN tool was used to identify sequence similarity. Multispecies alignment to identify conserved domains ≥ 95% conserved amino acids are highlighted. The Lipase family nucleophilic elbow is boxed with catalytic amino acid (serine) highlighted (*). Alignment was performed using Geneious using Clustal Omega alignment tool.

A show the full alignment. B shows the conserved sequences

Figure 8.A.2: Sequence alignment of PL002 and other lipases

Aligned sequences; 2 from the closest sequence similarity *Ciona intestinalis*, 3 from the brachiopod *Linguna anatina*, 4 from the golden apple snail *Pomacea canaliculata*, 5 from the scallop *Mizuhopecten yessoensis,* 6 from the little brown bat *Myotis lucifugus,* 7 from the central bearded dragon *Pogona vitticeps,* 8 from the star coral *Orbicella faveolata,* 9 from the West Indian manatee *Trichechus manatus latirostris,* 10 from the reedfish *Erpetoichthys calabaricus* and 11 from the lancelets *Branchiostoma belcheri* ≥ 95% conserved amino acids are highlighted. The Lipase family nucleophilic elbow is boxed with catalytic amino acid (serine) highlighted (*). Alignment was performed using Geneious using Clustal Omega alignment tool.

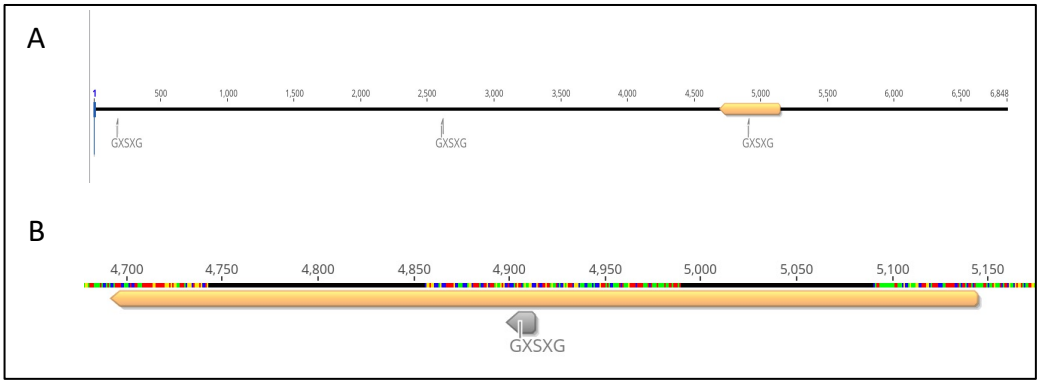

Figure 8.A.3: Open Reading Frame in the *Salpa thompsoni* genome

The image highlights conserved sequence GXSXG

0% zoom (A), 10% zoom (B) and 20% zoom (C)

Table 8.A.4: Top 10 BLASTP results aligning to PL001

Description	Max Score	Total Score	Query Cover	E Value	% Identity	NCBI Accession Number
lipase [uncultured Mediterranean phage]	337	337	79%	2e-113	64.05%	ANS04498.1
hypothetical protein CXT73_01935 [Euryarchaeota archaeon]	242	242	86%	2e-75	47.71%	RZD42941.1
hypothetical protein CXT73_01665 [Euryarchaeota archaeon]	231	231	81%	1e-71	49.40%	RZD43021.1
hypothetical protein [Candidatus Woesearchaeota archaeon]	216	216	88%	5e-66	42.55%	MAG49137.1
lipase family protein [Thaumarchaeota archaeon]	211	211	79%	1e-63	47.74%	NMJ87919.1
hypothetical protein CXT73_03135 [Euryarchaeota archaeon]	178	178	84%	7e-51	38.35%	RZD42392.1
hypothetical protein CXT73_05775 [Euryarchaeota archaeon]	164	164	84%	1e-45	36.23%	RZD41000.1
lipase family protein [Psychrosphaera saromensis]	99.8	99.8	58%	2e-20	31.22%	WP_105051833.1
lipase family protein [Oleispira antarctica]	92.0	92.0	51%	1e-17	35.50%	WP_046008945.1

VLEQFSTSHLGQYSVQQLGRKKKNWKLIIIGMILLLSSFEVVGEEGNRTTSPVSLESLIKMGEYS
KLIYTDKGVFAKGEVSPDDPEFYGLNKMIEKQYEVKKNEFSYYVIQEQGTTILIFRGTTNTKNIW
TAIDVRTFYDRRLDVNLHKGFRDAAALLLEDIYENYELDHTVYLTGHSLGGAIAQIIGMWIDSMK
DENGVKKYNVEIFTFGAPKVTTKFLFNEPKHWRVAIGSDPIPFMPSLPYVHSGIHIDPETLDWNE
THHEDSLWSIDSSDHSIKDYLDILYDHSECDAKCRGSQPIRE

Figure 8.A.5: Open Reading Frame translation of PL001

LCAVTVKMTYSSKPSSNNMSGGKSYTWTCSAFLKIILLTLTISPSKAAHPRVGKNETNNKKE
VCYKTYGCFKNDPPFNPKMPLPLGEKQLGTKFLLRTRENVNDYEITNQADIANSTFNASRPT
KVLIHGFVLGGKEIAPWVPTMADAILGKENVNVILVNWVQGAKTQYDQAVANTRMVGAQIHR
LINRLSRKHGAKANDFHLIGFSLGSHVAGFAGKASIKSGKQLGRISGLDPANPAFNSNSSEV
RLDRTDAKFVDVIHTDIRTILHISSGMNRSLGHIDFWPNGGESQPGCHNWNGGIFQGFQDMA
VCDHLRAPQLYIASIITTLPMIGYRCPNYDSFRRGTCLNCRGKVGSHKNNRCAVMGYYAEPP
RGSRKDAQVDYYLDTSDTSPYANRHYQVLIHWRKVPGKTTEEGQRASLFLRLHGEYMSSEPR
KLFLYKDLSTKYYHVYHNRTARFMITLPWDQDLGDLKKVTFWWQRQTCWHYIGCKNDENIFV
KRIRVLDAVEQKRYTFITPERLEHERVAPREILPNDKVEFVARQHHPKHKNSRSGRKGVEEA
DIVEPLLRQPMIVRRDTSSSSTSQSLSN

Figure 8.A.6: Open Reading Frame translation of PL002

Section B: Expression and Purification of Cold Active Lipases

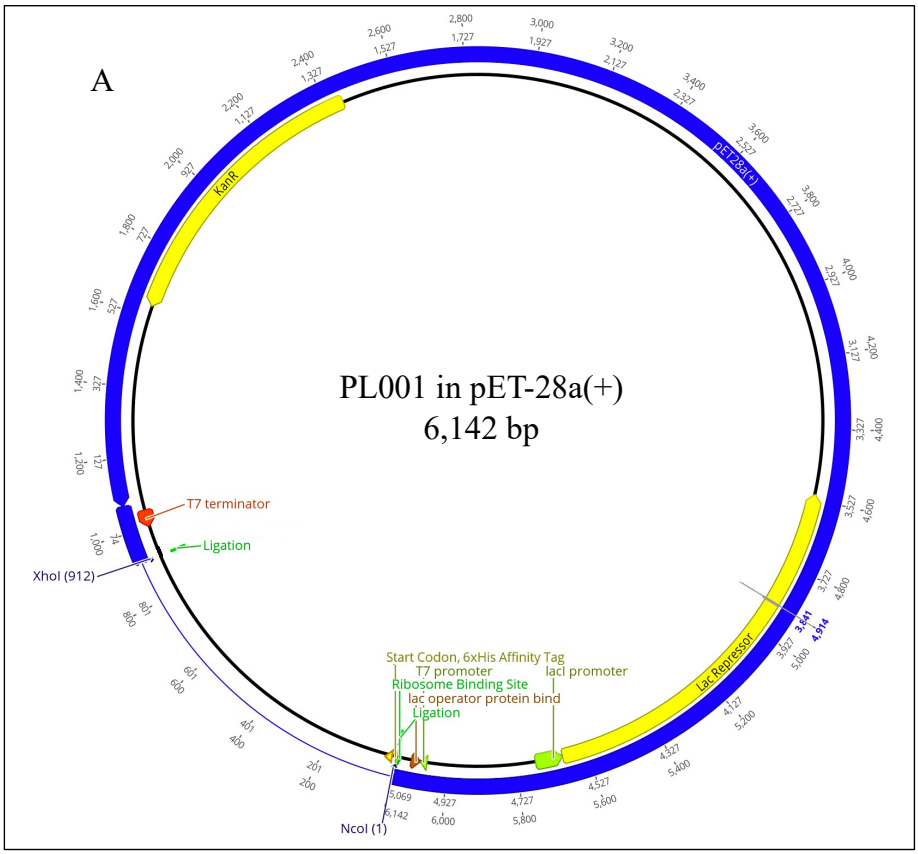

Figure 8.B.1: *Tara Ocean* lipase, PL001, expression construct

Synthesised expression construct formed from PL001 insert into pET-28a (+)

Table 8.B.2: Summary of PL001 Expression parameters

Experiment	Conditions				Analysis
	Temperature	pH	Induction Times	Cell Type	
PL001 and Negative control (PET-28a (+))	37°C	7.5	2 and 4 hours	BL21 PLysS	No clear band shown at the relevant size, 35kDa.
PL001 and Negative control (PET-28a (+))	15°C	7.5	4 hours and overnight	BL21 PLysS	Early formations of some protein expressed at 25kDa in the supernatant.
PL001 and Negative control with and without IPTG (pET-28a (+))	10°C	7.5	Overnight	BL21 PLysS	An emergence of a band found in the 25kDa range throughout the entire positive fraction and not in the negative controls.
PL001 and Negative control with and without IPTG (pET-28a (+))	5°C	7.5	Overnight	BL21 PLysS	An emergence of a band found in the 25kDa range throughout the entire positive fraction and not in the negative controls.
PL001 and Negative control (PET-28a (+)) with a range of different antibiotics and IPTG	10°C	7.5	24 Hours	BL21 PLysS	No clear conclusions, 25kDa band is present in the induced overnight with antibiotic cultures. (Figure 4.2)
PL001 and Negative control (PET-28a (+))	10°C	7.5	72 and 96 Hours	BL21 PLysS	Formation of the protein at 35kDa in the insoluble pellet range, (Figure.3)
PL001 and Negative control with a range of pH.	10°C	6,7.5 and 8	24 hours	BL21 PLysS and Arctic Express	No clear conclusions, 25kDa band is present in the induced overnight with antibiotic cultures.

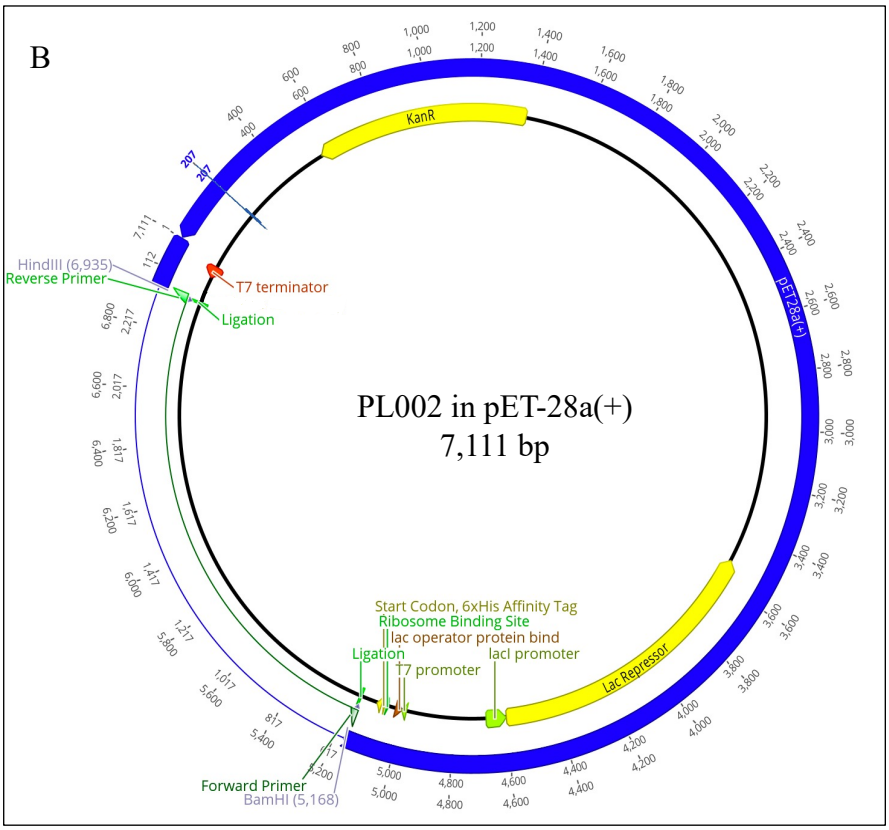

Figure 8.B.3: Salp lipase, PL002, expression construct

Synthesised expression construct formed from PL002 insert into pET-28a (+)

Table 8.B.4: Summary of PL002 Expression parameters

Experiment	Conditions				Analysis
	Temperature	pH	Induction Times	Cell Type	
PL002 and pET-28a (negative control)	16°C	7	24 and 48 hours	BL21	Nothing relevant
PL002 with Takara Biological Chaperones	16°C	7	24 and 48 hours	BL21	Very similar in size to chaperones, hard to distinguish
PL002 with Chemical chaperones (sorbitol)	16°C	7	24 and 48 hours	BL21	Addition of Sorbitol showed little effect.
Varying IPTG (0.5mM) with Biological Chaperones	16°C	7	48 hours	BL21	No effect
Varying IPTG (1mM) with Biological Chaperones	16°C	7	48 hours	BL21	Band is present, but due to chaperone sizes being similar it is hard to distinguish
Arctic Express	10°C	7	24hours and 48 hours	Arctic Express	Cell chaperone (60kda) interferes with PL002 our protein

Cloning of PL002

The identified salp lipase, PL002, was amplified using gradient PCR amplification. Primers were designed with the restriction sites, HindIII and BamHI at the N and C terminus respectively.

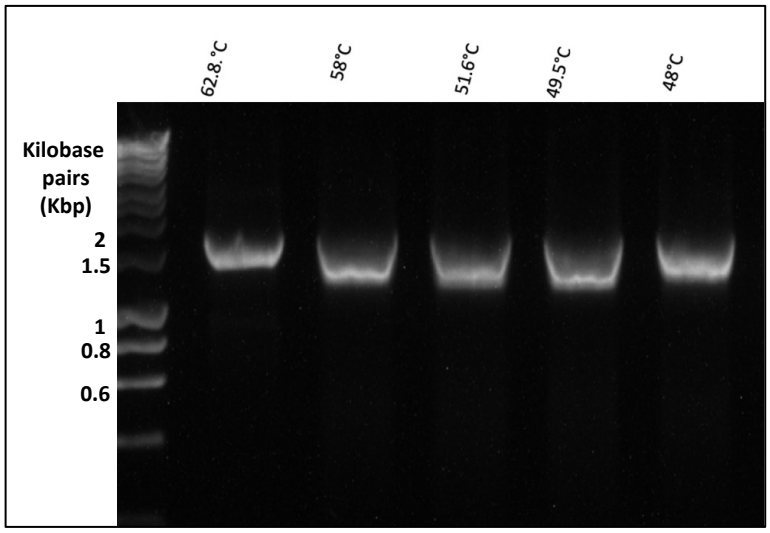

Figure 8.B.5: PCR reactions of PL002

1% DNA Agarose Gel with. Lanes 1 and 8 are the Hyperlader 1kb, lanes 2 to 6 are the PCR reactions for PL002, lane 7 is the PCR reaction for the positive control, BGL

The PL002 insert has a size of 1761 base pairs, calculated from the Geneious software, which can be seen throughout all the sample lanes. Hence, the optimised temperature of 62°C was used for further implication, Figure B.6.

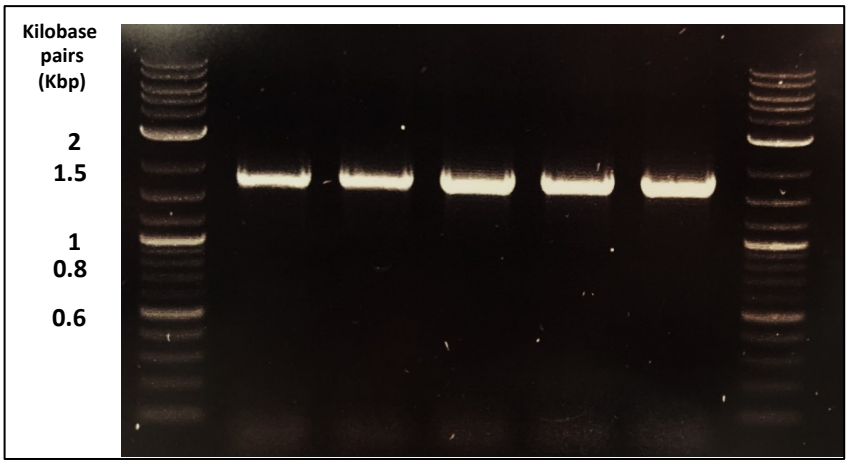

Figure 8.B.6: Q5 PCR reactions of PL002

1% agarose gel. Lanes 1 and 7 are the Quick-Load® 1 kb Plus DNA Ladder, lanes 2 to 6 are the Q5 PCR reactions for PL002.

These insert bands were extracted from the gel and used for restriction digest alongside the empty, pET-28a(+) vector to prepare the insert with sticky ends for successful cohesion to the vector (Smith, 1993). This was carried out using the restriction enzymes BamHI and HindIII. Using T4 DNA Ligase, ligations of ratios 1:1 and 3:1 were used. These were successfully grown on kanamycin selective agar petri dishes. Colonies were small and selected for a starter culture grown overnight. This was then miniprepped to extract viable plasmids. Figure B.7 shows the restriction digest results following miniprep. Here bands are shown near the region of the plasmid, 5.3Kbp. This suggests that the colonies grown from transformation stages were false positives and the plasmid religated onto itself.

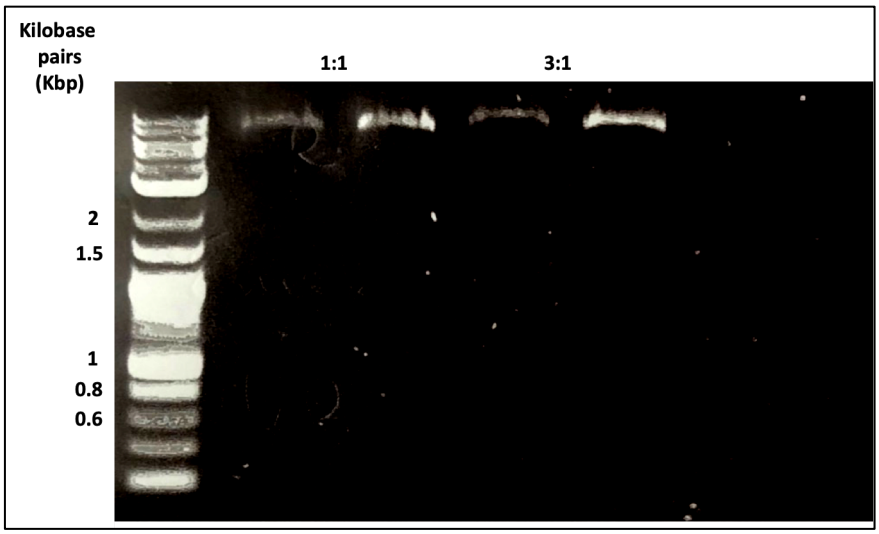

Figure 8.B.7: Miniprepped PL002

1% agarose gel with restriction digest samples.

Lane 1 is the Quick-Load® 1 kb Plus DNA Ladder, lanes 2 to 5 are transformed ligations of ratios 1:1 and 3:1.

Section C: Characterisation of Cold Active Lipases

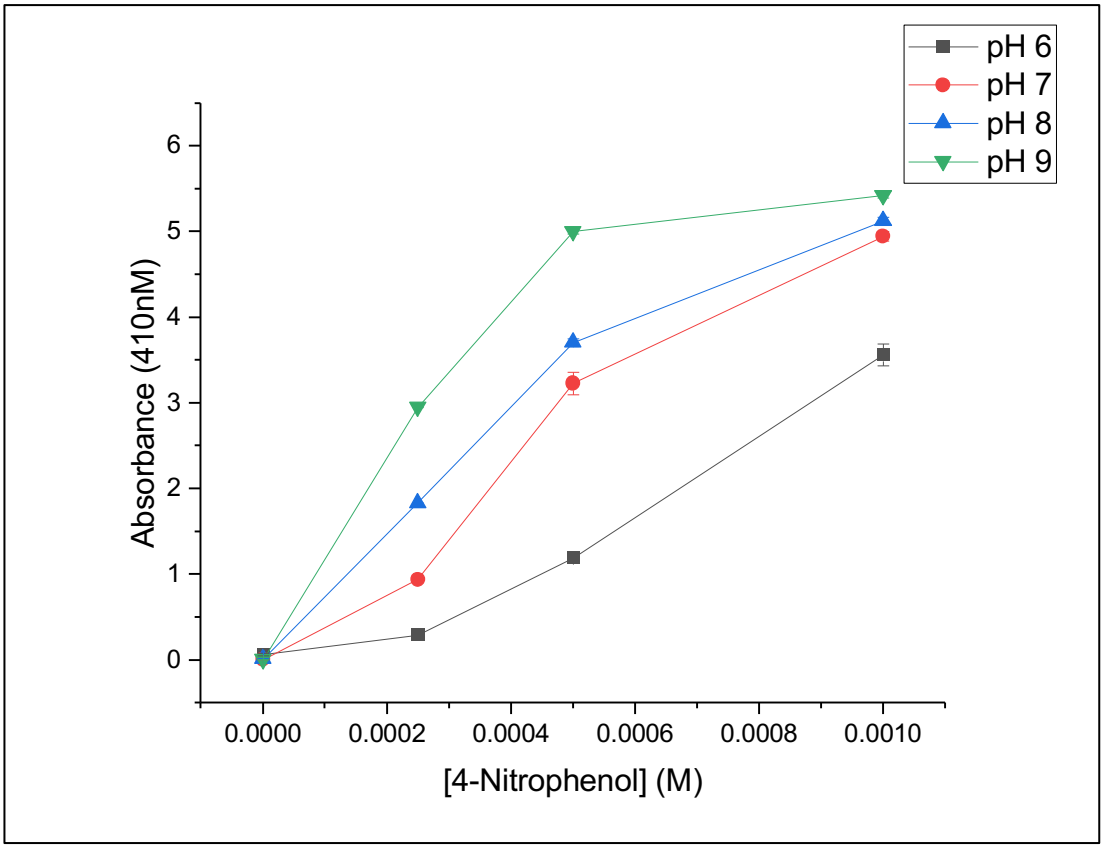

Figure 8.C.1: Standard curve of 4-Nitrophenol in relation to pH

Unless stated otherwise, pH profiles were expressed in relation to absorbance reads at 410nM. Each value represents the mean ± standard deviation (SD) of five replicate values.

Table 8.C.2: Specific activity of P-nitrophenyl butyrate based lipase reactions

Enzyme	Taxonomy	Temperature (°C)	Activity (U/mg)	Reference
Malbranchea cinnamomea	Fungus	40	263.3 ± 4.6	(Duan *et al.*, 2019)
Alkalispirillum sp. NM-ROO2	Bacteria	52 °C	38.1 ± 1.7	(Mesbah, 2019)
Aspergillus niger	Fungus	40	0.22	(Badgujar *et al.*, 2017)
Aspergillus niger	Fungus	30	1293	(Cong *et al.*, 2019)
Aspergillus oryzae	Fungus	45	7.9	(Q. Li *et al.*, 2021)
Bacillus licheniformis	Bacteria	90	15916	(Ugras, 2017)
Bacillus licheniformis – cold tolerant version	Bacteria	35	93.37 ± 2.45	(Zhao *et al.*, 2021)
Bacillus lipase	Bacteria	30	79.42	(Jain and Mishra, 2015)
Bacillus subtilis lipase A	Bacteria	25	9.4 ± 0.5	(Zhou *et al.*, 2019)
Burkholderia cepacia	Bacteria	25	29.11	(Badgujar and Bhanage, 2015)
Callosobruchus maculatus (beetle)	Animalia	37	0.36	(Malaikozhundan and Vinodhini, 2018)
Candida antarctica	Fungus	60	22.5 ± 0.5	(Carniel *et al.*, 2017)
Candida cylindracea	Fungus	40	0.83	(Badgujar *et al.*, 2017)
Candida rugosa	Fungus	40	0.28	(Badgujar *et al.*, 2017)
Candida rugosa	Fungus	25	12.15 ± 0.12	(de Morais *et al.*, 2016)
Ectomyelois ceratoniae (locust)	Animalia	30	0.4	(Ranjbar *et al.*, 2015)

Geotrichum candidum (human microbiome)	Fungus	25	11.48 ± 0.13	(de Morais *et al.*, 2016)
Lactobacillus rhamnosus	Bacteria	37	0.81	(Manasian *et al.*, 2020)
Marinactinospora thermotolerans	Bacteria	37	139.24	(Deng *et al.*, 2016)
Mucor javanicus	Fungus	40	0.21	(Badgujar *et al.*, 2017)
Mycobacterium tuberculosis	Fungus	37	35.71	(Lin *et al.*, 2017)
Oryza sativa (rice)	Plantae	35	4.73	(Chen *et al.*, 2019)
Paenibacillus pasadenensis	Bacteria	50	1165.57	(Gao *et al.*, 2018)
Pancreatic like lipase, Salpa thompsoni (Zooplankton)	Animalia	20	3.16 ± 0.14	
Penicillium expansum	Fungus	35	26.5	(Tang *et al.*, 2015)
Proteus sp. NH 2-2 – Ecoli expressed	Bacteria	20	24.16 ± 1.13	(Shao *et al.*, 2019)
Rhizomucor miehei	Fungus	50	0.177	(Yildirim *et al.*, 2019)
Rhizomucor miehei	Fungus	40	0.8	(Badgujar *et al.*, 2017)
Rhizopus oryzae	Fungus	40	112.7	(Zhao *et al.*, 2019)
Rhodothermus marinus	Bacteria	60	2073.3	(Memarpoor-Yazdi, Karbalaei-Heidari and Doroodmand, 2018)
Ricinus communis L – yeast expressed (Castor oil plant)	Plantae	40	47.902 ± 2.30	(Y. Li *et al.*, 2021)

Stomolophus meleagris (Jellyfish)	Animalia	55	0.80 ± 0.30	(Martínez-Pérez *et al.*, 2020)
Thermomyces lanuginosus	Fungus	30	2.74	(Tian *et al.*, 2017)
Thermomyces lanuginosus	Fungus	30	6	(Noro *et al.*, 2020)
Thermotoga maritima	Bacteria	70	64.3	(Tian *et al.*, 2015)
Vicia faba (faba bean)	Plantae	37	4500	(Lampi *et al.*, 2020)
Yarrowia lipolytica lipase 2	Fungus	40	140	(Wang *et al.*, 2015)
Yersinia enterocolitica	Bacteria	37	1093.4	(Ji *et al.*, 2015)

Section D: Stability and Activity of immobilised lipases

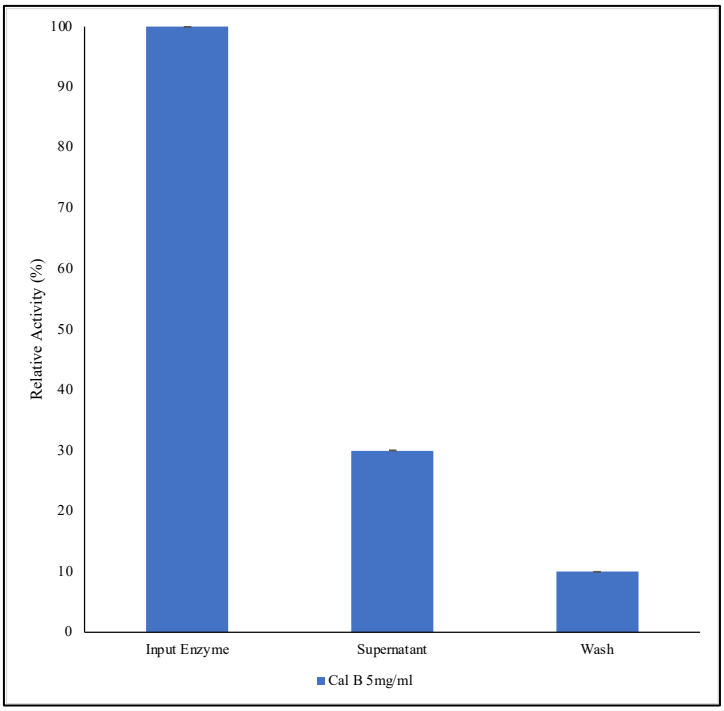

Figure 8.D.1: Activity profile from immoblisation stages

Relative activity of the immobilisation stages generated from Cal B (5 mg/ml) immobilised onto CNF membranes

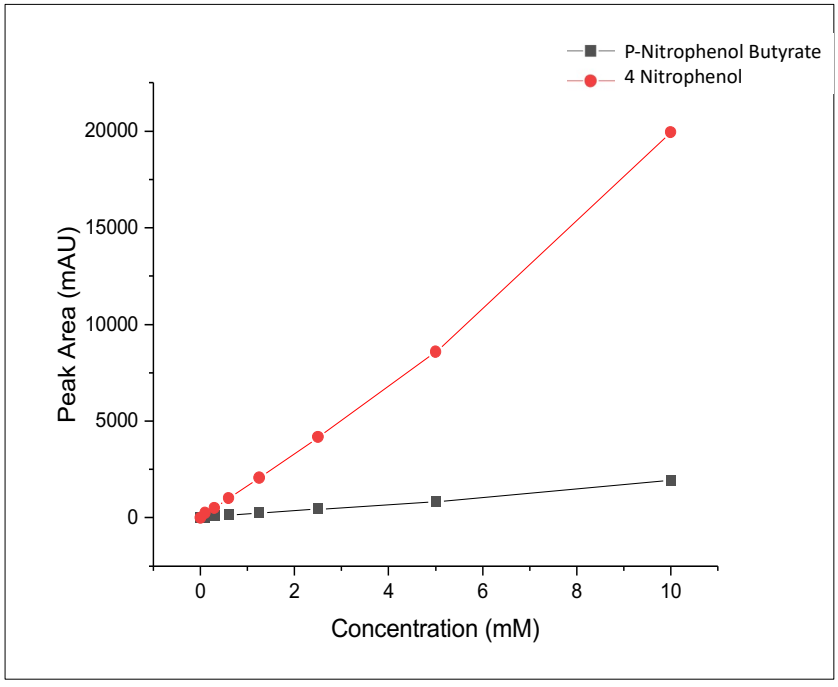

Figure 8.D.2: HPLC Standard curves of PNPB and 4 Nitrophenol

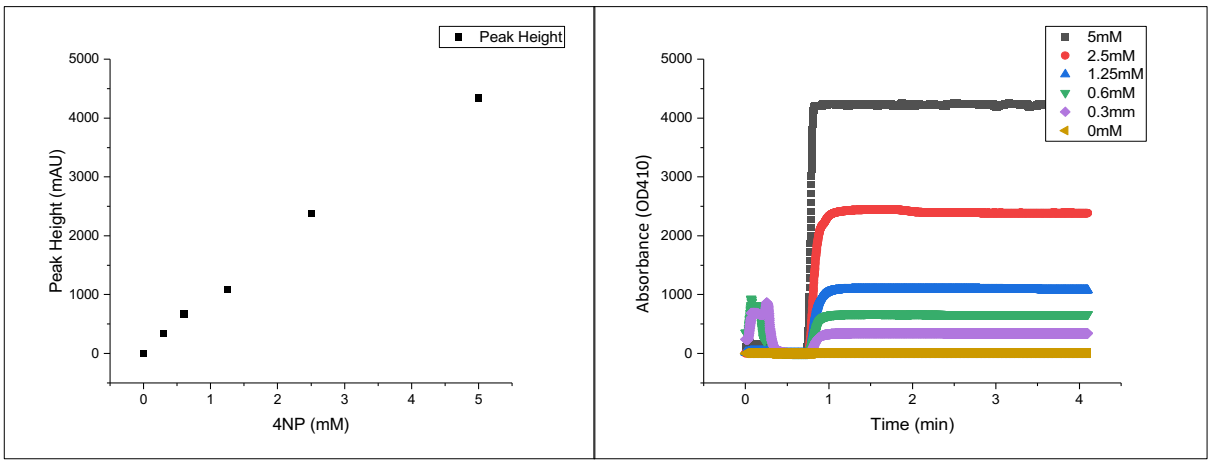

Figure 8.D.3: AKTA Avant standard curves of 4 Nitrophenol

Section E: Application of immobilised lipases to degrade polyesters

C13 NMR

A 500 MHz Bruker Avance Neo nuclear magnetic resonance (NMR) instrument, (UCL Chemistry, UK) was used for the carbon (13C) NMR spectra using a sealed internal capillary deuterium oxide (D2O) within the native aqueous sample and 1024 scans for each spectrum. Each experiment contained 750ul of sample.

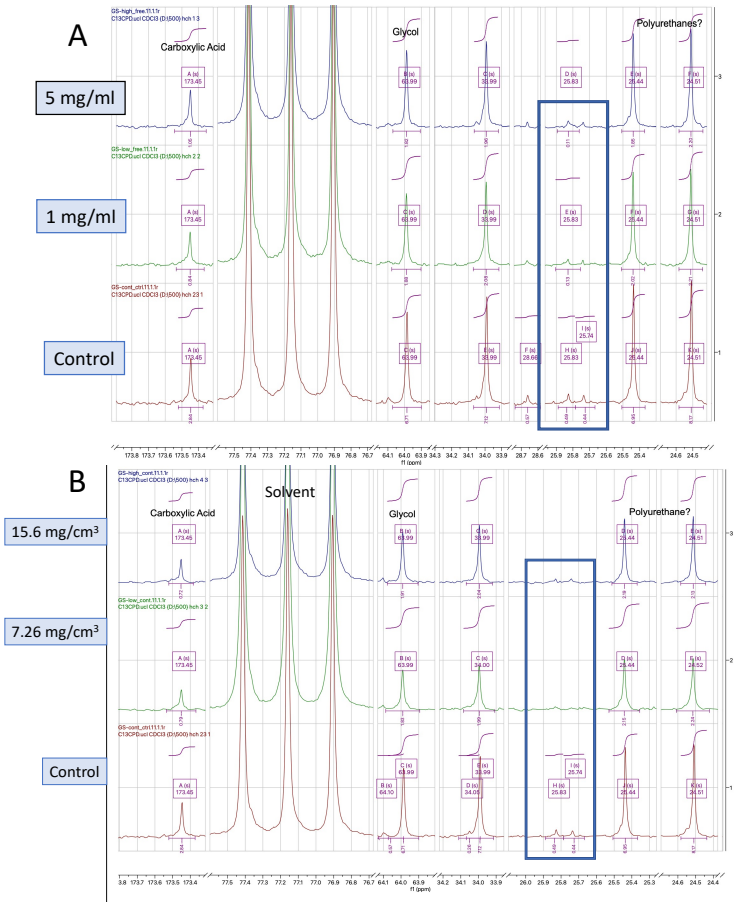

Figure 8.E.1: C13 NMR Spectra of Cal B treated Dispercoll

A) Free Cal B treated 0.01 mg/ml Dispercoll

B) Immobilised Cal B treated 0.01 mg/ml Dispercoll

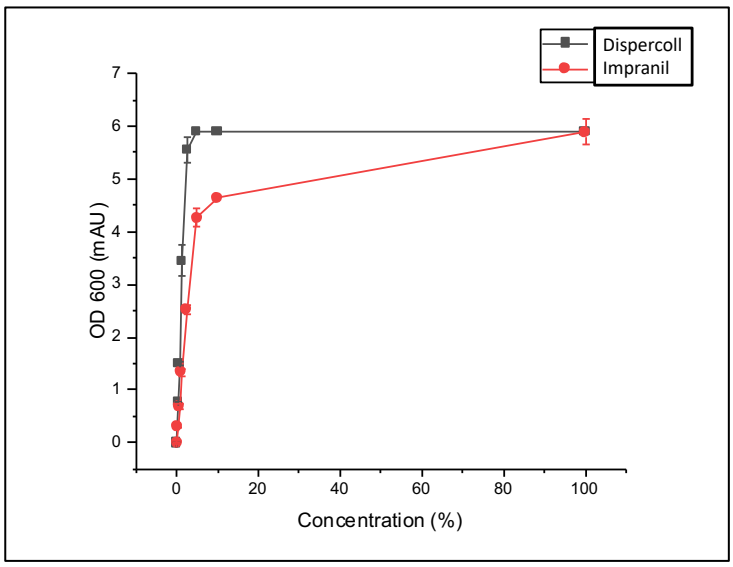

Figure 8.E.3: Dispercoll and Impranil Standard curves

10% is the upper limit before full saturation

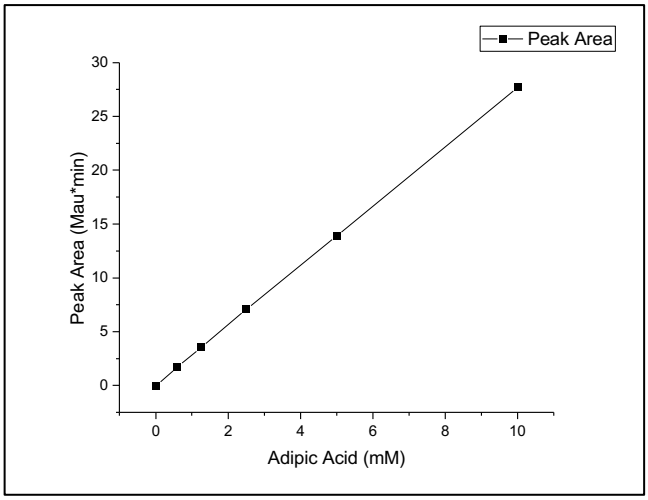

Figure 8.E.4: Standard curve of Adipic Acid

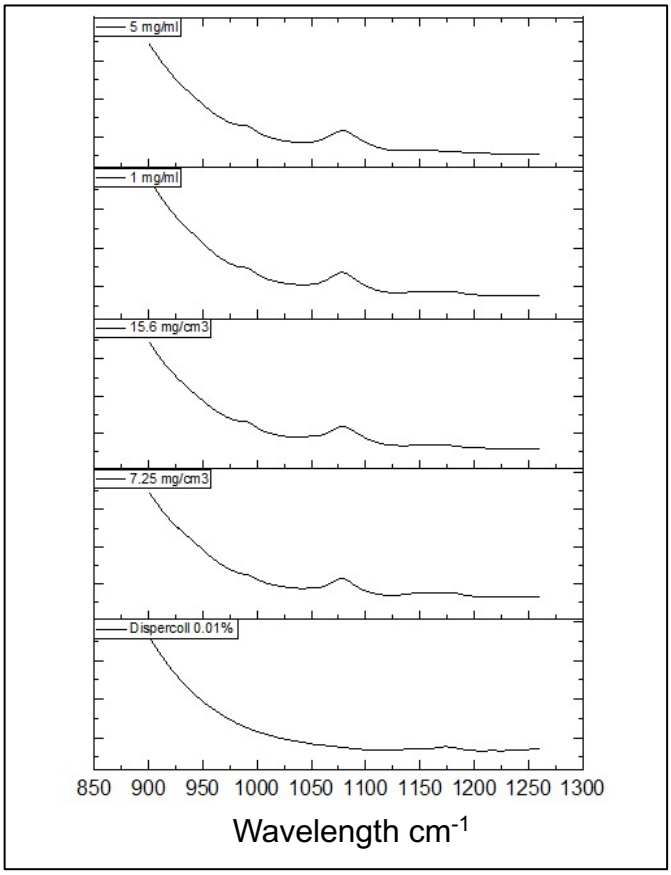

Figure 8.E.5: Stacked representative FTIR analysis of Dispercoll degradation

Immobilised and free sample particle size distribution in relation to untreated 0.01mg/ml Dispercoll control sample after 24 hours of incubations. Stacked graphs indicating changes reflecting Dispercoll degradation are observed in the signals at 990 cm^{-1} (C=C), 1080 cm^{-1} (C-O-C) and 1180 cm^{-1} (C-O)

References

A Roy, A Kucukural, Y. Z. (2010) *I-TASSER: a unified platform for automated protein structure and function prediction*, *Nature Protocols*. Available at: https://zhanggroup.org/I-TASSER/ (Accessed: 21 October 2021).

Abdul, A., Szita, N. and Baganz, F. (2013) 'Characterization and multi-step transketolase- ω -transaminase bioconversions in an immobilized enzyme microreactor (IEMR) with packed tube', *Journal of Biotechnology*. Elsevier B.V., 168(4), pp. 567–575. doi: 10.1016/j.jbiotec.2013.09.001.

Abdullah, N. and Chase, H. A. (2005) 'Removal of poly-histidine fusion tags from recombinant proteins purified by expanded bed adsorption', *Biotechnology and Bioengineering*, 92(4), pp. 501–513. doi: 10.1002/BIT.20633.

Agarwala, R. *et al.* (2018) 'Database resources of the National Center for Biotechnology Information', *Nucleic Acids Research*. Nucleic Acids Res, 46(D1), pp. D8–D13. doi: 10.1093/nar/gkx1095.

Agashe, D. *et al.* (2013) 'Good Codons, Bad Transcript: Large Reductions in Gene Expression and Fitness Arising from Synonymous Mutations in a Key Enzyme', *Molecular Biology and Evolution*. Oxford University Press, 30(3), pp. 549–560. doi: 10.1093/molbev/mss273.

Ahmad, N. N. *et al.* (2020) 'The role of surface exposed lysine in conformational stability and functional properties of lipase from staphylococcus family', *Molecules*, 25(17), pp. 1–19. doi: 10.3390/molecules25173858.

Aizouq, M. *et al.* (2020) 'Triacylglycerol and phytyl ester synthesis in *Synechocystis* sp. PCC6803', *Proceedings of the National Academy of Sciences*, 117(11), pp. 6216–6222. doi: 10.1073/pnas.1915930117.

Akbari, N. *et al.* (2010) 'High-level expression of lipase in Escherichia coli and recovery of active recombinant enzyme through in vitro refolding', *Protein Expression and Purification*. Academic Press, 70(1), pp. 75–80. doi: 10.1016/J.PEP.2009.08.009.

Akoh, C. C. *et al.* (2004) 'GDSL family of serine esterases/lipases', *Progress in Lipid Research*. Prog Lipid Res, 43(6), pp. 534–552. doi: 10.1016/j.plipres.2004.09.002.

Akutsu-Shigeno, Y. *et al.* (2006) 'Isolation of a bacterium that degrades urethane compounds and characterization of its urethane hydrolase', *Applied Microbiology and Biotechnology*. Springer, 70(4), pp. 422–429. doi: 10.1007/s00253-005-0071-1.

Ali, Y. Ben, Verger, R. and Abousalham, A. (2012) 'Lipases or Esterases: Does It Really Matter? Toward a New Bio-Physico-Chemical Classification', *Methods in Molecular Biology*. Humana Press, 861, pp. 31–51. doi: 10.1007/978-1-61779-600-5_2.

Almeida, F. L. C. *et al.* (2021) 'Trends in lipase immobilization: Bibliometric review and patent analysis', *Process Biochemistry*. Elsevier, 110, pp. 37–51. doi: 10.1016/J.PROCBIO.2021.07.005.

Almeida, J. M. *et al.* (2020) 'Metagenomics: Is it a powerful tool to obtain lipases for application in biocatalysis?', *Biochimica et Biophysica Acta - Proteins and Proteomics*. Elsevier, 1868(2), p. 140320. doi: 10.1016/j.bbapap.2019.140320.

de Almeida, J. M. *et al.* (2018) 'Tailoring recombinant lipases: keeping the His-tag favors

esterification reactions, removing it favors hydrolysis reactions', *Scientific Reports 2018 8:1*. Nature Publishing Group, 8(1), pp. 1–11. doi: 10.1038/s41598-018-27579-8.

Alotaibi, M. *et al.* (2018) 'Lipase immobilised on silica monoliths as continuous-flow microreactors for triglyceride transesterification', *Reaction Chemistry & Engineering*. The Royal Society of Chemistry, 3(1), pp. 68–74. doi: 10.1039/C7RE00162B.

Altschul, S. (1997) 'Gapped BLAST and PSI-BLAST: a new generation of protein database search programs', *Nucleic Acids Research*. Oxford University Press, 25(17), pp. 3389–3402. doi: 10.1093/nar/25.17.3389.

Alvarez, F. J. and Stella, V. J. (1989) 'The role of calcium ions and bile salts on the pancreatic lipase-catalyzed hydrolysis of triglyceride emulsions stabilized with lecithin', *Pharmaceutical research*. Pharm Res, 6(6), pp. 449–457. doi: 10.1023/A:1015956104500.

Angkawidjaja, C. and Kanaya, S. (2006) 'Family I.3 lipase: Bacterial lipases secreted by the type I secretion system', *Cellular and Molecular Life Sciences*, 63(23), pp. 2804–2817. doi: 10.1007/s00018-006-6172-x.

Angov, E. *et al.* (2008) 'Heterologous Protein Expression Is Enhanced by Harmonizing the Codon Usage Frequencies of the Target Gene with those of the Expression Host', *PLoS ONE*. Edited by C. Herman. Public Library of Science, 3(5), p. e2189. doi: 10.1371/journal.pone.0002189.

Ansari, S. A. and Husain, Q. (2012) 'Potential applications of enzymes immobilized on/in nano materials: A review', *Biotechnology Advances*, 30, pp. 512–523. doi: 10.1016/j.biotechadv.2011.09.005.

Ansorge-Schumacher, M. B. and Thum, O. (2013) 'Immobilised lipases in the cosmetics industry', *Chemical Society Reviews*, 42(15), p. 6475. doi: 10.1039/c3cs35484a.

Aoki, J. *et al.* (2002) 'Structure and function of phosphatidylserine-specific phospholipase A1', *Biochimica et Biophysica Acta (BBA) - Molecular and Cell Biology of Lipids*. Elsevier, 1582(1–3), pp. 26–32. doi: 10.1016/S1388-1981(02)00134-8.

Åqvist, J., Isaksen, G. V. and Brandsdal, B. O. (2017) 'Computation of enzyme cold adaptation', *Nature Reviews Chemistry 2017 1:7*. Nature Publishing Group, 1(7), pp. 1–14. doi: 10.1038/s41570-017-0051.

Arana-Peña, S. *et al.* (2020) 'Effects of Enzyme Loading and Immobilization Conditions on the Catalytic Features of Lipase From Pseudomonas fluorescens Immobilized on Octyl-Agarose Beads', *Frontiers in Bioengineering and Biotechnology*. Frontiers Media S.A., 8, p. 36. doi: 10.3389/fbioe.2020.00036.

Arita, M. *et al.* (2021) 'The international nucleotide sequence database collaboration', *Nucleic Acids Research*. Oxford Academic, 49(D1), pp. D121–D124. doi: 10.1093/NAR/GKAA967.

Arpigny, J. L. and Jaeger, K. E. (1999) *Bacterial lipolytic enzymes : classification and properties*, *Biochem. J*. doi: 10.1042/0264-6021:3430177.

Artimo P (2020) *ExPASy: SIB Bioinformatics Resource Portal*. Available at: https://www.expasy.org/about (Accessed: 5 April 2020).

Aslantas, Y. and Surmeli, N. B. (2019) 'Effects of N-terminal and C-terminal polyhistidine tag on the stability and function of the thermophilic P450 CYP119', *Bioinorganic Chemistry and Applications*. Hindawi Limited, 2019. doi: 10.1155/2019/8080697.

Attwood, T. . K. *et al.* (2003) *PRINTS and its automatic supplement, prePRINTS*, *Nucleic Acids*

Research. Oxford University Press. doi: 10.1093/NAR/GKG030.

Badgujar, K. C. and Bhanage, B. M. (2015) 'Immobilization of lipase on biocompatible co-polymer of polyvinyl alcohol and chitosan for synthesis of laurate compounds in supercritical carbon dioxide using response surface methodology', *Process Biochemistry*. Elsevier, 50(8), pp. 1224–1236. doi: 10.1016/j.procbio.2015.04.019.

Badgujar, V. C. *et al.* (2017) 'Immobilization of Rhizomucor miehei lipase on a polymeric film for synthesis of important fatty acid esters: kinetics and application studies', *Bioprocess and Biosystems Engineering*. Springer Verlag, 40(10), pp. 1463–1478. doi: 10.1007/S00449-017-1804-0/TABLES/3.

Barnes, H. (1997) 'Thixotropy - a review', *International Journal of Cosmetic Science*, 9(4), pp. 151–191. doi: 10.1111/j.1467-2494.1987.tb00472.x.

Basso, A. and Serban, S. (2019) 'Industrial applications of immobilized enzymes—A review', *Molecular Catalysis*. Elsevier, 479, p. 110607. doi: 10.1016/j.mcat.2019.110607.

Bateman, A. *et al.* (2021) 'UniProt: the universal protein knowledgebase in 2021', *Nucleic Acids Research*. Oxford Academic, 49(D1), pp. D480–D489. doi: 10.1093/nar/gkaa1100.

Bateman, A. and Sandford, R. (1999) 'The PLAT domain: A new piece in the PKD1 puzzle', *Current Biology*. Elsevier, 9(16), pp. R588–R590. doi: 10.1016/s0960-9822(99)80380-7.

Batta-Lona, P. *et al.* (2017) 'Transcriptomic profiles of spring and summer populations of the Southern Ocean salp, Salpa thompsoni, in the Western Antarctic Peninsula region', *Polar Biology*. Springer, 40(6), pp. 1261–1276. doi: 10.1007/s00300-016-2051-6.

Belval, L. *et al.* (2015) 'A fast and simple method to eliminate Cpn60 from functional recombinant proteins produced by E. coli Arctic Express', *Protein Expression and Purification*. Academic Press, 109, pp. 29–34. doi: 10.1016/J.PEP.2015.01.009.

Bender, M. L. and Turnquest, B. W. (1957) 'The Imidazole-catalyzed Hydrolysis of p-Nitrophenyl Acetate', *Journal of the American Chemical Society*. American Chemical Society, 79(7), pp. 1652–1655. doi: 10.1021/ja01564a034.

Berini, F. *et al.* (2017) 'Metagenomics: novel enzymes from non-culturable microbes', *FEMS Microbiology Letters*. Oxford Academic, 364(21), p. 211. doi: 10.1093/FEMSLE/FNX211.

Białecka-Florjańczyk, E. *et al.* (2012) 'Synthesis of 2-phenylethyl acetate in the presence of Yarrowia lipolytica KKP 379 biomass', *Journal of Molecular Catalysis B: Enzymatic*. Elsevier, 74(3–4), pp. 241–245. doi: 10.1016/J.MOLCATB.2011.10.010.

Bienert, S. *et al.* (2017) 'The SWISS-MODEL Repository—new features and functionality', *Nucleic Acids Research*. Oxford Academic, 45(D1), pp. D313–D319. doi: 10.1093/NAR/GKW1132.

Biffinger, J. C. *et al.* (2015) 'The applicability of Impranil® DLN for gauging the biodegradation of polyurethanes', *Polymer Degradation and Stability*. Elsevier Ltd, 120, pp. 178–185. doi: 10.1016/j.polymdegradstab.2015.06.020.

Bingham, E. (1922) *Fluidity and plasticity*. Available at: https://www.worldcat.org/title/fluidity-and-plasticity-by-eugene-c-bingham/oclc/1472704 (Accessed: 30 September 2021).

Blank, K., Morfill, J. and Gaub, H. E. (2006) 'Site-Specific Immobilization of Genetically Engineered Variants of Candida antarctica Lipase B', *ChemBioChem*, 7(9), pp. 1349–1351. doi: 10.1002/cbic.200600198.

Bone, Q., Carre, C. and Ryan, K. P. (2000) 'The endostyle and the feeding filter in salps (Tunicata)', *Journal of the Marine Biological Association of the United Kingdom*, 80(3), pp. 523–534. doi: 10.1017/S0025315400002228.

Bornhorst, J. A. and Falke, J. J. (2000) 'Purification of proteins using polyhistidine affinity tags', *Methods in Enzymology*. Academic Press Inc., pp. 245–254. doi: 10.1016/s0076-6879(00)26058-8.

Boudrant, J., Woodley, J. M. and Fernandez-Lafuente, R. (2020) 'Parameters necessary to define an immobilized enzyme preparation', *Process Biochemistry*. Elsevier, 90, pp. 66–80. doi: 10.1016/J.PROCBIO.2019.11.026.

Bourlat, S. J. *et al.* (2006) 'Deuterostome phylogeny reveals monophyletic chordates and the new phylum Xenoturbellida', *Nature*. Nature Publishing Group, 444(7115), pp. 85–88. doi: 10.1038/nature05241.

Bradford, M. (1976) 'A Rapid and Sensitive Method for the Quantitation of Microgram Quantities of Protein Utilizing the Principle of Protein-Dye Binding', *Analytical Biochemistry*. Elsevier BV, 72(1–2), pp. 248–254. doi: 10.1006/abio.1976.9999.

Brenna, E. *et al.* (2011) 'Biocatalytic Methods for the Synthesis of Enantioenriched Odor Active Compounds', 111, pp. 4036–4072. doi: 10.1021/cr100289r.

Brocca, S. *et al.* (2003) 'Sequence of the lid affects activity and specificity of Candida rugosa lipase isoenzymes.', *Protein science : a publication of the Protein Society*. Wiley-Blackwell, 12(10), pp. 2312–9. doi: 10.1110/ps.0304003.

Brown, A. and James, D. (2016) 'Precision control of recombinant gene transcription for CHO cell synthetic biology', *Biotechnology advances*. Biotechnol Adv, 34(5), pp. 492–503. doi: 10.1016/J.BIOTECHADV.2015.12.012.

Brumlik, M. J. and Buckley, J. T. (1996) 'Identification of the catalytic triad of the lipase/acyltransferase from Aeromonas hydrophila', *Journal of Bacteriology*. American Society for Microbiology, 178(7), pp. 2060–2064. doi: 10.1128/JB.178.7.2060-2064.1996.

Burham, H. *et al.* (2009) 'Enzymatic synthesis of palm-based ascorbyl esters', *Journal of Molecular Catalysis B: Enzymatic*. Elsevier, 58(1–4), pp. 153–157. doi: 10.1016/j.molcatb.2008.12.012.

Burnett, M. J. B. and Burnett, A. C. (2020) 'Therapeutic recombinant protein production in plants: Challenges and opportunities', *Plants, People, Planet*. John Wiley & Sons, Ltd, 2(2), pp. 121–132. doi: 10.1002/PPP3.10073.

Burnette, W. N. (1981) '"Western Blotting": Electrophoretic transfer of proteins from sodium dodecyl sulfate-polyacrylamide gels to unmodified nitrocellulose and radiographic detection with antibody and radioiodinated protein A', *Analytical Biochemistry*. Academic Press, 112(2), pp. 195–203. doi: 10.1016/0003-2697(81)90281-5.

Cao, L. (2006) 'Introduction: Immobilized Enzymes: Past, Present and Prospects', in *Carrier-bound Immobilized Enzymes*. Weinheim, FRG: Wiley-VCH Verlag GmbH & Co. KGaA, pp. 1–52. doi: 10.1002/3527607668.ch1.

Carniel, A. *et al.* (2017) 'Lipase from Candida antarctica (CALB) and cutinase from Humicola insolens act synergistically for PET hydrolysis to terephthalic acid', *Process Biochemistry*. Elsevier Ltd, 59, pp. 84–90. doi: 10.1016/j.procbio.2016.07.023.

Carson, M. *et al.* (2007) 'His-tag impact on structure', *Acta Crystallographica Section D Biological Crystallography*. International Union of Crystallography (IUCr), 63(3), pp. 295–

301. doi: 10.1107/S0907444906052024.

Cartier, G. *et al.* (2010) 'Cold Adaptation in DEAD-Box Proteins', *Biochemistry*. American Chemical Society, 49(12), pp. 2636–2646. doi: 10.1021/bi902082d.

Carvalho, F., Marques, M. P. C. and Fernandes, P. (2017) 'Sucrose hydrolysis in a bespoke capillary wall-coated microreactor', *Catalysts*. Multidisciplinary Digital Publishing Institute, 7(2), p. 42. doi: 10.3390/catal7020042.

Cavicchioli, R. *et al.* (2011) 'Biotechnological uses of enzymes from psychrophiles', *Microbial Biotechnology*, 4(4), pp. 449–460. doi: 10.1111/j.1751-7915.2011.00258.x.

Chandra, P. *et al.* (2020) 'Microbial lipases and their industrial applications: A comprehensive review', *Microbial Cell Factories*. BioMed Central Ltd, p. 169. doi: 10.1186/s12934-020-01428-8.

Chen, C.-C. *et al.* (2019) 'Two novel lipases purified from rice bran displaying lipolytic and esterification activities', *International Journal of Biological Macromolecules*. Elsevier, 139, pp. 298–306. doi: 10.1016/j.ijbiomac.2019.08.026.

Cheng, W. *et al.* (2019) 'Preparation and characterization of PDA/SiO2 nanofilm constructed macroporous monolith and its application in lipase immobilization', *Journal of the Taiwan Institute of Chemical Engineers*. Elsevier, 104, pp. 351–359. doi: 10.1016/j.jtice.2019.09.013.

Cherif, S. *et al.* (2011) 'A newly high alkaline lipase: an ideal choice for application in detergent formulations', *Lipids in Health and Disease*. BioMed Central, 10, p. 221. doi: 10.1186/1476-511X-10-221.

Chiuri, R. *et al.* (2009) 'Exploring Local Flexibility/Rigidity in Psychrophilic and Mesophilic Carbonic Anhydrases', *Biophysj*, 96, pp. 1586–1596. doi: 10.1016/j.bpj.2008.11.017.

Cho, S. S. *et al.* (2012) 'A neutral lipase applicable in biodiesel production from a newly isolated Streptomyces sp. CS326', *Bioprocess and Biosystems Engineering*. Springer, 35(1–2), pp. 227–234. doi: 10.1007/s00449-011-0598-8.

Colant, N. (2020) *Escherichia coli-based Cell-Free Protein Synthesis of Self-Assembling Particles for Vaccine Production and Gene Therapy*. UCL. Available at: https://discovery.ucl.ac.uk/id/eprint/10116761/1/Colant_Noelle_Thesis_Final.pdf (Accessed: 18 January 2022).

Colant, N. *et al.* (2021) 'A rational approach to improving titer in Escherichia coli-based cell-free protein synthesis reactions', *Biotechnology Progress*. American Chemical Society (ACS), 37(1), p. e3062. doi: 10.1002/BTPR.3062.

Colbourne, J. K. *et al.* (2011) 'The Ecoresponsive Genome of Daphnia pulex', *Science*. American Association for the Advancement of Science, 331(6017), pp. 555–561. doi: 10.1126/science.1197761.

Colli, A. N. and Bisang, J. M. (2011) 'Generalized study of the temporal behaviour in recirculating electrochemical reactor systems', *Electrochimica Acta*. Pergamon, 58(1), pp. 406–416. doi: 10.1016/j.electacta.2011.09.058.

Cong, S. *et al.* (2019) 'Synthesis of flavor esters by a novel lipase from Aspergillus niger in a soybean-solvent system', *3 Biotech*. Springer Verlag, 9(6), p. 244. doi: 10.1007/s13205-019-1778-5.

Connelly, P. W. (1999) 'The role of hepatic lipase in lipoprotein metabolism', *Clinica Chimica Acta*. Clin Chim Acta, 286(1–2), pp. 243–255. doi: 10.1016/S0009-8981(99)00105-9.

Contesini, F. J. *et al.* (2020) 'Advances in recombinant lipases: Production, engineering, immobilization and application in the pharmaceutical industry', *Catalysts*, 10(9), pp. 1–33. doi: 10.3390/catal10091032.

Cornish-Bowden, A. (1979) *Fundamentals of Enzyme Kinetics*. Elsevier. doi: 10.1016/C2013-0-04130-8.

Cotton, A. (2021) *Nature Inspired Engineering: bioprospecting for novel psychrophilic enzymes from the Antarctic tunicate, Salpa thompsoni*. University College London.

Covestro (2021) *Dispercoll® U 2682 | Covestro AG*. Available at: https://solutions.covestro.com/en/products/dispercoll/dispercoll-u-2682_80224622-21689466?SelectedCountry=GB (Accessed: 5 September 2021).

Coyle, R., Hardiman, G. and Driscoll, K. O. (2020) 'Microplastics in the marine environment: A review of their sources, distribution processes, uptake and exchange in ecosystems', *Case Studies in Chemical and Environmental Engineering*. Elsevier, 2, p. 100010. doi: 10.1016/J.CSCEE.2020.100010.

D'Amico, S. *et al.* (2002) 'Molecular basis of cold adaptation', in *Philosophical Transactions of the Royal Society B: Biological Sciences*, pp. 917–925. doi: 10.1098/rstb.2002.1105.

D'Amico, S. *et al.* (2003) 'Activity-Stability Relationships in Extremophilic Enzymes', *Journal of Biological Chemistry*. American Society for Biochemistry and Molecular Biology, 278(10), pp. 7891–7896. doi: 10.1074/jbc.M212508200.

Darvishi, F. (2012) 'Expression of native and mutant extracellular lipases fromYarrowia lipolytica in Saccharomyces cerevisiae', *Microbial biotechnology*. Wiley-Blackwell, 5(5), p. 634. doi: 10.1111/J.1751-7915.2012.00354.X.

Deepa, S. *et al.* (2012) 'Diversity and Antimicrobial Potential of Actinobacteria from Salt Pan Environment', *Global Advanced Research Journal of Microbiology*, 1(8), pp. 140–148. Available at: http://garj.org/garjm/index.htm (Accessed: 2 January 2022).

Demain, A. L. and Vaishnav, P. (2009) 'Production of recombinant proteins by microbes and higher organisms', *Biotechnology Advances*. Elsevier, 27(3), pp. 297–306. doi: 10.1016/J.BIOTECHADV.2009.01.008.

Denesyuk, A. *et al.* (2020) 'The acid-base-nucleophile catalytic triad in ABH-fold enzymes is coordinated by a set of structural elements', *PLOS ONE*. Public Library of Science, 15(2), p. e0229376. doi: 10.1371/JOURNAL.PONE.0229376.

Deng, D. *et al.* (2016) 'Functional Characterization of a Novel Marine Microbial GDSL Lipase and Its Utilization in the Resolution of (±)-1-Phenylethanol.', *Applied biochemistry and biotechnology*. Humana Press Inc., 179(1), pp. 75–93. doi: 10.1007/s12010-016-1980-4.

Dhake, K. P., Thakare, D. D. and Bhanage, B. M. (2013) 'Lipase: A potential biocatalyst for the synthesis of valuable flavour and fragrance ester compounds', *Flavour and Fragrance Journal*, 28(2), pp. 71–83. doi: 10.1002/ffj.3140.

Dods, S. R. *et al.* (2015) 'Fabricating electrospun cellulose nanofibre adsorbents for ion-exchange chromatography', *Journal of Chromatography A*. Elsevier, 1376, pp. 74–83. doi: 10.1016/J.CHROMA.2014.12.010.

Doran, P. (2013) *Bioprocess Engineering Principles*. Elsevier. doi: 10.1016/C2009-0-22348-8.

Duan, X. *et al.* (2019) 'Biochemical characterization of a novel lipase from Malbranchea

cinnamomea suitable for production of lipolyzed milkfat flavor and biodegradation of phthalate esters', *Food Chemistry*. Elsevier, 297, p. 124925. doi: 10.1016/j.foodchem.2019.05.199.

Dybern, B. I. (1967) 'The distribution and salinity tolerance of *Ciona intestinalis* (L.) F. *typica* with special reference to the waters around Southern Scandinavia', *Ophelia*. Taylor & Francis Group , 4(2), pp. 207–226. doi: 10.1080/00785326.1967.10409621.

Ekinci, A. P. *et al.* (2016) 'Partial purification and characterization of lipase from Geobacillus stearothermophilus AH22', *Journal of Enzyme Inhibition and Medicinal Chemistry*. Taylor & Francis, 31(2), pp. 325–331. doi: 10.3109/14756366.2015.1024677.

Elend, C. *et al.* (2007) 'Isolation and characterization of a metagenome-derived and cold-active lipase with high stereospecificity for (R)-ibuprofen esters', *Journal of Biotechnology*. Elsevier, 130(4), pp. 370–377. doi: 10.1016/j.jbiotec.2007.05.015.

Eriksen, M. *et al.* (2014) 'Plastic Pollution in the World's Oceans: More than 5 Trillion Plastic Pieces Weighing over 250,000 Tons Afloat at Sea', *PLOS ONE*. Public Library of Science, 9(12), p. e111913. doi: 10.1371/JOURNAL.PONE.0111913.

Esposito, D. and Chatterjee, D. K. (2006) 'Enhancement of soluble protein expression through the use of fusion tags'. doi: 10.1016/j.copbio.2006.06.003.

Febbraio, F. *et al.* (2011) 'Thermostable Esterase 2 from Alicyclobacillus acidocaldarius as Biosensor for the Detection of Organophosphate Pesticides', *Analytical Chemistry*, 83(5), pp. 1530–1536. doi: 10.1021/ac102025z.

Feller, G. (2013) 'Psychrophilic Enzymes: From Folding to Function and Biotechnology', *Scientifica*. Hindawi, 2013, pp. 1–28. doi: 10.1155/2013/512840.

Feller, G. and Gerday, C. (2003) 'Psychrophilic enzymes: Hot topics in cold adaptation', *Nature Reviews Microbiology*. doi: 10.1038/nrmicro773.

Feng, Q. *et al.* (2014) 'Electrospun Regenerated Cellulose Nanofibrous Membranes Surface-Grafted with Polymer Chains/Brushes via the Atom Transfer Radical Polymerization Method for Catalase Immobilization', *ACS Applied Materials & Interfaces*. American Chemical Society, 6(23), pp. 20958–20967. doi: 10.1021/am505722g.

Ferrer, M. *et al.* (2003) 'Chaperonins govern growth of Escherichia coli at low temperatures', *Nature Biotechnology*. Nature Publishing Group, 21(11), pp. 1266–1267. doi: 10.1038/nbt1103-1266.

Foley, T. L. *et al.* (2007) 'Site-specific protein modification: advances and applications This review comes from a themed issue on Proteomics and genomics Edited', *Current Opinion in Chemical Biology*, 11, pp. 12–19. doi: 10.1016/j.cbpa.2006.11.036.

Fox, B. G. and Blommel, P. G. (2009) 'Autoinduction of Protein Expression', *Current Protocols in Protein Science*. NIH Public Access, 56(1), p. Unit. doi: 10.1002/0471140864.ps0523s56.

Franca-Oliveira, G., Fornari, T. and Hernández-Ledesma, B. (2021) 'A review on the extraction and processing of natural source-derived proteins through eco-innovative approaches', *Processes*, 9(9). doi: 10.3390/pr9091626.

Francolini, I. *et al.* (2020) 'Enhanced performance of Candida rugosa lipase immobilized onto alkyl chain modified-magnetic nanocomposites', *Enzyme and Microbial Technology*. Elsevier, 132, p. 109439. doi: 10.1016/j.enzmictec.2019.109439.

Franssen, M. C. R. *et al.* (2013) 'Immobilised enzymes in biorenewables production',

Chemical Society Reviews. Royal Society of Chemistry, 42(15), p. 6491. doi: 10.1039/c3cs00004d.

Funabashi, M. *et al.* (2020) 'A metabolic pathway for bile acid dehydroxylation by the gut microbiome', *Nature*. NIH Public Access, 582(7813), p. 566. doi: 10.1038/S41586-020-2396-4.

Gama, N. V., Ferreira, A. and Barros-Timmons, A. (2018) 'Polyurethane Foams: Past, Present, and Future', *Materials*. Multidisciplinary Digital Publishing Institute (MDPI), 11(10). doi: 10.3390/MA11101841.

Ganasen, M. *et al.* (2016) 'Cold-adapted organic solvent tolerant alkalophilic family I.3 lipase from an Antarctic Pseudomonas', *International Journal of Biological Macromolecules*. Elsevier B.V., 92, pp. 1266–1276. doi: 10.1016/j.ijbiomac.2016.06.095.

Ganjalikhany, M. R. *et al.* (2012) 'Functional Motions of Candida antarctica Lipase B: A Survey through Open-Close Conformations', *PLoS ONE*. Edited by F. Fraternali, 7(7), p. e40327. doi: 10.1371/journal.pone.0040327.

Gao, J. *et al.* (2018) 'Cloning, overexpression, and characterization of a novel organic solvent-tolerant lipase from Paenibacillus pasadenensis CS0611', *Chinese Journal of Catalysis*. Elsevier, 39(5), pp. 937–945. doi: 10.1016/S1872-2067(18)63033-5.

García-Silvera, E. E. *et al.* (2018) 'Production and application of a thermostable lipase from *Serratia marcescens* in detergent formulation and biodiesel production', *Biotechnology and Applied Biochemistry*. Biotechnol Appl Biochem, 65(2), pp. 156–172. doi: 10.1002/bab.1565.

Gasteiger, E. *et al.* (2005) *Protein Identification and Analysis Tools on the ExPASy Server*. John M. Wa. Available at: https://web.expasy.org/protparam/protpar-ref.html (Accessed: 21 October 2021).

Gatti-Lafranconi, P. *et al.* (2010) 'Evolution of Stability in a Cold-Active Enzyme Elicits Specificity Relaxation and Highlights Substrate-Related Effects on Temperature Adaptation', *Journal of Molecular Biology*, 395(1), pp. 155–166. doi: 10.1016/j.jmb.2009.10.026.

Georlette, D. *et al.* (2003) 'Structural and Functional Adaptations to Extreme Temperatures in Psychrophilic, Mesophilic, and Thermophilic DNA Ligases*', *Journal of Biological Chemistry*, 278(39), pp. 37015–37023. doi: 10.1074/jbc.M305142200.

Gimmler, A. *et al.* (2016) 'The Tara Oceans voyage reveals global diversity and distribution patterns of marine planktonic ciliates.', *Scientific reports*. Nature Publishing Group, 6, p. 33555. doi: 10.1038/srep33555.

Gkini, O. A. *et al.* (2020) 'Kinetic analysis of the lipase-catalyzed hydrolysis of erythritol and pentaerythritol fatty acid esters: A biotechnological application for making low-calorie healthy food alternatives', *Catalysts*, 10(9). doi: 10.3390/catal10090965.

Glogauer, A. *et al.* (2011) 'Identification and characterization of a new true lipase isolated through metagenomic approach', *Microbial Cell Factories*. BioMed Central, 10(1), p. 54. doi: 10.1186/1475-2859-10-54.

Godeaux, J. E. a (1981) 'Functions of the endostyle in the tunicates', *Bulletin of marine science*, 45(2), pp. 228–242.

Gomes, A. M. V. *et al.* (2018) 'Comparison of Yeasts as Hosts for Recombinant Protein Production', *Microorganisms*. Multidisciplinary Digital Publishing Institute (MDPI), 6(2). doi: 10.3390/MICROORGANISMS6020038.

Goodall-Copestake, W. P. (2014) 'Morphological and molecular characterization of salps (Thalia spp.) from the Tristan da Cunha archipelago', *Journal of Plankton Research*. Oxford Academic, 36(3), pp. 883–888. doi: 10.1093/PLANKT/FBU013.

Goodall-Copestake, W. P. (2018) 'nrDNA:mtDNA copy number ratios as a comparative metric for evolutionary and conservation genetics', *Heredity 2018 121:2*. Nature Publishing Group, 121(2), pp. 105–111. doi: 10.1038/s41437-018-0088-8.

Gotor-Fernández, V., Busto, E. and Gotor, V. (2006) 'Candida antarctica Lipase B: An Ideal Biocatalyst for the Preparation of Nitrogenated Organic Compounds', *Advanced Synthesis & Catalysis*, 348(7–8), pp. 797–812. doi: 10.1002/adsc.200606057.

Gough, J. *et al.* (2001) 'Assignment of homology to genome sequences using a library of hidden Markov models that represent all proteins of known structure', *Journal of molecular biology*. J Mol Biol, 313(4), pp. 903–919. doi: 10.1006/JMBI.2001.5080.

Grande, F., Anderson, J. and Keys, A. (1970) 'Comparison of Effects of Palmitic and Stearic Acids in the Diet on Serum Cholesterol in Man', *The American Journal of Clinical Nutrition*, 23(9), pp. 1184–1193. doi: 10.1093/ajcn/23.9.1184.

Griffin, T. J. *et al.* (2007) 'Advancing mammalian cell culture engineering using genome-scale technologies', *Trends in Biotechnology*. Elsevier Current Trends, 25(9), pp. 401–408. doi: 10.1016/j.tibtech.2007.07.004.

Guerrand, D. (2016) 'Lipases industrial applications: focus on food and agroindustry'. doi: 10.1051/ocl/2017031.

Gupta, R. *et al.* (2003) 'Lipase assays for conventional and molecular screening: an overview', *Biotechnology and Applied Biochemistry*, 37(1), p. 63. doi: 10.1042/BA20020059.

Gustafsson, C. *et al.* (2012) 'Engineering genes for predictable protein expression', *Protein expression and purification*. Protein Expr Purif, 83(1), pp. 37–46. doi: 10.1016/J.PEP.2012.02.013.

Gustafsson, C., Govindarajan, S. and Minshull, J. (2004) 'Codon bias and heterologous protein expression', *Trends in Biotechnology*. Trends Biotechnol, 22(7), pp. 346–353. doi: 10.1016/j.tibtech.2004.04.006.

Guy, R. C. and Sahi, S. S. (2006) 'Application of a lipase in cake manufacture', *Journal of the Science of Food and Agriculture*, 86(11), pp. 1679–1687. doi: 10.1002/jsfa.2540.

Habeeb, A. F. and Hiramoto, R. (1968) 'Reaction of proteins with glutaraldehyde', *Archives of Biochemistry and Biophysics*, 126(1), pp. 16–26. doi: 10.1016/0003-9861(68)90554-7.

Harada, N. (2016) 'HPLC Separation of Diastereomers: Chiral Molecular Tools Useful for the Preparation of Enantiopure Compounds and Simultaneous Determination of Their Absolute Configurations', *Molecules*, 21(10), p. 1328. doi: 10.3390/molecules21101328.

von Harbou, L. *et al.* (2011) 'Salps in the Lazarev Sea, Southern Ocean: I. Feeding dynamics', *Marine Biology*, 158(9), pp. 2009–2026. doi: 10.1007/s00227-011-1709-4.

Hardick, O. *et al.* (2013) 'Nanofiber adsorbents for high productivity downstream processing', *Biotechnology and Bioengineering*. Wiley-Blackwell, 110(4), pp. 1119–1128. doi: 10.1002/bit.24765.

Hardick, O. *et al.* (2015) 'Nanofiber adsorbents for high productivity continuous downstream processing', *Journal of Biotechnology*. Elsevier, 213, pp. 74–82. doi: 10.1016/j.jbiotec.2015.01.031.

Hardick, O., Stevens, B. and Bracewell, D. G. (2011) 'Nanofibre fabrication in a temperature and humidity controlled environment for improved fibre consistency'. doi: 10.1007/s10853-011-5310-5.

Hartinger, D. *et al.* (2010) 'Enhancement of solubility in Escherichia coli and purification of an aminotransferase from Sphingopyxis sp. MTA144 for deamination of hydrolyzed fumonisin B1', *Microbial Cell Factories*. BioMed Central, 9(1), p. 62. doi: 10.1186/1475-2859-9-62.

Hitch, T. C. A. and Clavel, T. (2019) 'A proposed update for the classification and description of bacterial lipolytic enzymes', *PeerJ*. PeerJ Inc., 7(7), p. e7249. doi: 10.7717/peerj.7249.

Holm, C. *et al.* (1994) 'Identification of the active site serine of hormone-sensitive lipase by site-directed mutagenesis', *FEBS Letters*, 344(2–3), pp. 234–238. doi: 10.1016/0014-5793(94)00403-X.

Hong, P.-Y. *et al.* (2021) 'Production of Trans-Cinnamic Acid by Immobilization of the Bambusa oldhamii BoPAL1 and BoPAL2 Phenylalanine Ammonia-Lyases on Electrospun Nanofibers', *International Journal of Molecular Sciences*. MDPI, 22(20), p. 11184. doi: 10.3390/ijms222011184.

Horchani, H. *et al.* (2009) 'The N-terminal His-tag and the recombination process affect the biochemical properties of Staphylococcus aureus lipase produced in Escherichia coli', *Journal of Molecular Catalysis B: Enzymatic*, 61(3–4), pp. 194–201. doi: 10.1016/j.molcatb.2009.07.002.

Howard, G. T. and Blake, R. C. (1998) 'Growth of Pseudomonas fluorescens on a polyester–polyurethane and the purification and characterization of a polyurethanase–protease enzyme', *International Biodeterioration & Biodegradation*. Elsevier, 42(4), pp. 213–220. doi: 10.1016/S0964-8305(98)00051-1.

Huang, Q. *et al.* (2020) 'Enzymatic Self-Biodegradation of Poly(l -lactic acid) Films by Embedded Heat-Treated and Immobilized Proteinase K', *Biomacromolecules*, 21(8), pp. 3301–3307. doi: 10.1021/acs.biomac.0c00759.

Huang, S.-H., Liao, M.-H. and Chen, D.-H. (2003) 'Direct binding and characterization of lipase onto magnetic nanoparticles.', *Biotechnology progress*, 19(3), pp. 1095–100. doi: 10.1021/bp025587v.

Huang, X. J. *et al.* (2011) 'Immobilization of Candida rugosa lipase on electrospun cellulose nanofiber membrane', *Journal of Molecular Catalysis B: Enzymatic*. Elsevier, 70(3–4), pp. 95–100. doi: 10.1016/j.molcatb.2011.02.010.

Hung, C.-S. *et al.* (2016) 'Carbon Catabolite Repression and Impranil Polyurethane Degradation in Pseudomonas protegens Strain Pf-5'. doi: 10.1128/AEM.01448-16.

Ismail, A. R. and Baek, K. H. (2020) 'Lipase immobilization with support materials, preparation techniques, and applications: Present and future aspects', *International Journal of Biological Macromolecules*. Elsevier, 163, pp. 1624–1639. doi: 10.1016/J.IJBIOMAC.2020.09.021.

Jain, D. and Mishra, S. (2015) 'Multifunctional solvent stable Bacillus lipase mediated biotransformations in the context of food and fuel', *Journal of Molecular Catalysis B: Enzymatic*. Elsevier, 117, pp. 21–30. doi: 10.1016/j.molcatb.2015.04.002.

Ji, X. *et al.* (2015) 'Purification and characterization of an extracellular cold-adapted alkaline lipase produced by psychrotrophic bacterium *Yersinia enterocolitica* strain KM1', *Journal of Basic Microbiology*. Wiley-VCH Verlag, 55(6), pp. 718–728. doi: 10.1002/jobm.201400730.

Jia, F., Narasimhan, B. and Mallapragada, S. (2014) 'Materials-based strategies for multi-enzyme immobilization and co-localization: A review', *Biotechnology and Bioengineering*, 111(2), pp. 209–222. doi: 10.1002/bit.25136.

Jia, H. *et al.* (2002) 'Enzyme-carrying polymeric nanofibers prepared via electrospinning for use as unique biocatalysts', *Biotechnology Progress*, 18(5), pp. 1027–1032. doi: 10.1021/BP020042M.

Jiang, L. *et al.* (2014) '"Amano" lipase DF-catalyzed efficient synthesis of 2,2′-arylmethylene dicyclohexane-1,3-dione derivatives in anhydrous media', *Chinese Chemical Letters*. Elsevier, 25(8), pp. 1190–1192. doi: 10.1016/j.cclet.2014.04.007.

Jones, P. *et al.* (2014) 'InterProScan 5: genome-scale protein function classification.', *Bioinformatics (Oxford, England)*. Oxford University Press, 30(9), pp. 1236–40. doi: 10.1093/bioinformatics/btu031.

Jonkheijm, P. *et al.* (2008) 'Chemical Strategies for Generating Protein Biochips', *Angewandte Chemie International Edition*. Angew Chem Int Ed Engl, 47(50), pp. 9618–9647. doi: 10.1002/anie.200801711.

Joseph, B., Ramteke, P. W. and Thomas, G. (2008) 'Cold active microbial lipases: Some hot issues and recent developments', *Biotechnology Advances*, 26(5), pp. 457–470. doi: 10.1016/j.biotechadv.2008.05.003.

Jue, N. K. *et al.* (2016) 'Rapid Evolutionary Rates and Unique Genomic Signatures Discovered in the First Reference Genome for the Southern Ocean Salp, Salpa thompsoni (Urochordata, Thaliacea)', *Genome Biology and Evolution*, 8(10), pp. 3171–3186. doi: 10.1093/gbe/evw215.

Kamble, M. P., Shinde, S. D. and Yadav, G. D. (2016) 'Kinetic resolution of (R,S)-α-tetralol catalyzed by crosslinked Candida antarctica lipase B enzyme supported on mesocellular foam: A nanoscale enzyme reactor approach', *Journal of Molecular Catalysis B: Enzymatic*. Elsevier, 132, pp. 61–66. doi: 10.1016/j.molcatb.2016.06.013.

Kanwar, S. S. *et al.* (2005) 'Methods for inhibition of residual lipase activity in colorimetric assay: a comparative study.', *Indian journal of biochemistry & biophysics*, 42(4), pp. 233–7. Available at: https://pdfs.semanticscholar.org/b2e7/31c0a43d3011d02dfe2ee27b30aab84a3cd5.pdf (Accessed: 17 May 2018).

Karlsson, M. *et al.* (1997) 'cDNA cloning, tissue distribution, and identification of the catalytic triad of monoglyceride lipase. Evolutionary relationship to esterases, lysophospholipases, and haloperoxidases.', *The Journal of biological chemistry*. American Society for Biochemistry and Molecular Biology, 272(43), pp. 27218–23. doi: 10.1074/JBC.272.43.27218.

Karra-Châabouni, M. *et al.* (2006) 'Production of flavour esters by immobilized Staphylococcus simulans lipase in a solvent-free system', *Process Biochemistry*. Elsevier, 41(7), pp. 1692–1698. doi: 10.1016/J.PROCBIO.2006.02.022.

Käse, L. and Geuer, J. K. (2018) 'Phytoplankton Responses to Marine Climate Change – An Introduction', in *YOUMARES 8 – Oceans Across Boundaries: Learning from each other*. Cham: Springer International Publishing, pp. 55–71. doi: 10.1007/978-3-319-93284-2_5.

Kavitha, M. (2016) 'Cold active lipases – an update', *Frontiers in Life Science*, 9(3), pp. 226–238. doi: 10.1080/21553769.2016.1209134.

Kawaguchi, N. *et al.* (2018) 'A novel protocol for the preparation of active recombinant human pancreatic lipase from Escherichia coli', *Journal of biochemistry*. J Biochem, 164(6), pp. 407–

414. doi: 10.1093/JB/MVY067.

Kearse, M. *et al.* (2012) 'Geneious Basic: an integrated and extendable desktop software platform for the organization and analysis of sequence data.', *Bioinformatics (Oxford, England)*. Oxford University Press, 28(12), pp. 1647–9. doi: 10.1093/bioinformatics/bts199.

Khan, F. I. *et al.* (2017) 'The Lid Domain in Lipases: Structural and Functional Determinant of Enzymatic Properties', *Frontiers in Bioengineering and Biotechnology*. Frontiers Media SA, 5(MAR), p. 16. doi: 10.3389/fbioe.2017.00016.

Kim, E.-Y. *et al.* (2009) 'Novel Cold-Adapted Alkaline Lipase from an Intertidal Flat Metagenome and Proposal for a New Family of Bacterial Lipases', *Applied and Environmental Microbiology*, 75(1), pp. 257–260. doi: 10.1128/AEM.01400-08.

Kocot, K. M. *et al.* (2018) 'Phylogenomics offers resolution of major tunicate relationships', *Molecular Phylogenetics and Evolution*. Elsevier, 121(October 2017), pp. 166–173. doi: 10.1016/j.ympev.2018.01.005.

Koussoroplis, A.-M., Schwarzenberger, A. and Wacker, A. (2017) 'Diet quality determines lipase gene expression and lipase/esterase activity in Daphnia pulex', *Biology Open*. Company of Biologists, 6(2), pp. 210–216. doi: 10.1242/bio.022046.

Krause, M., Neubauer, A. and Neubauer, P. (2016) 'The fed-batch principle for the molecular biology lab: controlled nutrient diets in ready-made media improve production of recombinant proteins in Escherichia coli', *Microbial Cell Factories*. BioMed Central Ltd., 15(1), p. 110. doi: 10.1186/s12934-016-0513-8.

Kuhn, R. J. *et al.* (2010) 'CREON (Pancrelipase Delayed-Release Capsules) for the treatment of exocrine pancreatic insufficiency', *Advances in therapy*. Adv Ther, 27(12), pp. 895–916. doi: 10.1007/S12325-010-0085-7.

van Kuiken, B. A. and Behnke, W. D. (1994) 'The activation of porcine pancreatic lipase by cis-unsaturated fatty acids', *Biochimica et Biophysica Acta (BBA) - Lipids and Lipid Metabolism*, 1214(2), pp. 148–160. doi: 10.1016/0005-2760(94)90039-6.

Kulakova, L. *et al.* (2004) 'Cold-active esterase from Psychrobacter sp. Ant300: gene cloning, characterization, and the effects of Gly→Pro substitution near the active site on its catalytic activity and stability', *Biochimica et Biophysica Acta (BBA) - Proteins and Proteomics*. Elsevier, 1696(1), pp. 59–65. doi: 10.1016/j.bbapap.2003.09.008.

Kumar, A. *et al.* (2020) 'A Broad Temperature Active Lipase Purified From a Psychrotrophic Bacterium of Sikkim Himalaya With Potential Application in Detergent Formulation', *Frontiers in Bioengineering and Biotechnology*. Frontiers Media S.A., 8, p. 642. doi: 10.3389/fbioe.2020.00642.

Kumar, P. and Libchaber, A. (2013) 'Pressure and temperature dependence of growth and morphology of escherichia coli: Experiments and stochastic model', *Biophysical Journal*. The Biophysical Society, 105(3), pp. 783–793. doi: 10.1016/j.bpj.2013.06.029.

Kundys, A. *et al.* (2018) 'Candida antarctica Lipase B as Catalyst for Cyclic Esters Synthesis, Their Polymerization and Degradation of Aliphatic Polyesters', *J Polym Environ*, 26, pp. 396–407. doi: 10.1007/s10924-017-0945-1.

Kuo, C.-H. *et al.* (2014) 'Kinetics and optimization of lipase-catalyzed synthesis of rose fragrance 2-phenylethyl acetate through transesterification', *Process Biochemistry*. Elsevier, 49(3), pp. 437–444. doi: 10.1016/j.procbio.2013.12.012.

Kurtzman, C. P. (2009) 'Biotechnological strains of Komagataella (Pichia) pastoris are

Komagataella phaffii as determined from multigene sequence analysis', *Journal of industrial microbiology & biotechnology*. J Ind Microbiol Biotechnol, 36(11), pp. 1435–1438. doi: 10.1007/S10295-009-0638-4.

Lampi, A. M. *et al.* (2020) 'Potential of faba bean lipase and lipoxygenase to promote formation of volatile lipid oxidation products in food models', *Food Chemistry*. Elsevier, 311(November 2019), p. 125982. doi: 10.1016/j.foodchem.2019.125982.

Landers, A., Brown, H. and Strother, M. (2019) 'The effectiveness of pancreatic enzyme replacement therapy for malabsorption in advanced pancreatic cancer, a pilot study', *Palliative Care*. SAGE Publications, 12. doi: 10.1177/1178224218825270.

Langin, D. *et al.* (1993) 'Gene organization and primary structure of human hormone-sensitive lipase: possible significance of a sequence homology with a lipase of Moraxella TA144, an antarctic bacterium.', *Proceedings of the National Academy of Sciences of the United States of America*. National Academy of Sciences, 90(11), pp. 4897–901. doi: 10.1073/pnas.90.11.4897.

Lee, C. W., Jang, S.-H. H. and Chung, H.-S. S. (2017) 'Improving the stability of cold-adapted enzymes by immobilization', *Catalysts*. MDPI AG, 7(4). doi: 10.3390/catal7040112.

Lee, D. H. *et al.* (2010) 'Proteomic analysis of the effect of storage temperature on human serum', *Annals of Clinical and Laboratory Science*. Association of Clinical Scientists, 40(1), pp. 61–70.

Lee, J. H. *et al.* (2007) 'Stable and continuous long-term enzymatic reaction using an enzyme–nanofiber composite', *Applied Microbiology and Biotechnology*. Springer, 75(6), pp. 1301–1307. doi: 10.1007/s00253-007-0955-3.

Li, Q. *et al.* (2021) 'A novel lipase from Aspergillus oryzae WZ007 catalyzed synthesis of brivaracetam intermediate and its enzymatic characterization', *Chirality*. John Wiley and Sons Inc, 33(2), pp. 62–71. doi: 10.1002/chir.23286.

Li, Y. *et al.* (2021) 'Characterization of a novel sn1,3 lipase from Ricinus communis L. suitable for production of oleic acid-palmitic acid-glycerol oleate', *Scientific Reports*. Nature Research, 11(1). doi: 10.1038/S41598-021-86305-Z.

Lilly, M., Hornby, W. and Crook, E. (1966) 'The kinetics of carboxymethylcellulose–ficin in packed beds', *Biochemical Journal*, 100(3), pp. 718–723. doi: 10.1042/bj1000718.

Lin, Y. *et al.* (2017) 'Mycobacterium tuberculosis rv1400c encodes functional lipase/esterase', *Protein Expression and Purification*. Academic Press, 129, pp. 143–149. doi: 10.1016/j.pep.2016.04.013.

Liu, D. M. and Dong, C. (2020) 'Recent advances in nano-carrier immobilized enzymes and their applications', *Process Biochemistry*. Elsevier, 92, pp. 464–475. doi: 10.1016/J.PROCBIO.2020.02.005.

Liu, Y. *et al.* (2020) 'Purification, characterization and molecular cloning of a dicaffeoylquinic acid-hydrolyzing esterase from human-derived Lactobacillus fermentum LF-12', *Food & Function*. The Royal Society of Chemistry, 11(4), pp. 3235–3244. doi: 10.1039/D0FO00029A.

Lopes, D. B. *et al.* (2011) 'Lipase and esterase: to what extent can this classification be applied accurately?', *Ciência e Tecnologia de Alimentos*. SBCTA, 31(3), pp. 603–613. doi: 10.1590/S0101-20612011000300009.

Lowe, M. E. (2002) 'The triglyceride lipases of the pancreas', *Journal of Lipid Research*. Elsevier, 43(12), pp. 2007–2016. doi: 10.1194/jlr.R200012-JLR200.

Lu, S. *et al.* (2020) 'CDD/SPARCLE: the conserved domain database in 2020', *Nucleic acids research*. Nucleic Acids Res, 48(D1), pp. D265–D268. doi: 10.1093/NAR/GKZ991.

Madurawe, R. D. *et al.* (2000) 'A Recombinant Lipoprotein Antigen against Lyme Disease Expressed in E. coli: Fermentor Operating Strategies for Improved Yield', *Biotechnology Progress*. Biotechnol Prog, 16(4), pp. 571–576. doi: 10.1021/bp0000555.

Magnin, A. *et al.* (2020) 'Evaluation of biological degradation of polyurethanes', *Biotechnology Advances*. Elsevier, 39, p. 107457. doi: 10.1016/j.biotechadv.2019.107457.

Mala, J. G. S. and Takeuchi, S. (2008) 'Understanding structural features of microbial lipases-an overview', *Analytical chemistry insights*. SAGE Publications, 3, pp. 9–19.

Malaikozhundan, B. and Vinodhini, J. (2018) 'Nanopesticidal effects of Pongamia pinnata leaf extract coated zinc oxide nanoparticle against the Pulse beetle, Callosobruchus maculatus', *Materials Today Communications*. Elsevier, 14, pp. 106–115. doi: 10.1016/j.mtcomm.2017.12.015.

Manasian, P. *et al.* (2020) 'First Evidence of Acyl-Hydrolase/Lipase Activity From Human Probiotic Bacteria: Lactobacillus rhamnosus GG and Bifidobacterium longum NCC 2705', *Frontiers in Microbiology*. Frontiers Media S.A., 11, p. 1534. doi: 10.3389/fmicb.2020.01534.

Marjo, C. E. *et al.* (2017) 'ATR-FTIR as a tool for assessing potential for chemical ageing in Spandex/Lycra ® /elastane-based fabric collections', *Studies in Conservation*. Routledge, 62(6), pp. 343–353. doi: 10.1080/00393630.2016.1198868.

Martínez-Pérez, R. B. *et al.* (2020) 'Cannonball jellyfish digestion: an insight into the lipolytic enzymes of the digestive system', *PeerJ*. PeerJ Inc., 8, p. e9794. doi: 10.7717/peerj.9794.

Mateo, C. *et al.* (2005) 'Some special features of glyoxyl supports to immobilize proteins', *Enzyme and Microbial Technology*. Elsevier, 37(4), pp. 456–462. doi: 10.1016/j.enzmictec.2005.03.020.

Mateo, C., Grazu, V., *et al.* (2007) 'Immobilization of enzymes on heterofunctional epoxy supports', *Nature Protocols*. Nature Publishing Group, 2(5), pp. 1022–1033. doi: 10.1038/nprot.2007.133.

Mateo, C., Palomo, J. M., *et al.* (2007) 'Improvement of enzyme activity, stability and selectivity via immobilization techniques', *Enzyme and Microbial Technology*. Elsevier, 40(6), pp. 1451–1463. doi: 10.1016/j.enzmictec.2007.01.018.

Matsumura, S., Soeda, Y. and Toshima, K. (2006) 'Perspectives for synthesis and production of polyurethanes and related polymers by enzymes directed toward green and sustainable chemistry', *Applied Microbiology and Biotechnology*. Springer, 70(1), pp. 12–20. doi: 10.1007/s00253-005-0269-2.

Matte, C. R. *et al.* (2017) 'Physical-chemical properties of the support immobead 150 before and after the immobilization process of lipase', *Journal of the Brazilian Chemical Society*. Sociedade Brasileira de Quimica, 28(8), pp. 1430–1439. doi: 10.21577/0103-5053.20160319.

Mauro, V. P. (2018) 'Codon Optimization in the Production of Recombinant Biotherapeutics: Potential Risks and Considerations', *BioDrugs 2018 32:1*. Springer, 32(1), pp. 69–81. doi: 10.1007/S40259-018-0261-X.

Mavromatis, K. *et al.* (2002) 'Exploring the role of a glycine cluster in cold adaptation of an alkaline phosphatase', *European journal of biochemistry*. Eur J Biochem, 269(9), pp. 2330–2335. doi: 10.1046/J.1432-1033.2002.02895.X.

McCarthy, S. J. *et al.* (1997) 'In-vivo degradation of polyurethanes: transmission-FTIR microscopic characterization of polyurethanes sectioned by cryomicrotomy', *Biomaterials*, 18(21), pp. 1387–1409. doi: 10.1016/S0142-9612(97)00083-5.

McLaughlin, J. *et al.* (2019) 'Propionibacterium acnes and Acne Vulgaris: New Insights from the Integration of Population Genetic, Multi-Omic, Biochemical and Host-Microbe Studies', *Microorganisms*. Multidisciplinary Digital Publishing Institute (MDPI), 7(5). doi: 10.3390/MICROORGANISMS7050128.

Memarpoor-Yazdi, M., Karbalaei-Heidari, H. R. and Doroodmand, M. M. (2018) 'Enantioselective hydrolysis of ibuprofen ethyl ester by a thermophilic immobilized lipase, ELT, from Rhodothermus marinus', *Biochemical Engineering Journal*. Elsevier, 130, pp. 55–65. doi: 10.1016/j.bej.2017.11.016.

Menkhaus, T. J. *et al.* (2010) 'Electrospun nanofiber membranes surface functionalized with 3-dimensional nanolayers as an innovative adsorption medium with ultra-high capacity and throughput', *Chemical Communications*. The Royal Society of Chemistry, 46(21), pp. 3720–3722. doi: 10.1039/C001802C.

Mesbah, N. M. (2019) 'Covalent immobilization of a halophilic, alkalithermostable lipase LipR2 on Florisil® nanoparticles for production of alkyl levulinates', *Archives of Biochemistry and Biophysics*. Academic Press, 667, pp. 22–29. doi: 10.1016/j.abb.2019.04.004.

Messaoudi, A. *et al.* (2010) 'Classification of EC 3.1.1.3 bacterial true lipases using phylogenetic analysis', *African Journal of Biotechnology*, 9(48), pp. 8243–8247. doi: 10.5897/AJB10.721.

Metpally, R. P. R. and Reddy, B. V. B. (2009) 'Comparative proteome analysis of psychrophilic versus mesophilic bacterial species: Insights into the molecular basis of cold adaptation of proteins', *BMC Genomics*. BioMed Central, 10, p. 11. doi: 10.1186/1471-2164-10-11.

Mhetras, N., Mapare, V. and Gokhale, D. (2021) 'Cold Active Lipases: Biocatalytic Tools for Greener Technology', *Applied Biochemistry and Biotechnology*. Springer, 193(7), pp. 2245–2266. doi: 10.1007/s12010-021-03516-w.

Mingarro, I., González-Navarro, H. and Braco, L. (1995) 'Direct HPLC Monitoring of Lipase Activity in Reverse Micellar Media', *Journal of Liquid Chromatography*, 18(2), pp. 235–244. doi: 10.1080/10826079508009235.

Mistry, J. *et al.* (2021) 'Pfam: The protein families database in 2021', *Nucleic Acids Research*. Oxford Academic, 49(D1), pp. D412–D419. doi: 10.1093/nar/gkaa913.

Miyazaki, K. *et al.* (2000) 'Directed evolution study of temperature adaptation in a psychrophilic enzyme', *Journal of Molecular Biology*. Academic Press, 297(4), pp. 1015–1026. doi: 10.1006/jmbi.2000.3612.

Moeller, H. V. *et al.* (2019) 'Light-dependent grazing can drive formation and deepening of deep chlorophyll maxima', *Nature Communications 2019 10:1*. Nature Publishing Group, 10(1), pp. 1–8. doi: 10.1038/s41467-019-09591-2.

Mokhtar, N. F. *et al.* (2020) 'The immobilization of lipases on porous support by adsorption and hydrophobic interaction method', *Catalysts*, 10(7), pp. 1–17. doi: 10.3390/catal10070744.

Molitor, R. *et al.* (2020) 'Agar plate-based screening methods for the identification of polyester hydrolysis by Pseudomonas species', *Microbial Biotechnology*. John Wiley and Sons Ltd, 13(1), pp. 274–284. doi: 10.1111/1751-7915.13418.

Montaudo, G. *et al.* (1984) 'Mechanism of thermal degradation of polyurethanes. Effect of ammonium polyphosphate', *Macromolecules*, 17(8), pp. 1605–1614. doi: 10.1021/ma00138a032.

Montiel, L. M., Tyagi, R. D. and Valero, J. R. (2001) 'Wastewater Treatement Sludge as a Raw Material for the Production of Bacillus Thuringiensis Based Biopesticides', *Wat. Res*, 35(16), pp. 3807–3816.

de Morais, W. G. *et al.* (2016) 'Optimization of the production and characterization of lipase from Candida rugosa and Geotrichum candidum in soybean molasses by submerged fermentation', *Protein Expression and Purification*. Academic Press, 123, pp. 26–34. doi: 10.1016/j.pep.2016.04.001.

Mountaki, S. A. *et al.* (2021) 'Responsive Polyesters with Alkene and Carboxylic Acid Side-Groups for Tissue Engineering Applications', *Polymers*. MDPI AG, 13(10), p. 1636. doi: 10.3390/polym13101636.

Mussatto, S. I. *et al.* (2008) 'The effect of agitation speed, enzyme loading and substrate concentration on enzymatic hydrolysis of cellulose from brewer's spent grain', *Cellulose 2008 15:5*. Springer, 15(5), pp. 711–721. doi: 10.1007/S10570-008-9215-7.

Nair, S. *et al.* (2007) 'Improving Biocatalytic Activity of Enzyme-Loaded Nanofibers by Dispersing Entangled Nanofiber Structure'. doi: 10.1021/bm061004k.

Narayanan, N., Khan, M. and Chou, C. P. (2011) 'Enhancing functional expression of heterologous burkholderia lipase in Escherichia coli', *Molecular Biotechnology*. Springer, 47(2), pp. 130–143. doi: 10.1007/S12033-010-9320-3/FIGURES/9.

Nishizawa, M. *et al.* (1995) 'Stereoselective production of (+)-trans-chrysanthemic acid by a microbial esterase: cloning, nucleotide sequence, and overexpression of the esterase gene of Arthrobacter globiformis in Escherichia coli.', *Applied and Environmental Microbiology*, 61(9).

Noro, J. *et al.* (2020) 'Substrate hydrophobicity and enzyme modifiers play a major role in the activity of lipase from Thermomyces lanuginosus', *Catalysis Science & Technology*. The Royal Society of Chemistry, 10(17), pp. 5913–5924. doi: 10.1039/D0CY00912A.

Noureddini, H. and Gao, X. (2007) 'Characterization of sol-gel immobilized lipases', *Journal of Sol-Gel Science and Technology*. Springer, 41(1), pp. 31–41. doi: 10.1007/s10971-006-0124-7.

Okajima, S. *et al.* (2003) 'Lipase-Catalyzed Transformation of Poly(butylene adipate) and Poly(butylene succinate) into Repolymerizable Cyclic Oligomers', *Biomacromolecules*. American Chemical Society , 4(6), pp. 1514–1519. doi: 10.1021/bm034043u.

Ollis, D. *et al.* (1992) 'The α/β hydrolase fold', *Protein Engineering, Design and Selection*. Oxford Academic, 5(3), pp. 197–211. doi: 10.1093/protein/5.3.197.

Ortiz, C. *et al.* (2019) 'Novozym 435: The "perfect" lipase immobilized biocatalyst?', *Catalysis Science and Technology*. Royal Society of Chemistry, pp. 2380–2420. doi: 10.1039/c9cy00415g.

ØSterlund, T. *et al.* (1999) 'Domain identification of hormone-sensitive lipase by circular dichroism and fluorescence spectroscopy, limited proteolysis, and mass spectrometry', *The Journal of biological chemistry*. J Biol Chem, 274(22), pp. 15382–15388. doi: 10.1074/JBC.274.22.15382.

Osuna, Y. *et al.* (2015) 'Immobilization of Aspergillus niger lipase on chitosan-coated

magnetic nanoparticles using two covalent-binding methods', *Bioprocess and Biosystems Engineering*. Springer Verlag, 38(8), pp. 1437–1445. doi: 10.1007/s00449-015-1385-8.

Oyemitan, I. A. (2017) 'African Medicinal Spices of Genus Piper', in *Medicinal Spices and Vegetables from Africa*. Elsevier, pp. 581–597. doi: 10.1016/B978-0-12-809286-6.00027-3.

Ozcan, B. *et al.* (2009) 'Characterization of extracellular esterase and lipase activities from five halophilic archaeal strains', *Journal of Industrial Microbiology and Biotechnology*. Springer, 36(1), pp. 105–110. doi: 10.1007/s10295-008-0477-8.

Özdemir, F. İ., Tülek, A. and Erdoğan, D. (2021) 'Identification and Heterologous Production of a Lipase from Geobacillus kaustophilus DSM 7263T and Tailoring Its N-Terminal by a His-Tag Epitope', *Protein Journal*. Springer, 40(3), pp. 436–447. doi: 10.1007/S10930-021-09987-4/TABLES/2.

Palomo, J. M. *et al.* (2002) 'Modulation of the enantioselectivity of Candida antarctica B lipase via conformational engineering. Kinetic resolution of (±)-α-hydroxy-phenylacetic acid derivatives', *Tetrahedron: Asymmetry*. Pergamon, 13(12), pp. 1337–1345. doi: 10.1016/S0957-4166(02)00325-7.

Papaleo, E. *et al.* (2011) *Molecular Determinants of Enzyme Cold Adaptation: Comparative Struc-tural and Computational Studies of Cold-and Warm-Adapted Enzymes*, *Current Protein and Peptide Science*.

Park, C. G. *et al.* (2011) 'Cell-free synthesis and multifold screening of Candida antarctica lipase B (CalB) variants after combinatorial mutagenesis of hot spots', *Biotechnology Progress*, 27(1), pp. 47–53. doi: 10.1002/btpr.532.

Park, H. *et al.* (2012) 'Expression, immobilization and enzymatic properties of glutamate decarboxylase fused to a cellulose-binding domain', *International Journal of Molecular Sciences*. Molecular Diversity Preservation International, 13(1), pp. 358–368. doi: 10.3390/ijms13010358.

Park, Y.-K. *et al.* (2019) 'Efficient expression vectors and host strain for the production of recombinant proteins by Yarrowia lipolytica in process conditions', *Microbial Cell Factories*. BioMed Central Ltd., 18(1), p. 167. doi: 10.1186/s12934-019-1218-6.

Partini, M. and Pantani, R. (2007) 'FTIR analysis of hydrolysis in aliphatic polyesters', *Polymer Degradation and Stability*. Elsevier, 92(8), pp. 1491–1497. doi: 10.1016/j.polymdegradstab.2007.05.009.

de Pascale, D. *et al.* (2008) 'The cold-active Lip1 lipase from the Antarctic bacterium Pseudoalteromonas haloplanktis TAC125 is a member of a new bacterial lipolytic enzyme family', *Extremophiles*. Springer Japan, 12(3), pp. 311–323. doi: 10.1007/s00792-008-0163-9.

Patel, R. N., Banerjee, A. and Szarka, L. J. (1997) 'Stereoselective acetylation of [1-(hydroxy)-4-(3-phenyl)butyl]phosphonic acid, diethyl ester', *Tetrahedron: Asymmetry*. Pergamon, 8(7), pp. 1055–1059. doi: 10.1016/S0957-4166(97)00085-2.

Pedroche, J. *et al.* (2007) 'Effect of the support and experimental conditions in the intensity of the multipoint covalent attachment of proteins on glyoxyl-agarose supports: Correlation between enzyme–support linkages and thermal stability', *Enzyme and Microbial Technology*, 40(5), pp. 1160–1166. doi: 10.1016/j.enzmictec.2006.08.023.

Pei, Y., Hinchliffe, B. A. and Minelli, C. (2021) 'Measurement of the Size Distribution of Multimodal Colloidal Systems by Laser Diffraction', *ACS Omega*. American Chemical Society, 6(22), pp. 14049–14058. doi: 10.1021/acsomega.1c00411.

Perret, B. *et al.* (2002) 'Hepatic lipase: structure/function relationship, synthesis, and regulation.', *Journal of lipid research*. American Society for Biochemistry and Molecular Biology, 43(8), pp. 1163–9. doi: 10.1194/JLR.R100020-JLR200.

Pesant, S. S. *et al.* (2015) 'Open science resources for the discovery and analysis of Tara Oceans data', *Scientific Data 2015 2:1*. Nature Publishing Group, 2(1), pp. 1–16. doi: 10.1038/sdata.2015.23.

Peternel, Š. and Komel, R. (2011) 'Active Protein Aggregates Produced in Escherichia coli', *International Journal of Molecular Sciences*. Multidisciplinary Digital Publishing Institute (MDPI), 12(11), p. 8275. doi: 10.3390/IJMS12118275.

Pleiss, J., Fischer, M. and Schmid, R. D. (1998) 'Anatomy of lipase binding sites: the scissile fatty acid binding site', *Chemistry and Physics of Lipids*, 93(1–2), pp. 67–80. doi: 10.1016/S0009-3084(98)00030-9.

Pliego, J. *et al.* (2015) 'Monitoring Lipase/Esterase Activity by Stopped Flow in a Sequential Injection Analysis System Using p-Nitrophenyl Butyrate', *Sensors*, 15(2), pp. 2798–2811. doi: 10.3390/s150202798.

Pohlenz, H. D. *et al.* (1992) 'Purification and properties of an Arthrobacter oxydans P52 carbamate hydrolase specific for the herbicide phenmedipham and nucleotide sequence of the corresponding gene', *Journal of Bacteriology*, 174(20), pp. 6600–6607. doi: 10.1128/JB.174.20.6600-6607.1992.

Poppe, J. K. *et al.* (2013) 'Multipoint covalent immobilization of lipases on aldehyde-activated support: Characterization and application in transesterification reaction', *Journal of Molecular Catalysis B: Enzymatic*. Elsevier, 94, pp. 57–62. doi: 10.1016/j.molcatb.2013.05.017.

Poust, S. *et al.* (2014) 'Understanding the Role of Histidine in the GHSxG Acyltransferase Active Site Motif: Evidence for Histidine Stabilization of the Malonyl-Enzyme Intermediate', *PLOS ONE*. Public Library of Science, 9(10), p. e109421. doi: 10.1371/JOURNAL.PONE.0109421.

Quinn, D. M. *et al.* (1982) 'Lipoprotein lipase-catalyzed hydrolysis of water-soluble p-nitrophenyl esters. Inhibition by apolipoprotein C-II', *Biochemistry*. American Chemical Society, 21(26), pp. 6872–6879. doi: 10.1021/bi00269a038.

Racioppi, C. *et al.* (2017) 'Evolutionary loss of melanogenesis in the tunicate Molgula occulta', *EvoDevo*. BioMed Central Ltd., 8(1), p. 11. doi: 10.1186/s13227-017-0074-x.

Ranjbar, M. *et al.* (2015) 'Purification and characterization of a digestive lipase in the midgut of Ectomyelois ceratoniae Zeller (Lepidoptera: Pyralidae)', *Frontiers in Life Science*, 8(1), pp. 64–70. doi: 10.1080/21553769.2014.961616.

Rather, A. H. *et al.* (2022) 'Overview on immobilization of enzymes on synthetic polymeric nanofibers fabricated by electrospinning', *Biotechnology and Bioengineering*. John Wiley and Sons Inc, 119(1), pp. 9–33. doi: 10.1002/bit.27963.

Redeker, E. S. *et al.* (2013) 'Protein Engineering For Directed Immobilization'. doi: 10.1021/bc4002823.

Richardson, G. H., Nelson, J. H. and Farnham, M. G. (1971) 'Gastric Lipase Characterization and Utilization in Cheese Manufacture', *Journal of Dairy Science*, 54(5), pp. 643–647. doi: 10.3168/jds.S0022-0302(71)85900-3.

Rivera-Perez, C. (2015) 'Marine invertebrate lipases: Comparative and functional genomic analysis', *Comparative Biochemistry and Physiology Part D: Genomics and Proteomics*.

Elsevier, 15, pp. 39–48. doi: 10.1016/j.cbd.2015.06.001.

Rivera-Pérez, C. and García-Carreño, F. (2011) 'Effect of fasting on digestive gland lipase transcripts expression in Penaeus vannamei', *Marine Genomics*. Elsevier, 4(4), pp. 273–278. doi: 10.1016/J.MARGEN.2011.07.002.

Robinson, S. L., Piel, J. and Sunagawa, S. (2021) 'A roadmap for metagenomic enzyme discovery', *Natural Product Reports*, 38(11), pp. 1994–2023. doi: 10.1039/D1NP00006C.

Rodrigues, R. C. *et al.* (2009) 'Reactivation of covalently immobilized lipase from Thermomyces lanuginosus', *Process Biochemistry*. Elsevier, 44(6), pp. 641–646. doi: 10.1016/j.procbio.2009.02.001.

Rodrigues, R. C. *et al.* (2019) 'Immobilization of lipases on hydrophobic supports: immobilization mechanism, advantages, problems, and solutions', *Biotechnology Advances*. Elsevier, 37(5), pp. 746–770. doi: 10.1016/j.biotechadv.2019.04.003.

Rosano, G. L. and Ceccarelli, E. A. (2014) 'Recombinant protein expression in Escherichia coli: advances and challenges', *Frontiers in Microbiology*. Frontiers Media SA, 5, p. 172. doi: 10.3389/fmicb.2014.00172.

Roussel, A. *et al.* (1999) 'Crystal Structure of Human Gastric Lipase and Model of Lysosomal Acid Lipase, Two Lipolytic Enzymes of Medical Interest', *Journal of Biological Chemistry*, 274(24), pp. 16995–17002. doi: 10.1074/jbc.274.24.16995.

Ruiz, C. *et al.* (2004) 'Activation and inhibition of Candida rugosa and Bacillus-related lipases by saturated fatty acids, evaluated by a new colorimetric microassay', *Biochimica et Biophysica Acta - General Subjects*, 1672(3), pp. 184–191. doi: 10.1016/j.bbagen.2004.03.010.

SÁ, A. G. A. *et al.* (2017) 'A review on enzymatic synthesis of aromatic esters used as flavor ingredients for food, cosmetics and pharmaceuticals industries', *Trends in Food Science & Technology*. Elsevier, 69, pp. 95–105. doi: 10.1016/j.tifs.2017.09.004.

Saavedra, H. G. *et al.* (2018) 'Dynamic allostery can drive cold adaptation in enzymes', *Nature*, 558(7709), pp. 324–328. doi: 10.1038/s41586-018-0183-2.

Sahay, S. and Chouhan, D. (2018) 'Study on the potential of cold-active lipases from psychrotrophic fungi for detergent formulation', *Journal of Genetic Engineering and Biotechnology*. Academy of Scientific Research and Technology, 16(2), pp. 319–325. doi: 10.1016/j.jgeb.2018.04.006.

Sahdev, S., Khattar, S. K. and Saini, K. S. (2008) 'Production of active eukaryotic proteins through bacterial expression systems: A review of the existing biotechnology strategies', *Molecular and Cellular Biochemistry*. Springer, 307(1–2), pp. 249–264. doi: 10.1007/S11010-007-9603-6/TABLES/3.

Salwoom, L. *et al.* (2019) 'New recombinant cold-adapted and organic solvent tolerant lipase from psychrophilic pseudomonas sp. Lsk25, isolated from signy island antarctica', *International Journal of Molecular Sciences*, 20(6). doi: 10.3390/ijms20061264.

Sambrook, J. (1983) *Molecular Cloning. A Laboratory Manual*, *Biochemical Education*. Elsevier BV. doi: 10.1016/0307-4412(83)90068-7.

Sánchez-Carbente, M. del R. *et al.* (2017) 'The first description of a hormone-sensitive lipase from a basidiomycete: Structural insights and biochemical characterization revealed Bjerkandera adusta BaEstB as a novel esterase', *MicrobiologyOpen*. Wiley-Blackwell, 6(4), p. e00463. doi: 10.1002/MBO3.463.

Sander, D. *et al.* (2021) 'Metaproteomic Discovery and Characterization of a Novel Lipolytic Enzyme From an Indian Hot Spring', *Frontiers in Microbiology*. Frontiers Media S.A., 12, p. 1136. doi: 10.3389/fmicb.2021.672727.

De Santi, C. *et al.* (2014) 'A New Alkaliphilic Cold-Active Esterase from the Psychrophilic Marine Bacterium Rhodococcus sp.: Functional and Structural Studies and Biotechnological Potential', *Applied Biochemistry and Biotechnology*. Humana Press Inc., 172(6), pp. 3054–3068. doi: 10.1007/s12010-013-0713-1.

Saunders, N. F. W. *et al.* (2003) 'Mechanisms of thermal adaptation revealed from the genomes of the Antarctic Archaea Methanogenium frigidum and Methanococcoides burtonii', *Genome research*. Cold Spring Harbor Laboratory Press, 13(7), pp. 1580–8. doi: 10.1101/gr.1180903.

Sayer, C. *et al.* (2015) 'Structural studies of a thermophilic esterase from a new Planctomycetes species, Thermogutta terrifontis', *FEBS Journal*. John Wiley & Sons, Ltd, 282(15), pp. 2846–2857. doi: 10.1111/febs.13326.

Sayers, E. W. *et al.* (2022) 'Database resources of the national center for biotechnology information', *Nucleic acids research*. Nucleic Acids Res, 50(D1). doi: 10.1093/NAR/GKAB1112.

Schmuck, B., Sandgren, M. and Härd, T. (2018) 'The kinetics of TEM1 antibiotic degrading enzymes that are displayed on Ure2 protein nanofibrils in a flow reactor', *PLOS ONE*. Edited by K. M. G. Mallela. Public Library of Science, 13(4), p. e0196250. doi: 10.1371/journal.pone.0196250.

Schoffelen, S. and van Hest, J. C. (2013) 'Chemical approaches for the construction of multi-enzyme reaction systems', *Current Opinion in Structural Biology*. Elsevier Current Trends, 23(4), pp. 613–621. doi: 10.1016/j.sbi.2013.06.010.

Schumann, W. and Ferreira, L. C. S. (2004) 'Production of recombinant proteins in Escherichia coli', *Genetics and Molecular Biology*. Sociedade Brasileira de Genética, 27(3), pp. 442–453. doi: 10.1590/S1415-47572004000300022.

Seong, G. H., Heo, J. and Crooks, R. M. (2003) 'Measurement of Enzyme Kinetics Using a Continuous-Flow Microfluidic System', *Analytical Chemistry*. Kluwer Academic Publishers, 75(13), pp. 3161–3167. doi: 10.1021/ac034155b.

Sezonov, G., Joseleau-Petit, D. and D'Ari, R. (2007) 'Escherichia coli physiology in Luria-Bertani broth', *Journal of bacteriology*. J Bacteriol, 189(23), pp. 8746–8749. doi: 10.1128/JB.01368-07.

Shao, H. *et al.* (2019) 'Gene cloning, expression in E. coli, and in vitro refolding of a lipase from Proteus sp. NH 2-2 and its application for biodiesel production', *Biotechnology Letters*, 41(1), pp. 159–169. doi: 10.1007/s10529-018-2625-1.

Sharma, R., Chisti, Y. and Banerjee, U. C. (2001) 'Production, purification, characterization, and applications of lipases', *Biotechnology Advances*. Elsevier Inc., 19(8), pp. 627–662. doi: 10.1016/S0734-9750(01)00086-6.

Sheldon, R. A. and van Pelt, S. (2013) 'Enzyme immobilisation in biocatalysis: why, what and how', *Chem. Soc. Rev.*, 42(15), pp. 6223–6235. doi: 10.1039/C3CS60075K.

Shibasaki, S. (2009) 'Evaluation of the Biodegradability of Polyurethane and Its Derivatives by Using Lipase- Displaying Arming Yeast'.

Shilling, P. J. *et al.* (2020) 'Improved designs for pET expression plasmids increase protein production yield in Escherichia coli', *Communications Biology 2020 3:1*. Nature Publishing

Group, 3(1), pp. 1–8. doi: 10.1038/s42003-020-0939-8.

Siddiqui, K. S. *et al.* (2005) 'Role of Disulfide Bridges in the Activity and Stability of a Cold-Active α-Amylase', *Journal of Bacteriology*. American Society for Microbiology (ASM), 187(17), pp. 6206–6212. doi: 10.1128/JB.187.17.6206-6212.2005.

Siddiqui, K. S. *et al.* (2006) 'Role of lysine versus arginine in enzyme cold-adaptation: Modifying lysine to homo-arginine stabilizes the cold-adapted α-amylase from Pseudoalteramonas haloplanktis', *Proteins: Structure, Function, and Bioinformatics*. Proteins, 64(2), pp. 486–501. doi: 10.1002/prot.20989.

Siddiqui, K. S. and Cavicchioli, R. (2006) 'Cold-Adapted Enzymes', *Annual Review of Biochemistry*, 75(1), pp. 403–433. doi: 10.1146/annurev.biochem.75.103004.142723.

Silverstein, R. M. and Bassler, G. C. (1962) 'Spectrometric identification of organic compounds', *Journal of Chemical Education*. Division of Chemical Education , 39(11), p. 546. doi: 10.1021/ed039p546.

Siódmiak, T. *et al.* (2020) 'Evaluation of Designed Immobilized Catalytic Systems: Activity Enhancement of Lipase B from Candida antarctica', *Catalysts 2020, Vol. 10, Page 876*. Multidisciplinary Digital Publishing Institute, 10(8), p. 876. doi: 10.3390/CATAL10080876.

Smith, D. R. (1993) 'Restriction Endonuclease Digestion of DNA', in *Transgenesis Techniques*. New Jersey: Humana Press, pp. 427–432. doi: 10.1385/0-89603-245-0:427.

Soto, C. (2001) 'Protein misfolding and disease; protein refolding and therapy', *FEBS Letters*. FEBS Lett, 498(2–3), pp. 204–207. doi: 10.1016/S0014-5793(01)02486-3.

De Souza, M. C. M. *et al.* (2017) 'Production of flavor esters catalyzed by Lipase B from Candida antarctica immobilized on magnetic nanoparticles', *Brazilian Journal of Chemical Engineering*. Assoc. Brasiliera de Eng. Quimica / Braz. Soc. Chem. Eng., 34(3), pp. 681–690. doi: 10.1590/0104-6632.20170343s20150575.

Souza, P. M. P. *et al.* (2021) 'Enzyme-support interactions and inactivation conditions determine Thermomyces lanuginosus lipase inactivation pathways: Functional and florescence studies', *International Journal of Biological Macromolecules*. Elsevier, 191, pp. 79–91. doi: 10.1016/j.ijbiomac.2021.09.061.

Spriestersbach, A. *et al.* (2015) 'Purification of His-Tagged Proteins', in *Methods in Enzymology*. Academic Press Inc., pp. 1–15. doi: 10.1016/bs.mie.2014.11.003.

Stauch, B., Fisher, S. J. and Cianci, M. (2015) 'Open and closed states of Candida antarctica lipase B: protonation and the mechanism of interfacial activation', *Journal of lipid research*. J Lipid Res, 56(12), pp. 2348–2358. doi: 10.1194/JLR.M063388.

Stone, J. P. and Steinberg, D. K. (2016) 'Salp contributions to vertical carbon flux in the Sargasso Sea', *Deep Sea Research Part I: Oceanographic Research Papers*. Pergamon, 113, pp. 90–100. doi: 10.1016/J.DSR.2016.04.007.

Strocchi, M. *et al.* (2006) 'Low temperature-induced systems failure inEscherichia coli: Insights from rescue by cold-adapted chaperones', *PROTEOMICS*. Wiley-Blackwell, 6(1), pp. 193–206. doi: 10.1002/pmic.200500031.

Studier, F. W. (2014) 'Stable Expression Clones and Auto-Induction for Protein Production in E. coli', *Methods in Molecular Biology*. Humana Press, Totowa, NJ, 1091, pp. 17–32. doi: 10.1007/978-1-62703-691-7_2.

Suen, W.-C. *et al.* (2004) 'Improved activity and thermostability of Candida antarctica lipase

B by DNA family shuffling', *Protein Engineering Design and Selection*. Oxford University Press, 17(2), pp. 133–140. doi: 10.1093/protein/gzh017.

Sulaiman, S. *et al.* (2014) 'A Review: Potential Usage of Cellulose Nanofibers (CNF) for Enzyme Immobilization via Covalent Interactions'. doi: 10.1007/s12010-014-1417-x.

Sunagawa, S. *et al.* (2015) 'Structure and function of the global ocean microbiome', *Science*. American Association for the Advancement of Science, 348(6237). doi: 10.1126/science.1261359.

Supek, F. (2016) 'The Code of Silence: Widespread Associations Between Synonymous Codon Biases and Gene Function', *Journal of Molecular Evolution*. Springer, 82(1), pp. 65–73. doi: 10.1007/s00239-015-9714-8.

Sutherland, K. R., Madin, L. P. and Stocker, R. (2010) 'Filtration of submicrometer particles by pelagic tunicates'. doi: 10.1073/pnas.1003599107.

Swartz, J. R. (2001) 'Advances in Escherichia coli production of therapeutic proteins', *Current Opinion in Biotechnology*. Elsevier Ltd, 12(2), pp. 195–201. doi: 10.1016/S0958-1669(00)00199-3.

Szycher, M. (1991) 'High Performance Biomaterials : a Complete Guide to Medical and Pharmceutical Applications'.

Szycher, M. (2006) *Szycher's handbook of polyurethanes, second edition.* CRC Press.

Tang, L. *et al.* (2015) 'Lid hinge region of Penicillium expansum lipase affects enzyme activity and interfacial activation', *Process Biochemistry*. Elsevier, 50(8), pp. 1218–1223. doi: 10.1016/j.procbio.2015.04.022.

Tanokura, M. *et al.* (2015) 'Structural analysis of enzymes used for bioindustry and bioremediation', *Bioscience, Biotechnology, and Biochemistry*. Japan Society for Bioscience Biotechnology and Agrochemistry, 79(9), pp. 1391–1401. doi: 10.1080/09168451.2015.1052770.

Terpe, K. (2006) 'Overview of bacterial expression systems for heterologous protein production: from molecular and biochemical fundamentals to commercial systems', *Applied Microbiology and Biotechnology*. Springer, 72(2), pp. 211–222. doi: 10.1007/s00253-006-0465-8.

Thomas, T., Gilbert, J. and Meyer, F. (2012) 'Metagenomics - a guide from sampling to data analysis', *Microbial Informatics and Experimentation*, 2, p. 3. doi: 10.1186/2042-5783-2-3.

Tian, K. *et al.* (2017) 'Directed evolution of Thermomyces lanuginosus lipase to enhance methanol tolerance for efficient production of biodiesel from waste grease', *Bioresource Technology*. Elsevier, 245, pp. 1491–1497. doi: 10.1016/J.BIORTECH.2017.05.108.

Tian, R. *et al.* (2015) 'Expression and Characterization of a Novel Thermo-Alkalistable Lipase from Hyperthermophilic Bacterium Thermotoga maritima', *Applied Biochemistry and Biotechnology 2015 176:5*. Springer, 176(5), pp. 1482–1497. doi: 10.1007/S12010-015-1659-2.

Tišma, M. *et al.* (2019) 'Lipase Production by Solid-State Cultivation of Thermomyces Lanuginosus on By-Products from Cold-Pressing Oil Production', *Processes*, 7(7), p. 465. doi: 10.3390/pr7070465.

Troev, K. *et al.* (2000) 'A novel approach to recycling of polyurethanes: chemical degradation of flexible polyurethane foams by triethyl phosphate', *Polymer*. Elsevier, 41(19), pp. 7017–

7022. doi: 10.1016/S0032-3861(00)00054-9.

Truppo, M. D. and Hughes, G. (2011) 'Development of an Improved Immobilized CAL-B for the Enzymatic Resolution of a Key Intermediate to Odanacatib', *Organic Process Research & Development*. American Chemical Society, 15(5), pp. 1033–1035. doi: 10.1021/op200157c.

Tyagi, M. *et al.* (2009) 'Novel way of making high refractive index plastics; metal containing polymers for optical applications', *E-Polymers*, (100). doi: 10.1515/epoly.2009.9.1.1197.

Ugras, S. (2017) 'Characterization of a Thermophilic Lipase from Bacillus licheniformis Ht7 Isolated from Hayran Thermal Springs in Giresun', *Romanian Biotechnological Letters*, 22(1), p. 12297.

Upadhyay, L. S. B. and Verma, N. (2014) 'Dual immobilization of biomolecule on the glass surface using cysteine as a bifunctional linker', *Process Biochemistry*. Elsevier, 49(7), pp. 1139–1143. doi: 10.1016/J.PROCBIO.2014.04.003.

Uppenberg, J., Patkar, S., *et al.* (1994) 'Crystallization and preliminary X-ray studies of lipase B from Candida antarctica', *Journal of molecular biology*. J Mol Biol, 235(2), pp. 790–792. doi: 10.1006/JMBI.1994.1035.

Uppenberg, J., Oehrner, N., *et al.* (1994) 'The sequence, crystal structure determination and refinement of two crystal forms of lipase B from Candida antarctica', *Structure (London, England : 1993)*. Cell Press, 2(4), pp. 293–308. doi: 10.1016/S0969-2126(00)00031-9.

Uppenberg, J. *et al.* (1995) 'Crystallographic and molecular-modeling studies of lipase B from Candida antarctica reveal a stereospecificity pocket for secondary alcohols', *Biochemistry*. American Chemical Society, 34(51), pp. 16838–16851. doi: 10.1021/bi00051a035.

Utomo, R. N. C. *et al.* (2020) 'Defined Microbial Mixed Culture for Utilization of Polyurethane Monomers'.

Venkatachalam, S. *et al.* (2012) 'Degradation and Recyclability of Poly (Ethylene Terephthalate)', *Polyester*. IntechOpen. doi: 10.5772/48612.

Veno, J. *et al.* (2019) 'Insight into improved thermostability of cold-adapted staphylococcal lipase by glycine to cysteine mutation', *Molecules*. MDPI AG, 24(17). doi: 10.3390/molecules24173169.

Verma, M. L. *et al.* (2013) 'Enzyme Immobilisation on Amino-Functionalised Multi-Walled Carbon Nanotubes: Structural and Biocatalytic Characterisation'. doi: 10.1371/journal.pone.0073642.

Verma, M. L. and Puri, M. (2013) 'Nanobiotechnology as a novel paradigm for enzyme immobilisation and stabilisation with potential applications in biodiesel production', *Applied Microbiology and Biotechnology 2012 97:1*. Springer-Verlag, 97(1), pp. 23–39. doi: 10.1007/s00253-012-4535-9.

Walker, J. (2009) *Protein Protocols Edited by The Handbook SECOND EDITION*.

Wang, G. *et al.* (2015) 'Probing role of key residues in the divergent evolution of Yarrowia lipolytica lipase 2 and Aspergillus niger eruloyl esterase A', *Microbiological Research*. Urban & Fischer, 178, pp. 27–34. doi: 10.1016/j.micres.2015.05.011.

Wang, P. (2006) 'Nanoscale biocatalyst systems', *Current Opinion in Biotechnology*. Elsevier Current Trends, 17(6), pp. 574–579. doi: 10.1016/J.COPBIO.2006.10.009.

Wang, Q. *et al.* (2013) 'Optimization of Cold-Active Lipase Production from Psychrophilic Bacterium Moritella sp. 2-5-10-1 by Statistical Experimental Methods', *Bioscience,*

Biotechnology, and Biochemistry, 77(1), pp. 17–21. doi: 10.1271/bbb.120104.

Wang, W. *et al.* (2021) 'Rational engineering of low temperature activity in thermoalkalophilic Geobacillus thermocatenulatus lipase', *Biochemical Engineering Journal*. Elsevier, 174, p. 108093. doi: 10.1016/j.bej.2021.108093.

Wang, Y. *et al.* (2018) 'High-level expression and characterization of solvent-tolerant lipase', *Journal of Bioscience and Bioengineering*. Elsevier, 125(1), pp. 23–29. doi: 10.1016/j.jbiosc.2017.06.012.

Waterhouse, A. *et al.* (2018) 'SWISS-MODEL: homology modelling of protein structures and complexes', *Nucleic Acids Research*. Oxford Academic, 46(W1), pp. W296–W303. doi: 10.1093/nar/gky427.

Weimer, A. *et al.* (2020) 'Industrial biotechnology of Pseudomonas putida: advances and prospects', *Applied Microbiology and Biotechnology 2020 104:18*. Springer, 104(18), pp. 7745–7766. doi: 10.1007/S00253-020-10811-9.

Welch, M. *et al.* (2009) 'You're one in a googol: optimizing genes for protein expression', *Journal of The Royal Society Interface*. The Royal Society, 6(suppl_4), pp. 37–46. doi: 10.1098/rsif.2008.0520.focus.

Wen, J., Scoles, D. R. and Facelli, J. C. (2014) 'Structure prediction of polyglutamine disease proteins: comparison of methods', *BMC Bioinformatics*. BioMed Central Ltd., 15(S7), p. S11. doi: 10.1186/1471-2105-15-S7-S11.

Wilson, D. *et al.* (2009) 'SUPERFAMILY—sophisticated comparative genomics, data mining, visualization and phylogeny', *Nucleic Acids Research*. Oxford University Press, 37(suppl_1), pp. D380–D386. doi: 10.1093/nar/gkn762.

Winkler, F. K., D'Arcy, A. and Hunziker, W. (1990) 'Structure of human pancreatic lipase', *Nature*. Nature Publishing Group, 343(6260), pp. 771–774. doi: 10.1038/343771a0.

Winkler, U. K. and Stuckmann, M. (1979) 'Glycogen, hyaluronate, and some other polysaccharides greatly enhance the formation of exolipase by Serratia marcescens.', *Journal of Bacteriology*, 138(3).

Wrolstad, R. E. *et al.* (2004) *Handbook of Food Analytical Chemistry*, *Handbook of Food Analytical Chemistry: Water, Proteins, Enzjmes, Lipids, and Carbohydrates*. Hoboken, NJ, USA: John Wiley & Sons, Inc. doi: 10.1002/0471709085.

Xia, J. *et al.* (2015) 'Advances and Practices of Bioprocess Scale-up', *Advances in Biochemical Engineering/Biotechnology*. Springer, Berlin, Heidelberg, 152, pp. 137–151. doi: 10.1007/10_2014_293.

Xian, W. *et al.* (2018) 'Rheological and mechanical properties of thermoplastic polyurethane elastomer derived from CO_2 copolymer diol', *Journal of Applied Polymer Science*. John Wiley & Sons, Ltd, 135(11), p. 45974. doi: 10.1002/app.45974.

Xiang, M. *et al.* (2021) 'Heterologous expression and biochemical characterization of a cold-active lipase from Rhizopus microsporus suitable for oleate synthesis and bread making', *Biotechnology Letters*. Springer Science and Business Media B.V., 43(9), pp. 1921–1932. doi: 10.1007/s10529-021-03167-1.

Xiao, Y. *et al.* (2019) 'Constructing a Continuous Flow Bioreactor Based on a Hierarchically Porous Cellulose Monolith for Ultrafast and Nonstop Enzymatic Esterification/Transesterification', *ACS Sustainable Chemistry & Engineering*. American Chemical Society, 7(2), pp. 2056–2063. doi: 10.1021/acssuschemeng.8b04471.

Xie, Y. *et al.* (2014) 'Enhanced Enzyme Kinetic Stability by Increasing Rigidity within the Active Site', *Journal of Biological Chemistry*. American Society for Biochemistry and Molecular Biology Inc., 289(11), pp. 7994–8006. doi: 10.1074/jbc.M113.536045.

Xin, C. *et al.* (2020) 'Purification and Characterization of a Novel Lipase from Antarctic Krill', *J. Ocean Univ. China (Oceanic and Coastal Sea Research*, 19(1), pp. 209–215. doi: 10.1007/s11802-019-4174-1.

Xu, L. *et al.* (2022) 'An efficient and robust continuous-flow bioreactor for the enzymatic preparation of phytosterol esters based on hollow lipase microarray', *Food Chemistry*. Elsevier, 372, p. 131256. doi: 10.1016/j.foodchem.2021.131256.

Yabuuchi, E. *et al.* (1992) 'Proposal of Burkholderia gen. nov. and Transfer of Seven Species of the Genus Pseudomonas Homology Group II to the New Genus, with the Type Species Burkholderia cepacia (Palleroni and Holmes 1981) comb. nov.', *Microbiology and Immunology*. John Wiley & Sons, Ltd, 36(12), pp. 1251–1275. doi: 10.1111/j.1348-0421.1992.tb02129.x.

Yakimov, M. M. *et al.* (2003) 'Oleispira antarctica gen. nov., sp. nov., a novel hydrocarbonoclastic marine bacterium isolated from Antarctic coastal sea water', *International Journal of Systematic and Evolutionary Microbiology*. Int J Syst Evol Microbiol, 53(3), pp. 779–785. doi: 10.1099/ijs.0.02366-0.

Yan, B. X. and Sun Qing, Y. (1997) 'Glycine Residues Provide Flexibility for Enzyme Active Sites', *Journal of Biological Chemistry*. Elsevier, 272(6), pp. 3190–3194. doi: 10.1074/JBC.272.6.3190.

Yang, J. *et al.* (2015) 'The I-TASSER Suite: protein structure and function prediction', *Nature Methods*. NIH Public Access, 12(1), pp. 7–8. doi: 10.1038/nmeth.3213.

Yildirim, D. *et al.* (2019) 'Improvement of activity and stability of Rhizomucor miehei lipase by immobilization on nanoporous aluminium oxide and potassium sulfate microcrystals and their applications in the synthesis of aroma esters', *Biocatalysis and Biotransformation*. Taylor & Francis, 37(3), pp. 210–223. doi: 10.1080/10242422.2018.1530766.

Zarafeta, D. *et al.* (2016) 'Metagenomic mining for thermostable esterolytic enzymes uncovers a new family of bacterial esterases', *Scientific Reports*. Nature Publishing Group, 6(1), pp. 1–16. doi: 10.1038/srep38886.

Zdarta, J. *et al.* (2018) 'A general overview of support materials for enzyme immobilization: Characteristics, properties, practical utility', *Catalysts*, 8(2). doi: 10.3390/catal8020092.

Zeldis, J. R. and Décima, M. (2020) 'Mesozooplankton connect the microbial food web to higher trophic levels and vertical export in the New Zealand Subtropical Convergence Zone', *Deep-Sea Research Part I: Oceanographic Research Papers*. Elsevier Ltd, 155, p. 103146. doi: 10.1016/j.dsr.2019.103146.

Zhang, D. H., Yuwen, L. X. and Peng, L. J. (2013) 'Parameters affecting the performance of immobilized enzyme', *Journal of Chemistry*. doi: 10.1155/2013/946248.

Zhang, J. W. and Zeng, R. Y. (2008) 'Molecular Cloning and Expression of a Cold-Adapted Lipase Gene from an Antarctic Deep Sea Psychrotrophic Bacterium Pseudomonas sp. 7323', *Marine Biotechnology 2008 10:5*. Springer-Verlag, 10(5), pp. 612–621. doi: 10.1007/S10126-008-9099-4.

Zhang, Y. and Skolnick, J. (2004) 'Scoring function for automated assessment of protein structure template quality', *Proteins*. Proteins, 57(4), pp. 702–710. doi: 10.1002/PROT.20264.

Zhao *et al.* (2021) 'Characterization of a novel lipase from Bacillus licheniformis NCU CS-5 for applications in detergent industry and biodegradation of 2,4-D butyl ester', *International Journal of Biological Macromolecules*. Elsevier, 176, pp. 126–136. doi: 10.1016/J.IJBIOMAC.2021.01.214.

Zhao, J. *et al.* (2019) 'Enhanced Performance of Rhizopus oryzae Lipase by Reasonable Immobilization on Magnetic Nanoparticles and Its Application in Synthesis 1,3-Diacyglycerol', *Applied Biochemistry and Biotechnology 2019 188:3*. Springer, 188(3), pp. 677–689. doi: 10.1007/S12010-018-02947-2.

Zhou, Y. *et al.* (2019) 'The additive mutational effects from surface charge engineering: A compromise between enzyme activity, thermostability and ionic liquid tolerance', *Biochemical Engineering Journal*. Elsevier, 148, pp. 195–204. doi: 10.1016/j.bej.2018.07.020.

Zhu, G. *et al.* (2021) 'Structure and Function of Pancreatic Lipase-Related Protein 2 and Its Relationship With Pathological States', *Frontiers in Genetics*. Frontiers, 12, p. 1061. doi: 10.3389/fgene.2021.693538.

Zhu, J. and Sun, G. (2012) 'Lipase immobilization on glutaraldehyde-activated nanofibrous membranes for improved enzyme stabilities and activities', *Reactive and Functional Polymers*. Elsevier, 72(11), pp. 839–845. doi: 10.1016/j.reactfunctpolym.2012.08.001.

Zimmermann, J. L. *et al.* (2010) 'Thiol-based, site-specific and covalent immobilization of biomolecules for single-molecule experiments', *Nature Protocols*. Nature Publishing Group, 5(6), pp. 975–985. doi: 10.1038/nprot.2010.49.

Zisis, T. *et al.* (2015) 'Interfacial Activation of *Candida antarctica* Lipase B: Combined Evidence from Experiment and Simulation', *Biochemistry*. American Chemical Society, 54(38), pp. 5969–5979. doi: 10.1021/acs.biochem.5b00586.